Sunitinib-induced cardiotoxicity: the involvement of the mitogen-activated protein kinase kinase 7 pathway

Cooper, Samantha

Award date:
2018

Awarding institution:
Coventry University

Sunitinib-induced cardiotoxicity: the involvement of the mitogen-activated protein kinase kinase 7 pathway

By

Samantha Louise Cooper

Supervisory team: Dr Hardip Sandhu, Prof Helen Maddock, Dr Afthab Hussain, and Dr Christopher J Mee

September 2017

A thesis submitted in partial fulfilment of the University's requirements for the Degree of Doctor of Philosophy

Certificate of Ethical Approval

Applicant:

Samantha Cooper

Project Title:

The involvement of MKK7 in Sunitinib induced cardiotoxicity

This is to certify that the above named applicant has completed the Coventry University Ethical Approval process and their project has been confirmed and approved as Low Risk

Date of approval:

22 August 2016

Project Reference Number:

P45314

Acknowledgements

It is a pleasure to thank those who made this thesis possible. Firstly, I owe the deepest gratitude to my supervisors' Dr Hardip Sandhu, Professor Helen Maddock, Dr Afthab Hussain and Dr Christopher Mee, for all of their support, motivation and guidance over the past 4 years. I cannot thank you enough for opportunities to present my data at both national and international conferences, as well as encouragement to publish data that I have generated. You have all moulded me into the scientist I have become today.

In addition, I would like to express thanks Dr Mayel Gharanei, Dr Maryam Baba, Dr Igor Morozov, Dr Irmgard Haussman and Professor Rob James for their support and expert advice throughout this research project.

I am indebted to my many of my colleagues who have supported me; Mr Mark Bodycote and Mrs Bethan Grist for providing technical expertise and friendly advice. A special thank you to my lab colleagues Oana Chiuzbaian, Raja Kamarudin, Jasmin Bhandal, Refik Kuburas and Shabana Cassambai, who supported me and kept me sane. Your friendship has made Coventry University a really enjoyable place to work.

Finally, a massive thank you to my friends and family for being incredibly understanding, providing unyielding support and endless encouragement throughout. I couldn't have achieved any of this without you.

Thank you,

Samantha Louise Cooper

Abstract

Sunitinib is a potent multiple tyrosine kinase receptor inhibitor which possesses powerful anti-cancer properties. However, adverse cardiovascular events have been reported in treated patients.

Mitogen activated protein kinase (MAPK) signalling cascades play significant roles in the development of cardiac hypertrophy in response to external stresses. Interestingly, Sunitinib has been shown to produce an inhibitory effect on MAPK signalling. The stress signalling protein mitogen activated kinase kinase 7 (MKK7) is an elective upstream regulator of the c-Jun N-terminal kinase (JNK) pathway and is downstream to apoptosis signalling kinase 1 (ASK1). Specific deletion of MKK7, JNK and ASK1 in hearts has been shown to increase the sensitivity of cardiomyocytes to external stresses.

This thesis investigates Sunitinib-induced cardiotoxicity in 3 month, 12 month and 24 month old male Sprague-Dawley rats. Then, tests the involvement of the ASK1/MKK7/JNK and the protein kinase C α (PKCα) pathways in Sunitinib-induced cardiotoxicity in 3 month ages rats. The evaluation of potential cardioprotective compounds: NQDI-1 and 2Cl-IB-MECA were also investigated. Changes in cardiac injury specific microRNAs (miRNAs): miR-1, miR-27a, miR-133a and miR-133b levels and cancer specific miRNAs: miR-15a, miR-16-1 and miR-155 were measured in response to Sunitinib and cardioprotective adjunct therapy in both left ventricular tissue and the HL60 cell line.

Sunitinib produced a detrimental effect on haemodynamic function and significantly increased infarct size in all age groups tested. However, in the 24 month and 12 month groups the increase in infarct size was not as pronounced as in the 3 month group. Also,

haemodynamic dysfunction was present in all age groups, however, the level of dysfunction varied between the age groups tested. Ageing also demonstrated opposing expression patterns of cardiac injury specific miRNAs and MKK7 phosphorylation levels.

The adjunct therapy NQDI-1 partially attenuated Sunitinib-induced cardiotoxicity by facilitating a reduction in infarct size. However, NQDI-1 did not attenuate Sunitinib-induced declines in haemodynamic function. Interestingly, NQDI-1 attenuated Sunitinib's inhibition of ASK1/MKK7/JNK pathway and enhanced the anti-cancer properties of Sunitinib in HL60 cells.

The adjunct therapy IB-MECA abrogated both increases in infarct size and the declines in left ventricular developed pressure produced by Sunitinib treatment. However, the decline in heart rate was not attenuated by IB-MECA. IB-MECA attenuated Sunitinib's inhibition of MKK7 and JNK phosphorylation and the increase in PKCα phosphorylation in left ventricular tissue. Furthermore, IB-MECA did not jeopardise Sunitinib's anti-cancer properties.

In conclusion, data from this thesis demonstrated that Sunitinib caused cardiotoxicity in all age groups. Also, data highlighted the complexity of cellular signalling mechanisms produced by Sunitinib-induced cardiotoxicity. Inhibition of the ASK1/MKK7/JNK pathway and activation of PKC could be involved in Sunitinib-induced cardiotoxicity. However, the MKK7 signalling was altered by ageing. The use of miRNAs as markers for Sunitinib-induced cardiac injury and anti-cancer capabilities were inconclusive. However, both NQDI-1 and IB-MECA possess promising cardioprotective properties and did not diminish the anti-cancer properties of Sunitinib in HL60 cells.

Publications from this PhD project

Cooper, S., Sandhu, H., Mee, C., Hussain, A., & Maddock, H. (2017) Attenuation of Sunitinib-induced cardiotoxicity through the A3 adenosine receptor activation *European Journal of Pharmacology.* 814, 95-105. https://doi.org/10.1016/j.ejphar.2017.08.011

Cooper, S.L., Sandhu, H., Hussain, A., Mee, C. and Maddock, H. (2018) Involvement of mitogen activated kinase kinase 7 intracellular signalling pathway in Sunitinib-induced cardiotoxicity. *Toxicology*. 394 72-83 https://doi.org/10.1016/j.jbior.2017.10.004

Cooper, S.L., Mee, C., Hussain, A., Maddock, H.L. and Sandhu, H. (2017) Sunitinib-induced cardiotoxicity is age dependant and involves Mitogen Activated Kinase Kinase 7 (MKK7)**.**

***Submitted for publication in Aging US*.**

Cooper, S., Sandhu, H., Hussain, A., & Maddock, H. (2015). Involvement of mitogen activated kinase kinase 7 in tyrosine kinase inhibitor-induced myocardial injury. *Journal of Pharmacological and Toxicological Methods*, (75) 169. **Poster presentation at the Safety Pharmacology Society annual meeting, September 2014. Washington USA**

Maddock, H., Cooper, S., Sandhu, H., & Hussain, A. (2015) 198 Involvement of Mitogen Activated Kinase Kinase 7 in Tyrosine Kinase Inhibitor Induced Myocardial Injury *Heart* 101: A110. **Poster presentation at the British Cardiovascular Society Annual conference, June 2015. Manchester, UK.**

Cooper, S., Maddock, H., Hussain, A., & Sandhu, H. (2016). Mitogen activated kinase kinase 7 is involved in Sunitinib induced myocardial injury. *Journal of Pharmacological and*

Toxicological Methods, (81) 341. **Poster presentation at the Safety Pharmacology Society annual meeting, September 2015. Prague, Czech Republic.**

Cooper, S.L., Mee, C., Hussain, A., Maddock, H.L. and Sandhu, H. (2016) Age is a factor of the extent of anti-cancer Sunitinib therapy induced cardiotoxicity: Studying haemodynamic parameters and cardiotoxicity specific microRNA expression involved. **Poster presentation at the British Toxicology Society Annual Congress, April 2016. Manchester, UK.**

Cooper, S., Mee, C., Hussain, A., Maddock, H. and Sandhu, H., (2017) Sunitinib-Induced Cardiotoxicity is Age Dependant and Involves Mitogen Activated Kinase Kinase 7 (MKK7). *Journal of Pharmacological and Toxicological Methods*, (*88*) 216. **Poster presentation at the Safety Pharmacology Annual Meeting, September 2016. Vancouver, Canada.**

Contents Table

List of Figures

List of Tables

Abbreviations:

%	Percentage
µM	Micromole
A3AR	A3 adenosine receptor
AC	Adenylyl cyclase
AEBSF	β-glycaophosphate, 4-benzenesulfonyl fluoride hydrochloride
Akt	Protein Kinase B
AMP	Adenosine mono-phosphate
AMPK	Adenosine mono-phosphate kinase
ANF	Atrial natriuretic factor
AP-1	Activating protein 1
ASK1	Apoptosis signal regulated kinase 1
Atg-4	Autophagin-4
ATP	Adenosine triphosphate
BAD	BCL-2 antagonist of cell death
BAX	BCL2 associate X protein

BNP	B-type natriuretic peptide
BPM	Beats per minute
BSA	Bovine serum albumin
CAD	Coronary artery disease
cAMP	Cyclic adenosine mono-phosphate
cDNA	Complimentary deoxyribonucleic acid
CF	Coronary flow
CHF	Chronic Heart failure
C-KIT	Proto-oncogene c-Kit
CLL	Chronic lymphocytic leukaemia
Cmax	Maximum serum concentration
CML	Chronic myeloid leukaemia
CSF-1R	Colony stimulating factor-1 receptor
C_t	Cycle threshold
CT ΔΔ	Cycle threshold
cTn	Cardiac troponins

cTnT	Cardiac troponin T
DAG	Diacylglycerol
DMSO	Di-methyl sulfoxide
DNA	Deoxyribonucleic acid
DR	Death receptor
ECG	Electrocardiogram
ECL	Enhanced chemi-luminescence
EDTA	Ethylenediaminetetraacetic acid
EEF2	Eukaryotic elongation factor-2
EGFR	Epidermal growth factor receptor
ER	Endoplasmic reticulum
ERG	Ether-a-go-go related gene
ERK	Extracellular signal-regulated kinase
ETC	Electron transport chain
FBS	Foetal bovine serum
FGFR1	Fibroblast growth factor receptor 1

FLT-3	Fms-like tyrosine kinase-3 receptor
GADD45B	Growth arrest and DNA-damage-inducible beta
GAPDH	Glyceraldehyde 3-phosphate dehydrogenase
GDP	Guanosine diphosphate
GEF	Guanine nucleotide exchange factor
GIST	Gastrointestinal stromal tumour
GPCR	G protein coupled receptors
GSK3β	Glycogen synthase kinase 3β
GTP	Guanosine triphosphate
H^+	Hydrogen ions
H_2O_2	Hydrogen peroxide
HEPES	4-(2-hydroxyethyl)-1-piperazineethanesulfonic acid
HEPG2	Human hepatocellular cancer cell lines
HL60	Human leukaemia cancer cell line
HR	Heart rate
HRP	Horseradish peroxidase

IFN-γ	Interferon gamma
IG	Immunoglobulin
IL-3	Interleukin 3
iNOS	Inducible nitric oxide synthase
IR	Ischaemia reperfusion
IRI	Ischaemia reperfusion injury
JAK	Janus kinase
JIP	JNK interacting protein
JNK	c-Jun NH2-terminal kinase
KHB	Krebs Henseleit Buffer
LC3	Microtubule-associated protein 1 light chain 3
LV	Left ventricle
LVDP	Left ventricular developed pressure
LVEF	Left ventricular ejection fraction
MAPK	Mitogen activated protein kinases
MAPKK	Mitogen activated kinase kinase

Mdivi-1	Mitochondrial division inhibitor-1
MHC-β	Myosin heavy chain β
MI	Myocardial infarction
miRNA	MicroRNA
MKK7	Mitogen activated kinase kinase 7
MKKK	Mitogen activated kinase kinase kinase
mM	Millimole
mmHg	Millimetres of mercury
mtPTP	Mitochondrial permeability transition pore
mRNA	Messenger RNA
mtDNA	Mitochondrial DNA
mTOR	Murine target of rapamycin
MTT	3−[4,5−dimethylthia−zol−2−yl] −2,5−diphenyl tetrazolium bromide
NHE	Na+ /H+ exchanger
NF-κB	Nuclear factor kappa-light-chain enhancer of activated B cells
NK cell	Natural killer cell

NQO1	NAD(P)H: quinone oxidoreductases
NRTK	Non-receptor tyrosine kinases
NS	Not significant
NTC	Non-template control
PANC1	Pancreatic tumour cell line
PBS	Phosphate buffered saline
PCR	Polymerase chain reaction
PDGFR	Platelet derived growth factor receptor
PI3K	Phosphoinositide 3-kinase
PKC	Protein kinase C
PLC	Phospholipase C
Prkca	PKCα gene
PVDF	Hybond-P Polyvinyl Difluoride
Q	Quencher
Rn	Intensity of fluorescence
ROS	Reactive oxygen species

RT	Reverse transcriptase
RTK	Receptor tyrosine kinase
SEM	Standard error of mean
siRNA	Small interfering RNA
SR	Sarcoplasmic reticulum
SRC	Proto-oncogene tyrosine-protein kinase
SRF	Serum response factor
TAC	Transverse aortic constriction
TBS	Tris-buffered saline
TNFα	Tumour necrosis factor alpha
TNFαR	Tumour necrosis factor α receptor
TK	Tyrosine Kinase
TKI	Tyrosine kinase inhibitor
TRβ1	Thyroid hormone receptor β1
TTC	Triphenyltetrazolium chloride
UTR 3’	Untranslated region

VEGF	Vascular endothelial growth factor
VEGFR	Vascular endothelial growth factor receptor
VHL	Von Hipple-Lindau gene

1. Introduction

1.1 General introduction

Research within this thesis tested novel intracellular pathways associated with Sunitinib induced cardiotoxicity in 3 month, 12 month and 24 month aged Sprague-Dawley rat hearts. Then explored novel adjunct therapies which have the potential to reduce cardiac injury, by targeting key cardiotoxicity linked pathways in 3 month rats. The effect of specific adjunct therapy options was also investigated in a cancer cell model, examining the effects of the adjunct therapy drugs on Sunitinib's antineoplastic properties. Finally, the use of microRNAs (miRNAs) as indicators of both cardiac injury and cancer development were also investigated.

This introductory chapter summarises the anti-cancer effects of Sunitinib, potential mechanisms for Sunitinib-induced cardiac injury, the impact of ageing on Sunitinib induced cardiotoxicity, intracellular signalling pathways involved in Sunitinib-induced cardiotoxicity, potential cardioprotective adjunct therapies and miRNAs as potential biomarkers for cardiac injury and cancer progression.

1.2 Tyrosine kinases in cancer

The number of people diagnosed with cancer each year is drastically increasing (Siegel, Miller and Jemal 2015). Globally, it is estimated that 14.1 million new cancer cases are diagnosed each year (Torre et al. 2015). This increase is due to a combination of people living long enough for a detectable tumour to manifest, and vast improvements in the

methods of diagnosis. Fortunately, the number of people surviving cancer is also increasing due to effective new treatments.

Decades of rapid advancements in cancer research, has generated a wealth of knowledge, revealing the profound involvement of genome alterations during cancer development (Stratton, Campbell and Futreal 2009, Vogelstein et al. 2013). Cancer can arise through oncogene gain of function mutations, or mutations which cause a loss of tumour repressor genes function (Vogelstein et al. 2013). Both forms of genetic alteration can result in the progression of normal cells transforming into cancer cells (Ciriello et al. 2013).

Normal healthy cells have a protective mechanism which initiates programmed cell death in response to the activation of oncogene and suppression of tumour suppressor mutations (Roos and Kaina 2013). In contrast, cancer cells have evolved to tolerate genome complexity, which enables them to avoid apoptosis, commence uncontrolled proliferation and abnormal differentiation (Fernald and Kurokawa 2013). In particular, tyrosine kinases have been identified as a specific class of proteins which are involved in the progression of many cancers (Gschwind, Fischer and Ullrich 2004).

1.2.1 Tyrosine kinases in cancer development

Receptor tyrosine kinases (RTKs) and non-receptor tyrosine kinases (NRTKs) are a family of kinase proteins which have a pivotal role in signal transduction processes of the cell (Schlessinger 2000, Schlessinger 2014). Epidermal growth factor receptor (EGFR), vascular endothelial growth factor receptor (VEGFR) and platelet derived growth factor receptor (PDGFR) are key members of the RTK family (Robinson, Wu and Lin 2000). Structurally, RTK's comprise of an amino-terminal extracellular domain for ligand binding, characterised

by an immunoglobulin-like sequence, a lipophilic transmembrane segment and an intracellular carboxyl-terminal domain (Figure 1.1). Ligand binding causes a conformational change in protein structure, which allows RTK oligomerisation and auto-phosphorylation of tyrosine residues residing on the cytoplasmic domain (Figure 1.1) (Hubbard et al. 1994, Heldin 1995).

Figure 1.1: Structure of the human VEGFR-2.

This tyrosine kinase receptor consists of 1356 amino acids. The extracellular domain is composed of 7 immunoglobulin (IG) -like domains. The 2nd and 3rd IG-like domains are responsible for VEGF binding. The intracellular domain consists of 2 kinase domains and the C-terminal tail. The intracellular domain contains 5 highlighted tyrosine residues (Y951, Y1054, Y1059, Y1175 and Y1214) which are involved in SH2 domain binding of a number of signalling molecules (Holmes et al. 2007).

NRTKs are a family of intracellular proteins which relay intracellular signals. Both RTKs and NRTKs are enzymes which catalyse the transfer of γ phosphate from adenosine triphosphate (ATP) to target proteins (Lemmon and Schlessinger 2010). Numerous cytoplasmic signalling pathways, including Ras/Raf mitogen-activated protein kinase (MAPK) pathway and the protein kinase C (PKC) pathway have been shown to be regulated by NRTKs (Pawson 1995). Activation of these NRTKs elicits a downstream signalling cascade, culminating in cell proliferation related processes, including DNA synthesis, mitosis, cell growth, migration and differentiation (Madhusudan and Ganesan 2004, Schlessinger 2014), all of which are vital in normal cell growth (Figure 1.2).

Figure 1.2: Schematic overview of tyrosine kinase signalling pathways and potential therapeutic targets.

Receptor tyrosine kinases (RTKs) and non-receptor tyrosine kinases (NRTKs) are vital in many cellular processes. RTKs and NRTKs are proto-oncogenes and in cancer their activities can be upregulated and their expression levels can be increased. Therefore, they are promising targets for cancer therapy. Therapeutics can target: 1) the cytoplasmic domain of RTKs where the tyrosine kinase domain is situated, this prevents the intracellular signalling process of the target RTK from occurring. 2) Block ligand binding to the RTK, which prevents activation of the RTK protein. 3) Antibodies could be used to modulate the ligand, which can reduce the rate of RTK activity. 4) The use of RNA interference and antisense technology could be used to induce gene silencing and reduce RTK protein levels on cells. 5) Gene therapy in immune cells could be used to target cancer cell antigens. 6) Inhibition of NRTKs such as SrC and 7) BCR-ABL prevents signal transduction from RTKs. 8) therapies can also target downstream signal transduction pathways to specifically modulate a cellular function. Inhibition of each of the potential therapy targets listed could result in the reduction in cellular processes such as

cell proliferation, angiogenesis, cell migration and gene transcription. As well as, initiation of cell cycle senescence and apoptosis. (Madhusudan and Ganesan 2004).

Tyrosine kinases (TKs) are involved in many cases of tumorigenesis and their genes encompass the largest class of oncogenes (Porter and Vaillancourt 1998, Blume-Jensen and Hunter 2001). In the event of abnormal TK signalling, malignant transformation can occur. Malignant transformation in the process by which cells acquire the properties of cancer. During this process, mutations within TKs and their respective ligands can lead to over-expression of TKs or their ligands. This produces enhanced TK activity, which causes uncontrolled cell proliferation and tumour formation (Robertson, Tynan and Donoghue 2000).

An example of a TK gene involved in cancer is the Von Hipple-Lindau gene (VHL). Normally, VHL is a notable tumour suppressor gene. However, in approximately 80 % of cases of renal cell carcinoma, VHL is inactivated by deletion, mutation or methylation (Motzer et al. 2006). Inactivation of VHL causes an increase in FLT3 expression as well as an up regulation of hypoxia inducible factor 1, which induces the accumulation of proteins essential for adaption to low oxygen levels, such as vascular endothelial growth factor (VEGF) (Kaelin Jr 2008). This encourages the formation of new blood vessels through a process describes as angiogenesis.

1.2.1.1 Angiogenesis in cancer as a result of tyrosine kinases

During tumour growth, RTK VEGFR are highly expressed by hypoxic cells (Carmeliet and Jain 2000). The binding of VEGF to VEGFR initiates the recruitment of endothelial cells, this

stimulates proliferation and migration of the endothelial cells and therefore blood vessel formation (Goel and Mercurio 2013).

Angiogenesis is essential for enabling tumours to grow larger than 1-2 mm^3 (Hanahan and Weinberg 2011). Vessel formation in a tumour increases the availability of oxygen and other vital nutrients for the cancer cell mass to expand further. As tumours expand and metastasize, the characteristic symptoms of cancer (pain, fatigue, weight loss and dyspnoea) become more apparent (Walsh, Donnelly and Rybicki 2000).

RTKs, such as VEGFR, PDGFR and proto-oncogene c-Kit (c-KIT) are heavily involved in tumour development (Cao 2013, Matsumoto et al. 2013, Yao et al. 2013). These protein families promote angiogenesis and vascular permeability.

In cancer, tumour cells secrete VEGF which binds to VEGFR located on endothelial cells (Carmeliet 2005). This initiates vessel migration and formation, enabling the delivery of a blood supply to the tumour (Figure 1.3) (Otrock, Makarem and Shamseddine 2007). In addition to this, high levels of PDGFR and c-KIT are expressed in many tumours types (Heinrich et al. 2002, Hicklin and Ellis 2005). Activation of these proteins promotes tumour angiogenesis, proliferation and metastasis and therefore these proteins are suitable targets for treatment of many cancers. A class of very potent chemotherapy agents have been developed which inhibit TKs and therefore angiogenesis and they will be discussed later in this chapter (Shojaei 2012).

Figure 1.3: Schematic summarising tumour angiogenesis:

Angiogenic factors such as VEGF and PDGF are released by tumour cells, in response to hypoxic conditions. This induces the recruitment of vascular and lymphatic endothelial cells, which are incorporated into the tumour vasculature, through the activation of dimerised VEGFR and PDGFR. Through this process pre-existing vessels begin to migrate and proliferate towards the tumour mass. This establishes the blood supply to the tumour (adapted from Cristofanilli, Charnsangavej and Hortobagyi 2002).

1.2.1.2 Angiogenesis of the heart as a result of tyrosine kinases

In addition to cancer progression, angiogenesis is also a vital process during heart development (Oka et al. 2014). Similarly to tumours, as the heart develops and grows, the demand of oxygen and nutrients increases. To prevent the necrosis of oxygen and nutrient deficient tissue, angiogenesis is initiated (Riley and Smart 2011). Like in tumour cells, hypoxic regions of the heart release pro-angiogenic factors. Kobayashi et al (2017) demonstrated that high levels of VEGFA were present in the hypoxic tissue within mouse hearts (Kobayashi et al. 2017). As previously mentioned in figure 1.3, VEGF has a vital role in tumour angiogenesis. This highlights the similarities in processes of angiogenesis in tumour and heart tissues. Due to these similarities, potent anti-cancer agents which possess anti-angiogenic properties can have detrimental effects in the heart.

There are many cardiotoxic effects associated with anti-angiogenic agents, such as hypertension, arrhythmia, bleeding, venous thrombosis, pulmonary embolism, arterial thrombosis, coronary heart failure, left ventricle (LV) dysfunction and oedema (Shah and Morganroth 2015). The heart is highly susceptible to drug induced toxicity due to its high energetic metabolic demand and lack of regeneration capabilities (MacLellan and Schneider 2000, Kaakeh et al. 2012).

Shortly after birth, the cell-cycle activity of cardiomyocytes rapidly declines (Lee 2010). Because of this, cardiac hypertrophy is essential for heart growth and adaption to increasing work-loads (Foglia and Poss 2016). Therefore, pharmaceutical compounds which reduce metabolic activity or cause a loss of cardiomyocytes have the potential to cause adverse cardiovascular events, including heart failure (Xin, Olson and Bassel-Duby 2013).

1.3 Tyrosine kinase inhibitors

There are many TK abnormalities associated with a number of cancer types. For this reason, the tyrosine kinase inhibitor (TKI) class of anti-cancer pharmaceuticals were designed and created (Krause and Van Etten 2005).

TKIs are a very selective class of anti-cancer drugs. Previous anti-cancer therapeutics have been nonspecific cytotoxic drugs which target proliferating cells (Sawyers 2004). However, TKIs are selective for specific molecular TK targets. Initially, TKIs were designed to target tyrosine kinases by competitive inhibition of the ATP binding site (Zhang, Yang and Gray 2009). As RTKs and NRTKs are often over expressed in many cancers, inhibition of RTKs and NRTKs prevents cellular signalling transduction of pathways responsible for excessive cell growth and proliferation.

For example, the TKI Imatinib promotes natural killer cell (NK cell) activation, which upregulates the tumour suppressor interferon gamma (IFN-γ) (Borg et al. 2004). This feature of Imatinib has been exploited in the clinic and is used in the treatment of chronic eosinophilic leukaemia and gastrointestinal stromal tumours. However, Imatinib has been found to be less selective than originally thought, intolerance or resistance to Imatinib occurs is approximately 15-20% of cases (Hochhaus et al. 2009). Commonly, Imatinib resistance occurs in response to a point mutation in the ABL1 kinase domain of BCR-ABL1, which prevents Imatinib from binding (Burgess et al. 2005). In addition, in 90% of gastrointestinal stromal tumour (GIST) cases a secondary cKIT mutation is found which prevents Imatinib from binding (Heinrich et al. 2008). The high levels of Imatinib resistance

in patients has led to the development of new generation TKIs such as Sunitinib (Serrano et al. 2017).

1.3.1 The tyrosine kinase inhibitor: Sunitinib

1H-Pyrrole-3-carboxamide, N-(2-(diethylamino) ethyl)-5-((Z)-(5-fluoro-1, 2-dihydro-2-oxo-3H-indol-3-ylidene) methyl)-2, 4-dimethyl- or Sunitinib is an indolinone derivative multi-targeted tyrosine kinase inhibitor (Figure 1.4). Sunitinib features effective antineoplastic activity through inhibition of angiogenesis, cell proliferation, positive regulation of apoptosis and the inhibition of signal transduction (Christensen 2007).

Sunitinib is an effective treatment of GIST, pancreatic neuroendocrine tumour (PNET) and renal cell carcinoma (RCC) (Le Tourneau, Raymond and Faivre 2007). It is estimated that in 2015 there were 1 million people diagnosed with GIST, 1.4 million people diagnosed with PNET and 1.9 million diagnosed with RCC (Torre et al. 2015). It has been predicted that the number of diagnosed cases of GIST, PNET and RCC are increasing annually, which indicates that a large number of the population are potentially being treated with Sunitinib currently, though the exact number of patients is not available (Torre et al. 2015).

Sunitinib (Sutent, Pfizer) is available in 12.5 mg, 25 mg, 37.5 mg and 50 mg size capsules. Dosing information is provided by the patient's doctor upon receipt of their prescription. Dosing varies from person to person and this is mostly determined by the type of cancer being treated, either RCC, GIST or pancreatic neuroendocrine tumour PNET. However, all doses are administered by mouth, once daily (Pfizer, 2017).

For the treatment of RCC and GIST, 50 mg of Sunitinib is recommended and the dosing cycle consists of 28 days on-treatment and 14 days off-treatment. The number of cycle repeats is

determined by the patient's doctor. Whereas, PNET required 37.5 mg of Sunitinib daily, without an off-treatment period and the length of treatment is determined by the patient's doctor. Dose interruptions or adjustments of 12.5 mg may be recommended based on individual safety and tolerability (Pfizer, 2017).

Sunitinib inhibits cellular signalling associated with tumour formation by targeting multiple RTKs involved in tumour angiogenesis and proliferation (Motzer et al. 2006). In particular, Sunitinib is an inhibitor of VEGFR and PDGFR, c-KIT, colony stimulating factor-1 receptor (CSF-1R), Fms-like tyrosine kinase-3 receptor (FLT-3) and glial cell line-derived neurotrophic factor receptor. These TKs have a significant role in the development of clear-cell carcinoma.

Sunitinib inhibits TKs by competitively binding to the ATP-binding site domain of a number of receptor tyrosine kinases, notably: VEGFR-1, -2 and -3, PDGFR-α and –β, (O'Farrell et al. 2003, Roskoski Jr. 2007). Sunitinib's blockage of the ATP-binding domain leads to the inhibition of dysregulated or over-expressed TKs involved in the regulation of cell proliferation and cell survival. In addition, Sunitinib has anti-angiogenic properties. Sunitinib reduces blood supply to a tumour by targeting TKs such as VEGFR and PDGFR. This results in deprivation of nutrient to the tumour and prevents metastasis (Rini 2007).

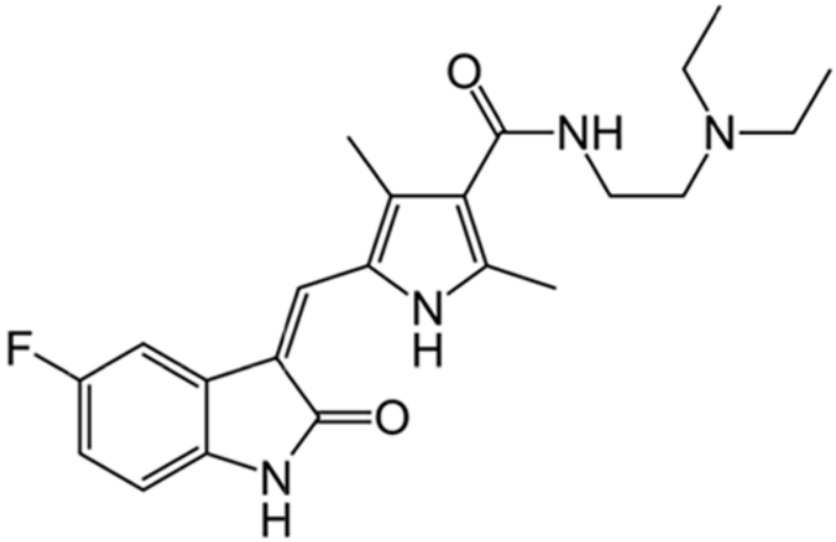

Figure 1.4: Chemical structure of Sunitinib (Remko, Bohác and Kováciková 2011).

1.4 Drug-induced cardiotoxicity and Sunitinib

As most cells in the human body proliferate and differentiate, it is difficult to produce chemotherapy drugs which are entirely selective for cancer cells. There is a limited knowledge base surrounding tissue specific cellular signalling pathways. This makes it almost impossible to predict the effect chemotherapy agents will have on the various tissues of the body. In particular, anti-angiogenic therapies have commonly caused: fatigue, hyperthyroidism, dyspnoea, gastrointestinal issues, cutaneous, anaemia, and cardiotoxic effects (Bhojani et al. 2008).

It is well established that chemotherapy agents have the potential to cause adverse effects in cardiomyocytes (Raschi et al. 2010). The cell biology of cardiomyocytes displays a substantial degree of similarity to that of cancer cells. Both have active stress signalling and

high-energy consumption (Cheng and Force 2010). Therefore, cardiomyocytes are highly susceptible to the cytotoxic effects of chemotherapy.

Many chemotherapy agents have been found to have cytotoxic effects on cardiomyocytes which can result in cardiac infarction, leading to a reduction in left ventricular ejection fraction (LVEF) in the heart (Monsuez et al. 2010). In addition to this, chemotherapy can induce cardiac repolarisation abnormalities such as QT prolongation, arrhythmia which is linked with myocardial dysfunction has also been found (Strevel, Ing and Siu 2007).

Unfortunately, many prescription drugs have been withdrawn from the market, as a consequence of these unpredicted cardiotoxic side-effects in patients (Botelho et al. 2016, Onakpoya, Heneghan and Aronson 2016). This therefore, illustrates a deficiency in cardiac safety analysis in preclinical trials (Morganroth 2007).

1.4.1 Sunitinib induced cardiotoxicity

Due to Sunitinib's broad intracellular molecular targets and many unpredicted off-target interactions, there is a plethora of side effects associated with its use (Aparicio-Gallego et al. 2011). Adverse cardiovascular effects have frequently been observed during and post-Sunitinib treatment in the clinic (Li et al. 2016). Cardiotoxicity produces alterations to haemodynamic flow, electrocardiographic (ECG) readings and LVEF (Monsuez et al. 2010).

1.4.2 Mechanisms of Sunitinib-induced cardiotoxicity

The exact mechanism by which cardiotoxicity is induced is still under consideration. It has been suggested that mitochondrial interactions with drugs such as anthracyclines causes the accumulation of reactive oxygen species (ROS) (Gouspillou et al. 2015). Lipids, proteins,

oxidative phosphorylation enzymes and mitochondrial DNA (mtDNA) are particularly susceptible to damage caused by ROS (Horenstein, Vander Heide and L'Ecuyer 2000, Sawyer et al. 2010).

Experimental investigation of the effect of Sunitinib on cardiomyocytes demonstrated a dose dependant reduction in cardiomyocyte survival (Chiusa et al. 2012). Sunitinib-induced cytotoxicity has been associated with an increased level of ROS generation (Zhuang et al. 2011). ROS damage can cause ATP synthesis disruption, which reduces the expression of sarcoplasmic reticulum calcium ATPase mRNA. This results in a decrease in heart contractility due to an increase in calcium levels within the cell, which results in Sunitinib-induced arrhythmia (Hare 2001).

Mutations of mtDNA can be caused by high levels of ROS (Ishikawa et al. 2008). This in turn can cause faulty oxidative phosphorylation machinery to be produced, as well as a decline in cardiac glutathione peroxidase activity, which can lead to further ROS being produced, inducing the formation of the mitochondrial permeability transition pore (mtPTP) (Brookes et al. 2004, Doenst, Nguyen and Abel 2013). High levels of ROS generated cellular damage induces cellular dysfunction and programmed cell death.

Programmed cell death is crucial for organ homeostasis as it controls cell numbers and eliminates damaged or abnormal cells. Apoptosis is the most typical form of programmed cell death. In very simplified terms, during apoptosis: cells shrink, undergo nuclear fragmentation, chromatin condensation, chromosomal DNA fragmentation and RNA degradation (Hengartner 2000), all of which results in cell death. Apoptosis is activated by two main pathways: the extrinsic and the intrinsic. The extrinsic pathway involving the binding of specific ligands to death receptors (DR) such as DR3, DR4, DR5, Fas and tumour

necrosis factor α receptor (TNFαR) (Varfolomeev et al. 1998, Gonzalvez and Ashkenazi 2010). This elicits a signal via specialised adaptor proteins, resulting in Caspase (cysteine protease) mediated cell death (Janicke et al. 1998).

In addition, the intrinsic pathway is activated in response to DNA or cellular damage (Fulda and Debatin 2006). This process involves the translocation of tBID, a pro-apoptotic protein, to mitochondria, which causes the release of cytochrome c (Wei et al. 2000). This again results in a Caspase cascade, causing either death receptor ligation or the release of mitochondria apoptotic mediators (Inoue et al. 2009). However, other forms of cell death are also increased in cardiac muscle cells in response to Sunitinib treatment, such as autophagy and programmed necrosis (Zhao et al. 2010).

In contrast, autophagy is a catabolic process in which misfolded proteins and cellular organelles are degraded. Autophagy occurs during conditions such as nutrient deficiency and hypoxia, which can be produced during Sunitinib treatment (Osawa and Shibuya 2013). Autophagy involves the cleavage of microtubule-associated protein 1 light chain 3 (LC3) by autophagin-4 (Atg-4) to generate LC3-I. Through the action of Atg-3 and Atg-7, LC3-I is further processed to LC3-II (Kroemer and Levine 2008). This results in the generation of phagophores. Phagophores are double membrane vesicles which grow and close around isolated cellular components. These components are then delivered to the lysosome, which enzymatically degrades the selected component (Tooze and Yoshimori 2010). Autophagic programmed cell death involves prolonged auto-digestion, during which there is a high turnover rate of proteins and organelles and the cell is pushed beyond its survival threshold (Tsujimoto and Shimizu 2005).

Necrosis is a process of caspase-independent cell death. Necrosis occurs in response to physical or chemical trauma on the cell, causing ATP depletion, dysfunctional Ca^{2+} regulation, mitochondrial abnormalities, increased ROS generation and stress signalling activation (Vanlangenakker, Berghe and Vandenabeele 2012). During this process, cellular organelles swell and the plasma membrane ruptures.

High levels of drug-induced cardiomyocyte cell death have a particularly destructive effect on the heart. As a consequence of cell death, areas of the heart lose the ability to function efficiently. This causes the heart to initiate cardiac remodelling, in an attempt to adapt to the increased level of stress and work load. The structure and function of cardiomyocytes is changed by cardiac remodelling and can produce decreased levels of cardiac output and lead to heart failure (Munzel et al. 2015). It is therefore important to investigate the level of drug-induced cytotoxicity a compound causes and to predict whether a compound has the potential to produce adverse cardiovascular events.

1.4.3 Investigation in to Sunitinib-induced cardiotoxicity

Adverse cardiovascular events are believed to be a result of lack of Sunitinib's specificity and selectivity. Karaman et al., (2008) demonstrated that Sunitinib bound to 57 out of 317 kinases tested. Sunitinib also causes depletion in ATP levels, due to the off-target inhibition of AMP-activated protein kinase (AMPK) or the inhibition of the ribosomal s6 kinase (RSK) complex (Force, Krause and Van Etten 2007, Kerkela et al. 2009). Cardiomyocytes have very limited ATP stores as the heart requires a lot of energy for constant contraction. In normal conditions the depletion of ATP leads to an increase in AMP and increased levels of activated AMPK, which activates catabolic pathways to limit the cellular consumption of ATP

(Kudo et al. 1995, Kudo et al. 1996). However, during Sunitinib treatment, the inhibition of AMPK prevents this energy-conserving process, which exacerbates the ATP decline further. This decline in ATP levels has been shown to cause mitochondrial dysfunction and initiate cell death processes.

In addition to this, Sunitinib has been shown to inhibit RSK. In normal conditions RSK regulates cellular survival by inhibiting the activation of the pro-apoptotic factor BCL-2 antagonist of cell death (BAD). However, during Sunitinib treatment, BAD is not inhibited. This enables activated Bad to initiate the caspase cascade and produce higher levels of apoptosis in the heart (Hasinoff, Patel and O'Hara 2008). Through the inhibition of AMPK and RSK, Sunitinib reduces the level of efficiently functioning cardiomyocytes in the heart, which causes a decline in heart contractility and therefore cardiac function (Kerkela et al. 2009) (Figure 1.5). The severe reduction in ATP and increased levels of apoptosis in cardiomyocytes associated with Sunitinib treatment could be responsible for the adverse cardiovascular events found in the clinic such as QT interval prolongation and declines in LVEF (Hartmann et al. 2009).

Figure 1.5: Schematic describing potential intracellular mechanisms of Sunitinib-induced cardiomyocyte apoptosis.

Inhibition of AMPK prevents the regulation of eukaryotic elongation factor-2 (EEF2), mammalian target of rapamycin (mTOR) and acetyl-Coenzyme A carboxylase which are responsible for energy consuming processes such as protein translation and lipid biosynthesis. This causes a severe ATP depletion. Sunitinib also inhibits RSK, which causes the release of BAD from RSK regulation. BAD can then activate BCL2 associate X protein (BAX) and cytochrome c release, which can initiate the intrinsic apoptotic pathway. Cardiomyocyte cell death and declines in ATP levels have been associated with compensatory cardiac hypertrophy and left ventricular (LV) dysfunction in the heart (Force, Krause and Van Etten 2007).

The following studies highlight the concerning level of cardiotoxicity associated with Sunitinib in the clinic. In a study by Chu et al. (2007), 97 patients with Imatinib-resistant GIST were given repeated cycles of Sunitinib over a 2 year period. During this time, 75 of the patients were enrolled into a cardiovascular study. 20% of patients undertaking Sunitinib treatment had a more than 50% decrease in LVEF, 8% of patients developed congestive heart failure and 1% developed myocardial infarction (Chu et al. 2007). This highlights the concerning level of cardiotoxicity which Sunitinib can generate over a long period of treatment.

In another study by Narayan et al. (2017), the level of Sunitinib-induced cardiotoxicity detected in patients receiving routine clinical treatment for metastatic renal cell carcinoma was assessed by echocardiography and biomarker phenotyping. Patients were assessed 3.5, 15 and 33 weeks after initiation of Sunitinib treatment. At each assessment, the cardiotoxic associated symptoms such as LVEF decline and cardiac damage were measured. An LVEF reduction of more than 10 % was considered to indicate LV dysfunction. The biomarkers Troponin I and B-type natriuretic peptide were assessed as predictors of LV dysfunction. All patients receiving Sunitinib treatment demonstrated declines in LVEF. In addition, 9.7 % of patients experienced substantial declines in LV function. Most cardiovascular events occurred within the first cycle of Sunitinib treatment. However, the majority of patients recovered to baseline after cardiovascular management (with anti-hypertensive drugs) and a Sunitinib dose reduction (Narayan et al. 2017). However, as this study was carried out over a short time, it is possible that latent adverse cardiovascular symptoms of Sunitinib treatment may have occurred after the “follow-up” visits ceased. In addition, patients with pre-existing cardiovascular conditions were excluded from this study. Therefore, this study

does not accurately account for the population who receive Sunitinib in the clinic, as patients may have pre-existing cardiovascular conditions when they initiate treatment.

Chu et al. (2007) identified more severe cardiovascular complications in the participants of their study. This is likely to be due to the study taking place over a 2 year time period, which meant that latent cardiovascular events caused by Sunitinib treatment were identified. Chu et al. also used a patient population that had received Imatinib treatment for GIST in the past. This may have increased the patients' susceptibility to Sunitinib-induced cardiotoxicity.

However, both studies used a middle-aged population with a mean age of 56 (Chu et al. 2007) and 63 (Narayan et al. 2017), whereas in the clinic, patients of all ages receive Sunitinib treatment. It would be interesting to see if the level of Sunitinib-induced cardiotoxicity varies with age.

1.4.4 Impact of age during drug-induced cardiotoxicity

Life expectancy at birth has increased substantially due to a combination of medical advances and improved quality of life. However, as a person ages, there is usually a decline in physical, social and cognitive function. In particular, ageing of the heart is a major risk factor for developing heart failure (Poulose and Raju 2014). Ageing in the heart is associated with left ventricular hypertrophy, diastolic dysfunction, heart valve degeneration, increased cardiac fibrosis, and decreased maximal exercise capacity (Dai, Rabinovitch and Ungvari 2012, Morita et al. 2009, Shioi and Inuzuka 2012). In addition, in later life many patients suffer with comorbidities, such as cancer, heart disease and diabetes. Therefore, in the clinic it is important for patient age to be considered before a potential cardiotoxic agent is administered.

Currently, there is very little information investigating the effect of Sunitinib treatment on an ageing population. Existing studies demonstrate similar levels of cardiotoxicity between patients <70 and >70 years old. However, elderly patients are more likely to display signs of fatigue, hypertension and stroke than younger patients (Hutson et al. 2014, Jang et al. 2016). The exact cause of this difference has not been fully investigated.

Historically, the use of rodents is essential in the drug discovery and development process (Vandamme 2014). Their use allows characterisation of disease pathophysiology, evaluation of mechanism of action of existing drugs, discover new drug targets and biomarkers and to estimate clinical dosing regimens and determine safety margins and toxicity. However, generally, a healthy "young" male animal of around 9-12 weeks, is dosed with an agent and the toxic effects are monitored. This does not accurately represent the total patient population, such as the elderly patients.

Also, as cardiotoxicity is one of the leading causes of drug attrition, it is now critical that early detection of drug-induced cardiotoxicity is established. At the clinical level it would be extremely beneficial to establish molecular markers which could be used to predict cardiac injury. Currently, preclinical cardiac safety assessments involve detection of cardiac injury biomarkers, such as troponin (Mair et al. 1995), as well as measurement of changes in cardiac morphology in organ and animal models. The identification of the specific cellular signalling processes involved in Sunitinib-induced cardiotoxicity could enable the development of effective cardioprotective therapy, without limiting Sunitinib's anti-cancer properties.

1.4.5 The relevance of the isolated Langendorff heart model in determining cardiotoxic side effects

Since its availability on the market in 2006, Sunitinib has been reported to produce adverse cardiovascular events. It has been reported that 20% of Sunitinib patients have experienced significant declines in left ventricular ejection fraction (LVEF), while 47% hypertension and 8% developed congestive heart failure (Chu et al., 2007; Motzer et al., 2007). Also, many patients did not experience cardiovascular side effects until two or more years after treatment (Chu et al., 2007), which highlights that the current preclinical studies include insufficient testing for the prediction of cardiac safety.

Henderson et al. 2013, demonstrated that the Langendorff isolated heart assay was a sensitive and predictive model for assessing changes in heart function induced by the tyrosine kinase inhibitors: Sunitinib, Sorafenib and Erlotinib. As a positive control for cardiac damage, Henderson et al. used carbonyl cyanide 4-(trifluoromethoxy)phenylhydrazone (FCCP) and isoproterenol along with modified Henseleit Krebs (MHK), while verapamil was used as a negative controls for cardiac damage to establish the cardiac injury caused by Sunitinib, Sorafenib and Erlotinib (Henderson et al., 2013).

In this thesis, the main method for analysing cardiac function in the response to Sunitinib perfusion (in the absence or presence of adjunct therapy) is the langendorff heart perfusion model (Bell, Mocanu and Yellon 2011). This technique involves the perfusion of the heart in a retrograde manner through the aorta. A cannula is inserted into the aorta and the retrograde perfusion forces the aortic valve to close. This forces direct perfusion of the coronary arteries (Langendorff 1895).

The heart can beat unaided, therefore, left ventricular function can be assessed. A balloon connected to a pressure transducer is inserted into the left ventricle and is used to monitor heart rate and left ventricular developed pressure. Coronary flow is measured by collecting the ejected perfusate (Bell, Mocanu and Yellon 2011).

One of the key benefits of using the Langendorff heart assay is that important aspects of *in vivo* conditions can be replicated, allowing insight into whole-organ function. This enables the monitoring of changes to heart function in response to drug under simulated physiological conditions (Hwang et al., 2010).

The use of the isolated Langendorff heart technique also allows the perfusion volume and content to be controlled. It has been reported that the clinical steady state blood concentrations of Sunitinib are between 0.01 and 1 µM in cancer patients treated with Sunitinib (Doherty et al., 2012, Goodman et al., 2007), therefore the chosen concentration of 1 µM of Sunitinib for this thesis was clinically relevant. A precise concentration of drug can be administered to the heart via the Langendorff technique, whereas in comparison, it would be difficult to establish clinically relevant concentrations of Sunitinib at the heart in an *in vivo* model due to variations in species size, metabolic activity, drug absorption and clearance (Toutain et al., 2010).

In addition to this, the Langendorff model enables the study of Sunitinib-induced changes to cardiac function in the absence of neurogenic and hormonal influences (Anderson et al., 2006). This is ideal for the study of compounds targeted for the use in humans in other species as there is an absence of external factors acting upon the heart, which may differ between species (Toutain et al., 2010). However, in relation to the clinic, it is important to

consider these variables as they may interfere with the pharmacokinetics and pharmacodynamics of a drug.

Therefore, the isolated Langendorff heart model is essentially an ideal method for determining the cardiac safety of a compound at clinically relevant concentrations prior to clinical trials. It can measure drug effect on left ventricular developed pressure, heart rate and coronary flow. The ability to predict potential cardiotoxic effects in the early stages of preclinical testing would be of a great benefit to future drug development as extremely cardiotoxic compounds could be eliminated from selection earlier. Also, from a clinical point of view, the Langendorff technique could be used to identify potential risks of the drug's which make it to market, enabling clinicians to monitor and manage possible side effects. However, as previously mentioned the effect of drug metabolism, drug interactions, pre-existing conditions, as well as neurogenic and hormonal influences cannot be measured by the Langendorff technique. In addition, the Langendorff model uses acute drug administration over a period of 125 minutes, therefore it does not represent the dosing used in the clinic, where cycles of Sunitinib treatment could be administered for months (Pfizer, 2017).

Therefore, *in vivo* and clinical studies would provide further insight into the potential cardiotoxic effects of a drug which have been highlighted by the Langendorff technique.

1.5 Intracellular signalling pathways associated with Sunitinib cardiotoxicity

As previously mentioned, traditionally, the methods used to identify patients at risk of cardiotoxicity involve the monitoring of cardiac function by measurement of LVEF. However,

LVEF assessment lacks sensitivity and changes are only detected once a significant amount of damage has occurred to the heart (Cardinale and Cipolla 2016).

Many proteins have been characterised as indicators of cardiac damage. Cardiac troponins (cTn) are deemed to be the "gold standard" biomarker of cardiac injury. cTn have a critical role in the contraction of the heart (Westfall and Metzger 2004). Elevation in cTn levels correlates with the extent of injury to the heart and they are highly selective and sensitive biomarkers (Korff, Katus and Giannitsis 2006). However, measurement of cTn does not identify the cause of cardiac injury. Therefore, assessment of proteins which are potentially associated with drug-induced cardiotoxicity should be carried out.

Sunitinib has been shown to alter the properties of the signal transduction pathways associated with RTKs in cancer cells. The main signalling pathways which have been identified are the PI3K, AKT, protein kinase C (PKC) and mitogen-activated protein kinase (MAPK)/ Ras signalling cascades (Figure 1.6). However, very little research has been carried out investigating the effect of Sunitinib on these pathways in the heart.

In general, the PI3K pathway has been studied more extensively. It has previously shown to be vital in cardiomyocyte cell survival (Jiang et al. 2016). Changes in the PKC family and MAPK signalling have been associated with cardiac hypertrophy, arrhythmia and cardiac injury (Rose, Force and Wang 2010).

We investigated the involvement of a MAPK cascade which included, apoptosis signalling kinase 1 (ASK1), mitogen-activated protein kinase kinase 7 (MKK7) and c-Jun NH2-terminal kinase (JNK) in Sunitinib-induced cardiotoxicity. Plus, briefly measured changes in PKCα phosphorylation levels in Sunitinib induced cardiotoxicity.

Figure 1.6: Schematic of the possible effects of Sunitinib on intracellular mechanisms in a cancer cell.

The inhibition of RTKs by Sunitinib reduces the level of PI3K/AKT/mTOR, MAPK and PKC signalling, which produces the anti-tumour effects of Sunitinib.

Inhibition of the same pathways in the heart have been liked to cardiac dysfunction (Aparicio-Gallego et al. 2011).

1.5.1 The stress activated mitogen-activated kinase kinase 7 (MKK7) pathway

Mitogen-activated kinase kinase 7 (MKK7) is a member of the MAP kinase kinase (MAPKK) super family. MAPKKs facilitate a variety of cellular functions in response to exogenous and endogenous stimuli (Foltz et al. 1998). The human mkk7 gene is located on chromosome 19 (mkk7 gene location in rodents: chromosome 8 in mouse and chromosome 12 in rat) (Tournier et al. 1999). The MKK7 transcript is alternately spliced to generate a group of MKK7 proteins with different N-termini (α, β and γ) and different C-termini (1 and 2) (Tournier et al. 1999). All of the splice variants contain the S-K-A-K-T motif in the kinase domain. This motif contains the serine and threonine residues by which MKK7 is phosphorylated by several MAP Kinase Kinase Kinases (MKKKs) (Takekawa, Tatebayashi and Saito 2005). To facilitate phosphorylation of the serine and threonine the MKKKs must dock to the DVD site of MKK7, which is found in its C-terminus region (Takekawa, Tatebayashi and Saito 2005).

MKK7 is responsible for the regulation of JNK, a protein which will be discussed later in the chapter. Activation of MKK7 signal transduction results in vital cellular processes including: proliferation, differentiation, apoptosis and tumorigenesis (Schramek et al. 2011).

Interestingly, MKK7 has been shown to have an important role in embryonic development. Deletion of the MKK7 gene in mice results in embryonic lethality (Wang, Destrument and Tournier 2007). Therefore, much of the research investigating the functionality of MKK7 has been carried out in mouse embryonic fibroblasts. The deletion of the mkk7 gene was shown to produce reduced levels of proliferation and cause premature cell senescence through the

initiation of G2/M cell cycle arrest in response to UV- and γ-irradiation (Wada et al. 2004). Therefore, it is possible that MKK7 could be involved in stress signalling in the heart.

1.5.1.1 MKK7 signalling in the heart

A number of studies have investigated the involvement of MKK7 in the development of cardiac complications. Wang et al., (1998) investigated the role of MKK7 in cardiac hypertrophy. Transgenic neonatal cardiomyocytes were produced which expressed a constitutively active mutant of MKK7 (Wang et al. 1998). Using this mutant, Wang et al., demonstrated a direct increase in JNK activation by MKK7, which produced characteristic indicators of cardiac hypertrophy. This therefore demonstrates that increased levels of MKK7 may be responsible for the progression of cardiac hypertrophy.

This was further investigated by Wang et al., (2008) who demonstrated the inhibition of MKK7 by growth arrest and DNA-damage-inducible beta (GADD45B) counteracted the cardiomyocyte hypertrophy and elevated atrial naturetic factor (ANF) caused by MKK7 overexpression (Wang et al. 2008). However, as these studies were only conducted in cardiomyocytes, it is difficult to determine whether MKK7 would produce a hypertrophic effect *in vivo*.

Mitchell et al., (2006) used a transgenic mouse model with cardiac specific activated mutants of MKK7 to assess changes in gene expression, using cDNA microarrays (Mitchell et al. 2006). Over 200 genes were significantly changed compared to control animals. The altered genes were synonymous with restrictive cardiomyopathy phenotypes. This suggests that increased levels of MKK7 increases susceptibility of an individual to develop cardiomyopathy.

Contrastingly, Liu et al. (2011) used cardiac specific MKK7 knock-out, mouse models to demonstrate the involvement of MKK7 in heart failure. A pressure overload was exerted on the heart, through transverse aortic constriction (TAC). After a week, the MKK7 knock-out mice began to exhibit deterioration of ventricular function and signs of heart failure, compared to both sham wild type and TAC wild type mice. Liu et al. (2011) also carried out cell death assays which measured proteins associated with apoptosis and cardiomyocyte dysfunction such as ANP, BNP, Troponin I, TGF-β, MnSOD, p53, BAX and BAD (Liu et al. 2011). They found a significant increase in cardiomyocyte apoptosis, alongside elevated levels of MnSOD and p53. It was determined that MKK7 has a vital role in protecting the heart from hypertrophic remodelling and cardiomyocytes apoptosis during stress. Also, the requirement of MKK7 to prevent the transition into heart failure (Liu et al. 2011).

The above studies therefore highlight the vital role of MKK7 in the maintenance of heart homeostasis. An up regulation of MKK7 demonstrated an increase in cardiac hypertrophic and heart failure phenotypes (Wang et al. 1998). However, if MKK7 is removed entirely from cardiomyocytes, there is profound cardiomyocyte cell death and susceptibility to heart failure is increased (Liu et al. 2011).

1.5.1.2 MKK7 signalling in cancer

MKK7 has also be shown to be an appropriate target for anti-cancer therapy. Inactivation of MKK7 signalling in murine lung and mammary cancer demonstrated that MKK7 had an important role in delaying the progression of malignancies (Schramek et al. 2011). This highlights the potential tumour suppressor role of MKK7.

In addition, Tang et al. (2012) found an up-regulation of MKK7 in hepatoma cells with Alpinetin treatment. Alpinetin is a novel plant flavonoid, which possess strong anti-tumour properties. Through this up-regulation, cell cycle arrest occurred in the G0/G1 phase of the cell cycle (Tang et al. 2012). This suggests that by agonistic modulation of MKK7 it may be possible to both enhance anticancer properties of chemotherapy agents, as well as, limit apoptosis as the cell cycle is arrested.

This thesis aims to investigate the involvement of MKK7 in Sunitinib induced cardiotoxicity. MKK7 contains an ATP binding domain with sequence homology to that of the target proteins of Sunitinib. It is therefore possible that Sunitinib has an inhibitory effect on the JNK signalling cascade (Aparicio-Gallego et al. 2011). With reduced MKK7 activity demonstrating both an incline towards cardiomyocyte damage and a reversal of anti-tumour effects of chemotherapy, it would be interesting to assess both the changes in expression levels and levels of phosphorylated MKK7 in the presence of Sunitinib.

In the future, it may possible to identify a link between MKK7 expression and TKI induced cardiotoxicity. It is also possible that MKK7 inhibition has a vital role in the progression of TKI induced cardiotoxicity. It is imperative to investigate this so that preventative treatment can be discovered.

1.5.2 Down-stream pathway mediator from MKK7: c-Jun NH_2-terminal Kinase (JNK)

As a consequence of exposure to stressful stimuli, mammalian cells elicit a cellular response in the form of c-Jun NH_2-terminal Kinase (JNK) activation (Raman, Chen and Cobb 2007). Stimuli include cytokines, interleukin-1, transforming growth factor-β, platelet-derived

growth factor, epidermal growth factor, reactive oxygen species, and environmental stress such as hypoxia, ischaemia and radiation (Rosette and Karin 1996).

JNK is a member of the MAPK family (Minden and Karin 1997). In mammalian genomes: jnk1, jnk2 and jnk3 encode a family of 3 JNK isoforms: JNK1, JNK2 and JNK3. The jnk1 gene is located on chromosome 10 in humans (chromosome 14 of mice and chromosome 16 of rats), jnk2 is located on human chromosome 5 (chromosome 11 of mice and chromosome 10 of rats) and jnk3 is located on chromosome 4 of humans (chromosome 5 of mice and chromosome 14 of rats) (Davis 2000). There are a total of 10 splice variants, meaning that each jnk gene codes 2-4 alternatively spliced transcripts, each of 46 to 55 kDa in size (Casanova et al. 1996). The difference in transcript occurs in the subdomain IX and the C-terminal, making it difficult to identify the exact functional properties of each splice variant. JNK1 and JNK 2 are ubiquitously expressed, whereas JNK3 is mostly expressed in the brain, heart and testis (Wagner and Nebreda 2009).

The JNK signalling cascade comprises of a 3 tier phosphorelay system: MAP kinase kinase kinases (MKKK's) phosphorylate MAPKKs and MAPKKs phosphorylate the MAPKs, in this case, JNK (Davis 2000).

There are at least 20 MKKKs, 14 of which are known to contribute to JNK activation (Dhanasekaran et al. 2007). In addition to this, scaffold proteins such as JNK interacting protein (JIP), play an important role in the mediation of signalling complexes (Whitmarsh et al. 2001). Scaffold proteins facilitate the assembly of protein complexes (Good, Zalatan and Lim 2011, Su, Xu and Zhang 2015). Like many JNK-interacting proteins, JIP1 contains the conserved JNK-binding domain (Ho et al. 2006). Complex formation increases the proximity of relevant signalling proteins, allowing efficient cell signalling. In the JNK MAP kinase

pathway, JIP1 holds all three member kinases together, allowing efficient catalysis, reducing cross talk and ensuring specific signalling (Moon and Park 2014, Whitmarsh 2006).

The MKKKs directly phosphorylate MKK4 and MKK7. JNKs are phosphorylated on Thr and Tyr residues within a Thr-Pro-Tyr motif of the protein kinase subdomain VIII, specifically by MKK7 (Kishimoto et al. 2003). Activation of this MAP-kinase signalling cascade generally results in phosphorylation of JNK nuclear substrates, leading to regulation of gene expression. Activating protein 1 (AP-1) is a collective name for transcription factors which modulate a variety of DNA binding sites, such as Jun, Fos or ATF (Karin, Liu and Zandi 1997). In JNK signalling, AP-1 typically binds to the c-Jun DNA binding site. In addition to this, JNK proteins associate with proteins of the plasma membrane, implying a more complex functionality of JNK than just gene regulation (Gupta et al. 1996). At a cellular level, activation of JNK results in either apoptosis or promotion of cell survival. The choice of fate seems to depend on the cell type and on the stimulating signal (Chang and Karin 2001).

In cardiomyocytes, JNK signalling is vital for the maintenance and organisation of the cytoskeleton and sarcomere structure (Windak et al. 2013). The c-Jun AP-1 molecule has been found to specifically stimulate α-adrenergic growth response in cardiomyocytes (Taimor et al. 2004). Furthermore, by abrogating endogenous AP-1 activation, it is possible to inhibit cardiomyocyte hypertrophy (Omura et al. 2002). Using Cre-loxP mediated transgenisis another group have shown that a constitutively active JNK mutant in mice leads to cardiac hypertrophy and pathology in adult hearts (Petrich, Molkentin and Wang 2003). This highlights the crucial role of AP-1 in the progression of cardiac remodelling as a result of stressful conditions.

Many JNK knock out models have been used to determine the role of JNK in the development of cardiac dysfunction (Kaiser et al. 2005, Tachibana et al. 2006). Tachibana et al. (2006) demonstrated with the selective deletion of all three JNKs (jnk1$^{-/-}$, jnk2$^{-/-}$ and jnk3$^{-/-}$) cardiac hypertrophy ensued when a pressure over load is applied in mice (Tachibana et al. 2006). However, JNK1$^{-/-}$ mice in particular displayed significant reductions in fractional shortening and eventually developed cardiac dysfunction after 12 weeks. Kaiser et al. (2005) demonstrated the importance of JNK in ischaemia-reperfusion injury. They showed that a reduction in JNK activity in the heart resulted in a reduced level of cardiac injury and cellular apoptosis (Kaiser et al. 2005). However, by using mouse models which over express MKK7 in the heart; the same group demonstrated an increase in c-Jun Kinase activity but also cause significant protection against ischaemia-reperfusion injury (Kaiser et al. 2005). This all in all highlights the complexity of JNK signalling.

1.5.3 Upstream mediator from MKK7: apoptosis signal-regulating kinase 1 (ASK1)

Apoptosis signal-regulating kinase 1 (ASK1) is a member of the MAPKKK family. Generally, MAPKKK's have an essential role in cellular stress by directly phosphorylating MAPKKs, such as MKK7. ASK1 is an upstream activator of MKK7 and a regulator of the JNK pathway (Ichijo et al. 1997).

ASK1 has been shown to be activated by a variety of stimuli, such as oxidative stress, endoplasmic reticulum stress, calcium overload, and lipopolysaccharide and stress signalling ligands such as TNFα (Ichijo et al. 1997, Saitoh et al. 1998, Chen et al. 1999a).

Many studies investigated the structure and function of ASK1 (Bunkoczi et al. 2007). In its resting state, ASK1 forms a homo-oligomer, which is stabilised by the C-terminal coiled-coil domain of the protein (Saitoh et al. 1998). In addition, the N-terminal of ASK1 is bound to the reduced redox-regulated protein thioredoxin (Saitoh et al. 1998). During cellular oxidative stress thioredoxin becomes oxidised. This oxidation causes the formation of a disulphide bridge between Cysteine 32 and 35 residues. This causes a conformational change in the structure of thioredoxin, exposing the hydrophobic region of ASK1. This mechanism results in the disassociation of thioredoxin from the N-terminal of ASK1 and allows auto-phosphorylation to occur at the threonine 838 site of the activation loop (Bunkoczi et al. 2007). Therefore, oxidation of thioredoxin causes the dissociation of the heterodimer and activates ASK1 so that it can initiate its MAPK cascade.

ASK1 has been shown to initiate pro-apoptotic effects in cells. In 1999, Zhang et al. demonstrated that anti-cancer drugs such as cisplatin have direct agonistic effects on ASK1 and the pro-apoptotic pathway (Zhang, Chen and Fu 1999).

To further investigate the role of ASK1 on apoptosis, Tobiume et al. (2001) used ASK1 knockouts ($ASK1^{-/-}$) in mice to show that ASK1 is a vital mediator of apoptosis in response to oxidative cellular stress (Tobiume et al. 2001). Sustained activation of JNK and p38 pathways was lost when cells were treated with TNF and H_2O_2. Embryonic fibroblasts demonstrated resistance to apoptosis during oxidative cellular stress. This demonstrated that removal of ASK1 protected cells from apoptosis.

Liu et al. (2009) created transgenic mice with cardiac-specific inducible over expression of ASK1 (Liu et al. 2009). Interestingly, this mutation did not induce cardiac hypertrophy. However, an increased level of myocyte cell death was detected. This resulted in a

significantly increased susceptibility to cardiomyopathy and in some cases myocardial infarction. This study shows the importance of ASK1 in cell death of cardiomyocytes. A drug which is an agonist of the ASK1/MKK7/JNK pathway is highly likely to cause cardiotoxicity.

He et al. (2003) demonstrated that ASK1 has an essential role in the regulation of cardiac contractile function. Cardiac troponin T (cTnT) is a substrate of ASK1. The induction of mutations at the ASK1 phosphorylation sites (T194/S198) of cTnT reduced activation of cTnT by ASK1 and caused contractile dysfunction in cardiomyocytes. Furthermore, overexpression of constitutively active ASK1 induced an increase in cTnT phosphorylation and inhibited shortening of cardiomyocytes (He et al. 2003). This highlights the importance of ASK1 in the regulation of cardiac contractile function.

Moreover, by investigating the effect of ischemia-reperfusion on $ASK1^{-/-}$ compared to wild type mice, Watanabe et al. (2005) showed that ASK1 is involved in necrosis as well as apoptosis. Wild type mice exhibited a significant increase in necrotic injury (Watanabe et al. 2005). However, $ASK1^{-/-}$ mice displayed a significant reduction in infarct size. Additionally, cellular studies revealed that $ASK1^{-/-}$ cardiomyocytes were more resistant to H_2O_2 and Ca^{2+} induced apoptosis and necrosis (Watanabe et al. 2005). This suggests that inhibition of ASK1 could have a cardioprotective effect.

1.5.4 PKC in cardiac function

The PKC family are Ca^{2+}, diacylglycerol (DAG), and/or phospholipid-activated serine/threonine kinases (Newton 2001). Structurally, PKC proteins are defined by a highly-conserved C-terminal, catalytic domain, which contains the motifs required for ATP or substrate binding. A flexible hinge region separates the C-terminal region from the N-

terminal regulatory domain. Differences found in the N-terminal categorise the PKC proteins into the distinct PKC subfamilies, which are classed as conventional (α, βI, βII and γ), novel (δ, ε, θ and η) and atypical (ζ and I/λ) (Steinberg 2008).

In general, PKC proteins are involved in the regulation of cell survival, growth, proliferation, migration and apoptosis (Poole et al. 2004). Interestingly, the PKC isoforms behave differently depending on cell type and location within the cell. For example, there is evidence demonstrating translocation of PKC isozymes to the nucleus allows PKC to modulate the cell cycle. Specifically, PKCα and PKCε regulate cyclins D1 and D3 (Detjen et al. 2000, Fima et al. 2001). Therefore, PKC can affect the G_1/S-phase of the cell cycle, which is the stage at which a cell becomes predisposed to either become quiescent or differentiate and initiate proliferation (Arand and Sage 2017).

All of the PKC isozymes are expressed in human and rat heart tissue. In particular, PKCα, βI, βII and γ are expressed in the ventricles (Simonis et al. 2007). However, the most prevalent isoform in the human heart is PKCα.

Due to its impact of cell survival and high prevalence in the heart, PKCα is considered to be essential in a number of cardiac functional processes (Hahn et al. 2003). Braz et al. 2004, demonstrated with the deletion of the PKCα gene (Prkca) that PKCα is a negative regulator of heart contractility in mice (Braz et al. 2004). The same study also demonstrated that the deletion of Prkca prevented the onset of heart failure associated with long-term pressure overload in a genetic model of dilated cardiomyopathy. A similar study by Hambleton et al. (2007) confirmed these findings by using a cardiomyocyte specific double negative Prkca knock-out transgenic mouse model and PKCα inhibitory compounds (Hambleton et al. 2007). This demonstrated that the inhibition of PKCα in cardiomyocytes provides protection

against heart failure and dilated cardiomyopathy, by enhancing contractility of the heart. In addition to this, significantly increased levels of PKCα were found in the left and right ventricular homogenates of rat hearts after surgically induced myocardial infarction and had developed heart failure (Wang et al. 2003). This further implicates PKCα in cardiac dysfunction.

As PKCα has been shown to have a vital role in the heart, it would be interesting to identify whether PKCα's signalling is effected by Sunitinib treatment. Further understanding of specific proteins involved in Sunitinib induced cardiotoxicity could enable the development of effective adjunctive treatments.

1.6 Cardioprotection by adjunctive therapy

The introduction of more targeted therapies, such as Sunitinib has resulted in considerable improvements in cancer survival rates. As cancer becomes more of a chronic illness, long and short-term cardiotoxic effects of chemotherapy are being reported at an increasing rate. An assessment of Sunitinib's long-term safety in 5739 patients revealed that moderate cardiovascular events occurred in 24% of patients and severe cardiovascular events occurred in <1% of patients (Porta et al. 2016). In addition, Surveillance of a Medicare database identified 171 out of 670 patients aged >65 years who received Sunitinib or Sorafenib had cardiovascular event (Jang et al. 2016). It was revealed that the majority of cardiovascular events occurred during the first year of treatment. However, as more research is concentrated on the cardiac safety of chemotherapy agents, it is beginning to become apparent that lasting long-term damage to the cardiovascular system ensues. In Denmark, a nationwide cohort study of patients diagnosed with soft tissue sarcoma

between 1997 and 2011 revealed that Doxorubicin treatment was a strong predictor of heart failure later in life (Shantakumar et al. 2016). It has been suggested that patients who have survived cancer after being treated with Sunitinib, may also develop heart failure later in life (Lenihan and Cardinale 2012).

It has been hypothesised that cardiovascular damage occurs as a result of negative effects on structural and functional properties of the endothelium and cardiomyocytes, during chemotherapy treatment (Svilaas et al. 2016). This has highlighted the requirement for further understanding of the mechanisms of Sunitinib-induced cardiotoxicity so that a mechanism of cardioprotection can be used.

The use of cardioprotective therapies in combination with Sunitinib has been previously investigated. However, the ability of these treatments to protect the heart has been limited due to Sunitinib targeting >30 different kinases. Notably, the inhibition of angiogenic growth factors and the compromise of energy homeostasis through inhibition of AMPK by Sunitinib are thought to be key in the development of cardiotoxicity (Izumiya et al. 2006, Kerkela et al. 2009). To counteract this, the use of angiotensin-converting enzyme (ACE) inhibitors, Beta-blockers and AMPK agonists have been proposed as cardioprotective agents (Dirix, Maes and Sweldens 2007, Hasinoff, Patel and O'Hara 2008).

ACE inhibitors have been shown to prevent the decline in LVEF associated with the use of high-dose chemotherapy agents (Cardinale et al. 2006). However, ACE inhibitor treatment did not produce long-term cardioprotective effects. Over the 6 years following a combination of ACE inhibitor and anthracycline treatment patients produced progressive declines in left ventricular end-systolic wall stress, though this was still not as severe patients who received anthracycline alone (Silber et al. 2004). Beyond 6 years, the benefits

of ACE inhibitors were diminished and further cardiac dysfunction was identified (Lipshultz et al. 2002). Yet, interestingly, the combination of ACE inhibitors and Beta-blockers has been shown to be highly effective against hypertension and reductions in LVEF in patients receiving Trastuzumab (Oliva et al. 2012). During Sunitinib treatment, ACE inhibitors are administered to manage hypotension (Joensuu et al. 2011). However, there is no clinical evidence suggesting that the use of ACE inhibitors or Beta-blockers will produce sufficient cardioprotective effects against Sunitinib-induced cardiotoxicity.

Furthermore, AMPK agonists have been predicted as potential cardioprotective agents. An AMPK-constitutively active mutant in cardiomyocytes treated with Sunitinib demonstrated partial resistance to Sunitinib-induced apoptosis (Kerkela et al. 2009). Interestingly, Metformin has been shown to improve left ventricular function by increasing AMPK activity (Gundewar et al. 2009, Zhou et al. 2001), (Shen, Ke and Wu 2017). Also, Metformin has produced cardioprotective effects against Doxorubicin-induced cardiotoxicity, by attenuating Doxorubicin-induced oxidative stress, energy starvation and structural changes in the myocardium (Ashour et al. 2012). However, Metformin lacks cardioprotective abilities against Sunitinib treatment in cardiomyocytes (Hasinoff, Patel and O'Hara 2008). It is therefore vital to further investigate potential cardioprotective agents to reduce the risk of cardiovascular events associated with Sunitinib therapy.

1.6.1 ASK-1 inhibitor: NQDI-1

Ethyl 2, 7-dioxo-2, 7-dihydro-3*H*-naphtho [1, 2, 3-*de*] quinoline-1-carboxylate (NQDI-1) is a selective inhibitor for ASK-1. It has a K_i of 500nM and IC_{50} of 3µM for ASK1 (Volynets et al.

2011). However, as this is a relatively new drug the mechanism of inhibition is not yet fully characterised.

Presently, there is no published data where NQDI-1 has been used in heart tissue. However, NQDI-1 has been shown to protect cells against apoptosis, attenuate hypoxic and ischaemic cerebral injury and ischaemic renal injury (Eter 2013, Hao et al. 2016, Nomura et al. 2013).

Inhibition of ASK1 with NQDI-1 has been shown to completely prevent caspase 3 and caspase 9 activation and cell death in neuronal cells, after treatment with H_20_2 (Nomura et al. 2013). This confirms the involvement of ASK1 in ROS induced cell death and highlights the protective properties of NQDI-1.

Furthermore, the administration of NQDI-1 to animal models of acute ischaemic renal failure caused attenuation of renal dysfunction and also reduced the level of apoptosis compared to untreated animals (Eter 2013). This demonstrated the ability of NQDI-1 to protect against ischaemic injury by the inhibition of ASK1 and therefore, apoptosis and oxidative stress.

Similarly, a study investigating the effect of NQDI-1 treatment on neonatal rats which have received brain hypoxia ischaemia (Hao et al. 2016). Hao et al. (2016) found that NQDI-1 attenuated hypoxic-ischaemic cerebral injury by inhibiting cellular apoptosis. Untreated animals with brain injuries were found to have increased levels of ASK1 in neurons and astrocytes compared to sham controls, which confirms the involvement of ASK1 signalling in cerebral injury.

Interestingly, in hamsters expressing severe cardiomyopathy phenotypes, ASK1 inhibition has been shown to supress the progression of ventricular remodelling and fibrosis of

hamster hearts (Hikoso et al. 2007). It could be possible that NQDI-1 has protective properties in the heart.

This highlights the pharmacological potential of NQDI-1 in the protection of whole organs from cellular damage. As well as this, due to the level of cellular damage caused as a result of many drug treatments and its characteristic ability to reduce tissue infarction, NQDI-1 may be a potential cardioprotective agent for Sunitinib induced cardiotoxicity.

1.6.2 A3 adenosine receptor: IB-MECA

1-[2-Chloro-6-[[(3-iodophenyl) methyl] amino]-9*H*-purin-9-yl]-1-deoxy-*N*-methyl-β-D-ribofuranuronamide (IB-MECA) is a selective A3 adenosine receptor (A3AR) agonist (Fishman et al. 2001). The A3AR is one of the four distinct adenosine receptors: A_1, A_{2A}, A_{2B} and A_3.

Adenosine receptors are a part of the G protein-coupled receptor (GPCR) family. GPCRs are one of the largest and diverse membrane protein families, which are coded by over 800 genes in the human genome (Fredriksson et al. 2003). GPCRs are characterised by 7 transmembrane spanning, α-helical domains, which are separated by alternating intracellular and extracellular loop regions. The N-terminus and extracellular loops are responsible for ligand binding (Carlsson et al. 2010). When a ligand binds to the central binding pocket, the receptor experiences a conformational change through the fifth and sixth transmembrane helix, this exposes a cavity which enables the coupling of G proteins to the receptor (Scheerer et al. 2008). The G proteins which associate with GPCRs form a heterotrimeric complex, including the Gα, Gβ and Gγ subunits (Figure 1.7). In the GPCRs active-state, the Gα is directly bound to the intracellular loops, which function as the

guanine nucleotide exchange factor (GEF). During G protein activation, the Gα exchanges a guanosine diphosphate (GDP) for a guanosine triphosphate (GTP). This causes the G protein to dissociate from the GPCR and then regulate effector proteins, including cyclic AMP (cAMP) and phospholipase C (PLC) (Figure 1.7). The intracellular C-terminus of the G protein heterotrimer contains the serine/threonine phosphorylation sites for protein kinases. This allows regulation of a variety of intracellular signalling pathways such as PKC, MAPK, PKA, and GRK (Rosenbaum, Rasmussen and Kobilka 2009).

Figure 1.7: Classical structure of G protein coupled receptors and their activation.

In a resting state the GPCR made up of 7 tras-membrane helices is bound with a Gα protein. The Gα protein is bound to a GDP and the Gβ and Gγ subunits.

Upon ligand binding, the receptor becomes active. This causes the Gα subunit to dissociate from the GPCR and the Gβ and Gγ subunits, as the GDP is

exchanged for a GTP. The Gα is now able to activate other signalling molecules within the cell (Li et al. 2002).

Adenosine is the endogenous ligand of the adenosine receptor family. The affinity of adenosine varies between the 4 adenosine receptor subtypes. The A_1 and A_{2A} subtypes have a strong binding affinity for adenosine, whereas the A_3 and A_{2B} have a lower affinity (Fredholm et al. 2011). In normoxic conditions, adenosine concentrations are in the low nano-molar range, however, its levels may rise due to high levels of ATP dephosphorylation in response to a high metabolic rate or hypoxic conditions.

Binding of adenosine initiates either an increase of intracellular cyclic adenosine monophosphate (cAMP) by A_{2A} and A_{2b} adenosine receptor subtypes or inhibition of cAMP activity by A_1 and A_3 adenosine receptor subtypes (Figure 1.8) (Fredholm et al. 2011). cAMP regulates important cellular processes such as, immune function, growth differentiation, gene expression and metabolism. An imbalance of cAMP signalling has been implicated in a number of pathologies, including: diabetes, inflammation and heart diseases (Guellich, Mehel and Fischmeister 2014, Levy, Zhou and Zippin 2016, Miller et al. 2013). Therefore, regulation of vital cell signalling pathways such as cAMP, through pharmacological adenosine receptor activation or inhibition is of high interest.

In particular, activation of the A3AR with IB-MECA has been shown to inhibit cAMP accumulation (Abedi et al. 2014). In addition to this, activation of A3ARs with IB-MECA has also been shown to increase the levels of PLC (Abbracchio et al. 1995). PLC is an upstream regulator of cellular signalling processes involving PKC and calcium dependant signalling pathways (Rohacs 2013) (Figure 1.8).

Figure 1.8: Schematic of the downstream targets of the A_3 adenosine receptor (A3AR).

The Gα subunit dissociates from the A3AR and the Gβγ subunits. The G protein can now: open the K_{ATP} channels, inhibit the catalytic activity of adenylyl cyclase (AC) and therefore the production of cAMP. 2) Activate PLC, which in turn increases cellular levels of Ca^{2+} and PLC induces PI3K and AKT phosphorylation. Stimulate RhoA and PDL activate MAPK family proteins including ERK, JNK and P38. All of which results in the regulation of various transcription factors, shown in the nucleus (Borea et al. 2015).

1.6.2.1 Cardioprotection by IB-MECA through the activation of A3ARs

A3AR have an important role in the regulation of the cardiovascular system. A3ARs are highly expressed in cardiomyocytes and activation of the A3AR has been shown to provide protective effects against myocardial ischaemia (Liu et al. 1994, Maddock, Mocanu and

Yellon 2002, Hussain et al. 2014). IB-MECA has been shown to have powerful cardioprotective effects against cardiac damage caused by hypoxia, ischemia/reperfusion injury and anti-cancer treatment with Doxorubicin (Shneyvays et al. 2002).

The key cardioprotective functions of IB-MECA are to reduce ischemia and infarct size, following ischaemia reperfusion injury. This is thought to be achieved through many cellular mechanisms. Firstly, activation of mitochondrial K_{ATP} channels has been shown to be critical in A3AR activation (Zhao and Kukreja 2002). A3AR cause the activation of PKC, nuclear factor kappa-light-chain enhancer of activated B cells (NF-κB), inducible nitric oxide synthase (iNOS), MAPK/ERK and Akt/PI3K stress signalling pathways (Xu et al. 2006).

In a study by Emanuelov *et al*. (2010), Doxorubicin treatment led to left ventricular dysfunction due to mitochondrial dysfunction and Ca^{2+} overload in cardiomyocytes with reduced ATP production (Emanuelov et al. 2010). There was an increased level of Ca^{2+} in the cytosol and in the mitochondria, due to the limited uptake of Ca^{2+} from the sarcoplasmic reticulum (SR), which caused insufficient Ca^{2+} levels in the SR to mediated contraction. Co-administration of IB-MECA attenuated the harmful effect of Doxorubicin by restoring the SR Ca^{2+} levels through activation of sarcoplasmic reticulum Ca^{2+} ATPase ATP2A2 (SERCA2a), thus preventing Ca^{2+} overload in cardiomyocytes and restoring the function of the mitochondria.

It is therefore possible that co-treatment of IB-MECA during Sunitinib therapy could be used to modulate the stress signalling created by Sunitinib induced cardiotoxicity and offer a protective effect.

1.7 microRNAs as indicators of cardiotoxicity and cancer.

The short non-coding RNAs known as microRNA (miRNA) are approximately 22 nucleotides long and perform the negative regulation of mRNA transcripts by repressing translation or mRNA degradation (Bagga et al. 2005). miRNAs are directed by sequence specific, Watson-Crick pairings between the miRNA nucleotides and the complimentary sites found within the 3' untranslated region of its target mRNA (Bartel 2004). Once bound to the complimentary region, the miRNA prevents the target mRNA from being translated (Figure 1.9). For mRNA targets, this has a direct effect on protein levels (Baek et al. 2008).

Regulation through miRNAs is vital during prenatal development. This was demonstrated by the deletion of Dicer protein, which is responsible miRNA biogenesis (Bernstein et al. 2003) (Figure 1.9). This deletion caused arrested development and lethality during gastrulation.

As well as this, specific Dicer deletions in the heart of mice did not affect gastrulation. However, mice carrying this deletion demonstrated altered cardiac contractility as a result of sarcoplasmic disarray. This caused a decline in cardiac function, leading to heart failure and eventually lethality (Chen et al. 2008). This highlights the importance of miRNA regulation of cardiac function in addition to development.

miRNAs have been shown to be involved in cardiomyocyte differentiation and response to stress. Changes in miRNA levels have been associated with cardiac injury (Babiarz et al. 2011). Van Rooji et al. (2008) investigated the expression of miRNAs during cardiac hypertrophy, which is caused in response to stress (van Rooij, Marshall and Olson 2008). More than 12 miRNAs were found to be up or down-regulated in response to stress induced cardiac hypertrophy. The miRNAs are up- or down-regulated during heart failure are could

potentially be selective markers for cardiac injury (van Rooij and Olson 2007). miRNA expression profiling has identified miRNAs which are linked to cardiovascular injury, therefore miRNAs have been implicated as predictors of cardiac damage. The 4 miRNAs known to be associated with such cardiac injury we have focused on are miR-1, miR-27a, miR-133a and miR-133b (van Rooij et al. 2006).

Figure 1.9: Schematic showing the process of the microRNA (miRNA) processing pathway and miRNA's role in the inhibition of gene expression at a translational level.
Firstly, miRNA undergoes transcription by RNA polymerase II/III. The primary transcript (>1kb) folds into a local stem-loop structure known as pri-miRNA, which contains the miRNA sequence. Pri-miRNA is then processed in the nucleus by the Drosha and DGCR8 Microprocessor complex into a shorter hairpin-shaped RNA of ~65 nucleotides known as pre-miRNA. Pre-miRNA is exported to the cytoplasm through a nuclear pore by the exportin 5-Ran-GTP transport complex. Upon entering the cytoplasm, the pre-miRNA is cleaved by Dicer (regulated by cofactors, TRBP in humans) close to the terminal loop, leaving a small RNA duplex. The loop is degraded. The small RNA duplex is loaded onto an AGO protein to form an effector complex known as the RNA-induced silencing complex (RISC). The AGO protein removes the passenger strand from the RNA duplex, leaving the mature miRNA. The mature miRNA can now base pair with its mRNA target, initiating processes such cleavage, repressing translation and de-adenylation of the target mRNA. (Winter et al. 2009).

1.7.1 miR-1 and miR-133a

miR-1 is co-expressed with miR-133a as they are located on the same miRNA cluster. In the heart and they regulate the cardiac conduction system, maintaining heart beat rhythm (Zhao and Srivastava 2007, Zhao et al. 2007). During cardiac disease, there is an altered expression of these miRNAs, suggesting that they are important modifiers of gene expression in the progression of heart failure (Vegter et al. 2016).

Yang et al., (2007) demonstrated in coronary heart disease and in infarcted rat hearts there is an over expression of miR-1 and this caused a reduced level of conduction during muscle contraction (Yang et al. 2007). This is as result of miR-1's inhibitory role on the potassium channel, potassium voltage-gated channel subfamily J member 2 (KCNJ2) and gap-junction protein connexin. A reduction in myocyte repolarisation is a causative factor in patients with a long QT interval (Chen et al. 1999b).

In addition to this, another target of miR-1 is Hand2, a protein which has a role in cardiac morphogenesis. This inhibition or "knock-out" of Hand2 results in ventricular myocyte failure (Srivastava 2006). This suggests that over-expression of miR-1 promotes apoptosis. Ai et al (2010) showed an up-regulation of miR-1 in the circulation of patients who have acute myocardial infarction (Ai et al. 2010).

He et al (2011) found miR-1 to be down regulated during ischaemia reperfusion, but up-regulated by ischaemic post conditioning (He et al. 2011). This suggests a potential cardioprotective effect of miR-1. However, Gidlof et al (2013) found no change in expression in patients who had experienced myocardial infarction (Gidlöf et al. 2013). Gidlof suggested

other studies were too focused of the acute stage of myocardial infarction and used much smaller cohorts.

miR-133a is known to have the opposite effect to miR-1 in cardiovascular tissue during cardiovascular diseases. The down-regulation of miR-133a is associated with cardiac hypertrophy (van Rooij et al. 2006, Care et al. 2007). Liu et al., (2008) demonstrated that miR-133a is important in maintaining healthy cardiomyocytes (Liu et al. 2008). The knock-out of miR-133a generated abnormalities in important cell survival pathways and was found to be lethal in most cases, suggesting a role in development. Survivors developed myocardial fibrosis and eventually died of heart failure. In addition, miR-133a targets small RhoA and Cdc42, which are GTP-binding proteins involved in hypertrophy (Care et al. 2007). Suppression of miR-133a allows hypertrophy to occur. These findings suggest that miR-133a has an anti-apoptotic and hypertrophic role (Xu et al. 2007).

Also, it has been established that miR-133a has a partial complimentary target site in the 3'UTR region of ether-a-go-go (ERG). This implies that miR-133a inhibits ERG when it is over expressed. A reduction in ERG levels causes the delayed myocyte repolarisation attributed to a long QT interval (Xiao et al. 2007).

1.7.2 miR-27a

Research has indicated that miR-27a is up-regulated during cardiac hypertrophy and heart failure (van Rooij et al. 2006). By using virus mediated small interfering RNA (siRNA) against Dicer, Nishi et al. (2011) demonstrated that miR-27a indirectly regulates myosin heavy chain β (MHC-β) through its inhibitory role on thyroid hormone receptor β1 (TRβ1) (Nishi et al.

2011). TRβ1 negatively regulates MHC-β, therefore, over expression of miR-27 increases MHC-β levels. An increase in MHC-β is associated with cardiac hypertrophy.

However, Dong et al (2009) found an increased expression of miR-27a in non-infarcted heart tissue compared to infarcted heart tissue (Dong et al. 2009). Additionally, Marfella et al (2013) found a significant decrease in miR-27a in patients who have suffered with severe heart attack and a further decrease after 1 year of cardiac resynchronization therapy (Marfella et al. 2013). This suggests that miR-27a has an important role in the progression of heart failure. Any change in expression could be a result of cardiac damage.

1.7.3 miR-133b

miR-133b has been found to regulate the development and differentiation of neonatal cardiomyocytes by inhibiting the cell cycle protein serum response factor (Ekhteraei Tousi et al. 2013). This inhibition decreases cardiomyocyte proliferation (Koutsoulidou et al. 2011). The down-regulation of miR-133b has been associated with an increased expression of b-type natriuretic peptide (BNP), skeletal α-actin and ANF (Sucharov, Bristow and Port 2008), all of which are known biomarkers for cardiotoxicity and muscle damage.

Additionally, in a clinical setting, increases in miR-133b expression positively correlate with an increase in central venous pressure and cardiac output (Wang et al. 2013). Wang et al., (2013) also demonstrated that high levels of miR-133b reflect early myocardial injury (Wang et al. 2013).

Although, miRNAs have been thought to be extremely sensitive biomarkers for cardiotoxicity, there is a substantial amount of conflicting published data. This suggests that the role of miRNAs, miR-1, miR-27a, miR-133a and miR-133b in particular is very complex

and needs to be further investigated to gain a clear picture as to whether up- or down-regulation of these molecules is directly proportional to the extent of cardiac damage. For this reason, the study of proteomics and protein biomarkers is generally investigated alongside miRNAs.

1.7.4 The involvement of miRNA in cancer

In addition, the expression pattern of miRNAs is frequently dysregulated in tumour cells (Lin and Gregory 2015). These miRNAs have important gene regulation functions as they interact with their specific target mRNA(s) and induce RNA silencing and therefore regulate the level of translation of target proteins (figure 1.9). It has been reported that a large number of miRNA genes are located in cancer associated genomic regions. Because of this, miRNAs have been reported in many types of cancer, including: breast, colon, haemolytic, liver, lung and thyroid (Reddy 2015).

miRNAs could be used as potential biomarkers for cancer diagnostics as previous studies have shown that miRNA expression profiles can be used to distinguish between healthy tissue and cancerous tissue (Cheng 2015). Studies have shown that over-expression of miR-155 and deletion of the miR-15a/16 cluster will cause initiation of B cell lymphomas, especially in diffuse large B cell lymphomas, Hodgkin lymphomas, and certain types of Burkitt lymphomas (Costinean et al. 2006, Klein et al. 2010). The gene of miR-155 was previously described as an avian leucosis virus, proviral DNA insertion site or the BIC oncogene. This BIC oncogene (RNA) was shown to associate with myc, a regulator gene which codes for a transcription factor. This association induced haematopoietic tumours (Tam, Ben-Yehuda and Hayward 1997). Therefore, over-expression of miR-155 induced

haematopoietic cancers, however miR-155 deficient mice have been shown to produce defective B and T cells (Rodriguez et al. 2007). This suggests that miR-155 is required for normal immune function.

Contrastingly, is has been alluded that the miR-15a and miR-16-1 cluster of miRNAs are tumour suppressor genes. This cluster is located on chromosome 13 (13q14) and is often found to be deleted in cases of chronic lymphocytic leukaemia (CLL) and prostate cancer (Rowntree et al. 2002, Bonci et al. 2008). Additionally, point mutations downstream of the miR-16-1, which reduces expression of miR-16-1 has been observed in CLL cases (Calin et al. 2005).

The knowledge of changes in up/down regulation of specific miRNAs could identify tumour miRNA expression signatures specific to the tumour type (Calin and Croce 2006).

1.8 Aims, objectives and hypothesis

1.8.1 Aims

The aims of this thesis were to:

- Investigate whether Sunitinib induces cardiotoxicity in Langendorff heart models, using Sprague-Dawley rats at 3, 12 and 24 months of age.
- Establish whether the stress signalling MKK7 pathway, as well as PKCα are involved in Sunitinib-induced cardiotoxicity.
- Identify compounds which may have the ability to produce cardioprotective effects counteracting the Sunitinib-induced cardiotoxicity while not interfering with the anti-cancer properties of Sunitinib in HL60 cells.

1.8.2 Objectives:

The objectives of this thesis were to:

• Determine the cardiotoxic effects of a clinically relevant concentration of Sunitinib in a Langendorff isolated heart model and study the effect of ageing on the level of Sunitinib-induced cardiotoxicity.

• Determine the effects of Sunitinib on signalling proteins of the MKK7 and PKCα pathway.

• Investigate the level of cardioprotection generated by co-administration of Sunitinib with NQDI-1 or IB-MECA.

• Assess the expression levels of relevant miRNAs to identify cardiac injury and cancer progression in cardiac tissue and HL60 cells.

1.8.3 Hypotheses

The Hypotheses of this thesis are listed below:

- Sunitinib treatment will have adverse effects on the haemodynamic function of the heart, increase the infarct size to risk ratio and affect the expression profiles of miRNAs associated with myocardial injury compared to vehicle controls.
- Age will have an effect on the level and formation of cardiotoxicity.
- The ASK1 inhibitor, NQDI-1 will protect against the cardiotoxic effects of Sunitinib treatment.
- Activation of the A3 adenosine receptor with IB-MECA will protect against the adverse effects of Sunitinib treatment.
- The anti-cancer properties of Sunitinib in HL60 cells will not be affected by adjunct therapy of NQDI-1 or IB-MECA.
- Levels of cancer specific miRNAs will change in response to Sunitinib and the adjunct therapies NQDI-1 and IB-MECA treatment of HL60 cells compared to untreated controls HL60 cells.

2. Materials and Methods

2.1 Animals and ethical procedure

Adult male Sprague-Dawley rats (300-350 g in body weight) were purchased from Charles River UK Ltd (UK) and housed suitably in the Coventry University Animal House (Coventry, UK). All animals received humane care and free access to a standard diet following "The Guidance on the Operation of the Animals (scientific procedures) Act of 1986" (Porta et al. 2013). This project received ethical approval from Coventry University (UK). All efforts were made to minimize animal suffering and to reduce the number of animals used in the experiments. Rats were sacrificed by cervical dislocation (Schedule 1 Home Office procedure).

Female rats were not considered for this thesis as the hormone cycling associated with the female anatomy has the potential to add an additional uncontrollable variable (Buoncervello et al. 2017). In addition, previous studies have shown that oestrogens play an important role in cardiovascular injury through regulation of cardiac stem cells and protection against oxidative stress (Kuhar et al. 2007 and Lagranha et al. 2010).

2.2 Reagents

2.2.1 Drugs

N-(2-diethylaminoethyl)-5-[(*Z*)-(5-fluoro-2-oxo-1H-indol-3-ylidene) methyl]-2,4-dimethyl-1*H*-pyrrole-3-carboxamide (Sunitinib Malate), 2,7-Dihydro-2,7-dioxo-3*H*-naphtho[1,2,3-*de*] quinoline-1-carboxylic acid ethyl ester (NQDI-1) and 2-chloro-N^6-(3-Iodobenzyl) adenosine-

5’-N-methyluronamide (2-CL-IB-MECA/IB-MECA) were purchased from Sigma-Aldrich (UK) and dissolved in dimethyl sulfoxide (DMSO) from Sigma-Aldrich (UK). Sunitinib and NQDI-1 made up to a stock concentration of 25 mM and IB-MECA made up to 1 mM stock concentration. All were stored at -20 °C; aliquots were thawed at room temperature prior to experimental use.

2.2.2 Salts and general reagents

NaCl, NaHCO3, KCl, $MgSO_4.7H_2O$, KH_2PO_4, $CaCl_2$, $Na_2HPO_4.2H_2O$, NaH_2PO_4, NaF, HCl, Glucose, Taurine, Sodium dodecyl sulphate, Sodium Pyruvate, HEPES, Creatine, Glycine, Tris base, Ethylenediaminetetraacetic acid (EDTA), β-glycaophosphate, 4-benzenesulfonyl fluoride hydrochloride (AEBSF), glycerol, 2-mercaptoethanol, bromophenol blue, formaldehyde, methanol, L-Glutamine, bovine serum albumin (BSA) all purchased from Fischer Scientific, UK.

2, 3, 5-Triphenyl-2H-tetrazolium chloride (TTC), 3- [4, 5 –dimethylthiazol-2-yl]-2, 5 diphenyl tetrazolium bromide (MTT), Triton X-100, protease inhibitor cocktail tablets and Phosphate buffered saline (Sigma-Aldrich, UK).

2.2.3 RNA extraction and PCR reagents

RNase/DNase free ethanol purchased from Fischer (UK). RNAlater, ZAP solution, RNase free H_20, oligo (dt) cellulose isolation kit, SYBR® Green Master Mix purchased from Ambion (UK). miRNA isolation kit: mirVana miRNA isolation kit, without phenol, Acid phenol: chloroform, TRIzol plus RNA purification kit purchased from Invitrogen (UK). RNA Reverse Transcription

Kit, TaqMan Universal PCR Master Mix purchased from Applied Biosystems (USA). The iTaq universal SYBR green super mix was purchased from BioRad (UK).

2.2.3.1 Primers

U6 snRNA, rno-miR-1, hsa-miR-15a, hsa-miR-16-1, hsa-miR-27a, hsa-miR-133a, hsa-miR-133b and hsa-miR-155, Primer assays purchased from Applied Biosystems (USA). GAPDH Forward and reverse primer, MKK7 forward and reverse primer purchased from Invitrogen, Life Technologies (UK).

2.2.4 Cell culture and MTT assay

Human leukaemia cancer (HL60) cell line (obtained from Coventry University's Cell Bank). RPMI 1640 media without L-Glutamine, in DMEM media without L-glutamine, antibiotic solution (10 000 U/ml penicillin and 10 000 µg/ml streptomycin), Foetal bovine serum (Biosera, UK).

2.2.5 Western Blot and flow cytometry studies

4–15 % Mini-PROTEAN® TGX™ Gel for MKK7, any KDa Mini-PROTEAN® TGX™ Gel, 8-20 % Mini-PROTEAN® TGX™ Gel, Trans-Blot® Turbo™ PVDF membrane purchased from BioRad (UK), Super Signal West Femto kit purchased from PIERCE biotechnologies (UK).

2.2.5.1 Antibodies

Phospho-MKK7 (Ser271/Thr275), Total MKK7, Phospho-ASK1 (Thr 845), Total ASK1, Phospho-SAPK/JNK (Thr183/Tyr185), Total SAPK/JNK rabbit mAb antibodies, Total GAPDH, Alexa flour@488 conjugated secondary antibody anti-rabbit IgG, HRP-linked antibody and

anti-biotin, HRP-linked antibody were purchased from Cell Signalling Technologies (UK). Antibodies anti-PKC α (phospho T497) and total PKC were from Abcam (UK).

2.2.6 Animals and Ethics

Adult male Sprague-Dawley rats (300-350 g in body weight) were purchased from Charles River UK Ltd (UK) and housed suitably. They received humane care and had free access to standard diet according to "The Guidance on the Operation of the Animals (scientific procedures) Act of 1986". Animals were selected at random for all treatment groups and the collected tissue was blinded for infarct size assessment. The experiments were performed following approval of the protocol by the Coventry University Ethics Committee. All efforts were made to minimize animal suffering and to reduce the number of animals used in the experiments. Rats were sacrificed by cervical dislocation and death was confirmed by exsanguination (Schedule 1 Home Office procedure).

2.3 Langendorff perfused isolated heart assay

2.3.1 Background of the Langendorff model

The Langendorff system is a classic technique for investigating acute changes in heart physiology. Frog hearts were the first isolated perfused hearts to be developed by Elias Cyon et al. at the Carl Ludwig institute in 1866. In 1895 perfusion of isolated mammalian hearts was pioneered by Oscar Langendorff (Zimmer 1998).

The Langendorff system forces fluid to retrogradely flow into the aorta. The aortic valve is closed under pressure and as a consequence the perfusate enters the coronary arterial vasculature through the ostia at the aortic root. The perfusion buffer flows through the vascular bed and drains into the right atrium (Bell, Mocanu and Yellon 2011, Langendorff 1895). Effluent is ejected from the heart chambers, generating a flow representative of the vasodilation and vasoconstriction of the blood vessels within the hearts. Measurements of left ventricular pressure and heart rate can be measured by the insertion of a force/pressure transducer system into the left ventricle (Figure 2.1).

This preparation was originally applied to the study of heart biology by physiologists and biochemists. The isolated heart model is also used by pharmacologists to assess the effects of various drugs on cardiac muscle contraction, heart rate and coronary vasculature. In addition, the Langendorff system is essential in the study of the effect of changes in gene expression and protein levels as this allows the identification and development of novel therapies which protect cardiac tissue from damage.

Figure 2.1: Schematic of Langendorff experimental apparatus.

Oxygenated perfusate (Kerbs buffer) flows via gravitational force through the cannulated aorta of a rat heart. The perfusate is forced retrogradely to the coronary arteries of the rat heart. The Thermal chamber is a warming jacket surrounding the heart, maintaining the temperature of the heart at 37 °C. An iso-volumic balloon is inserted into the left atrium. This is connected to the force transducer which is connected to a computer and records changes in heart rate (bpm) and left ventricular developed pressure (mmHg). Perfusate that leaves the heart is measured and coronary flow (ml/min) can be calculated (Skrzypiec-Spring et al. 2007).

2.3.2 Langendorff protocol

Rats were sacrificed by cervical dislocation and conformation of death by exsanguinations (Schedule 1 Home Office procedure) and confirmed by exsanguination. Afterwards the hearts were immediately excised and placed into ice-cold (<4 °C) Krebs Henseleit buffer (KH) (118.5 mM NaCl, 25 mM $NaHCO_3$, 4.8 mM KCl, 1.2 mM $MgSO_4$, 1.2 mM KH_2PO_4, 1.7 mM $CaCl_2$, and 12 mM glucose, pH 7.4). The hearts were mounted onto the Langendorff system

immediately after dissection procedure and retrogradely perfused with KH buffer (Figure 2.1). The KH buffer was continuously gassed with 95 % O_2 and 5 % CO_2 and maintained at 37 ± 0.5 °C using a water-jacketed Langendorff system and organ chamber.

The left atrium was removed and a latex iso-volumic balloon was carefully introduced into the left ventricle and inflated by 2 ml of H_2O (Figure. 2.1). Functional recordings were taken via a physiological pressure transducer connected to a Powerlab (AD Instruments Ltd. Chalgrove, UK) and visualised on a monitor. Left ventricular pressure (LVDP) and heart rate (HR) were measured by the Powerlab system (Figure. 2.2). Coronary flow (CF) was measured by collecting the perfusate, and was recorded as the volume (ml) of fluid pumped out of the heart in one min divided by the weight of the heart.

Each Langendorff assay was conducted for 145 mins: 20 min stabilisation period followed by 125 mins of drug or vehicle perfusion in normoxic conditions. All recordings were measured at regular intervals (every 5 mins for the first 55 mins and every 15 mins after that till the end of the experiment).

The specific drug treatments are listed in Chapters 3, 4 and 5.

Hearts were then either weighed, wrapped in plastic film and stored at -20 °C overnight for 2, 3, 5-Triphenyl-2H-tetrazolium chloride (TTC) staining (see section 2.4) or the left ventricle was dissected free and collected and was divided into two parts: one half was immersed in 500 µl of RNAlater and stored at -20 °C for microRNA (miRNA) (see section 2.6) or mRNA (see section 2.7) analysis by real-time PCR analysis, while the other half was wrapped in foil, snap frozen in liquid nitrogen and stored at -80 °C for Western blot analysis (see section 2.9).

2.3.3 Quantifying Langendorff haemodynamic results

Raw data recorded from Labchart 7 with PowerLAB (ADInstruments, New Zealand) readings provided the haemodynamic analysis of HR and LVDP parameters. CF measurements were manually recorded by collecting perfusate for 1 min at each time point. Each time point was normalised to the average of the last 10 mins of the stabilisation period of each parameter.

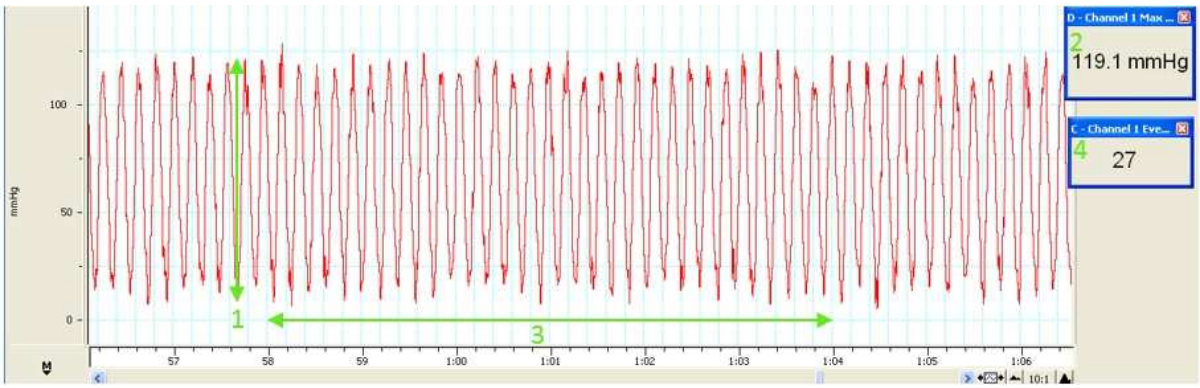

Figure 2.2: Screen shot of the trace produced during a control Langendorff experiment in LabChart. 1) is the trace peak length, this is the pressure exerted in the left ventricle during a heartbeat. 2) The LVDP reading was 119.1 mmHg for an average of 6 secs. 3) Each peak represents a heartbeat. 4) The number of beats in 6 secs for this trace was 27 beats, multiply this number by 10 to give 270 beats per min.

2.3.4 Haemodynamic data analysis

Haemodynamic data were analysed using Microsoft Excel. HR and LVDP were calculated as the percentage of the last 10 minutes of the stabilisation and coronary flow was first corrected for heart weight and then calculated as the percentage of the average of the last 10 minutes of the stabilisation period.

Graphs were plotted in GraphPad Prism (version 5.03, GraphPad Software, Inc. USA).

All statistical analysis was done by one-way ANOVA or student's t-test using the IBM program SPSS, (USA) with the LSD post hoc test. Data expressed as mean ± SEM P-values < 0.05 were considered statistically significant.

2.4 Triphenyltetrazolium Chloride Assay

2.4.1 Background of the triphenyltetrazolium chloride assay

2, 3, 5-Triphenyl-2H-tetrazolium chloride (TTC) staining is one of the most conventional methods for detection of infarcted areas of the heart in animal experiments. TTC is reduced to triphenyltetrazolium formazan in areas where dehydrogenase activity is present and stains the tissue red. Dehydrogenase activity is evident of the presence of functional mitochondria; therefore, red stained tissue is viable. Tissue which is not stained and appears pale is fibrous and infarcted (Figure. 2.3).

2.4.2 Triphenyltetrazolium Chloride Assay protocol

After a Langendorff experiment whole hearts were stored at -20 °C over-night. The following day the hearts were sliced into 2 mm thick transverse sections and incubated in 0.1 % TTC solution in phosphate buffer (2 ml of 100 mM $NaH_2PO_4.2H_2O$ and 8 ml of 100 mM NaH_2PO_4, pH 7.4) at 37 °C for 15 mins and fixed in 10 % formaldehyde for 4 hrs.

After 4 hrs, the formaldehyde solution was removed and heart slices were placed between two Perspex sheets and compressed by bulldog clips. The heart slices were blinded and traced onto acetate sheets using different coloured markers to represent areas of infarct and viable tissue. The viable tissue stained red and infarct tissue appeared pale (Figure. 2.3).

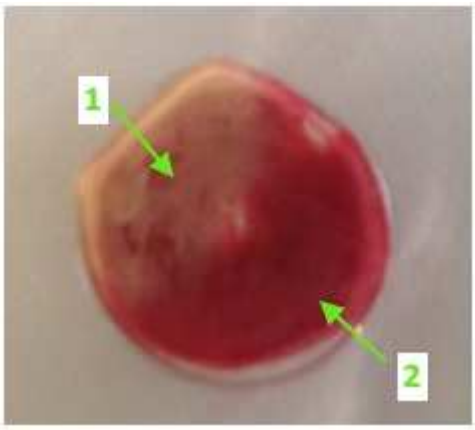

Figure 2.3: TTC stained heart slice, highlighting the areas of 1) infarcted tissue and 2) viable tissue.

2.4.3 Triphenyltetrazolium Chloride Assay data analysis

The acetate film was scanned into a computer and by using computerised planimetry (Imagetool 3.0, UTHSCSA). Measurements of total heart slice area, total area of infarcted tissue (Infarct) and area of viable tissue (Risk) was recorded. The calculation: (Infarct/Risk) x 100 provided the infarct to risk ratio (%). The infarct to risk ratio (%) was calculated for each slice and then an average was taken for an infarct ratio of the whole heart. Statistical analysis of infarct sizes within drug treatment groups was carried out using One-way ANOVA or Students T-test using the SPSS software package (IBM, USA).

2.5 Reverse transcription and real-time PCR

The polymerase chain reaction (PCR) is one of the key technologies used in present-day life sciences. The process involves repeated heating and cooling cycles of a solution of DNA, gene specific DNA primers, DNA polymerase and dNTPs. Generally, the PCR mixture is heated to 94-96 °C which allows denaturation of the double stranded DNA. The mixture is then cooled to approximately 50-65 °C to allow the annealing of primers to the target DNA

transcript. DNA polymerase then extends the primers, copying the target section of DNA at an optimum temperature of approximately 70-74 °C. This process is then repeated 40 times. This results in exponential amplification of the unique DNA target. DNA is amplified for purposes such as diagnosis and monitoring of genetic diseases, forensics and the study of gene function.

However, in addition to this, PCR can be used to quantify gene expression. A target messenger RNA (mRNA) or micro RNA (miRNA) is reverse transcribed using the reverse transcriptase enzyme. This reaction produces complimentary DNA (cDNA). The amount of cDNA produced by the reverse transcription process is relative to the original amount of target mRNA or miRNA. With the addition of a fluorescent marker with in specific primers, PCR can then be used to quantify the relative level of the original mRNA from the cDNA (Figure. 2.4).

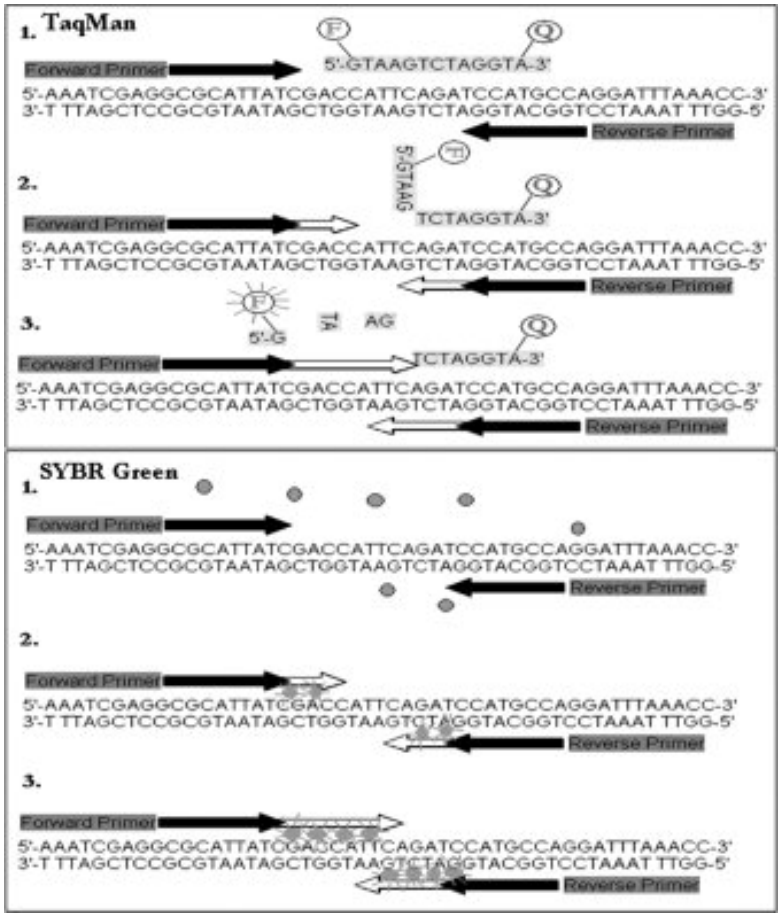

Figure 2.4: Schematic of real-time PCR using TaqMan or SYBR Green.

TaqMan: 1) The primers and probes which are labelled with a fluorophore (R) and a quencher (Q)) anneal target sequence. While the fluorophore and quencher are in close proximity, the fluorescent signal is blocked 2) Polymerase performs elongation of the primers by adding nucleotides. Elongation continues until taq Pol falls off, generating the product of cycle 1. During elongation, the probe is displaced, enabling the fluorescent signal to be emitted. 3) Fluorescence can be detected as the probe is degraded. The intensity of fluorescence corresponds to the number of DNA copies. SYBR Green: 1) Before the PCR reaction SYBR Green is free in the reaction mix solution and a small amount of fluorescence is emitted. 2) As primers are extended by Taq *polymerase, SYBR Green is inserted into the double stranded DNA. 3) After many template replications occurs there are more concentrated levels of SYBR Green which emit fluorescence. The fluorescence increases as strands are replicated (Thornton and Basu 2011).*

The intensity of fluorescence (Rn) emitted by each sample at each reaction cycle is detected by a PCR machine. The magnitude of signal generated during PCR can be calculated (ΔRn). A graph of ΔRn (RFU) vs copy number is plotted (Figure. 2.5). The number of PCR cycles it takes for fluorescence levels of a target cDNA to surpass the background fluorescence is the cycle threshold (C_t). Therefore, the lower the C_t value the more target mRNA or miRNA was present in the starting sample. This value was normalised to the C_t of a house keeping gene, such as GAPDH, which should remain at a consistent level in all research samples. This allows comparisons of different samples during various treatments/conditions to be made.

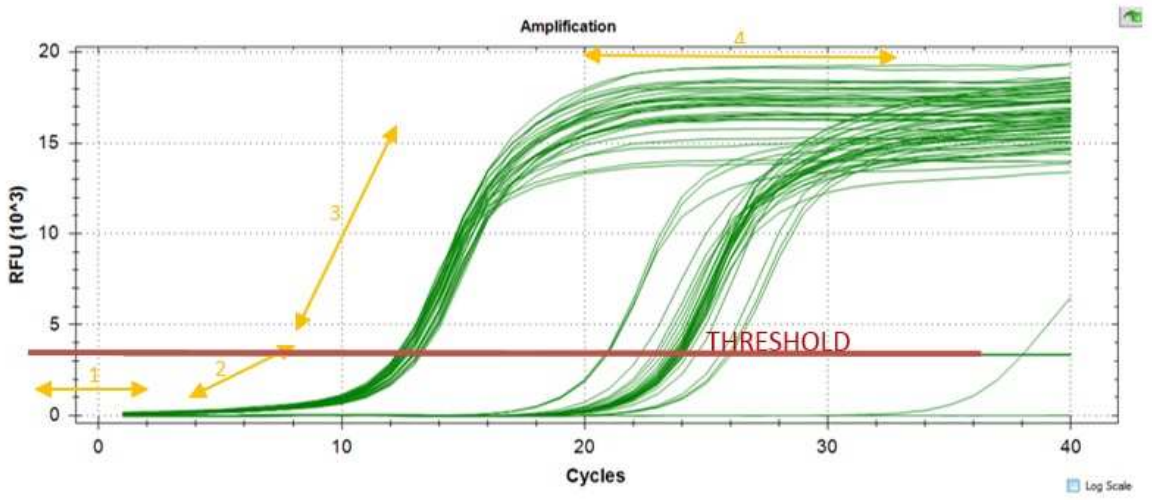

Figure 2.5: PCR amplification graph showing fluorescence intensity vs PCR cycle number.
The orange arrows identify the stages of real-time PCR. 1) Linear ground phase. 2) Early exponential phase. 3) log-linear phase. 4) Plateau phase. The red line represents the level of fluorescence required for a target amplification to be detected (C_t).

Quantitative reverse transcriptase PCR was used to analyse the expression of cardiac injury specific miRNAs (miR-1, miR-27a, miR-133a and miR-133b), as well as miRNAs involved in cancer development (miR-155, miR-15a and miR-16-1), and MKK7 mRNA.

Following Langendorff perfusion, hearts were dissected and the left ventricle was removed and chopped into small pieces. The tissue was transferred into 2ml RNA/DNA free microfuge tubes and 1 ml of RNAlater (Ambion life technologies, UK) was added to them and stored at -20 °C until analysis by real-time PCR.

2.6 Reverse transcription and real-time PCR: for the determination of microRNA expression in the myocardium protocol

2.6.1 RNA extraction

It is possible to extract high-quality miRNA from a variety of tissue and cell sources. Commonly, RNAs are extracted by chemical extraction and then purified by solid-phase extraction. Chemical extraction uses concentrated chaotropic salts such as guanidinium thiocyanate, in combination with phenol and chloroform. The general steps include cell lysis to disrupt cell structure to produce a lysate, nuclease inactivation and separation of RNA from cell debris. After, centrifugation at a high speed the lysate-guandinium thiocyanate-phenol-chloroform solution shows visible separation of RNA from DNA, protein and cell debris. RNA is found in the top clear layer of the mixture. This method provides isolation of very pure RNA; however, the RNA requires desalting. Desalting is achieved by solid-phase extraction. Therefore, ethanol is added and the solution is passed through a glass-fibre

filter. The glass fibre immobilises the RNA and is only released when a non-ionic solution is added. This will produce ultra-pure RNA.

2.6.1.1 Lysing heart tissue

The homogeniser (IKA Overtechnical T25) was cleaned with RNase/DNase free ethanol, ZAP solution and RNase free H_20. The RNAlater solution was discarded and 1 ml of lysis buffer solution (mirVANA kit, Ambion, UK) was added to the microfuge tubes on ice. The samples were then homogenised AT 12000 rpm using the IKA Overtechnical T25 in ice, making sure that the samples remained cool to prevent denaturation of the RNAs. 30 µl of Homogenate Additive (mirVANA kit, Ambion, UK) was added and the tubes were incubated on ice for 10 mins.

2.6.1.2 Lysing HL60 cells

After drug incubation (described in chapter 5) HL60 cells were transferred to centrifuge tubes and centrifuged at 1000rpm for 10 mins. The supernatant was removed and the cell pellet was resuspended in 1ml of phosphate buffered saline (PBS). The cells were centrifuged again at 1000rpm and resuspended in PBS. The cells were then kept on ice.

The PBS was then removed and 600 µl of Lysis/Binding solution (mirVANA kit, Ambion, UK) was added. To fully lyse the cells the lysate was vortexed. 60 µl of Homogenate additive (mirVANA kit, Ambion, UK) was added and the tubes were incubated on ice for 10 mins.

2.6.2 miRNA isolation (heart tissue and HL60 cells)

300 µl of chloroform was added to the tubes. The samples were vortexed and centrifuged at 12,000 rpm for 5 mins at room temperature. The upper phase (containing RNA) was

transferred to new RNase free microfuge tubes and the lower phase was discarded. The upper phase volume was estimated and a 1.25 X volume of RNase free ethanol was added. This was centrifuged through a spin column into a collection tube for 15 secs at 12,000 rpm at room temperature. The effluent was discarded and the spin column was washed with 500 µl of Wash Solution 1 (mirVANA kit, Ambion, UK) and then centrifuged for 15 secs at 12,000 rpm at room temperature. The effluent was discarded. The spin column was now washed with 500 µl Wash Solution 2/3 (mirVANA kit, Ambion, UK) twice, centrifuging for 15 secs at 12,000 rpm at room temperature. The spin column was then centrifuged for 1 min at 12,000 rpm in an emptied collection tube.

The spin column was placed in a new RNase free collection tube and 50 µl of 95°C warm RNase free water was added to it. This was incubated for 1 min on ice. The spin column/ collection tubes were centrifuged for 20 secs, at 12,000 rpm, at room temperature. The collected effluent contained the extracted miRNA.

The RNA quantity and quality were measured by a nanochip bioanalyser (Quiagen) and nanoid spectrophotometry (Nanoid Technology, Delaware, USA). Extracted miRNA was stored at -80 °C until further analysis.

2.6.3 Reverse transcription reaction of target miRNAs

500 ng of miRNA (either from tissue or cell) was reverse transcribed into cDNA for using primers specific for U6 snRNA, hsa-miR-155, hsa-miR-15a, hsa-miR-16-1, rno-miR-1, hsa-miR-27a, hsa-miR-133a or hsa-miR-133b using the Applied Biosystems MicroRNA Reverse Transcription Kit (Applied Biosystems, USA) according to the manufacturer's instructions.

DNA/RNA free microfuge PCR tubes were labelled and the substances added to each tube are found in table 2.1.

Table 2.1: The recipe for each PCR tube during the reverse transcription and PCR of the miRNAs. Please note only the miRNA primers of interest were added.

Multi reverse transcriptase	1 µl
100mM Dntp	0.2 µl
10x RT buffer	3 µl
RNase inhibitor	0.2 µl
U6 snRNA RT PCR primer	0.5 µl
rno-miR-1 RT PCR primer	0.5 µl
hsa-miR-27a RT PCR primer	0.5 µl
hsa -miR-133a RT PCR primer	0.5 µl
hsa -miR-133b RT PCR primer	0.5 µl
hsa-miR-15a RT PCR primer	0.5 µl
miR-16-1 RT PCR primer	0.5 µl
hsa-miR-155 RT PCR primer	0.5 µl
miRNA (from extracted from sample)	500 ng/µl (using nanodrop results)
H_2O	Make up to 30 µl

The reverse transcription PCR reaction was performed with the following setup: 16 °C for 30 min, 42 °C for 30 mins and 85 °C for 5 mins and then at 4 °C (until used for real-time PCR or stored). cDNA was stored at -20 °C until further analysis.

2.6.4 Real-time PCR reaction of target miRNAs from heart tissue or HL60 cells

Real-time PCR was performed using a standard TaqMan Universal PCR Master Mix (Applied Biosystems, USA) protocol on the 7500 HT Real-time PCR sequence detection system (Applied Biosystems, USA). The 7500 Fast Real-time PCR sequence detection software SDS version 1.4 (Applied Biosystems, UK) monitored the amplification of DNA in real-time by optics and imaging system via the binding of SYBR Green fluorescent dye to double-stranded DNA. A 20 µl reaction mixture containing 100 ng cDNA, specific Applied Biosystems primer assays and the TaqMan Universal PCR Master Mix was used in the Real-time PCR reaction. A non-template control was included in all experiments.

Using a qPCR plate template, design the layout for the reaction for each drug treatment group (Figure 2.6) duplicates with each primer for each sample and non-template controls (NTC) for each individual primer set (U6 snRNA, rno-miR-1, hsa-miR-27a, hsa-miR-133a, hsa-miR-133b, hsa-miR-155, hsa-miR-15a, and hsa-miR-16-1) were made. Each 20 µl reaction contained the following:

Table 2.2 : shows the recipe for each real-time PCR well during the experiment.

cDNA	3 µl
Individual Primer set	0.5 µl
SYBER green	10 µl
H_2O	6.5 µl

plate 1	1	2	3	4	5	6	7	8	9	10	11	12
A	U6	U6	U6	U6	U6	U6	U6	U6	U6	U6	U6	U6
B	miR-1	miR-1	miR-1	miR-1	miR-1	miR-1	miR-1	miR-1	miR-1	miR-1	miR-1	miR-1
C	miR-27a	miR-27a	miR-27a	miR-27a	miR-27a	miR-27a	miR-27a	miR-27a	miR-27a	miR-27a	miR-27a	miR-27a
D	miR-133a	miR-133a	miR-133a	miR-133a	miR-133a	miR-133a	miR-133a	miR-133a	miR-133a	miR-133a	miR-133a	miR-133a
E	miR-133b	miR-133b	miR-133b	miR-133b	miR-133b	miR-133b	miR-133b	miR-133b	miR-133b	miR-133b	miR-133b	miR-133b
F	miR-155	miR-155	miR-155	miR-155	miR-155	miR-155	miR-155	miR-155	miR-155	miR-155	miR-155	miR-155
G	miR-15a	miR-15a	miR-15a	miR-15a	miR-15a	miR-15a	miR-15a	miR-15a	miR-15a	miR-15a	miR-15a	miR-15a
H	U6	miR-1	miR-27a	miR-133a	miR-133b	miR-155	miR-15a	miR-16-1				
plate 2	1	2	3	4	5	6	7	8	9	10	11	12
A	miR-16-1	miR-16-1	miR-16-1	miR-16-1	miR-16-1	miR-16-1	miR-16-1	miR-16-1	miR-16-1	miR-16-1	miR-16-1	miR-16-1

Figure 2.6: Template for the qPCR reaction for miRNAs (U6, miR-1, miR27a, miR-133a, miR-133b, miR-155, miR-15, and miR-16-1) in one drug treatment group (n=6).

Yellow=1n, blue=2n, red=3n, green=4n, orange=5n, navy=6n and black= non-template control. Shown on 96 well PCR plates.

The real-time PCR machine was programmed to: 1) 2 mins at 50 °C, 2) 10 mins at 95 °C, 3) 15 secs at 95 °C, 4) 1 min at 60 °C, Repeat steps 3) and 4) 40 times.

2.6.5 Quantifying miRNA real-time PCR analysis

The ΔΔ cycle threshold (CT) values for the Sunitinib, 2-Cl-IB-MECA and NQDI-1 treated groups were compared with the control group. U6 was used as an internal reference. The relative amount of miRNA was calculated using the ΔΔCT method, with CT values for the specific miRNA primers in relation to the CT values of U6 snRNA using the following miRNA ratio formula (Sandhu, 2010).;

$X_0/R_0=2^{CTR-CTX}$

Where; X_0 = original amount of target miRNA

R_0 = original amount of U6

CTR = CT value for U6, and

CTX = CT value for the target miRNA.

2.6.6 Data analysis of miRNA profiles

Fold changes in the miRNA expressions were plotted in bar chart graphs and assessed for statistical differences using ANOVA or students t-test using GraphPad Prism version 5 (GraphPad Software, Inc. USA) and SPSS software (IBM, USA)). All values were expressed as mean ± SEM. P-values ≤0.05 were considered statistically significant.

2.7 Reverse transcription and real-time PCR analysis of MKK7 mRNA in heart tissue

Following Langendorff perfusion, hearts were dissected and the left ventricle tissue was removed and chopped into small pieces. The tissue was transferred into 2 ml RNA/DNA free microfuge tubes and 500 µl of RNAlater (Ambion life technologies, UK) was added to them and stored at -20 °C until required, or the tissue was snap frozen and stored at -80 °C until later use.

2.7.1 mRNA isolation from heart tissue

For RNA isolation 2 different kits were used. The Oligo (dT) cellulose isolation kit (Ambion, UK) for pure mRNA and TRIzol plus RNA purification kit (Invitrogen, UK).

2.7.1.1 Oligo (dT) cellulose mRNA isolation kit

The homogeniser (IKA Overtechnical T25) was cleaned with RNase/DNase free ethanol (Fischer, UK), ZAP solution and RNase free H_20 (Ambion, UK). The RNAlater solution was discarded and 600 µl of lysis buffer solution (Albion life technology, UK) was added to the microfuge tubes. The samples where then homogenised on ice. A volume of 1400 µl dilution solution (Albion life technology, UK) was added to the homogenised solution and was centrifuged at 14,000 rpm using the MIKRO 200R Zentrifugen, Hettich, UK for 15 mins at 4 °C. The supernatant was transferred into fresh RNase/DNase free microfuge tubes. A tube of Oligo (dt) Cellulose (Ambion, UK) was added to the lysate and incubate at room temperature for 15 mins with gentle agitation and rocking. The Oligo cellulose step allows

the hybridization between poly (A) sequences found on most mRNAs and the Oligo (dT) Cellulose.

Next, the samples were centrifuged at 6,000 rpm for 3 mins at room temperature. The supernatant was discarded and the pellet was resuspended in 1 ml of Lysate Wash (Ambion, UK) by vortexing (Vortex-Genie 2, Scientific industries, USA). The lysate/Oligo (dT) cellulose mixture was centrifuged at 6,000 rpm for 3 mins at room temperature. The supernatant was discarded and 600 µl of Lysate Wash was added. The sample was then vortexed to resuspend the pellet.

The lysate/Oligo (dT) cellulose slurry was transferred to a spin column and collection tube and centrifuged at 7,000 rpm for 20 secs. The flow through was discarded and the spin column was transferred to a fresh collection tube. A volume of 100 µl of RNA Storage solution (Ambion, UK) which has been warmed to 68-75 °C was added to the spin column and the mixture was agitated to create a paste like solution and centrifuged for 20 secs at 7,000 rpm. The spin column was left in the same collection tube and 100 µl RNA Storage solution was added again and spun for 20 secs at 7,000 rpm. The collected effluent contained the poly (A) tail linked mRNA.

A volume of 200µl 2x Binding solution (Ambion, UK) was added to the Oligo (dT) cellulose in the spin column and mixed gently. The previously collected poly (A) tail linked mRNA effluent was transferred back to the spin column, vortexed and incubated at 68-75 °C for 5 mins. Next, the solution was incubated at room temperature for 15 mins with gentle agitation. After, the mixture was transferred to a new spin column and fresh collection tube. The tubes were spun at 7,000 rpm for 20 secs and the effluent was discarded.

A volume of 500 µl Wash solution 1 (Ambion, UK) was added to the spin column, which was vortexed and centrifuged at 6,000 rpm for 3 mins and the flow through was discarded twice. Afterwards, the column was washed twice with 500 µl of Wash Solution 2 (Ambion, UK) by vortexing and centrifugation at 6,000 rpm for 3 mins.

The spin column was placed into a fresh collection tube. A volume of 200 µl RNA storage solution (68-75°C) was added. The mixture was agitated and centrifuged at 7,000 rpm for 20 secs. The purified mRNA concentrate was collected from the bottom of the collection tube. Nanodrop (Nanoid Technology, Delaware, USA) at 260 nm was used to determine the amount of purified mRNA. The mRNA was then stored at -80 °C until further analysis.

Generally, the nanodrop was unable to measure the amount of mRNA present. Therefore, we used 10 µl of mRNA for each reverse transcription and also used a second mRNA isolation kit to verify results.

2.7.1.2 Total RNA isolation by the TRIzol plus PNA purification kit.

The homogeniser (IKA Overtechnical T25) was cleaned with RNase/DNase free ethanol (Fischer, UK), ZAP solution and RNase free H_20 (Ambion, UK). Then, 50mg of snap frozen tissue, which had been collected following the Langendorff perfusion experiment was homogenised in 1 ml of TRIzol reagent, Invitrogen (UK). The lysate was then incubated at room temperature for 5 mins to allow full dissociation of nucleoprotein complexes. 200 µl of chloroform was added to the lysate and then shaken vigorously by hand for 15 secs. This was then incubated at room temperature for 2-3 mins. The sample was then centrifuged at 12000 rpm for 15 mins at 4 °C, using the MIKRO 200R Zentrifugen (Hettich, UK). After

centrifugation, the mixture was separated into a lower, red phenol-chloroform phase, an interphase and a colourless upper phase, which contained the RNA.

Approximately 600 µl the upper phase was transferred to a fresh RNase-free tube. The same volume of 70 % ethanol was added and mixed well by vortexing.

Up to 700 µl of the ethanol/RNA solution was transferred to a spin cartridge in a collection tube. This was then centrifuged at 12000 rpm for 15 secs, at room temperature. The flow-through was discarded and spin column was re-inserted into the same collection tube. This was repeated until all of the ethanol/RNA solution had been passed through the spin column.

The total RNA was trapped in the spin cartridge. The spin cartridge was washed firstly with 700 µl of Wash Buffer 1, centrifuged at 12000 rpm for 15 secs. The flow-through was discarded and the spin column was inserted into a new collection tube. Next, the spin column was washed with 500 µl of Wash Buffer 2 and centrifuged at 12000 rpm for 15 secs. The flow-through was discarded and the spin column was re-inserted into the same collection tube. The spin column was again washed with 500 µl of Wash Buffer 2, centrifuged at 12000 rpm for 15 secs, the flow-through was discarded and re-inserted into the collection tube. To dry the spin column, the collection tube and spin column was centrifuged at 12000 rpm for 1 min. The spin column was then inserted into a recovery tube.

100 µl of RNase free water was added to the centre of the spin cartridge and incubated at room temperature for 1 min. The spin tube and the recovery tube were then centrifuged at 14000 rpm for 2 mins at room temperature. The recovery tube contained the purified RNA.

This was then nano-dropped (Nanoid Technology, Delaware, USA) to quantify the amount of total RNA extracted and stored at -80 °C until required.

2.7.2 Reverse transcription PCR reaction:

MKK7 real-time PCR reactions were normalised to GAPDH mRNA expression levels. GAPDH is a house keeping gene, therefore should be expressed at a consistent level.

Primers (all from Invitrogen, Life Technologies, UK):

GAPDH Forward primer: GAACGGGAAGCTCACTGG

GAPDH Reverse primer: GCCTGCTTCACCACCTTCT

MKK7 forward primer: CCCCGTAAAATCACAAAGAAAATCC

MKK7 reverse primer: GGCGGACACACACTCATAAAACAGA

RNase/DNase free microfuge PCR tubes were labelled (one set for MKK7 primers and one for GAPDH) and to each tube for MKK7 or GAPDH the following was added (tables 2.3 and 2.4):

Table 2.3: The recipe for each PCR tube during the reverse transcription and PCR of the MKK7 or GAPDH mRNAs using the Oligo (dT) cellulose mRNA isolation kit.

Multi reverse transcriptase	1 µl
100mM dNTP	0. 2 µl
10x RT buffer	2.5 µl
RNase inhibitor	0.2 µl
Forward primer of target mRNA	1 µl
Reverse primer of target mRNA	1 µl
mRNA (from sample)	10 µl
H_2O	9.1 µl

Table 2.4: the recipe for each PCR tube during the reverse transcription and PCR of the MKK7 or GAPDH mRNAs using the TRIzol plus RNA purification kit

Multi reverse transcriptase	1 µl
100mM dNTP	0. 2 µl
10x RT buffer	2.0 µl
RNase inhibitor	0.2 µl
Forward primer of target mRNA	0.2 µl
Reverse primer of target mRNA	0.2 µl
mRNA 1000ng (from sample)	---
H_2O	Make up to 20µl

The 7500 HT real-time PCR sequence detection system (Applied Biosystems, USA) was programmed to: 30 mins at 16 °C, 30 mins at 42 °C, 5 mins at 85°C and ∞ at 4 °C. Once the mRNA was processed into cDNA it was stored at -20 °C, until required for the next step.

2.7.3 Real-time PCR reaction

The quantitative PCR reactions were performed in duplicate with the SYBR® Green Master Mix, (Life sciences, Ambion, UK), GAPDH and MKK7 primers on real-time PCR machine (7500 HT real-time PCR sequence detection system from Applied Bio systems, USA).

The qPCR plate template (Figure. 2.7) was used to design the layout for the reaction. Duplicates were made for each primer for each sample and Non-template controls (NTC) for each primer (MKK7 and GAPDH) were added to the plate.

	1	2	3	4	5	6	7	8	9	10	11	12
A	MKK7	MKK7	MKK7	MKK7			GAPDH	GAPDH	GAPDH	GAPDH		
B	MKK7	MKK7	MKK7	MKK7			GAPDH	GAPDH	GAPDH	GAPDH		
C	MKK7	MKK7	MKK7	MKK7			GAPDH	GAPDH	GAPDH	GAPDH		
D	MKK7	MKK7	MKK7	MKK7			GAPDH	GAPDH	GAPDH	GAPDH		
E	MKK7	MKK7	MKK7	MKK7			GAPDH	GAPDH	GAPDH	GAPDH		
F	MKK7	MKK7	MKK7	MKK7			GAPDH	GAPDH	GAPDH	GAPDH		
G	MKK7	MKK7	MKK7	MKK7			GAPDH	GAPDH	GAPDH	GAPDH		
H	MKK7	MKK7					GAPDH	GAPDH				

Figure 2.7: Real-time PCR template.

Yellow: normoxic control samples, Red: Sunitinib (1µM) samples, Blue: NQDI-1 (2.5 µM) samples, Green: NQDI-1 (2.5 µM) with Sunitinib (1 µM) samples,

Black: Non-template Control samples (all in duplicate).

For each qPCR reaction, the following was added: (per specific primer set).

Table 2.5: The recipe for each real-time PCR well during the experiment.

cDNA	4 µl
Forward Primer	1 µl
Reverse Primer	1 µl
SYBER green	10 µl
H_2O	4 µl

The real-time PCR machine was programmed to: 1) 2 mins at 50°C, 2) 10 mins at 95°C, 3) 15 secs at 95°C, 4) 1 min at 60°C. Steps 3) and 4) were repeated 40 times.

2.7.4 Quantifying the changes in MKK7 mRNA levels in the heart after Sunitinib with and without NQDI-1 treatment

The ΔΔ cycle threshold (CT) values for the drug treatment groups were compared to the control group. The data obtained was analysed using SDS software. The mRNA data was then analysed using the comparative ΔΔCT method (Sandhu, 2010). GAPDH mRNA was used as an internal reference to normalise MKK7 mRNA. The relative amount of mRNA was calculated with the CT values for the different primers in relation to the CT values of GAPDH mRNA using the following mRNA ratio formula;

$X_0/R_0=2^{CTR-CTX}$

Where; X_0 = original amount of target mRNA

R_0 = original amount of GAPDH

CTR = CT value for GAPDH, and

CTX = CT value for the MKK7 mRNA.

2.7.5 MKK7 mRNA measurement data analysis

Fold changes in the mRNA expressions were presented in bar chart graphs and assessed for statistical differences using ANOVA or Students t-test using GraphPad Prism version 5 (GraphPad Software, Inc. USA) and SPSS software (IBM, USA). All values were expressed as mean ± SEM. P-values of $P < 0.05$ was considered statistically significant.

2.8 MTT assay for analysis of cytotoxicity

2.8.1 MTT assay background

Similar to the TTC tissue staining assay, the MTT assay is based on the conversion of a tetrazolium salt, MTT (3- [4, 5 –dimethylthiazol-2-yl]-2, 5 diphenyl tetrazolium bromide) into formazan crystals by functioning mitochondria. Within the mitochondria succinate dehydrogenase cleaves the tetrazolium ring of MTT, leaving insoluble purple formazan. The formazan concentration can be measured by optical density.

In principle, when mitochondria are active MTT is reduced by dehydrogenase enzymes, which produces a colour change in the solution to purple. Therefore, the MTT assay measures cell viability by assuming mitochondrial activity is present in live cells. An increase in formazan crystals production and therefore a stronger purple colour represents a higher

number of viable cells. Lack of formazan crystals and a purple colour denotes low cell viability levels.

2.8.1.1 HL60 cell MTT assay protocol

Human leukaemia cancer cell line (HL60) were cultured in RPMI 1640 media without L-Glutamine, which was supplemented with 10 % foetal bovine serum (FBS), 2 mM L-glutamine, HEPES and 0.1 % antibiotic solution (10 000 U/ml penicillin and 10 000 µg/ml streptomycin) (Biosera, UK) in a T75 cm^2 flask and incubated at 37 °C, 95 % O_2 and 5 % CO_2 in a Nuaire incubator (triplered laboratory technology, UK). 100 µl of HL60 cells were transferred to a 96-well plate at a cell density of $1x10^5$ cells/ml and then incubated over night at 37°C in the Nuaire incubator. 20 µl of filtered, sterile drug was added to each well. The specific drug treatments used are described in chapters 4 and 5.

The 96-well plated containing the drug treated HL60 cells was then incubated for 24 hrs at 37 °C in the Nuaire incubator. The plate was removed from the incubator and 50 µl of filtered, sterile MTT solution (5 mg MTT powder/ml PBS) was added to each well. The 96-well plate was then incubated for 24 hrs at 37 °C in the Nuaire incubator. Once removed from the incubator, the 96-well plate was centrifuged at 1000 rpm (using a plate centrifuge). The supernatant was removed and discarded. Then, 50 µl of DMSO was added to each well to lyse the cells and release the purple formazan crystals. The level of formazan created was detected by spectrophotometry on the plate reader (Anthos Labtech AR 2001 Multiplate Reader (*Anthos Labtec* Instruments, Austria) at 492 nm.

HL60 cells were used in these studies because Teng et al. (2013) previously demonstrated that Sunitinib induces G1 cell cycle arrest and increases levels of apoptosis in HL60 cells (Teng et al. 2013).

2.8.2 Quantification of the MTT assay

The mean absorbance of each treatment group was obtained and the absorbance for the drug alone was subtracted from this. This was calculated as a percentage of the mean absorbance of the control group and plotted using GraphPad Prism (version 5.03, GraphPad Software, Inc. USA).

2.9 Western blot for the determination of p-MKK7, p-ASK1, p-JNK and p-PKCα

2.9.1 Western blot background

The western blot technique is an immunoblotting method used to separate and identify proteins. Firstly, proteins are isolated and purified from tissue or cells. The protein is then denatured and held in its primary structure in a solution. The protein samples are then separated by size and charge by sodium dodecyl sulphate-polyacrylamide gel electrophoresis (SDS-PAGE). Once fully separated all proteins of the same weight will lie in the same band across the gel. The proteins are then electrophoretically transferred to a PVDF or cellulose membrane, where the protein of interest can be probed for by primary anti-bodies. For detection, a horseradish peroxidase (HRP) tagged secondary antibody binds to the primary antibody. A substrate for the HRP is added and a signal is generated. From

the signal intensity, it is possible to quantify the protein of interest (Gershoni and Palade 1982).

The western blot technique is used in research to study the level of protein activation or presences of a protein in various tissues and cells. This immunoblotting technique is essential in clinical diagnosis and quantifying gene products.

2.9.2 Protein isolation

2.9.2.1 Total protein isolation from heart tissue

The Langendorff system was used to collect tissue samples for western blot analysis as in the TTC protocol. However, once the experiment was terminated the left ventricles was removed, snap frozen in liquid nitrogen and stored at -80 °C until required. The left ventricular tissue was lysed in lysis buffer (NaCl 0.1 M, Tris base 10 µM, EDTA 1 mM, Sodium pyrophosphate 2 mM, NaF 2 mM, β-glycaophosphate 2 mM, AEBSF 0.1 mg/ml, protease cocktail tablet 1/1.5, pH 7.6) using a homogeniser (IKA Overtechnical T25). The homogenised samples were then centrifuged at 11,000 rpm at 4 °C for 10 mins. The supernatant was collected. From this, protein concentration was determined using nanodrop (Nanoid Technology, Delaware, USA) at 280nm. Protein was then diluted 1:1 with 2X Laemmili Sample buffer (125 mM Tris-HCl [pH 6.8], 20 % Glycerol, 4 % SDS, 10 % 2-mercaptoethanol, 0.004 % bromophenol blue, pH 7.4) to give 90 mg/ml of protein per sample, by heating to 95°C for 5 mins. The samples were stored at -20 °C until further analysis.

2.9.2.2 Protein isolation from HL60 cells

HL60 cells were plated at $5x10^6$ cells/well into a 6 well plate. The treated cells were transferred to centrifuge tubes and centrifuged at 900 rpm for 5 mins. The supernatant containing media and drug was removed and 500 µL of PBS was added. The cells were resuspended and centrifuged again at 900 rpm, the PBS was discarded (this step was repeated). A volume of 500 µl of ice cold lysis buffer (25 mM HEPES, 100 mM NaCl, 1 mM EDTA, 10 % (v/v) Glycerol, 1 % (v/v) Triton X-100 and 1 protease inhibitor tablet per 10 ml of buffer). The cells were then incubated on ice for 30 mins. The cells were then centrifuged for 20 mins at 12000 rpm at 4 °C. The supernatant (containing the isolated protein) was transferred to a fresh Eppendorf tube. The amount of protein isolated was quantified using a Nanodrop. The isolated protein was then diluted 1:1 with 2X Laemmili sample buffer and heated to 95 °C for 5 mins. The protein was ready to use at this stage, but could also be stored at -20 °C until required.

2.9.3 Gel electrophoresis

80 mg/ml of protein was loaded on to a pre-made gel (4–15 % Mini-PROTEAN® TGX™ Gel for MKK7, any KDa Mini-PROTEAN® TGX™ Gel for JNK and PKC, 8-20 % Mini-PROTEAN® TGX™ Gel for ASK1 (BioRad, UK) using gel loading tips (Fischer, UK). Markers used: Precision Plus Protein Kaleidoscope and Biotinylated Protein Ladder (Cell Signalling Technologies, UK) with bands of known molecular weights to allow identification of the target protein. The gel was placed into a Mini-Protean 3 electrode assembly unit, into a clamping frame and lowered into a Mini Tank. The tank contained running buffer (Glycine 0.2 M, SDS 3.5 mM, and Tris base 0.25 M). Running buffer was also added to the inner chamber of the system to allow a

current to flow. Using a BioRad mini protean II system (Bio-Rad, UK) the proteins in samples were separated by electrophoresis (50 mA, 200 V for 60 mins) (Figure. 2.8).

Figure 2.8: Image of protein sample loading on to a gel and the start of electrophoresis using the BioRad mini Protean ii system.

2.9.4 Protein transfer from gel onto a PVDF membrane

Separated proteins were electrophoretically transferred onto a Bond-P Polyvinylidene Di fluoride (PVDF) (Trans-Blot® Turbo™ PVDF membrane, Bio-Rad, UK) by the Trans-Blot Turbo transfer system (Bio-Rad, UK). This was assembled in accordance to the manufacturer's guidelines. The Setting used was for the transfer of mixed molecular weighted proteins (25 V, 1.3 A for 7 mins per 2 mini gels).

2.9.5 Probe for target phosphorylated protein

PVDF membranes were blocked with 5 % milk (powder) in (Tris buffered saline with tween) TBS-T for 1 hour on an orbital shaker. Membranes were then incubated overnight in 1:1000

Phosphorylated protein antibody (MKK7, ASK1, JNK or PKCα) antibodies in 5 % BSA in TBS-T at 4 °C with gentle agitation on an orbital shaker. Membranes were washed with TBS-T 3 times for 5 mins to remove any unbound MKK7 antibody. Next, membranes were incubated with secondary antibody; a HRP tagged Anti-rabbit IGg 1:10 000 and anti-biotin antibody 1:7 500 dilution (Cell Signalling Technology, UK) in 5 % milk in TBS-T for 1 hour. Membranes were again washed with TBS-T 3 times for 5 mins to remove unbound secondary antibody.

2.9.6 Protein immuno-detection

Protein detection carried out by enhanced chemi-luminescence (ECL). Membranes were placed on acetate sheet and 1ml of 1:1 mixture of Luminol/Enhancer and Stable Peroxide Buffer from the Super Signal West Femto kit (PIERCE biotechnologies, UK) was added. This was then incubated in the dark for 5 mins at room temperature. Excess solution was dripped off the acetate sheet and then the membrane was placed into the Chemidoc MP imaging system (Bio-Rad, UK). The system was programmed to chemi blots and an automatic detection of the oxidation reaction between horseradish peroxidase and luminol which produced a low intensity light at 428 nm.

2.9.7 Probing for target total protein and band detection

Membranes were boiled for 5 mins to remove bound antibodies. Membranes were then blocked with 5 % milk in TBST for 1 hour at room temperature. The membranes were then incubated with Total-protein Antibody (of MKK7, ASK1, JNK or PKC) (Cell Signalling Technology, UK) over night, with gentle agitation at 4 °C. Membranes were then washed for 5 mins with TBST, 3 times followed by incubation in the secondary antibody (1:10,000 dilution in the antibody dilution buffer) with Anti-rabbit antibody HRP linked IgG and HRP linked anti-

biotin antibody on an orbital shaker at room temperature for 1 hour. The membrane underwent a further 3 washes with TBST (for 5 mins) before being analysed again by ECL.

2.9.8 Quantifying Western blot results

Phosphorylated protein (MKK7, ASK1, JNK or PKCα) levels were normalised to Total protein levels of the same protein (total MKK7, ASK1, JNK or PKC). Results were expressed as a percentage of the density of phosphorylated protein (MKK7, ASK1, JNK or PKCα) relative to the density of total protein (MKK7, ASK1, JNK and PKC) using Image Lab 4.1 from BioRad (UK). Significance of the data was measured by ANOVA in the SPSS program (IBM, USA). P-values <0.05 was noted as being significant.

2.10 Adult rat cardiomyocyte isolation

Cardiomyocytes were enzymatically isolated from 12 week old Sprague Dawley rats, following cervical dislocation and heart excision. Hearts were mounted onto a modified Langendorff apparatus and perfused with a modified Krebs buffer (NaCl 116 mM, KCl 5.4 mM, $MgSO_4.7H_2O$ 0.4 nM, Glucose 10 mM, Taurine 20 mM, Pyruvate 5 mM, $Na_2HPO_4.2H_2O$ 0.9 mM and $NaHCO_3$ 25 mM: dissolved in ddH_2O). The buffer was the oxygenated with 95 % O_2 and 5 % CO_2 at 37°C to maintain a pH of 7.4. Once the heart had stabilised, a collagenase buffer (0.03mg Liberase (TH Research Grade, Roche) in 65 ml of modified Krebs buffer plus in 65 ml and 1 M $CaCl_2$, pH 7.4) was administered 10 mins later to the heart at a rate of 7.5 ml/min for approximately 7 mins with a peristatic pump. The heart was then detached from the apparatus. The atria were removed and discarded. The ventricles were chopped and mechanically digested in the collagenase buffer.

Nylon mesh was used to filter cells from undigested tissue into restoration buffer (NaCl 116 mM, KCL 5.4 mM, $MgSO_4$ 0.4 mM, glucose 10 mM, Taurine 20 mM, Pyruvate 5 mM, $NaHPO_4$ 0.9 mM, Creatine 5 mM, $CaCl_2$ 50 µM, 2 g BSA and 1% antibiotic solution (10 000 U/ml penicillin and 10 000 µg/ml streptomycin), pH 7.4 at 37 °C). The $CaCl_2$ concentration was increased to regular intervals to a final concentration of 1.25 mM.

Cardiomyocytes were counted using a haemocytometer and resuspended in restoration buffer at a density of 100,000 cells/ml. The cells were then aliquoted into a 24 well plate (1 ml per well) and the treatment groups are described in chapter 5. The cells were then incubated at 37 °C at normoxic conditions in the Nuaire DH autoflow CO_2 air jacketed incubator (Caerphilly, UK) for 2 hrs.

2.11 Flow cytometry

Flow cytometry is a widely used method for analysing the expression of cell surface and intracellular molecules. Rapid measurements of illuminated particles or cells are made as they flow in a fluid stream past a sensing point. The flow cytometer has the ability to count cells and record the light scattering (both optical and fluorescent) feature of each of the cells being investigated. This may be as a result of cell staining with dyes or fluorescently tagged monoclonal antibodies, which target extracellular surface proteins or intracellular proteins of interest. As the amount of fluorescent probe present in a cell is proportional to the level of molecule or protein of interest, it is possible to quantify the relative amount of molecule or protein present in a number of cells. Light from a laser beam acts as an excitation source. As the light hits the fluorescent particle, the fluorophore is excited and emits a different wavelength of light. The intensity of the light emitted is measured for each

cell by the flow cytometer. The level of light emitted is directly proportional to the level of target molecule or protein present.

In addition, the light scattering caused by a cell can provide structural and morphological information of cells. This allows the flow cytometer to distinguish between cell types.

2.11.1 Flow cytometry analysis for p-MKK7 in drug treated cardiomyocytes

Following cardiomyocyte isolation, the drug treated cells were transferred into labelled 1.5 ml microfuge tubes and centrifuged at 1,200 rpm for 2 mins. The supernatant was discarded and the cell pellets were resuspended in 250 µl of 3 % formaldehyde in phosphate buffered saline (PBS). Cells were then fixed for 10 mins at 37 °C and then put on ice for 1 min before being centrifuged at 1,200 rpm for 2 mins. The supernatant was removed and 250 µl of ice cold methanol (90 %) was added. The cells were incubated on ice for 30 mins and were stored at -20 °C until required.

Next, the cells were washed with incubation buffer (0.5 % BSA in PBS) twice and blocked for 10 mins with incubation buffer. Then cells were centrifuged at 1,200 rpm for 2 mins.

The cells were then stained with phosphor-MKK7 antibody at a 1:100 concentration and a fluorescent conjugated secondary antibody (Alexa flour@488 conjugated secondary antibody) (1:100) was added. Cells were incubated in the dark for 1 hour at room temperature.

The cells were then centrifuged at 1,200 rpm for 2 mins, supernatant removed and then washed with incubation buffer twice. Afterwards, they were spun a final time at 1,200 rpm

and the pellet was resuspended in 500 µl PBS. Samples were analysed using flow cytometry on the FL1 channel (FACS, Becton Dickinson, Oxford, UK).

2.11.2 Quantifying Flow cytometry results

Expression levels were measured using flow cytometry. The flow cytometry machine shines a laser beam on to the cells and the fluorophore attached to the secondary antibody is excited and emits a light of a different wave length, which only happens when it is bound to the conjugated MKK7 secondary antibody. Alexa Fluor is excited by a 488 nm laser and emits light at 519 nm. The flow cytometry machine then detects the intensity of florescence emitted at 519 nm and this is directly proportional to the level of activated MKK7 within the cardiomyocytes. Total MKK7 levels were also determined using the same protocol to allow normalisation of samples.

2.11.3 Data analysis

Results were expressed as mean % of total MKK7 levels and presented as bar chart graphs in GraphPad prism (version 5.03, GraphPad Software, Inc. USA). Data was analysed using One-way ANOVA with the LSD post hoc test or Students t-test when only 2 groups are being compared by the SPSS (IBM, USA) program.

3. Ageing results in different responses to Sunitinib induced cardiotoxicity: Investigating the involvement of MKK7 and miRNAs in Sunitinib cardiotoxicity.

3.1 Abstract

The anti-cancer drug, Sunitinib is linked to adverse cardiovascular events. However, its impact on ageing is under investigated. Mitogen activated kinase kinase 7 (MKK7) has been shown to be involved in cardiac injury development. Sunitinib-induced cardiotoxicity in 3, 12 and 24 month old male Sprague-Dawley rats and the associated involvement of MKK7 was investigated.

Isolated Langendorff-perfused hearts were treated with Sunitinib (1 μM) for 125 min, whilst cardiac function and infarct size were measured. Left ventricular cardiac samples were analysed by qRT-PCR for expression of MKK7 mRNA or cardiac injury associated microRNAs (miR-1, miR-27a, miR-133a and miR-133b). Western blot analysis measured MKK7 phosphorylation (p-MKK7).

Infarct size was significantly increased in all age groups. Haemodynamic alterations were observed following Sunitinib administration, left ventricular developed pressure (LVDP) was decreased in all age groups, while heart rate (HR) was decreased only in the 3 month and 12 month groups.

Sunitinib treatment decreased miR-27a levels in all age groups, while miR-133a and miR-133b levels were increased in 3 month, but decreased in the 24 month groups. MKK7 mRNA levels and p-MKK7 levels were significantly decreased in the 3 month group following Sunitinib treatment. However, MKK7 mRNA levels were increased in the 24 month group and p-MKK7 levels were increased in 12 month group following Sunitinib treatment.

This study highlights the complexity of drug-induced cardiotoxicity in the ageing heart. Plus, the involvement of cardiac injury associated miRNAs and MKK7 in age related response to Sunitinib-induced cardiotoxicity.

3.2 Introduction

Life expectancy has increased substantially due to a combination of medical advancements and improved quality of life (Chetty et al. 2016). With the ever-expanding elderly population, the number of elderly patients with cancer is unfortunately increasing (Torre et al. 2015).

The median age of patients diagnosed with cancer is 66 years, and the risk of developing cancer increases with age in both males and females (Stewart and Wild 2017). Due to ageing of the population and the cardiotoxic nature of cancer treatment, there is an increasing number of elderly patients with cancer and comorbid cardiovascular diseases (Atkinson et al. 2007). It is therefore vital to unravel the pathways linked to development of cardiovascular diseases during anti-cancer treatment in elderly cancer patients.

Ageing of the heart involves progressive deteriorations in its structure and function, and is a leading risk factor for cardiovascular morbidity and mortality (Hagström et al. 2016). In

particular, ageing of the heart is linked with left ventricular hypertrophy, diastolic dysfunction, and valve degeneration, increased cardiac fibrosis, and decreased maximal exercise capacity (Dai, Rabinovitch and Ungvari 2012, Morita et al. 2009, Shioi and Inuzuka 2012). Needless to say, ageing of the heart causes it to become extremely vulnerable to external stress, such as cardiotoxic anti-cancer therapy.

Sunitinib is a multi-targeted TKI used in the treatment of many forms of cancer (Le Tourneau, Raymond and Faivre 2007). Sunitinib inhibits cellular signalling associated with tumour formation by targeting multiple RTKs. Sunitinib inhibits TKs by competitively binding to the ATP-binding site domain of a number of receptor tyrosine kinases, notably: VEGFR 1-3 and PDGFR α and β, (O'Farrell et al. 2003). Binding to the ATP-binding domain causes the inhibition of dysregulated or over expressed TKs involved in the regulation of angiogenesis cell proliferation and cell survival (Ferrara and Kerbel 2005, Mendel et al. 2003). However, due to Sunitinib's broad molecular targets and a lack of kinase selectivity, there are many side effects associated with its use, including cardiotoxicity. Sunitinib induced cardiotoxicity causes adverse effects in cardiomyocytes (Raschi and De Ponti 2012), which can lead to cardiac ischaemia and produce arrhythmias in the heart (Cohen et al. 2011). Also, in the clinic, left ventricular hypertrophy, hypertension and heart failure development have been reported in response to Sunitinib treatment (Gupta and Maitland 2011).

The stress activated protein, MKK7, belongs to the MAPK kinase superfamily, which are involved in proliferation, differentiation, apoptosis and tumorigenesis (Schramek et al. 2011, Chang and Karin 2001, Sundarrajan et al. 2003).

MKK7 contains a highly-conserved ATP binding domain (Song et al. 2013). Interestingly, Sunitinib is an ATP analogue and competitively inhibits the ATP binding domain of its target

proteins (Roskoski 2007, Shukla et al. 2009). Hence, it might be possible that Sunitinib could have an inhibitory effect on the MKK7 signalling cascade. As inhibition of MKK7 activity has been directly correlated with an increase in cardiomyocyte damage (Liu et al. 2011), it would be interesting to assess changes in MKK7 expression levels, in the presence of Sunitinib, at various age stages. Establishing an age dependant involvement of MKK7 during Sunitinib-induced cardiotoxicity would enhance our understanding of cardiac ageing pathways, during stress stimuli and could lead to reform of anti-cancer therapy, by implementing effective adjunct therapy.

This study investigates for the first time the involvement of the MKK7 pathway in the Sunitinib-induced cardiotoxicity at various age stages via the assessment of cardiac function and injury on ageing rat hearts using a Langendorff perfused heart model. Three age groups of Sprague-Dawley rats were used: *Young* (3 months), *Middle-aged* (12 months) and *Elderly* (24 months). Furthermore, the differential expression patterns of cardiotoxicity-linked: miRNAs miR-1, miR-27a, miR-133a and miR-133b, is determined within the specific age groups.

The miRNAs investigated during this study (i.e. miR-1, miR-27a, miR-133a and miR-133b) produce differential expression patterns during the progression of heart failure (Akat et al. 2014, Tijsen, Pinto and Creemers 2012). Changes in cardiac injury specific miRNA profiles could indicate the level of Sunitinib-induced cardiac injury and whether age contributes to the level of cardiac injury generated by Sunitinib. Plus, the stress signalling molecule, MKK7 was investigated at an mRNA and protein level, to identify whether it is involved in Sunitinib-induced cardiotoxicity in all age groups.

3.2.1 Hypothesis

The use of the isolated Langendorff heart model will demonstrate that Sunitinib treatment will have adverse effects on the haemodynamic function of the heart, increase in the infarct size to risk ratio and effect the expression profiles of miRNAs associated with myocardial injury compared to normoxic controls in all age groups. Also, the level of cardiotoxicity will differ between age groups.

3.3 Materials and methods

3.3.1 Materials

Sunitinib malate and triphenyl-tetrazolium chloride were purchased from Sigma Aldrich (UK) and dissolved in dimethyl sulphoxide (DMSO) and stored at -20 °C. Krebs perfusate salts were from Fisher Scientific (UK). Ambion MicroPoly(A)Purist kit, Ambion mirVana miRNA Isolation Kit, Reverse Transcription Kit, Applied Biosystems MicroRNA Reverse Transcription Kit, TaqMan Universal master mix II (no UNG), MKK7 mRNA primers, Applied Biosystems primers assays (U6, rno-miR-1, hsa-miR-27a, hsa-miR-133a, and hsa-miR-133b) were purchased from Life Technologies (USA). The iTaq Universal SYBR Green Supermix was purchased from BioRad (UK). Phospho-MKK7 (Ser271/Thr275), Total MKK7 rabbit mAb antibodies and anti-rabbit IgG, HRP-linked antibody and anti-biotin, HRP-linked antibody were purchased from Cell signalling technologies (UK).

3.3.2 Animals and Ethics

Adult male Sprague-Dawley rats (300-350 g in body weight); were purchased from Charles River UK Ltd (UK) and housed suitably, received humane care and had free access to

standard diet according to “The Guidance on the Operation of the Animals (scientific procedures) Act of 1986”. 30 rats were aged until 12 month old (500-600g in body weight) and 30 rats were aged until 24 months old (650-750g in body weight). Animals were selected at random for drug treatment groups and the collected tissue was blinded for infarct size assessment. The experiments were performed after approval of the protocol by the Coventry University Ethics Committee. All efforts were made to minimize animal suffering and to reduce the number of animals used in the experiments. A total of 79 animals were used for this study and the data from 64 rats were included, while data from 15 rats were excluded from analysis due to the established haemodynamic exclusion criteria.

3.3.3 Langendorff perfusion model

Rats were sacrificed by cervical dislocation and death was confirmed by exsanguination (Schedule 1 Home Office procedure) and the hearts were rapidly excised and placed into ice-cold Krebs Henseleit (KH) buffer (118.5 mM NaCl, 25 mM $NaHCO_3$, 4.8 mM KCl, 1.2 mM $MgSO_4$, 1.2 mM KH_2PO_4, 1.7 mM $CaCl_2$, and 12 mM glucose, pH7.4). The hearts were mounted onto the Langendorff system and retrogradely perfused with KH buffer. The pH of the KH buffer was maintained at 7.4 by gassing continuously with 95 % O_2 and 5 % CO_2 and maintained at 37 ± 0.5 °C using a water-jacketed organ chamber. The left atrium was removed and a latex iso-volumic balloon was carefully introduced into the left ventricle and inflated up to 5-10 mmHg. Functional recordings (LVDP and HR) were taken via a physiological pressure transducer and data recorded using Powerlab, AD Instruments Ltd. (UK). Coronary flow (CF) was measured by collecting and measuring the volume of perfusate

for 1 minute, thereafter it was disposed of. All haemodynamic parameters were measured at 5 minute and then 15 minute intervals after 35 minutes of drug treatment.

Each Langendorff study was conducted for 145 minutes: a 20 minute stabilisation period and 125 minutes of drug or vehicle perfusion in normoxic conditions. Generally, the hearts became stable after 10 minutes, therefore all haemodynamic parameters were normalised to the last 10 minutes of the stabilisation period to take into account the variations between individual starting HR, LVDP and CF levels. Hearts were included in the study with a LVDP between 80-150 mmHg, a HR between 225-325 beats per minute, and a CF between 3.5-12.0 ml/g (weight of the rat heart) during the stabilisation period. Haemodynamic effects are presented as a percentage of the mean stabilisation period for each parameter to allow clear comparison across drug groups. The maximal change in LVDP, HR, and CF were calculated by calculating mean ± SEM at the specific time points in Control and Sunitinib treated hearts in all 3 age groups. The single time point showing the maximal drop or increase in LVDP, HR, and CF was selected from this calculation.

Sunitinib malate (1 µM) was administered throughout the perfusion period. The dose of 1 µM Sunitinib was chosen in line with previous studies (Henderson et al. 2013). Langendorff perfused hearts treated with vehicle (i.e. DMSO) were recorded as Control group. The hearts were then weighed and either stored at -20 °C for TTC staining or the left ventricular tissue was dissected free and immersed in RNAlater from Ambion (USA) for qRT-PCR or snap frozen by liquid nitrogen for Western blot analysis.

3.3.4 Infarct size analysis

Frozen whole hearts were sliced into approximately 2 mm thick transverse sections and incubated in 0.1 % TTC solution in phosphate buffer (2 ml of 100 mM $NaH_2PO_4.2H_2O$ and 8 ml of 100 mM NaH_2PO_4) at 37 °C for 15 minutes and fixed in 10% formaldehyde (Fisher Scientific, UK) for 4 hours. The risk zone and infarct areas were traced onto acetate sheets. The tissue at risk stained red and infarct tissue appeared pale. The acetate sheet was scanned and ImageTool from UTHSCSA software (USA) was used to measure the area of infarct and the area of risk. A ratio of infarct to risk size was calculated (as a percentage) for each slice. An average was taken of all of the slices from each heart to give the percentage infarct size of the whole heart. The mean of infarct to risk ratio for each heart was normalised to heart weight and the mean ± SEM for each treatment and age group was plotted as a bar chart. The infarct size determination was randomised and blinded.

3.3.5 Analysis of miRNA expression profiles

The miRNA was isolated from left ventricular tissue using the *mir*Vana miRNA Isolation Kit. The miRNA quantity and quality were measured by NanoDrop from Nanoid Technology (USA). A total of 500 ng miRNA was reverse transcribed into cDNA using primers specific for housekeeping reference RNA U6 snRNA and target miRNAs: rno-miR-1, hsa-miR-27a, hsa-miR-133a or hsa-miR-133b (please note all human hsa-miRNAs assays are compatible with rat samples) using the MicroRNA Reverse Transcription Kit according to the manufacturer's instructions. The reverse transcription quantitative PCR reaction was performed with the following setup: 16 °C for 30 min, 42°C for 30 min and 85 °C for 5 min and ∞ at 4°C. The qRT-PCR was performed using the TaqMan Universal PCR Master Mix II (no UNG) protocol

on the 7500 HT Real Time PCR sequence detection system from Applied Biosystems (USA). A 20µl reaction mixture containing 100 ng cDNA, specific miRNA primer assays mentioned above and the TaqMan Universal PCR Master Mix was used in the qRT-PCR reaction in triplicates. A non-template Control was included in all experiments. The real time PCR reaction was performed using the program: 1) 2 minutes at 50°C, 2) 10 minutes at 95°C, 3) 15 seconds at 95°C, 4) 1 minute at 60°C. Steps 3) and 4) were repeated 40 times. Analysis of qRT-PCR data of miRNAs was performed using the Ct values for U6 snRNA as reference for the comparison of the relative amount of miRNAs (rno-miR-1, hsa-miR-27a, hsa-miR-133a and hsa-miR-133b). The values of each of the miRNA was calculated to compare their ratios. The formula used was $X_0/R_0=2^{CTR-CTX}$, where X_0 is the original amount of target miRNA, R_0 is the original amount of U6 snRNA, CTR is the CT value for U6 snRNA, and CTX is the CT value MKK7 mRNA (Sandhu, Ansar and Edvinsson 2010). Averages of the Ct values for each sample group (Control and Sunitinib treated hearts) and each individual primer set were calculated and bar charts were plotted with mean ± SEM. The mean of the Control group was set as 1 for all miRNAs.

3.3.6 Measurement of MKK7 mRNA expression

Total mRNA was extracted from left ventricular tissue using The Ambion MicroPoly (A) Purist kit. Extracted mRNA was processed directly to cDNA by reverse transcription using Reverse Transcription Kit with the respective primers for MKK7 (MKK7 forward primer: CCCCGTAAAATCACAAAGAAAATCC and MKK7 reverse primer: GGCGGACACACACTCATAAAACAGA) and housekeeping gene GAPDH (GAPDH Forward primer: GAACGGGAAGCTCACTGG and GAPDH Reverse primer: GCCTGCTTCACCACCTTCT) according to the instructions from the manufacturer. The reverse transcription PCR reaction

was performed with the following setup: 16 °C for 30 minutes, 42°C for 30 minutes and 85 °C for 5 minutes. The qRT-PCR reactions were performed with the iTaq Universal SYBR Green Supermix from, GAPDH and MKK7 mRNA primer sets on the 7500 HT Real Time PCR machine from Applied Biosystems (USA) using the program: 1) 2 minutes at 50°C, 2) 10 minutes at 95°C, 3) 15 seconds at 95°C, 4) 1 minute at 60°C. Steps 3) and 4) were repeated 40 times.

Analysis of qRT-PCR data of MKK7 mRNA were performed using the Ct values for GAPDH mRNA as reference for the comparison of the relative amount MKK7 mRNA. The formula used was $X_0/R_0=2^{CTR-CTX}$, where X_0 is the original amount of MKK7 mRNA, R_0 is the original amount of GAPDH mRNA, CTR is the CT value for GAPDH mRNA, and CTX is the CT value for MKK7 mRNA (Sandhu, Ansar and Edvinsson 2010). Averages of the Ct values for each sample group (Control and Sunitinib treated hearts) and MKK7 was calculated and bar charts were plotted with mean ± SEM. The mean of the Control group was set as 1 for the MKK7 mRNA study.

3.3.7 Western blot detection of phosphorylated MKK7

A total of 50 ± 5 mg of the frozen left ventricular tissue was lysed in lysis buffer (NaCl 0.1 M, Tris base 10 µM, EDTA 1 mM, sodium pyrophosphate 2 mM, NaF 2 mM, β-glycaophosphate 2 mM, 4-(2-Aminoethyl) benzene sulfonyl fluoride hydrochloride (0.1 mg/ml, 1/1.5 of protease cocktail tablet) using a IKA Overtechnical T25homogeniser at 11,000 RPM. The supernatant was measured for protein content using NanoDrop from Nanoid Technology (USA). Then 80 µg of protein was loaded to 4–15 % Mini-Protean TGX Gel from BioRad (UK) and separated at 200 V for 60 minutes. After separation, the proteins were transferred to

the Bond-P polyvinylidene difluoride membrane from BioRad (UK) by using the Trans-Blot Turbo transfer system from BioRad (UK) and probed for the Phosphorylated (Ser^{271}/Thr^{275})-MKK7 (p-MKK7). The blots were stripped by boiling and the PVDF membrane was used for total MKK7. The relative changes in the p-MKK7 protein levels were measured and corrected for differences in protein loading as established by probing for total MKK7.

For Western blot analysis, phosphorylated antibody levels were normalised to total antibody levels in order to correlate for unequal loading of protein and differential blot transfer and to identify the level of active versus inactive protein levels. Results were expressed as a percentage of the density of phosphorylated protein relative to the density of total protein using Image Lab 4.1 from BioRad (UK).

3.3.8 Data analysis and statistics

Results are presented as mean ± standard error of the mean (SEM). The significance of all data sets were measured by the IBM SPSS program (USA) or GraphPad Prism version 5 (USA) as described in the figure legends. P-values <0.05 were considered statistically significant.

3.4 Results

3.4.1 Haemodynamic parameters LVDP, HR and CF

In this study, we recorded the LVDP, HR, and CF haemodynamic parameters to determine whether 1µM Sunitinib produces signs of cardiac dysfunction during a 125 minute Langendorff perfusion in 3 month, 12 month and 24 month Sprague-Dawley rat hearts (Tables 3.1-3.3, Figures 3.1-3.3). Raw data for each parameter can be found in Tables 3.1-

3.3. Due to variations within control experiments between the age groups, the raw data has also been normalised to the stabilisation period in figures 3.1-3.3.

3.4.1.1 Left Ventricular Developed Pressure

The raw data demonstrated that LVDP (mmHg) varied between age groups. There was a tendency for the 12 month control group to have a higher LVDP compared to both 3 month and 24 month controls. This difference was significant at many of the time points (Table 3.1). Also, the 12 month group treated with Sunitinib was found to have a significantly higher LVDP compared to both 3 month and 24 month controls at many of the time points (Table 3.1).

When drug treatment groups were normalised to the stabilisation period, Sunitinib treatment significantly decreased LVDP (% of stabilisation period) in the 3 month and 24 month age groups compared to their group controls (Figures 3.1 i-iii). There was also a tendency for a decline in LVPD in the 12 month group treated with Sunitinib compared to control (this was significant at 125 mins when a Student's T-test was carried out). The time points at which significant difference in LVDP occurred between Control and Sunitinib groups in the 3 age groups can be found in the appendices (Table 0.1). Sunitinib treatment caused a maximum % drop in LVDP at the following time points for each age group: 125 min in the 3 month group (Control: 85.26 ± 3.72 %; Sunitinib: 70.39 ± 3.58 %, 17.45 ± 3.96 % drop, $p<0.001$), at 125 min for the 12 month group (Control: 80.32 ± 1.72 %; Sunitinib: 69.47 ± 1.41 %, 13.51 ± 1.61 % drop, $p<0.05$), and at 95 min for the 24 month group (Control: 76.70 ± 0.87 %; Sunitinib: 56.08 ± 2.43 %, 26.88 ± 2.83 % drop, $p<0.001$) (Figure 3.2). The 24 month group produced the largest drop in LVDP and this was significant compared to the 3 month group ($p<0.05$) (Figure 3.2).

Table 3.1: Left ventricular developed Pressure (mmHg) raw data values obtained during a 125 minute of langendorff control or Sunitinib (1 µM) perfusion.

Groups: 3 month (n=9), 12 month (n=6) and 24 month (Control: n=3; Sunitinib: n=5) old Sprague-Dawely rat hearts. Data expressed at mean ± S.E.M. Statistics: 12 month and 24 month vs 3 month control: a (p<0.05) and aa (p<0.01); 12 month and 24 month vs 3 month Sunitinib: A (p<0.05) and AA (p<0.01); 24 month vs 12 month control: b (p<0.05) and B (p<0.05); 24 month vs 12 month Sunitinib: BB (p<0.01) and BBB (p<0.001). Two-way ANOVA, Tukey post hoc.

LVDP	**Control**			**Sunitinib**		
Time	3 month	12 month	24 month	3 month	12 month	24 month
0	112.15 ± 3.09	138.50 ± 8.22	118.77 ± 14.43	113.21 ± 3.13	143.82 ± 4.96^{A}	125.82 ± 12.92
5	123.77 ± 2.96	136.55 ± 5.66	109.83 ± 16.70	138.17 ± 8.01	142.95 ± 5.84	112.06 ± 5.28
10	119.93 ± 2.90	142.85 ± 16.26	119.97 ± 11.63	131.19 ± 7.22	141.67 ± 6.34	104.18 ± 13.19^{B}
15	116.01 ± 3.03	140.88 ± 14.27	122.55 ± 8.38	122.76 ± 8.44	140.18 ± 6.15	95.21 ± 11.56^{BB}
20	116.98 ± 3.46	144.30 ± 11.30	110.01 ± 12.90	112.67 ± 5.98	133.40 ± 5.98	94.77 ± 13.00^{BB}
25	112.87 ± 3.58	145.90 ± 14.50^{a}	112.78 ± 12.22	112.12 ± 4.99	134.52 ± 4.56	97.86 ± 13.85^{B}
30	115.84 ± 3.50	145.35 ± 14.71^{a}	115.38 ± 13.53	106.30 ± 5.56	135.07 ± 4.08^{A}	92.37 ± 11.87^{BB}
35	113.97 ± 4.49	142.13 ± 13.07	111.74 ± 12.62	106.92 ± 3.87	135.93 ± 5.02^{A}	90.16 ± 10.83^{BBB}
50	110.06 ± 6.35	142.68 ± 9.65^{a}	101.84 ± 12.23^{b}	96.97 ± 5.89	127.00 ± 5.34^{A}	86.77 ± 9.05^{BB}
65	107.63 ± 7.18	136.48 ± 10.89^{a}	92.16 ± 11.38^{a,b}	92.67 ± 4.65	124.89 ± 6.41^{A}	74.53 ± 4.21^{BBB}
80	101.16 ± 5.24	134.70 ± 14.11^{aa}	90.00 ± 9.41^{b}	91.29 ± 4.23	116.96 ± 4.93	71.43 ± 6.19^{BB}
95	98.19 ± 2.23	132.35 ± 8.40^{aa}	90.45 ± 7.44^{b}	92.84 ± 5.48	113.52 ± 6.04	69.83 ± 6.02^{BB}
110	93.20 ± 2.76	128.00 ± 9.44^{aa}	89.25 ± 7.40^{b}	84.55 ± 4.01	105.05 ± 3.70	72.47 ± 10.48^{B}
125	92.71 ± 2.31	123.65 ± 6.67^{a}	86.70 ± 7.46	80.16 ± 3.97	97.35 ± 2.86	69.44 ± 8.92

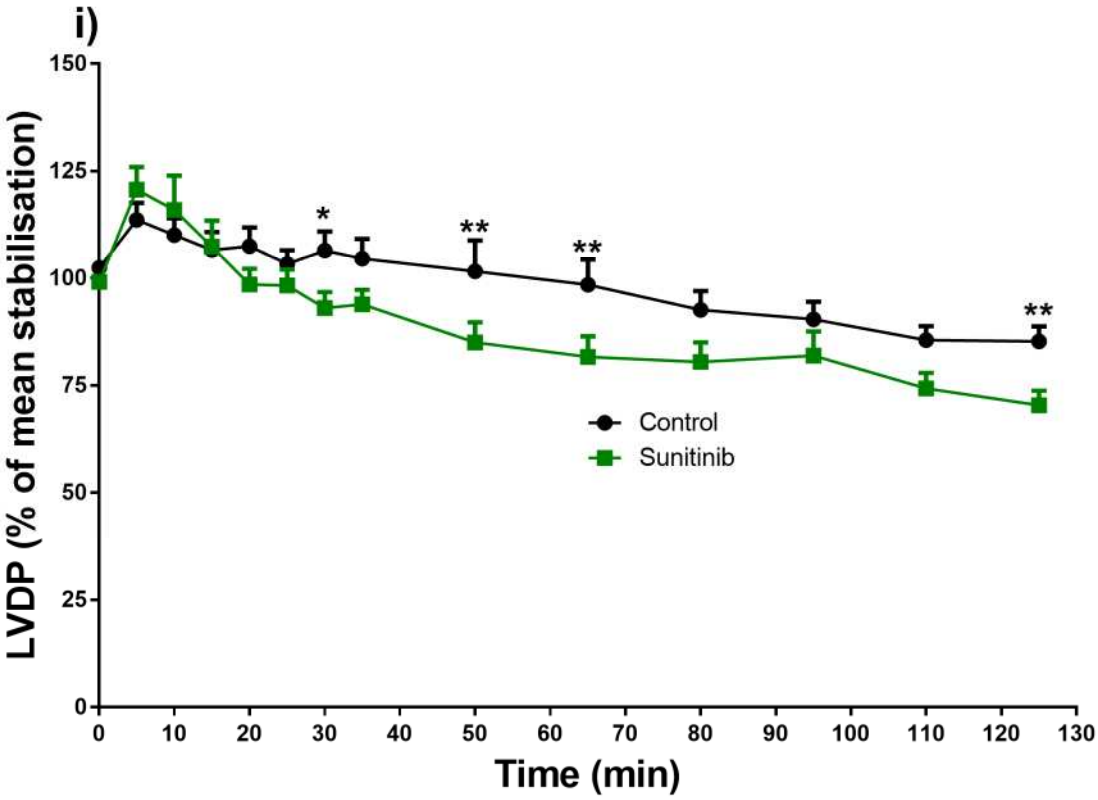
i)
LVDP (% of mean stabilisation)
150
125
100
75
50
25
0
0
10
20
30
40
50
60
70
80
90
100
110
120
130
Time (min)
*
**
**
**
Control
Sunitinib

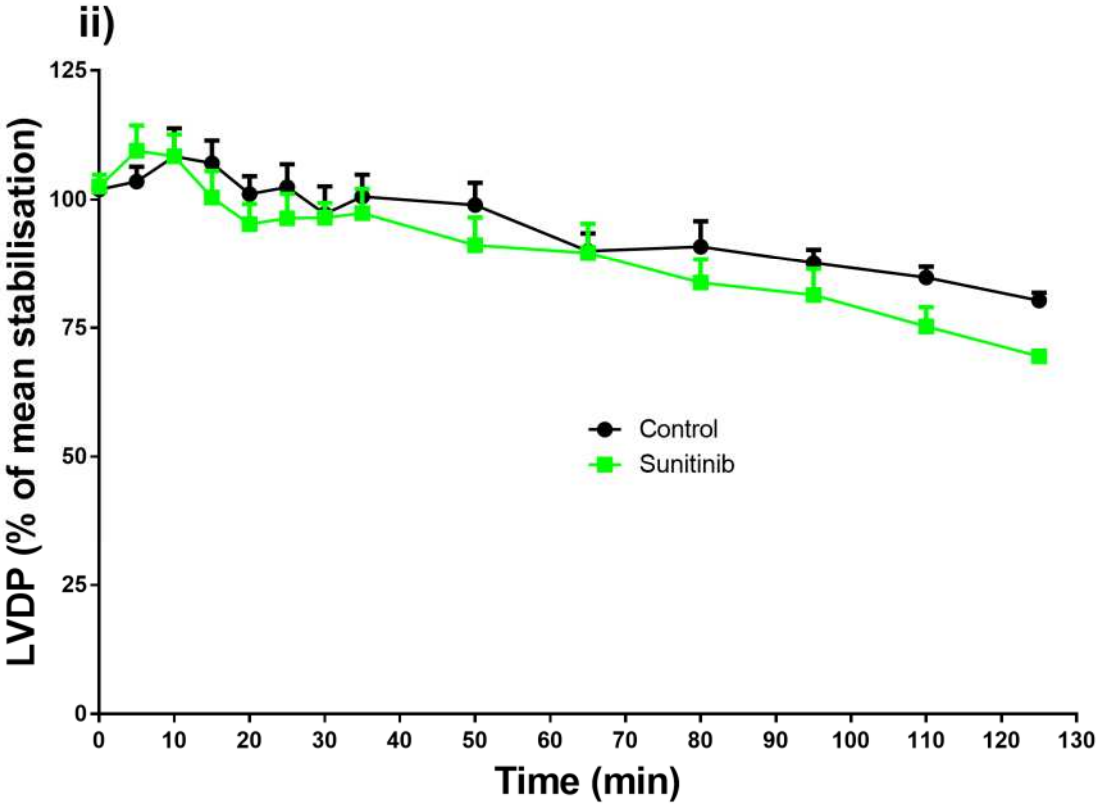
ii)
LVDP (% of mean stabilisation)
125
100
75
50
25
0
0
10
20
30
40
50
60
70
80
90
100
110
120
130
Time (min)
Control
Sunitinib

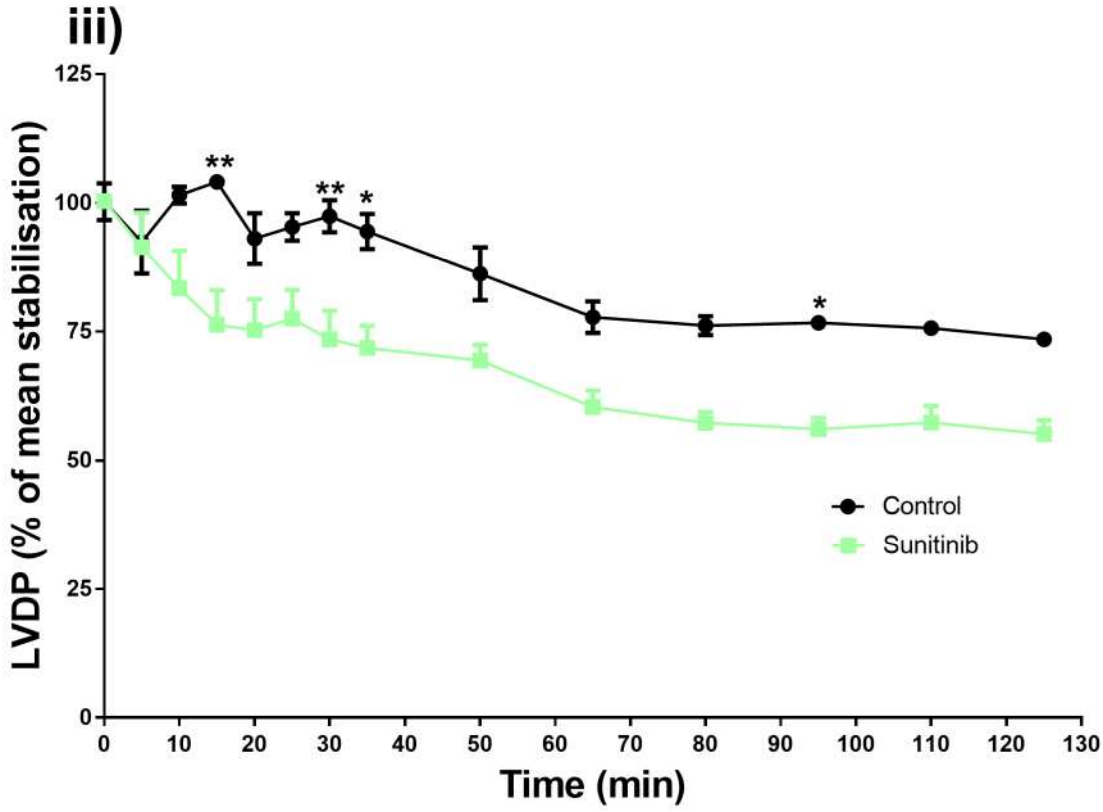

Figure 3.1: Representation of changes in LVDP (mmHg) measured during Langendorff experiments over time relative to the stabilisation period.

*Starting from drug treatment with control and Sunitinib (1 µM) in: i) 3 month old rats (n = 9), ii) 12 month old rats (n = 6), iii) 24 month old rats (Control n = 3, Sunitinib n = 5). Data expressed as mean ± S.E.M. Statistics: * = p < 0.05, **= p < 0.01 groups compared by Two-way repeated measures ANOVA, Bonferroni post hoc test.*

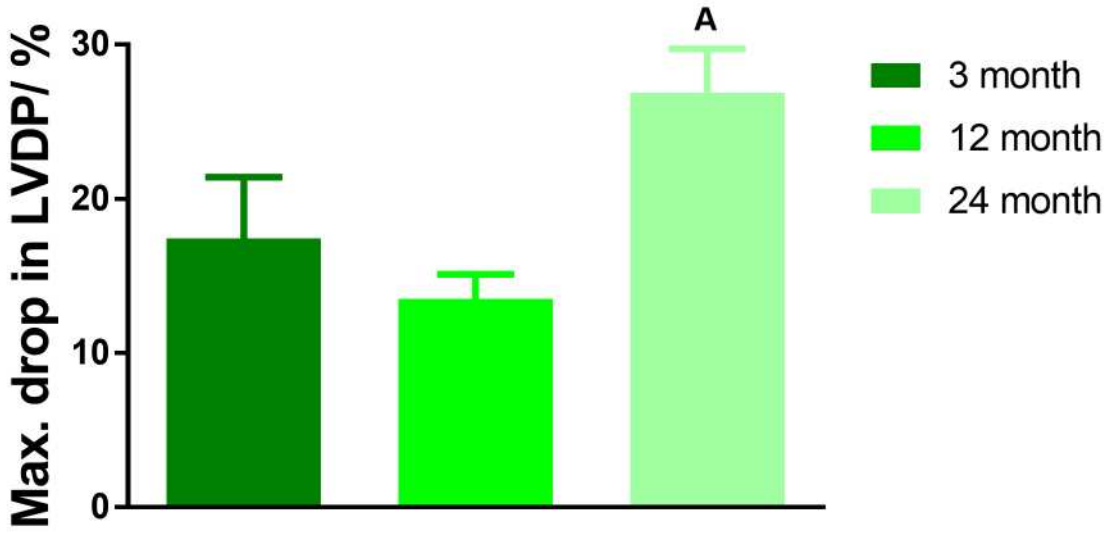

Figure 3.2: The maximum drop in LVDP during the 125 minute Sunitinib (1 µM) perfusion.

3 month produces a maximum drop at 125 minutes (n=9), 12 month produces a maximum drop at 125 minutes (n=6) and 24 month produces a maximum drop at 95 minutes (Control: n=3; Sunitinib: n=5), data presented as a percentage reduction in LVDP compared to control at the same point.

Stats: One-way ANOVA comparing 3 month vs 12 month, 3 month vs 24 month and 12 month vs 24 month. A = p<0.05 vs 3 month.

3.4.1.2 Heart Rate

The HR (beats per min) raw data demonstrated that there was a tendency for the 24 month control group to have a lower HR compared to both 3 month and 12 month controls; significant differences found at all of the time points (Table 3.2). There were also significant differences between the Sunitinib treated groups. The 3 month group had a significantly higher HR than the 12 and 24 month groups treated with Sunitinib at time point 80 mins. Also, at time point 125 mins, the 12 month group treated with Sunitinib had a significantly

lower HR compared to its group control and the 3 month group treated with Sunitinib (Table 3.2).

When the HR were normalised to the stabilisation period, Sunitinib treatment significantly reduced the HR (% of stabilisation period) of the 3 month and 12 month groups, compared to control (Figure 3.3i-ii and Table 3.2)). The 12 month group also experienced significant decreases in HR after 80 mins of Sunitinib perfusion, compared to control.

Throughout the 125 minutes of Sunitinib perfusion the HR for 24 month group was not significantly different to control (Figure 3.3iii). The time points at which significant difference in HR occurred between Control and Sunitinib groups in the 3 age groups can be found in the appendices (Table 0.2).

Sunitinib treatment resulted in a maximum % drop in HR: at 125 min in the 3 month group (Control: 100.48 ± 2.35 %; Sunitinib: 79.78 ± 5.29 %, 20.60 ± 4.97 % drop, $p<0.01$), at 125 min for the 12 month group (Control: 98.00 ±3.03 %; Sunitinib: 79.73 ± 3.15 %, 18.64 ± 2.94% drop, $p<0.01$), and at 30 min for the 24 month group (Control: 98.23 ± 4.16 %; Sunitinib: 87.71 ± 6.02%, 10.97 ± 5.45 % drop, non-significant decrease) (Figure 3.4). There were no significant differences in maximum % drop in HR between all of the age groups. However, there was a tendency for the maximum % drop in HR to reduce with age increase.

Table 3.2: Heart rate (bpm) raw data values obtained during a 125 minute of langendorff control or Sunitinib (1 µM) perfusion.

Groups: 3 month (n=9), 12 month (n=6) and 24 month (Control: n=3; Sunitinib: n=5) old Sprague-Dawely rat hearts. Data expressed at mean ± S.E.M. Statistics: 12 month and 24 month vs 3 month control: a (p<0.05) and aa (p<0.01); 12 month and 24 month vs 3 month Sunitinib: A (p<0.05) and AA (p<0.01); 24 month vs 12 month control: b (p<0.05) and bb (p<0.01). Two-way ANOVA, Tukey post hoc.

HR	**Control**			**Sunitinib**		
Time	3 month	12 month	24 month	3 month	12 month	24 month
0	262.22 ± 6.80	262.00 ± 19.17	196.67 ± 10.80^{a}	275.56 ± 7.93	242.00 ± 13.42	224.00 ± 19.56
5	257.78 ± 6.56	270.00 ± 19.04	196.67 ± 8.16^{b}	271.11 ± 9.91	238.00 ± 13.87	220.00 ± 23.18
10	256.67 ± 7.29	262.00 ± 22.75	190.00 ± 7.07^{a,b}	262.22 ± 8.06	240.00 ± 13.23	222.00 ± 24.60
15	256.67 ± 6.85	262.00 ± 19.81	196.67 ± 10.80^{a}	255.56 ± 7.31	234.00 ± 9.08	220.00 ± 21.51
20	256.67 ± 6.85	252.00 ± 18.17	193.33 ± 8.16^{a}	250.00 ± 7.50	228.00 ± 8.94	214.00 ± 23.87
25	262.22 ± 7.86	252.00 ± 20.43	200.00 ± 14.14^{a}	256.67 ± 9.35	234.00 ± 5.70	212.00 ± 20.74
30	262.22 ± 8.06	254.00 ± 23.08	193.33 ± 14.72^{a}	248.89 ± 7.59	226.00 ± 4.47	208.00 ± 21.62
35	271.11 ± 7.80	254.00 ± 23.08	190.00 ± 7.07^{aa}	255.56 ± 7.31	234.00 ± 8.37	214.00 ± 19.56
50	256.67 ± 7.71	252.00 ± 18.17	180.00 ± 7.07^{aa,b}	250.00 ± 7.91	218.00 ± 5.48	216.00 ± 21.10
65	257.78 ± 8.62	256.00 ± 23.61	183.33 ± 8.16^{aa,b}	254.44 ± 8.86	218.00 ± 5.48	214.00 ± 17.89
80	255.56 ± 9.86	256.00 ± 20.80	180.00 ± 7.07^{aa,b}	250.00 ± 6.61	200.00 ± 6.12^{A}	212.00 ± 17.82^{A}
95	261.11 ± 7.99	256.00 ± 25.88	183.33 ± 10.80^{aa,b}	248.89 ± 7.80	208.00 ± 8.22	214.00 ± 14.83
110	263.33 ± 9.68	258.00 ± 21.62	186.67 ± 8.16^{aa,b}	252.22 ± 7.45	200.00 ± 6.12	216.00 ± 11.51
125	265.56 ± 9.20	258.00 ± 23.02	180.00 ± 14.14^{aa,bb}	245.56 ± 6.15	194.00 ± 4.47^{bb,A}	216.00 ± 17.89

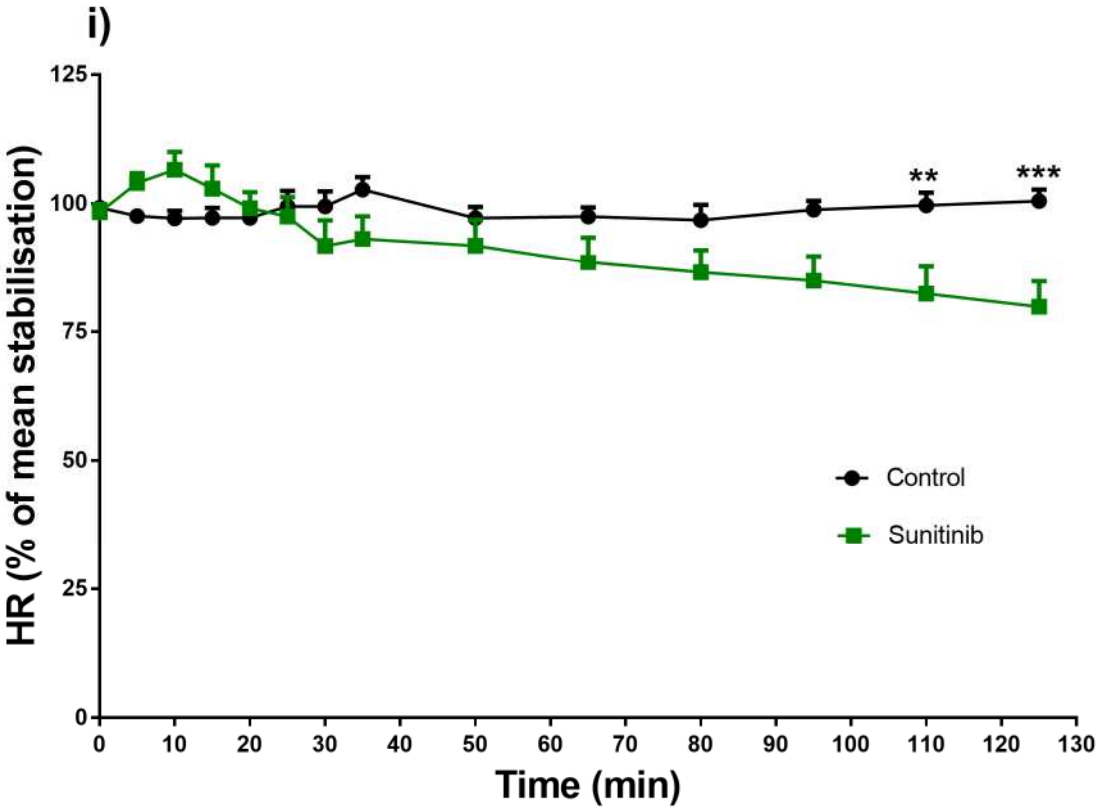
i)
HR (% of mean stabilisation)
Time (min)
Control
Sunitinib
**
***

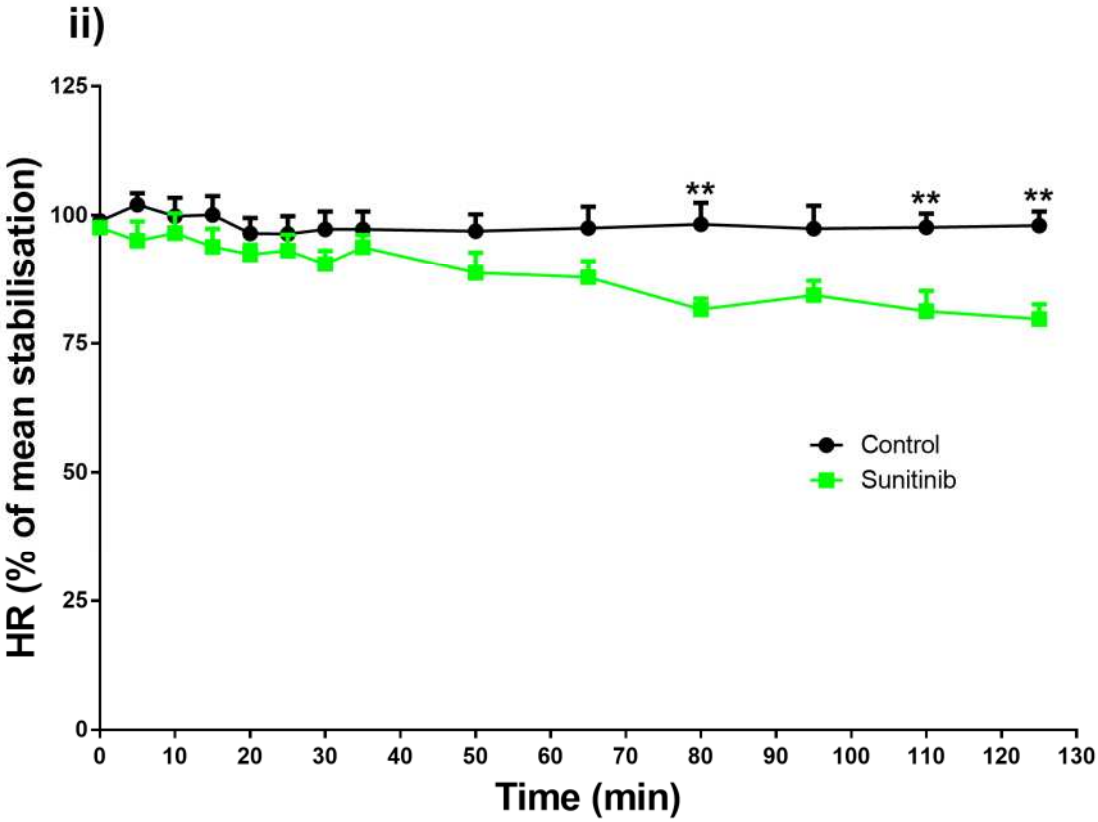
ii)
HR (% of mean stabilisation)
Time (min)
Control
Sunitinib
**
**
**

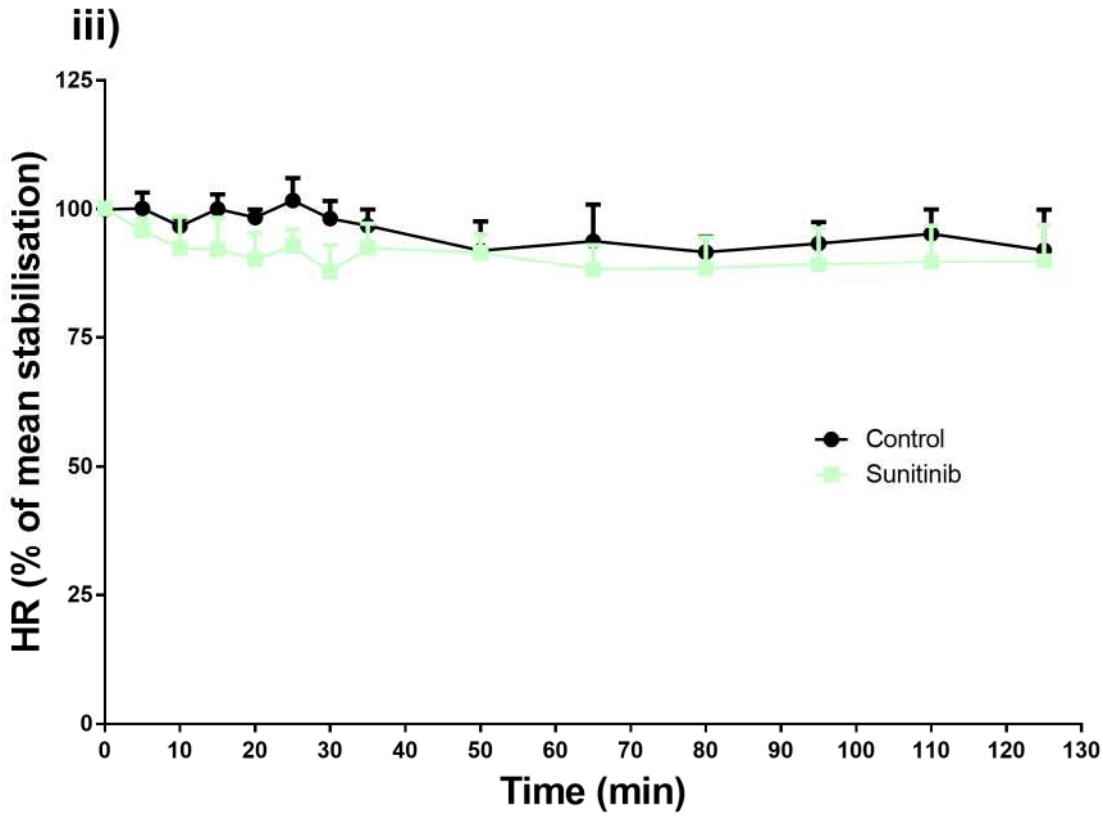

Figure 3.3*: Representation of changes in HR (bpm) measured during Langendorff experiments over time relative to the stabilisation period.*

*Starting from drug treatment of control and Sunitinib (1 µM) in i) 3 month old rats (n = 9), ii) 12 month old rats (n = 6), iii) 24 month old rats (Control n = 3, Sunitinib n = 5). Data expressed as mean ± S.E.M. Statistics: * = p < 0.05, **= p < 0.001 groups compared by two-way repeated measures ANOVA, Bonferroni post hoc.*

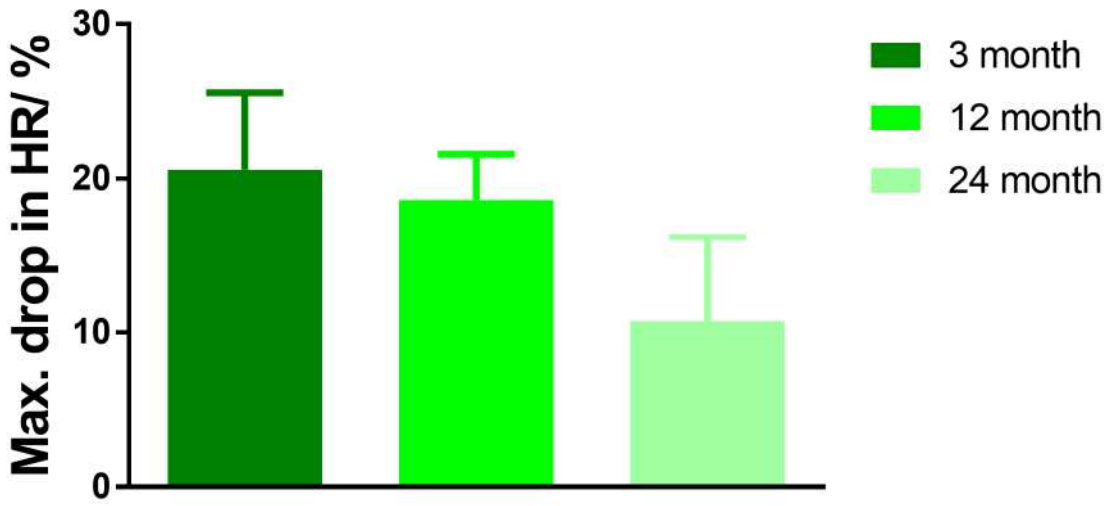

Figure 3.4: The maximum drop in HR (bpm) during the 125 minute Sunitinib (1 µM) perfusion. 3 month produces a maximum drop at 125 minutes (n=9), 12 month produces a maximum drop at 125 minutes (n=6) and 24 month produces a maximum drop at 30 minutes (control: n=3; Sunitinib n=5), data presented as a percentage reduction in HR compared to control at the same point. Stats: One-way ANOVA comparing 3 month vs 12 month, 3 month vs 24 month and 12 month vs 24 month.

3.4.1.3 Coronary Flow

The CF (ml/min/g) raw data demonstrated that there was a tendency for the 24 month control group to have a lower CF compared to both 3 month and 12 month controls. This was significant at many of the time points (Table 3.3). There were also significant differences between the Sunitinib treated groups. The 12 month group has a significantly higher CF than the 3 month group treated with Sunitinib between time point's 35-95 mins and also compared to the 24 month group treated with Sunitinib at time point 65 mins. Interestingly, between time points' 35-65 mins, the 24 month group treated with Sunitinib had a significantly higher CF compared to its group control (Table 3.2).

When the CF was normalised to the stabilisation period, the CF (% of stabilisation period) was not significantly altered in any age group, however, there was a tendency for an increase in CF in the first 25 minutes of Sunitinib treatment in the 3 month group (Figure 3.5i-iii and Table 3.3 of the appendix).

In response to Sunitinib treatment, the maximum % increase in CF was observed at 10 mins in the 3 month group (Control: 89.46 ± 2.98 %; Sunitinib: 106.54 ± 3.69 %, 19.10 ± 3.89 % drop, $p<0.01$), at 5 mins in the 12 month group (Control: 103.17 ± 2.02 %; Sunitinib: 118.93 ± 10.19 %, 15.27 ± 9.02 % drop, non-significant increase), and at 50 mins for the 24 month group (Control: 90.30 ± 2.24 %; Sunitinib: 92.98 ± 4.32 %, 2.98 ± 4.28 % drop, NS) (Figure 3.4). There were no significant differences in maximum % drop in CF between all of the age groups (data not shown). It should be noted there were high levels of variation in all groups during CF measurement.

Table 3.3: Coronary Flow (ml/min/g) raw data values obtained during a 125 minute of langendorff control or Sunitinib (1 µM) perfusion.

Groups: 3 month (n=9), 12 month (n=6) and 24 month (Control: n=3; Sunitinib: n=5) old Sprague-Dawely rat hearts. Data expressed at mean ± S.E.M. Statistics: 12 month and 24 month vs 3 month control: a (p<0.05); 12 month and 24 month vs 3 month Sunitinib: A (p<0.05) and AA (p<0.01); 24 month vs 12 month control: b (p<0.05); 24 month vs 12 month Sunitinib: B (p<0.05); cc (p<0.01) vs 24 month control. Two-way ANOVA, Tukey post hoc.

CF	**Control**			**Sunitinib**		
Time	3 month	12 month	24 month	3 month	12 month	24 month
0	7.29 ± 0.42	6.94 ± 0.22	3.81 ± 0.17^{a}	6.10 ± 0.80	7.44 ± 0.91	5.57 ± 0.90
5	7.68 ± 0.38	7.17 ± 0.28	3.81 ± 0.17^{a}	6.18 ± 0.82	8.58 ± 0.79	5.47 ± 0.83
10	7.93 ± 0.59	7.36 ± 0.42	3.98 ± 0.14^{a}	5.91 ± 0.87	8.32 ± 0.82	5.48 ± 0.57
15	7.67 ± 0.65	7.40 ± 0.56	3.81 ± 0.12^{a}	5.75 ± 0.75	7.96 ± 0.67	5.09 ± 0.74
20	7.36 ± 0.50	7.35 ± 0.39	3.73 ± 0.08^{a}	5.85 ± 0.83	7.70 ± 0.76	5.24 ± 0.88
25	7.21 ± 0.47	7.65 ± 0.45	3.73 ± 0.14^{a,b}	5.87 ± 0.88	8.05 ± 0.71	5.02 ± 1.04
30	6.79 ± 0.52	7.37 ± 0.38	3.73 ± 0.14	5.58 ± 0.85	8.12 ± 0.70	5.16 ± 0.94
35	6.91 ± 0.53	7.55 ± 0.42	3.49 ± 0.08^{b}	5.45 ± 0.90	8.24 ± 0.73^{A}	5.10 ± 0.75^{cc}
50	6.81 ± 0.56	7.55 ± 0.59	3.41 ± 0.05^{b}	4.84 ± 0.93	8.04 ± 0.78^{A}	5.08 ± 0.68^{cc}
65	6.59 ± 0.58	6.82 ± 0.61	3.41 ± 0.05	4.51 ± 0.85	7.93 ± 0.79^{AA}	4.68 ± 0.58^{cc,B}
80	6.43 ± 0.51	6.85 ± 0.70	3.41 ± 0.05	4.35 ± 0.85	7.07 ± 0.62	4.54 ± 0.82
95	6.31 ± 0.57	6.24 ± 0.89	3.25 ± 0.09	4.06 ± 0.62	6.92 ± 0.51^{A}	4.54 ± 0.74
110	6.12 ± 0.57	6.29 ± 0.93	3.25 ± 0.09	3.89 ± 0.61	6.19 ± 0.55	4.22 ± 0.84
125	5.93 ± 0.56	5.78 ± 0.76	3.17 ± 0.06	3.89 ± 0.62	5.55 ± 0.72	3.87 ± 0.69

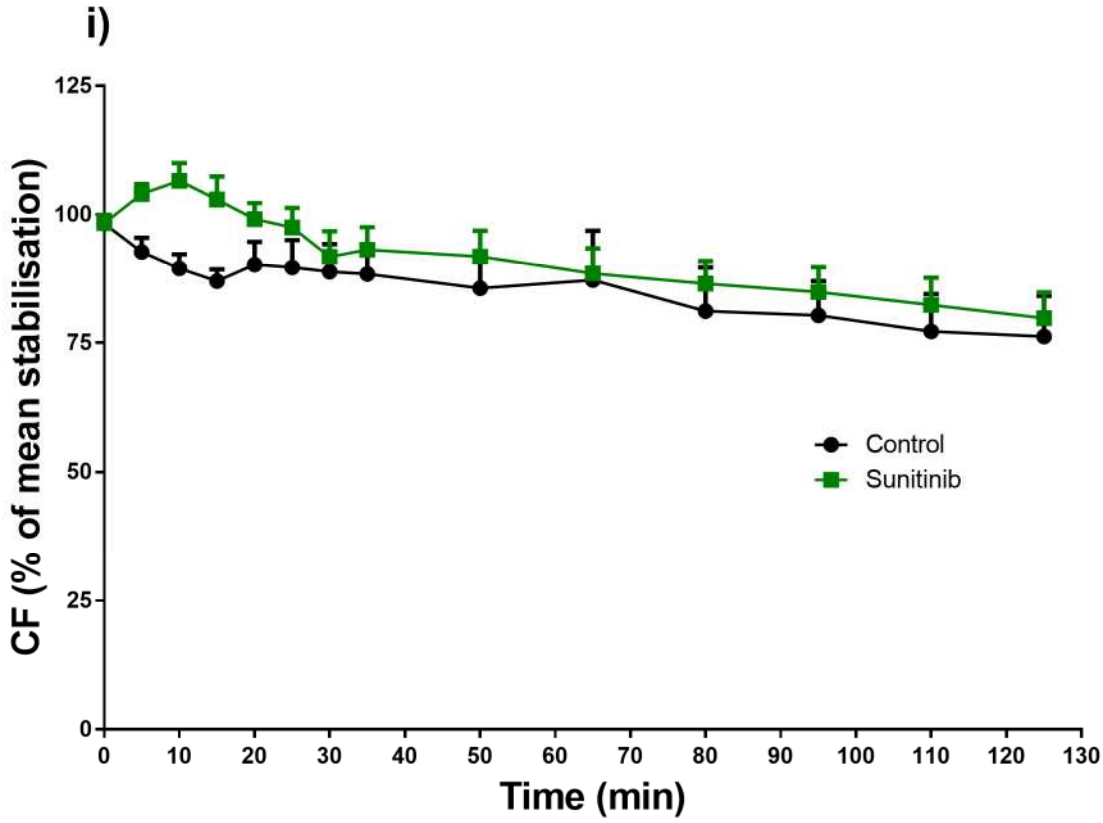
i)
CF (% of mean stabilisation)
125
100
75
50
25
0
0
10
20
30
40
50
60
70
80
90
100
110
120
130
Time (min)
Control
Sunitinib

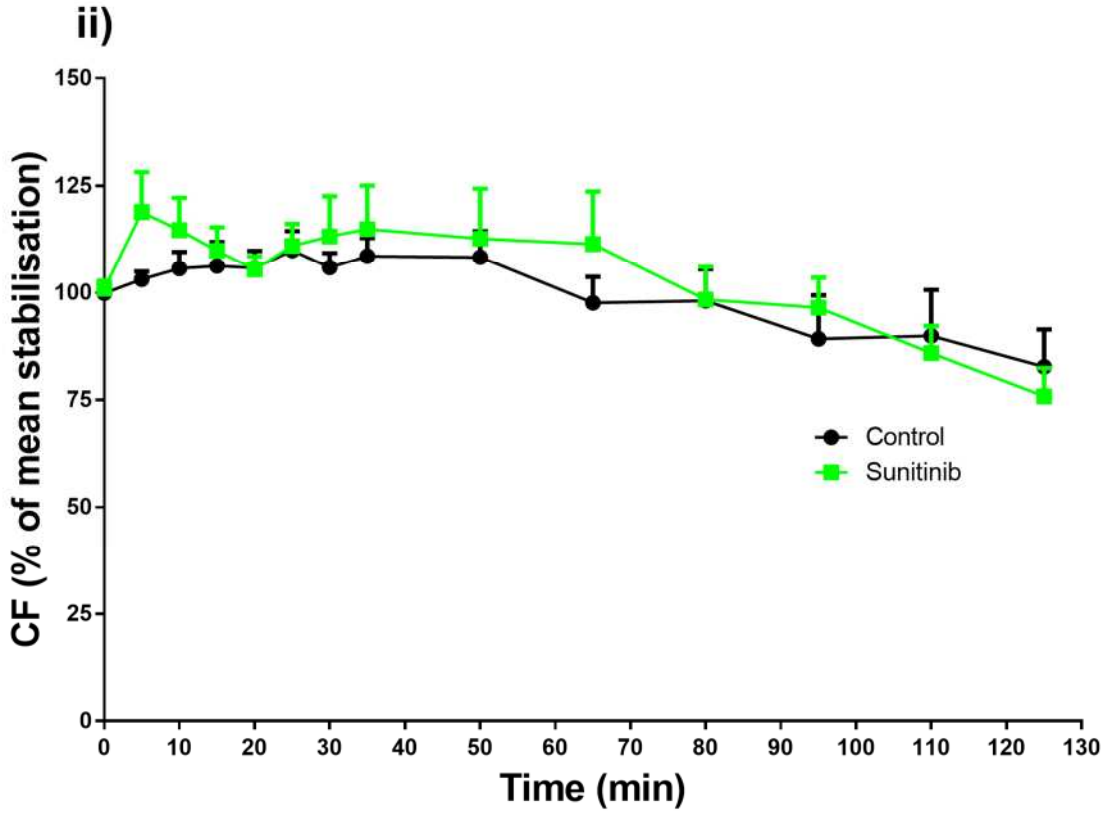
ii)
CF (% of mean stabilisation)
150
125
100
75
50
25
0
0
10
20
30
40
50
60
70
80
90
100
110
120
130
Time (min)
Control
Sunitinib

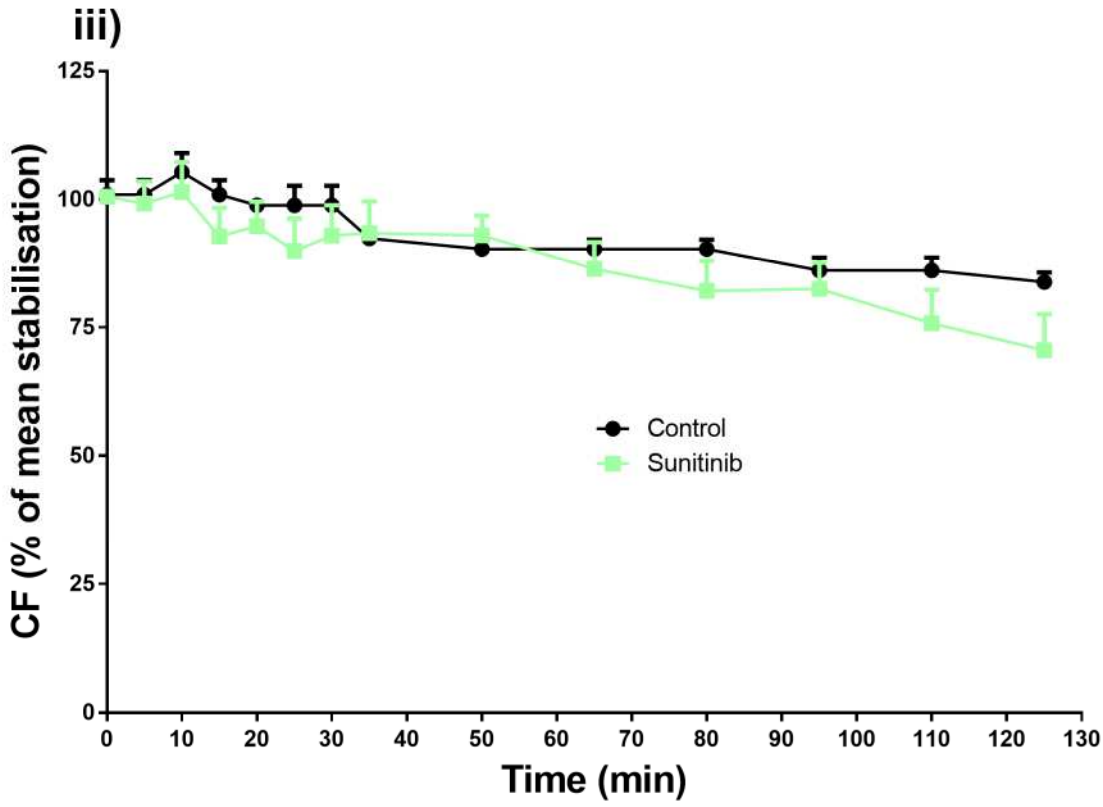

Figure 3.5*: Representation of changes in CF (ml/heart weight g) measured during Langendorff experiments over time relative to the stabilisation period.*

Starting from drug treatment with control and Sunitinib (1 μM*) in i) 3 month old rats (n = 9), ii) 12 month old rats (n = 6), iii) 24 month old rats (Control n = 3, Sunitinib n = 5). Data expressed as mean ± S.E.M. Statistical analysis by two-way repeated measures ANOVA, Bonferroni post hoc.*

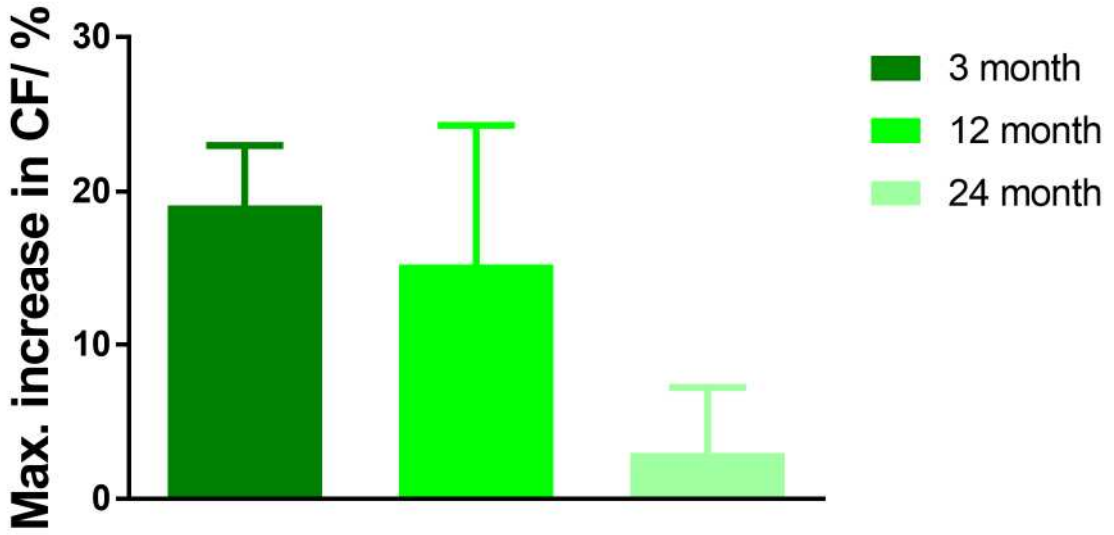

Figure 3.6: The maximum increase in CF during the 125 minute Sunitinib (1 µM) perfusion. 3 month produces a maximum drop at 10 minutes (n=9), 12 month produces a maximum drop at 5 minutes (n=6) and 24 month produces a maximum drop at 50 minutes (Control: n=3; Sunitinib n=5), data presented as a percentage reduction in CF compared to control at the same point. Stats: One-way ANOVA comparing 3 month vs 12 month, 3 month vs 24 month and 12 month vs 24 month.

3.4.2 Infarct size assessment

Sunitinib treatment produced significant increases in infarct size (normalised to heart weight) in all age groups, compared to group controls: 5.1 fold increase in the 3 month group (control= 3.29 ± 0.55 %/g, Sunitinib 17.14 ± 0.39%/g, $p<0.001$), 3.3 fold increase in the 12 month group (control= 3.06 ± 0.09 %/g, Sunitinib= 10.19 ± 0.84 %/g, $p<0.001$) and a 2.5 fold increase in the 24 month group (control = 2.25 ± 0.21 %/g, Sunitinib = 5.53 ± 0.15 %/g, $p<0.001$) (Figure 3.7).

The average heart weights for each group is shown is table 3.4. The 3 month group hearts were significantly smaller than both the 12 and 24 month groups.

When the infarct sizes were normalised to the age group's specific control heart infarct size, we observed a significantly higher infarct size in the 3 month group compared to both 12 month and 24 month rats following Sunitinib treatment ($p<0.001$ in both cases). The 12 month group treated with Sunitinib also had a significantly larger infarct size compared to the 24 month group ($p<0.01$) (Figure 3.7). The infarct sizes of the control groups were at similar levels in all 3 age groups.

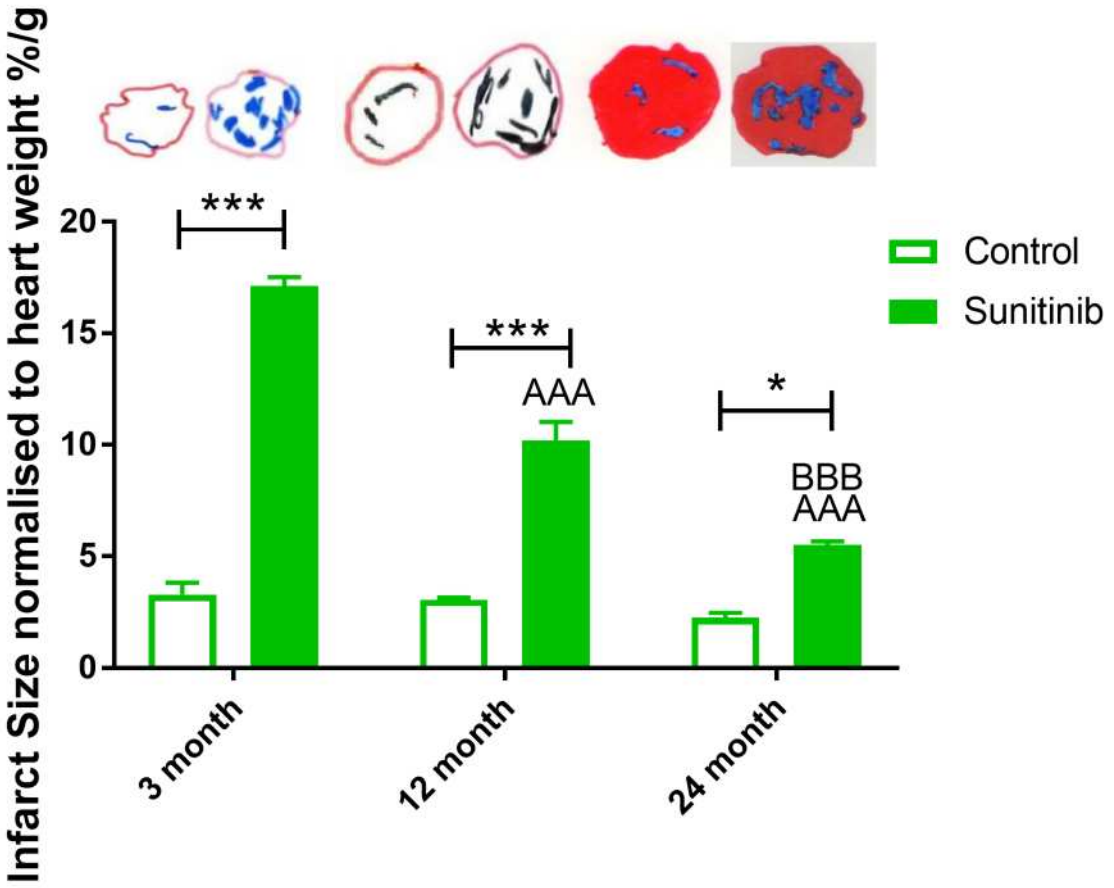

Figure 3.7: Infarct to whole heart ratio assessment establishes Sunitinib-induced cardiotoxicity. The hearts were drug perfused with Sunitinib (1 µM) for 125 min in an isolated Langendorff heart model. The infarct size measurements were normalised to heart weight. Groups: Control and Sunitinib (1 µM) in A) 3 month rats (n = 9), B) 12 month rats (n = 6) and C) 24 month rats (Control n = 3, Sunitinib n = 5). Statistics t-test between Control vs Sunitinib (*) of each age group. Statistics: Two-way ANOVA, Bonferroni post hoc. Comparing Control vs Sunitinib of the same age group Data expressed as mean ± S.E.M. = P<0.05, * = p<0.001 and *** = p<0.001. Comparing Sunitinib treatment of each age group, vs 3 month = A and vs 12 month = B.*

*Table 3.4: Heart weights (g) of each age group. Data expressed as mean ± S.E.M. Statistics: One-way ANOVA, post hoc Tukey (***=p<0.001 compared to 3 month group).*

3 Month	**12 month**	**24 month**
2.41 ± 0.05 g	3.39 ± 0.12 g***	3.86 ± 0.30 g***

3.4.3 Profiles of cardiac injury associated miRNAs

MicroRNAs have important roles in tissue formation and function, in response to injury and disease (Chen et al. 2008). The miRNAs miR-1, miR-27a, miR-133a and miR-133b have been shown to produce differential expression patterns during the progression of heart failure (Akat et al. 2014, Tijsen, Pinto and Creemers 2012). Here we investigated the effect Sunitinib (1 µM) treatment produced on the expression profiles of miRNAs associated with cardiac damage: miR-1, miR-27a, miR-133a and miR-133b (Figure 3.8).

Sunitinib treatment did not significantly alter the expression levels of miR-1 in any of the age groups, compared to group controls (Figure 3.8). Following Sunitinib treatment, a significant reduction in miR-27a expression was observed in all age groups, compared to specific group controls (0.40 fold decrease in 3 month group, $p<0.001$; 0.43 fold decrease in 12 month group, $p<0.05$; 0.69 fold decrease in 24 month group, $p<0.05$) (Figure 3.8).

Interestingly, Sunitinib treatment caused a 2.7 fold ($p<0.001$) increase in miR-133a expression in the 3 month group, compared to its group control. However, Sunitinib treatment produced a significant 0.7 fold ($p<0.001$) decrease in miR-133a levels in the 24 month group, compared to its control group. Plus, a tendency for decrease in miR-133a was also found in 12 month old rats after Sunitinib treatment (Figure 3.8).

Similarly to miR-133a, Sunitinib treatment significantly increased miR-133b levels in 3 month old rats by 3.79 fold ($p<0.01$) and in the 24 month group Sunitinib treatment caused significant 0.7 fold (0.01) decrease in miR-133b compared to its control. Also, there was a tendency for a decrease in miR-133b, in response to Sunitinib treatment in the 12 month group (Figure 3.8).

Following Sunitinib treatment, comparisons between the age groups found miR-133a and miR-133b levels to be significantly increased in the 3 month group compared to both the 12 month group and the 24 month group ($p<0.01$). There was a tendency for an increase in miR-1 and miR-27a levels with age in response to Sunitinib treatment, however there were no significant differences between the age groups.

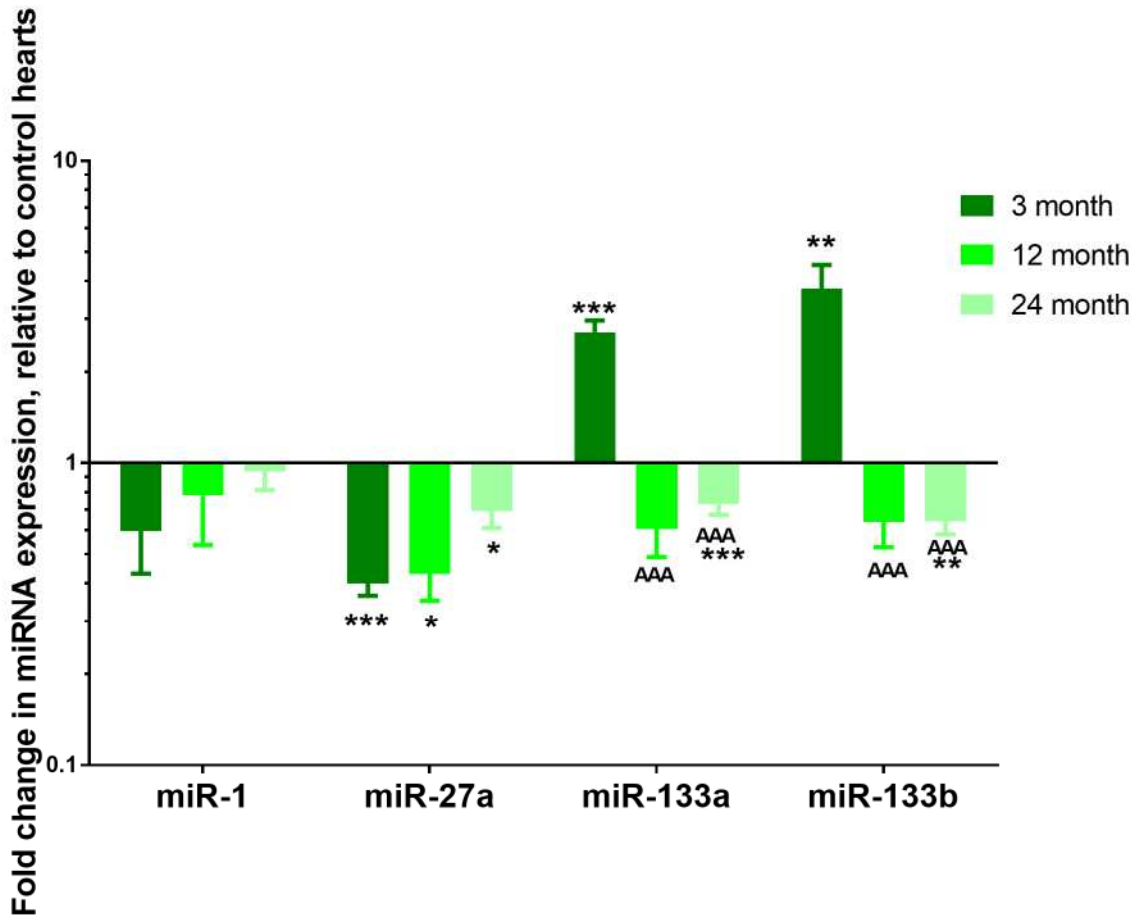

Figure 3.8: The effect of Sunitinib (1 µM) on cardiac damage specific miRNAs expression following 125 minute drug perfusion in an isolated heart Langendorff model.

The qRT-PCR results are shown as the ratio of target miRNA normalised to U6 with control group miRNA ratio set as 1 of miRNAs miR-1, miR-27a, miR-133a and miR-133b. Comparing the effect of Sunitinib treatment on miRNA expression in the 3 age groups. 3 month (control n= 9, Sunitinib n = 11), 12 month (n = 6) and 24 month (n = 6). Data expressed as mean ± S.E.M. = P<0.05, * = p<0.001 and *** = p<0.001. Statistics: Two-way ANOVA comparing Control vs Sunitinib (*) of each age group. One-way ANOVA comparing Sunitinib treatment of each age group, vs 3 month = A (AAA = p<0.001).*

3.4.4 MKK7 mRNA expression

MKK7 is a stress signalling protein which has previously been shown have an important role

in protecting the heart from heart failure (Liu et al. 2011). As Sunitinib produces adverse effects in the heart (Ewer et al. 2014), it would be important to establish whether MKK7 levels are altered in response to Sunitinib treatment. Therefore, firstly we investigated whether MKK7 mRNA levels are altered in response to Sunitinib induced cardiac injury (Figure 3.9).

MKK7 mRNA profiling in response to Sunitinib treatment revealed a significant 0.3 fold ($p<0.05$) decrease in 3 month old rats (Figure 3.9i), compared to its age group control. Contrastingly, Sunitinib treatment significantly increased MKK7 mRNA levels 10.17 fold ($p<0.01$) in the 24 month group (Figure 3.9iii), compared to its group control. There was also a tendency for an increase in MKK7 mRNA expression in 12 month rats after Sunitinib treatment (Figure 3.9ii), compared to its group control, however, this was not significant.

Sunitinib-induced alteration of MKK7 mRNA was normalised to the specific age group controls. We observed a significant increases in MKK7 mRNA in the 24 month group, compared to both the 3 and 12 month groups. There was also a tendency for the Sunitinib treatment to increase MKK7 mRNA levels in an age dependant manner (Figure 3.9iV).

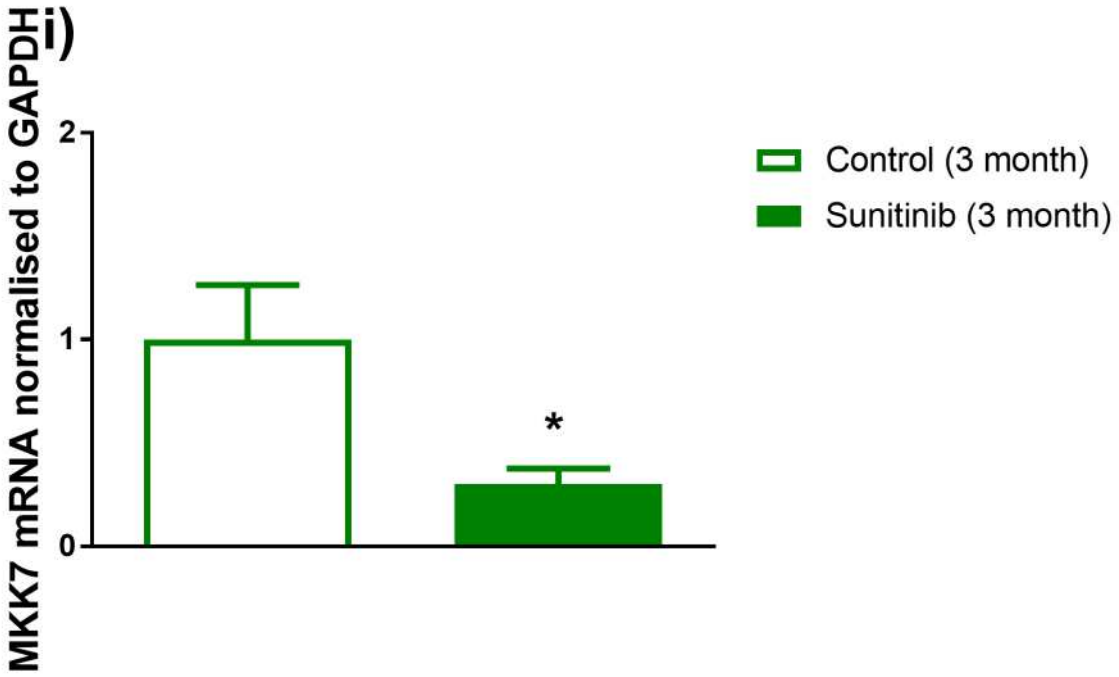
i)
MKK7 mRNA normalised to GAPDH
2
1
0
*
Control (3 month)
Sunitinib (3 month)

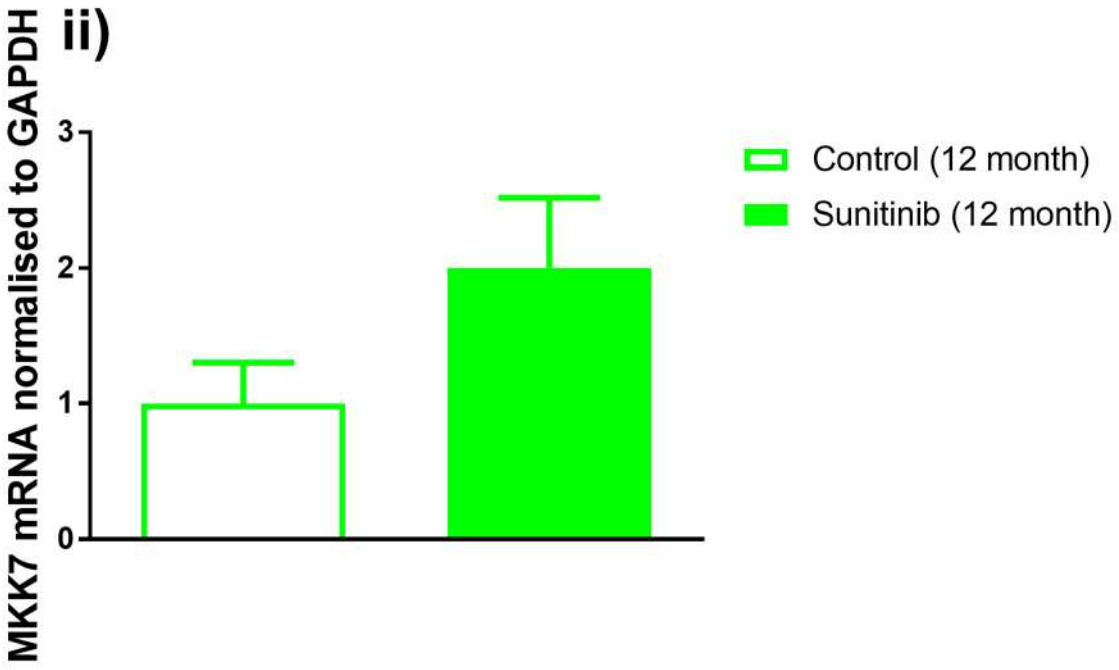
ii)
MKK7 mRNA normalised to GAPDH
3
2
1
0
Control (12 month)
Sunitinib (12 month)

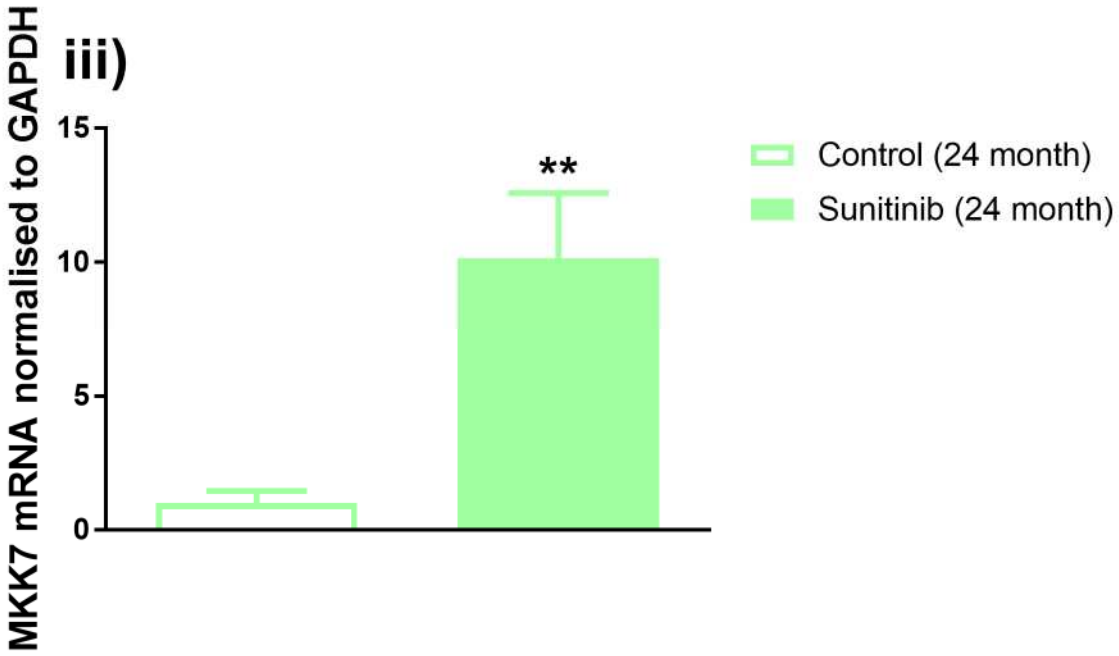
iii)
MKK7 mRNA normalised to GAPDH
15
10
5
0
**
Control (24 month)
Sunitinib (24 month)

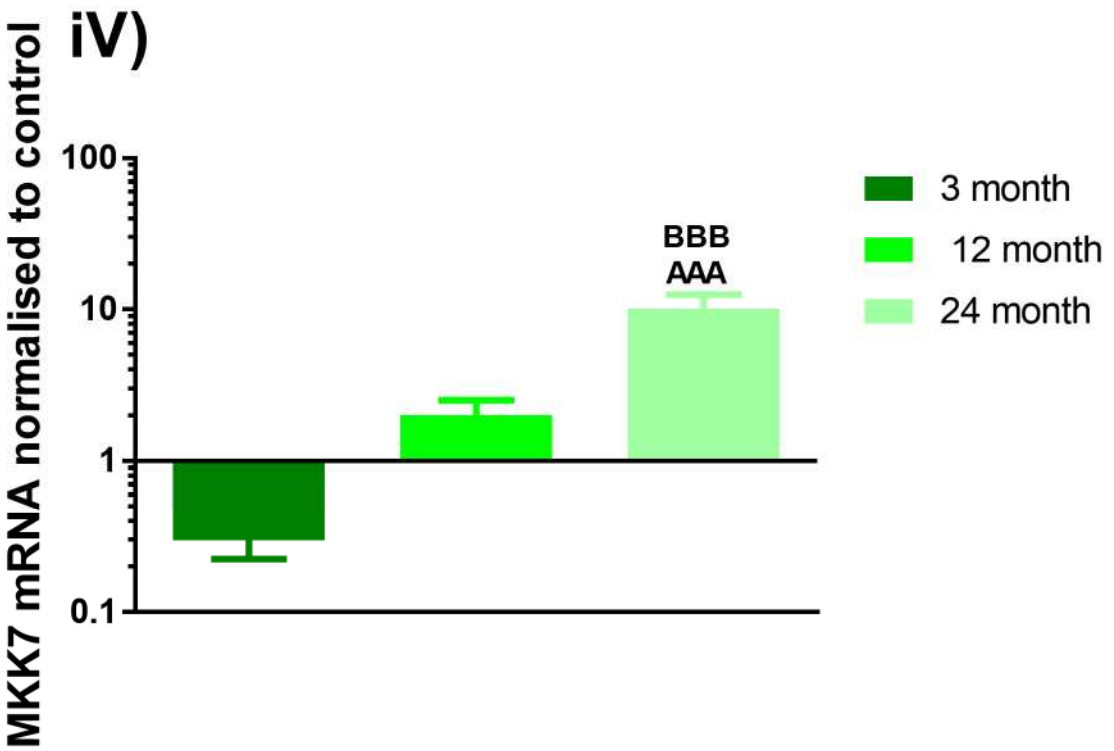

Figure 3.9: The qRT-PCR assessment of MKK7 mRNA expression levels in an isolated heart Langendorff model.

The qRT-PCR results are shown as the ratio of MKK7 mRNA expression in Sunitinib treatment (1µM) normalised to GAPDH with control group ratio set as 1. i-iii) MKK7 mRNA profiles after Sunitinib treatment in all age groups after being normalised to the control of the same age group. Data expressed as mean ± S.E.M. = P<0.05, ** = p<0.01 and *** = p<0.001. Groups: i) 3 month (Control n = 8, Sunitinib n= 6) ii) 12 month (n = 7) iii) 24 month (n = 5). Statistics: Student's t-test between Control vs Sunitinib (*) of each age group. iv) Combined aged data investigating the effect of Sunitinib treatment on MKK7 mRNA levels. Presented on a log_{10} scale. One-way ANOVA comparing Sunitinib treatment of each age group, vs 3 month = A, vs 12 month = B and vs 24 month = C (Where, AAA or BBB represents p<0.001).*

3.4.5 Phosphorylated MKK7 protein levels

Previous research has demonstrated the important role of MKK7 in the heart. MKK7 has been shown to have altered levels of activation in response to cellular stresses in the heart (Petrich and Wang 2004). In addition, alterations in the level of protein activation have been shown age specific (Jiang, Moffat and Narayanan 1993). Therefore, we investigated the effect of Sunitinib induced cardiac injury on MKK7 phosphorylation levels in different age groups.

In the 3 month group, p-MKK7 levels were significantly decreased after Sunitinib treatment compared to control (control=78.83±8.45%, Sunitinib=45.69±2.15%, $p<0.05$). Contrarily, the 12 month group demonstrated a significant increase in p-MKK7 levels after Sunitinib treatment, compared to control (control= 55.88±3.19%, Sunitinib= 71.42±4.87%, $p<0.05$). Sunitinib treatment did not significantly alter the p-MKK7 levels of the 24 month group (Figure 3.10i).

There was a significant increase in p-MKK7 levels in the 12 month group compared to the 3 month group in response the Sunitinib treatment, when normalised to the specific group controls (3 month: 0.60 fold decrease, 12 month: 1.38 fold increase $p<0.01$). Also, p-MKK7 levels were significantly reduced in the 24 month group compared to the 12 month group (24 month: 0.94 fold decrease, $p<0.05$) (Figure 3.10ii).

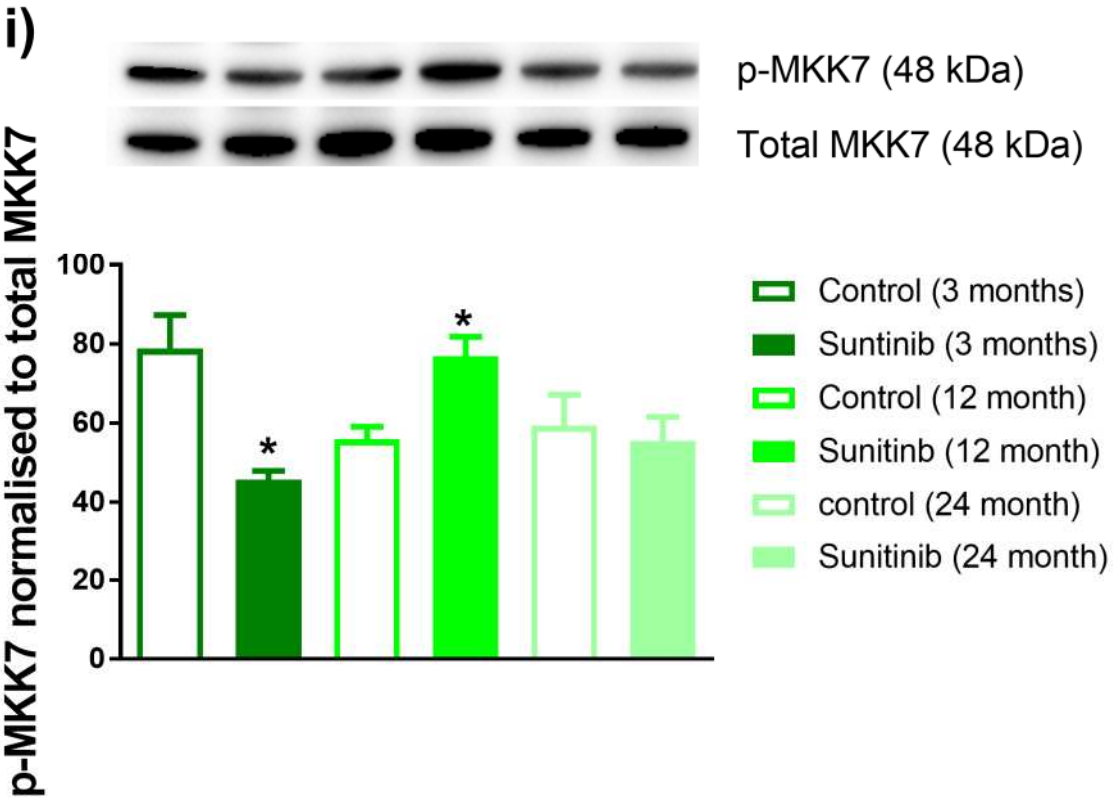
i)
p-MKK7 (48 kDa)
Total MKK7 (48 kDa)
p-MKK7 normalised to total MKK7
100
80
60
40
20
0
*
*
Control (3 months)
Suntinib (3 months)
Control (12 month)
Sunitinb (12 month)
control (24 month)
Sunitinib (24 month)

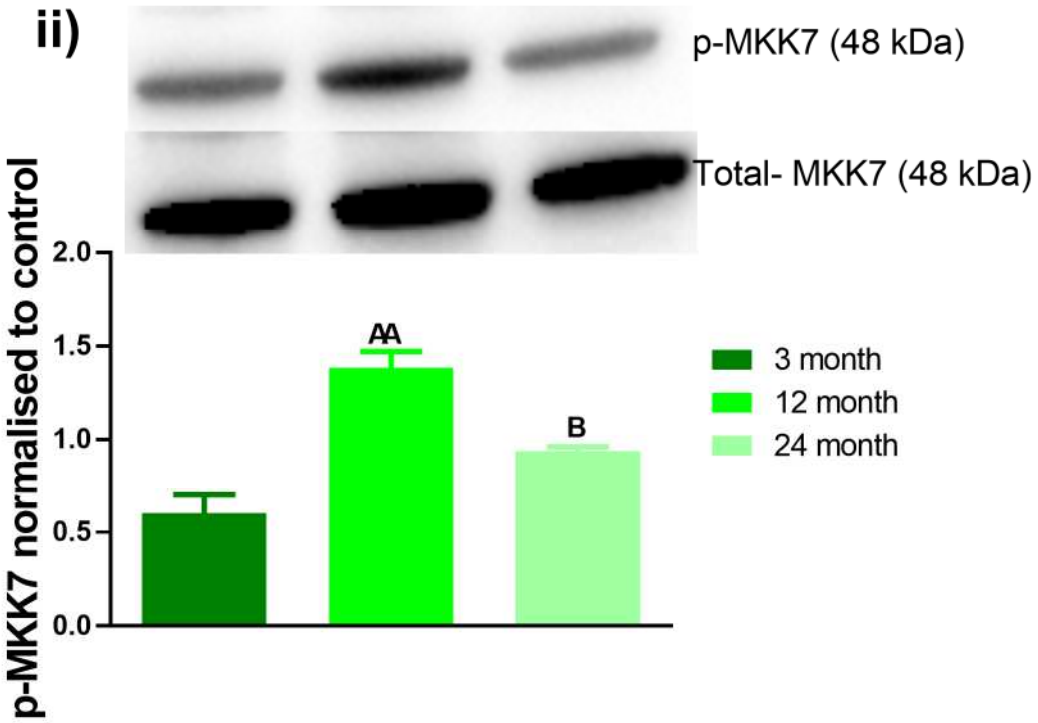

Figure 3.10: Western blot assessment of MKK7 phosphorylation levels in an isolated heart Langendorff model after 120 minutes of Sunitinib (1µM) perfusion.

*Data expressed as mean ± S.E.M., * = p<0.05, * = p<0.01 and *** = p<0.001. i) P-MKK7 levels are presented as a percentage of total MKK7 found in the heart tissue. Statistics: Student's t-test was carried out between Control vs Sunitinib (*) of each age group (n=3). ii) The Sunitinib treatment group were then normalised to the control (control = 1) of the same age group to allow for comparison of p-MKK7 levels in the different age groups (n=3). Statistics: One-way ANOVA comparing vs 3 month = A, vs 12 month = B and vs 24 month = C.*

3.5 Discussion

In the clinic, the level of cardiotoxicity generated by Sunitinib treatment is largely under estimated (Schmidinger et al. 2008). This is evident by the increasing number of cancer survivors, developing acute and delayed toxicities later in life (Lipshultz et al. 2013).

Age is a well-established risk factor which may predispose a patient to cardiotoxicity and as Sunitinib treatment is administered to patients at a variety of ages (from paediatrics to patients over 65), it is important to identify the level of Sunitinib-induced cardiotoxicity produced in various age groups (Hutson et al. 2014, Janeway et al. 2009, Pai and Nahata 2000). Hence, we investigated age associated differences in Sunitinib-induced cardiotoxicity by measuring changes in haemodynamic parameters (LVDP, HR and CF) and the level of heart tissue infarction in 3 month, 12 month and 24 month rats.

The present study demonstrated that raw haemodynamic data differed between age groups during both control and Sunitinib treatment. In particular, the 24 month group had reduced levels of LVDP, HR and CF in control groups compared to the other age groups. This was an expected finding as ageing is associated with a reduction in cardiac output (Parikh et al. 2016). For this reason, the raw haemodynamic data was normalised to the stabilisation period, so that a percentage change in haemodynamic parameter could be observed and comparisons between age and drug treatment group could be drawn.

3.5.1 Sunitinib is cardiotoxic in all three age groups

Following, normalisation to the stabilisation period there was a significant percentage decrease in LVDP in all 3 age groups. Left ventricular dysfunction is one of the main adverse

cardiac side-effects of Sunitinib treatment, after hypertension (Chu et al. 2007). During a 3 year study, which followed 48 patients, undertaking Sunitinib treatment, Telli et al. reported significant declines in left ventricular ejection fraction in 21% of patients and 15% of patients developed symptoms of heart failure in patients aged between 32 and 81 years (Telli et al. 2008).

Chu et al. also demonstrated deterioration of myocardial contractility in response to Sunitinib treatment in patients with an average age of 54 years (Chu et al. 2007). Left ventricular dysfunction and a decline in cardiac contractility have been linked to mitochondrial dysfunction, which occurs as a result of the inhibition of ribosomal S6 kinase and AMP-activated protein kinase by Sunitinib (Hasinoff and Patel 2010, Kerkela et al. 2009).

Interestingly, in the presented study the 24 month group produced the largest maximum drop in LVDP. Sunitinib has been shown to produce non-reversible adverse cardiovascular effects in elderly patients between 4-44 days of the onset of treatment (Brunello et al. 2012, Khakoo et al. 2008). The heart has a high energy demand and through ageing essential cellular processes, including autophagy, become dysfunctional (Peart et al. 2014). This results in an accumulation of impaired cellular machinery, such as mitochondria. In turn, this reduces the level of ATP available for cardiomyocytes and reduces heart function, both of which have been linked to age associated heart failure (Moyzis, Sadoshima and Gustafsson 2015). It is likely that Sunitinib caused a further depletion in ATP levels in aged hearts through the inhibition of AMPK which lead to a decline in left ventricular function (Force, Krause and Van Etten 2007). The younger hearts may facilitate a more efficient process of autophagy and cell death pathways, which prevent the accumulation of dysfunctional mitochondrial and protein signalling (Zhao et al. 2010). However, this needs to be

investigated in further detail by directly investigating mitochondria dysfunction (Brand and Nicholls 2011), as well as, autophagy and cell death pathway responses to Sunitinib (Knaapen et al. 2001, Yeap et al. 2013).

Heart rate was also significantly affected by Sunitinib treatment. Both the 3 month and 12 month group demonstrated significant declines in heart rate. In Langendorff studies, Henderson et al. observed a dose-dependent decline in HR under ischaemic conditions (Henderson et al. 2013). In the clinic, declines in HR are a common side effect of Sunitinib treatment (Azizi, Chedid and Oudard 2008). Bello et al. demonstrated that Sunitinib induces QT-interval prolongation in patients and there is a dose-dependent increased risk of ventricular arrhythmias with Sunitinib treatment (Bello et al. 2009). At a cellular level, Sunitinib had been shown to block the cardiac hERG channel which is associated with long QT syndrome (Doherty et al. 2013).

Interestingly, Sunitinib treatment did not generate declines in HR in the 24 month group. This could be due the 24 month group having a much lower heart rate at baseline and in the control hearts. Over time, the heart enlarges in response to increase in haemodynamic load, neuro-hormonal and pro-hypertrophic signalling (Gosse 2005). Remodelling fundamentally begins with molecular changes, such as altered cell growth regulation and protein expression. This results in impairment of myocardial performance and causes a lower heart rate (Lupón et al. 2015). Perhaps, a lower HR at baseline as shown by the HR raw data, prevented Sunitinib from reducing it further.

Furthermore, we investigated the level of Sunitinib-induced infarct size. All of the age groups demonstrated significant increases in infarct size after Sunitinib treatment, compared to control hearts. Henderson et al. measured troponin levels as a marker for

myocyte injury. The group demonstrated significant increases in troponin levels release from hearts treated with 1 µM Sunitinib, indicating that Sunitinib caused direct injury to the cardiomyocytes (Henderson et al. 2013).

In a study using induced pluripotent stem cell-derived cardiomyocytes, Cohen et al. discovered that Sunitinib treatment resulted in a reduction in ATP and increased oxidised gluthione levels, which was thought to induce apoptosis (Cohen et al. 2011). In addition to this, 1 µM Sunitinib treatment of isolated human myocardium tissue and isolated mouse left ventricular myocytes, was shown to produce a significant decline in intracellular Ca^{2+} levels and an increase in levels of reactive oxygen species (ROS) generation, which can cause apoptosis (Rainer et al. 2012).

In the present study, the 3 month group produced a much larger infarct size than both the 12 and 24 month groups. It has been established that younger patients (<20 years) are highly susceptible to cardiac injury during and after cancer therapy (Hancock, Tucker and Hoppe 1993). The cardiovascular system of the developing child/adolescent is thought to be particularly vulnerable to toxicities (Oeffinger et al. 2006). QT-interval prolongation and a decrease in ejection fraction has been reported in children during the first cycle of Sunitinib treatment, however, these cardiovascular effects were reversed following further cycles of Sunitinib treatment (Dubois et al. 2011). This suggests that younger heart tissue could have an initial sensitivity to Sunitinib induced cardiotoxicity. Our current study confirms this as the 3 month group demonstrated significant declines in LVDP, HR and infarct size in response to Sunitinib treatment.

Interestingly, the 12 and 24 month old rat hearts produced smaller infarct sizes than 3 month old rats after Sunitinib treatment. Capitanio et al (2016) demonstrated that elements

of heart protection could be present in disease-free ageing of Sprague Dawely rats. There was an activation of cellular protective mechanisms such as a reduction in ROS generation, resistance to apoptosis and inhibition of mtPTP opening (Capitanio et al. 2016). Therefore, the 12 and 24 month group could have developed resistance to cell death and tissue injury through ageing.

However, the huge decline in LVDP in response to Sunitinib in the 24 month group is indicative of cardiovascular dysfunction (Chu et al. 2007). Previous studies have shown that younger animals tolerate significantly larger infarct sizes without producing left ventricular dysfunction and other symptoms of coronary heart failure compared to aged animals (Gould et al. 2002). Bujak et al. (2008) demonstrated that younger animals effectively recruit myofibroblasts to infarcted areas and then generate collagen-based scars. However, elderly animals were shown to form defective scar tissue, which was postulated as being due to a reduced myofibroblast density in elderly heart tissue. In addition to this, Bujak et al. demonstrated that healing defects in elderly mice resulted in adverse cardiac remodelling and enhanced systolic dysfunction, which were not correlated to infarct size, but instead to the lack of tensile strength in the tissue scaring (Bujak et al. 2008). Further investigation into the contractility properties of aged heart tissue and myofibroblast recruitment in response to Sunitinib treatment is required to establish why Sunitinib treatment caused the heart of 24 month rats to produce reductions in function, yet produced smaller infarct sizes than younger animals, relative to Control.

3.5.2 Key cardiac injury linked miRNAs are altered by Sunitinib treatment

Short non-coding RNA microRNAs (miRNAs) carry out the negative regulation of mRNA transcripts by repressing translation (Bagga et al. 2005). Specific miRNAs expression patterns have been linked to cardiomyocyte differentiation and in response to stress (Babiarz et al. 2011) and have also been shown to be differentially expressed during the development of heart failure (Thum et al. 2007).

miRNAs regulate the expression and function of eukaryotic genomes. Changes in the expression of certain miRNAs could be indicative of specific diseases or medical conditions (Lu et al. 2008). miR-1, miR-27a, miR-133a and miR-133b expression profiles tend to be altered during cardiac injury and during the progression of heart failure (Akat et al. 2014, Tijsen, Pinto and Creemers 2012). We show Sunitinib induced changes in 3 of the miRNAs investigated (miR-27a, miR-133a and miR-133b) in the 3 age groups investigated.

In response to Sunitinib, miR-27a was reduced in all age groups. miR-27a has been shown to downregulate FOXO-1 protein, a transcription factor which regulates genes involved in the apoptotic response, cell cycle, and cellular metabolism (Guttilla and White 2009). It has also been observed that over expression of FOXO1 resulted in decreased cell viability because of inhibition of cell cycle and induction of apoptosis. A down regulation of miR-27a has been linked to an increased sensitivity to Adriamycin induced apoptosis (Zhang et al. 2010). This suggests that miRNA-27a is an effective regulator of apoptosis.

In coronary sinus samples, miRNA27a was significantly downregulated in heart failure patients (Marques et al. 2016). The significant decrease in miR-27a expression during Sunitinib treatment during the current study follows the same trend in expression as

patients with heart failure and apoptosis at a cellular level, which could suggest that a down-regulation of miR-27a predicts an increase in cell death or heart tissue damage within the heart, as we have shown an increase in infarct size in all age groups.

Interestingly, miR-133a and miR133b are both significantly upregulated in 3 month rats but downregulated in 24 month old rats in response to Sunitinib treatment. miR-133a has a partial complimentary target site in the 3'UTR region of the human ether-a-go-go related gene (*ERG*) potassium channel transcripts, implying that miR-133a overexpression inhibits the *ERG* potassium channel expression. A reduction in ERG potassium channel expression results in delayed myocyte repolarisation, which is attributed to a long QT interval (Xiao et al., 2007). Therefore, the increase in miR-133a found in the 3 month group suggests an increase in ERG inhibition, which could be responsible for a slower heart rate.

Sunitinib treatment of both the 12 month and the 24 month group demonstrated significant reductions in miR-133a. This could suggest that Sunitinib causes attenuation of the *ERG* potassium channel expression by miR-133a may have taken place (Bello et al. 2009). However, Sunitinib also induced significant reductions in HR in the12 month group. This suggests that alternate mechanisms to Sunitinib-induced ERG inhibition could be occurring in older animals. This highlights the complexity of Sunitinib-induced HR reductions at different ages.

In addition, miR-133a has been shown to be upregulated during oxidative stress (Izarra et al. 2014). Plus, in cardiomyocytes miR-133b has been shown to be upregulated during apoptosis, but downregulated during hypertrophy (Ramasamy et al. 2015). This could suggest that Sunitinib treatment resulted in increased levels of oxidative stress and cell death, in the 3 month group, which resulted in a larger infarct size compared to 12 month

and 24 month groups. miRNAs have previously been shown to be differentially expressed when young rodent hearts are compared to aged rodent hearts (Zhang, Azhar and Wei 2012). Perhaps, ageing provides alternate signalling mechanisms which reduces levels of Sunitinib-induced cell death or heart tissue damage. This needs to be investigated further.

3.5.3 The level of MKK7 transcription and protein phosphorylation is altered by Sunitinib treatment and the age of rats treated

MKK7 has a vital role in cellular stress response and is fundamental in regulating cell survival, proliferation and cell death (Foltz et al. 1998). Here we show the level of MKK7 transcription and MKK7 protein phosphorylation is affected by ageing and Sunitinib treatment.

In 3 month old rat hearts treated with Sunitinib, there is a significant reduction in both MKK7 mRNA and phosphorylated MKK7, compared to Control. Inactivation of MKK7 has been shown to result in embryonic lethality, defective hepatocyte proliferation and in embryonic fibroblasts, MKK7 knockdown causes impaired proliferation, premature senescence and G2/M cell cycle arrest (Wada et al. 2004). Plus, as demonstrated by Liu et al., loss of MKK7 enhanced the deterioration of ventricular function following pressure overload (Liu et al. 2011). Therefore, a reduction in MKK7 transcription could be responsible for the increases sensitivity to Sunitinib induced cardiotoxicity, as shown by the increase in infarct size compared to Control and to the other age groups investigated.

Sunitinib treatment significantly increased the levels of MKK7 mRNA in the 12 month group and there was a tendency for an increased in MKK7 mRNA levels in the 24 month group. Interestingly Hsieh et al. 2003, also demonstrated an increased level of MKK7 activation in

response to ROS generation in 24 month mice compared to 3 month mice (Hsieh et al. 2003). Previously, over expression of MKK7 has also been shown to produce characteristic features of myocardial hypertrophy, which may have contributed to the loss of contractile function and cardiomyocyte viability following ischaemia/reperfusion injury (Wang et al. 1998). In turn, studies investigating cardiac hypertrophy have shown activated MKK7 levels to be significantly higher than in controls (Wang et al. 2008). This could suggest that the increase in MKK7 mRNA in the 12 month and 24 month groups and phosphorylated MKK7 in the 12 month group could indicant a hypertrophic response to Sunitinib treatment. Previous research has indicated an increased level of MAPK signalling associated with ageing. In particular, rats aged 12 months and over were found to have significantly higher levels of phosphorylated JNK in kidney tissue in normoxic conditions (Kim et al. 2002). However, this group did not investigate activation of the MAPK pathways in response to stress.

In the present study, Sunitinib treatment of the 24 month group did not alter levels of p-MKK7, but significantly increased MKK7 mRNA levels. Atypical gene Control underlies the age-related decline in physiologic function and age-associated diseases (Rahman et al. 2013). This decline in gene regulation can reduce the ability for cells to cope with stress (Révész et al. 2014). This could explain the significant Sunitinib-induced decrease in LVDP found in the 24 month group, compared to the 3 month group, yet the 3 month group exhibited a smaller infarct size compared to 24 month group following Sunitinib treatment.

In addition, resistance to stress is important as it is key to animal survival and longevity. It is evident that individuals with longer life spans produce a stronger resistance to environmental and or physiological stress (Pérez et al. 2009). It has been shown that over expression of a variety of stress-related proteins in specific tissues leads to a longer life span

(Saunders and Verdin 2009). Here we show that an increase in MKK7 mRNA levels in response to Sunitinib treatment resulted in smaller infarct sizes. Perhaps overtime cells adapt cellular processes, including MKK7 signalling, to increase resistance to initiation of cell death pathways (Gosse 2005).

3.6 Conclusion

This study shows that all age groups exhibited signs of Sunitinib-induced cardiotoxicity. However, we conclude that ageing strengthens the hearts ability to resist Sunitinib-induced heart tissue death, but increases detrimental effects on haemodynamic function. The younger group (3 months old) appeared to be more sensitive to toxicities in the early stages of treatment, with reductions in haemodynamic parameters and significantly larger infarct size. In addition, this chapter reveals for the first time that MKK7 has a role in Sunitinib-induced cardiotoxicity. Sunitinib treatment of the younger animals produced an inhibitory effect on MKK7 phosphorylation and reduced the levels of left ventricular MKK7 mRNA levels. The reduction in MKK7 levels could be responsible for the larger increase in infarct size found in the younger group. This could be due to younger animals having underdeveloped cellular signalling pathways, which are not mature enough to cope with the toxicities associated with Sunitinib treatment.

The middle-aged group (12 months old) treated with Sunitinib were also more resistant to left ventricular symptoms of cardiotoxicity, compared to the elderly group. The middle-aged group also produced an increased level of MKK7 phosphorylation which could have produced adaptive hypertrophic responses, and may have delayed the onset of tissue infarction. However, the elderly group demonstrated a high resistance to Sunitinib-induced

heart tissue damage. Perhaps this was achieved through a resistance to stress as MKK7 phosphorylation levels were unchanged compared to control.

Discovering the role of proteins involved in the development of Sunitinib-induced cardiotoxicity could lead to the identification of biomarkers, which could be monitored during treatment. If levels of biomarkers reach the levels known to be associated with toxicity, treatment could be stopped much sooner than when just an electrocardiogram is used. In addition, identification of proteins involved in cardiotoxicity could allow the discovery of cardioprotective agents which could be used to reduce the level of cardiac damage during Sunitinib treatment. In future investigations, it would be interesting to identify whether agonists or antagonists of MKK7 would influence the level of Sunitinib induced cardiotoxicity.

Finally, this study also highlighted the importance of evaluating the different responses aging can produce in response to drug treatments. This should be considered in preclinical drug testing.

4. Sunitinib-induced cardiotoxicity is partially attenuated through the inhibition of ASK1

4.1 Abstract

The tyrosine kinase inhibitor, Sunitinib is used to treat cancer and is linked to severe adverse cardiovascular events. Mitogen activated kinase kinase 7 (MKK7) is involved in the development of cardiac injury and is a component of the c-Jun N-terminal kinase (JNK) signal transduction pathway. Apoptosis signal-regulating kinase 1 (ASK1) is the upstream activator of MKK7 and is specifically inhibited by ethyl 2, 7-dioxo-2, 7-dihydro-3*H*-naphtho [1, 2, 3-*de*] quinoline-1-carboxylic acid ethyl ester (NQDI-1). This study investigates the role of ASK1, MKK7 and JNK during in Sunitinib-induced cardiotoxicity.

Isolated, male, Sprague-Dawley rat, Langendorff-perfused, hearts were treated with Sunitinib in the presence and absence of NQDI-1 for 125 min, whilst cardiac function and infarct size were measured. Left ventricular cardiac samples were analysed by qRT-PCR for MKK7 mRNA expression and myocardial injury associated microRNAs (miR-1, miR-27a, miR-133a and miR-133b) or Western blot analysis to measure ASK1/MKK7/JNK phosphorylation.

Administration of Sunitinib (1 μM) during Langendorff perfusion significantly increased infarct size, decreased heart rate (HR) and decreased left ventricular developed pressure (LVDP). As well as, increased miR-133a expression and decreased phosphorylation of the ASK1/MKK7/JNK pathway compared to control. Co-administration of NQDI-1 (2.5 μM) attenuated the increase in infarct size induced by Sunitinib administration alone, reversed the miR-133a expression pattern and increased phosphorylated levels of ASK1/MKK7/JNK.

The detrimental effects Sunitinib induced in the haemodynamic parameters were not attenuated by NQDI-1 co-administration. These findings suggest that the ASK1/MKK7/JNK intracellular signalling pathway is important in Sunitinib-induced cardiotoxicity. The anti-cancer properties of Sunitinib were also assessed using the 3-(4, 5-Dimethulthiazol-2-yl)-2, 5-Diphenyltetrazolium Bromide (MTT) cell viability assay. Sunitinib significantly decreased the cell viability of human acute myeloid leukaemia 60 cell line (HL60). The combination of Sunitinib (1 nM - 10 µM) with NQDI-1 (2.5 µM) enhanced the cancer-fighting properties of Sunitinib. Investigations into the ASK1/MKK7/JNK transduction pathway could lead to development of cardioprotective adjunct therapy, which could prevent Sunitinib-induced cardiac injury.

4.1 Introduction

The tyrosine kinase inhibitor (TKI) Sunitinib is used in the treatment of many cancers (Faivre et al. 2006). Sunitinib prevents tumour cell survival and angiogenesis by inhibiting a variety of growth factor and cytokine receptors, including platelet derived growth factor receptors (PDGFRs), vascular endothelial growth factor receptors (VEGFRs) and proto-oncogenes c-Kit and RET (Force, Krause and Van Etten 2007).

However, Sunitinib is also associated with a lack of kinase selectivity, which potentially results in cardiotoxic adverse effects (Force, Krause and Van Etten 2007). In the clinic, Sunitinib treatment is associated with: QT prolongation (Bello et al. 2009), left ventricular dysfunction (Shah and Morganroth 2015) and development of heart failure (Ewer et al. 2014). These findings are consistent with many other successful chemotherapy agents which are linked to severe drug-induced cardiotoxicity (Hahn, Lenihan and Ky 2014)

including electrophysiological changes and LV dysfunction which can cause heart failure in some patients (Aggarwal, Kamboj and Arora 2013).

In vivo studies have revealed that Sunitinib induces: left ventricular hypertrophy, hypertension and heart failure (Gupta and Maitland 2011). Also, *in vitro* studies have shown Sunitinib to cause mitochondrial injury and cardiomyocyte apoptosis through an increase in caspase-9 and cytochrome C release in both mice and in cultured rat cardiomyocytes (Chu et al. 2007). Other indicators of apoptosis, such as an increase in caspase-3/7, have also been detected after Sunitinib treatment in rat myocytes (Hasinoff, Patel and O'Hara 2008).

MKK7 facilitates cellular responses to exogenous and endogenous stimuli (Foltz et al. 1998). The activation of JNK by MKK7 results in the initiation of cellular processes including: proliferation, differentiation and apoptosis (Schramek et al. 2011, Chang and Karin 2001, Sundarrajan et al. 2003). MKK7 has a vital role in protecting the heart from hypertrophic remodelling, which occurs via cardiomyocyte apoptosis and heart failure (Liu et al. 2011). Whereas, JNK signalling is vital for the maintenance and organisation of the cytoskeleton and sarcomere structure in cardiomyocytes (Windak et al. 2013).

Interestingly, Sunitinib has been shown to inhibit MAPK signalling (Aparicio-Gallego et al. 2011). In addition to this, Sunitinib is an ATP analogue and competitively inhibits the ATP binding domain of its target proteins (Roskoski 2007, Shukla et al. 2009). MKK7 also contains a highly-conserved ATP binding domain (Song et al. 2013). It is also possible that Sunitinib could directly interact with the MKK7, and inhibit the MKK7/JNK transduction pathway and thereby reduce MKK7 pathway activation.

It is important to determine the relationship between MKK7 expression and Sunitinib induced cardiotoxicity by measuring the alteration of MKK7 mRNA and phosphorylated MKK7 levels in the presence of Sunitinib. Determining the relationship between Sunitinib and MKK7 could lead to a greater understanding of its off-target mechanism of action and lead to the improvement of future drug discovery programmes or novel cardioprotective adjunct therapies.

Short non-coding RNA microRNAs (miRNAs) carry out the negative regulation of mRNA transcripts by repressing translation (Bagga et al. 2005). Specific miRNAs expression patterns have been linked to cardiomyocyte differentiation and in response to stress (Babiarz et al. 2011) and have also been shown to be differentially expressed during the development of heart failure (Thum et al. 2007). The miRNAs miR-1, miR-27a, miR-133a and miR-133b produce differential expression patterns during the progression of heart failure (Akat et al. 2014, Tijsen, Pinto and Creemers 2012). It is important to identify miRNA expression profiles in response to drug-induced cardiotoxicity, as similar patterns in miRNA expression to those identified during heart failure may indicate the early onset of cardiotoxicity at a molecular level.

As there is not a commercially available selective, MKK7 inhibitor, we have chosen to investigate inhibition of the upstream kinase ASK1, which is linked to MKK7 activation (Ichijo et al. 1997). ASK1 is activated in response to oxidative stress and stress-induced vascular endothelial growth factor (VEGF) suppression in the heart (Nako et al. 2012). Izumiya et al. (2003) used ASK1 deficient transgenic mice to assess the role of ASK1 in cardiac hypertrophy. Both wild type and ASK1 deficient mice developed hypertension when stimulated with angiotensin II. Interestingly, the ASK1 deficient mice did not produce signs

of cardiac hypertrophy. Cardiac remodelling, in addition activation of ASK1, p38 and JNK was severely attenuated. This study emphasised the importance of ASK1 in cardiac hypertrophy and remodelling signalling (Izumiya et al. 2003).

ASK1 is selectively inhibited by NQDI-1 with high specificity with a K_i of 500nM and IC_{50} of 3µM (Volynets et al. 2011). However, as this is a relatively new drug, a complete pharmacological profile has not been fully characterised.

ASK1 inhibition has previously been shown to offer protection against ischaemia reperfusion injury (Toldo et al. 2012) and has also been shown to supress the progression of ventricular remodelling and fibrosis in hamsters expressing severe cardiomyopathy phenotypes (Hikoso et al. 2007). These findings highlight the potential of NQDI-1 as a valuable asset to inhibit cardiac injury via the ASK1/MKK7/JNK pathway.

This novel study investigated the involvement of the ASK1/MKK7/JNK pathway in the Sunitinib-induced cardiotoxicity via the assessment of cardiac function and infarct in conjunction with relevant intracellular signalling mediators. Furthermore, we assessed the anti-cancer properties of Sunitinib and determined whether co-administration of Sunitinib with NQDI-1 affected the anti-cancer/apoptotic effect of Sunitinib in HL60 cells.

4.1.2 Hypothesis

The used of the ASK1 inhibitor NQDI-1 as an adjunct therapy with Sunitinib in the Langendorff isolated heart model will demonstrate protective properties against the cardiotoxic effects of Sunitinib treatment. In addition, miRNAs we successfully identify the cardioprotective effects of NQDI-1.

4.3 Materials and methods

4.3.1 Materials

Sunitinib malate and NQDI-1 were purchased from Sigma Aldrich (UK). Both drugs were dissolved in dimethyl sulphoxide (DMSO) and stored at -20 °C. Krebs perfusate salts were from either VWR International (UK) or Fisher Scientific (UK). Phospho-ASK1 (Thr 845) and Total ASK1 were purchased from Abcam (UK). Phospho-MKK7 (Ser271/Thr275), Total MKK7, Phospho-SAPK/JNK (Thr183/Tyr185), Total SAPK/JNK rabbit mAb antibodies, anti-rabbit IgG, HRP-linked antibody and anti-biotin, HRP-linked antibody were purchased from Cell signalling technologies (UK). The Ambion MicroPoly (A) Purist kit, Ambion mirVana miRNA Isolation Kit and Reverse Transcription Kit were from Life Technologies (USA). The mRNA primers and the Applied Biosystems primers assays (U6, rno-miR-1, hsa-miR-27a, hsa-miR-133a, and hsa-miR-133b) were purchased from Invitrogen (UK). The iTaq Universal SYBR Green Supermix was purchased from BioRad (UK). The HL60 cell line was obtained from the European Collection of Cell Culture (UK).

4.3.2 Animals and Ethics

Adult male Sprague-Dawley rats (300-350 g in body weight) were purchased from Charles River UK Ltd (UK) and housed suitably. They received humane care and had free access to standard diet according to “The Guidance on the Operation of the Animals (scientific procedures) Act of 1986”. Animals were selected at random for all treatment groups and the collected tissue was blinded for infarct size assessment. The experiments were performed following approval of the protocol by the Coventry University Ethics Committee. All efforts were made to minimize animal suffering and to reduce the number of animals used in the

experiments. Rats were sacrificed by cervical dislocation (Schedule 1 Home Office procedure).

A total of 80 animals were used for this study and the data from 68 rats were included, while data from 12 rats were excluded from analysis due to the established haemodynamic exclusion criteria. No animals were culled due to ill health.

4.3.3 Langendorff perfusion model

The hearts were rapidly excised after the rats were sacrificed and placed into ice-cold Krebs Henseleit (KH) buffer (118.5 mM NaCl, 25 mM $NaHCO_3$, 4.8 mM KCl, 1.2 mM $MgSO_4$, 1.2 mM KH_2PO_4, 1.7 mM $CaCl_2$, and 12 mM glucose, pH 7.4). The hearts were mounted onto the Langendorff system and retrogradely perfused with KH buffer. The pH of the KH buffer was maintained at 7.4 by gassing continuously with 95 % O_2 and 5 % CO_2 and maintained at 37 ± 0.5 °C using a water-jacketed organ chamber. The left atrium was removed and a latex iso-volumic balloon was carefully introduced into the left ventricle and inflated up to 5-10 mmHg. Functional recordings (LVDP and HR) were taken via a physiological pressure transducer and data recorded using Powerlab, AD Instruments Ltd. (UK). Coronary flow (CF) was measured by collecting and measuring the volume of perfusate for 1 minute, thereafter it was disposed of. All haemodynamic parameters were measured at 5 minute and then 15 minute intervals after 35 minutes of drug treatment.

Each Langendorff study was conducted using the protocol for naïve Langendorff studies (Gharanei et al. 2013). In summary, each Langendorff experiment was carried out for 145 minutes: a 20 minute stabilisation period and 125 minutes of drug or vehicle perfusion in normoxic conditions.

The hearts were not paced as this study assessed the changes in heart rate caused by Sunitinib. Instead, the hearts were stabilised for a period of 20 minutes. Generally, the hearts became stable after 10 minutes, therefore all haemodynamic parameters were normalised to the last 10 minutes of the stabilisation period (%) to take into account the variations between individual starting HR, LVDP and CF levels. Hearts were included in the study with a HR between 225-325 beats per minute, a LVDP between 80-150 mmHg and a CF between 3.5-12.0 ml/g (weight of the rat heart) during the stabilisation period. Sunitinib malate (1 µM) was administered throughout the perfusion period in the presence or absence of NQDI-1 (2.5 µM).

The clinically relevant dose of 1 µM Sunitinib was chosen in line with previous studies by (Henderson et al. 2013). Additionally, it has been reported that the plasma concentration of Sunitinib has a Cmax in the rage of 0.5–1.4µM (Doherty et al. 2013). While, the dose of 2.5 µM NQDI-1 was chosen following a thorough literature review. Calculations for NDQI-1's IC_{50} for ASK-1 range between 500 nM-3 µM (Eaton et al. 2014, Song et al. 2015, Volynets et al. 2011). NQDI-1 is not yet used in the clinic, therefore a clinically relevant dose has not been reported.

Langendorff perfused hearts treated with vehicle were recorded as the control group. The hearts were then weighed and either stored at -20 °C for 2,3,5-Triphenyl-2H-tetrazolium chloride (TTC) staining or the left ventricular tissue was dissected free and immersed in RNAlater from Ambion (USA) for qRT-PCR or snap frozen by liquid nitrogen for Western blot analysis.

4.3.4 Infarct size analysis

Frozen whole hearts were sliced into approximately 2 mm thick transverse sections and incubated in 0.1 % TTC solution in phosphate buffer (2 ml of 100 mM $NaH_2PO_4.2H_2O$ and 8 ml of 100 mM NaH_2PO_4, pH 7.4) at 37 °C for 15 minutes and fixed in 10% formaldehyde (Fisher Scientific, UK) for 4 hours. The risk zone and infarct areas were traced onto acetate sheets. The tissue at risk stained red and infarct tissue appeared pale. The acetate sheet was scanned and ImageTool from UTHSCSA (USA) software was used to measure the area of infarct and the area of risk. A ratio of infarct to risk size was calculated (as a percentage) for each slice. An average was taken of all of the slices from each heart to give the percentage infarct size of the whole heart. The mean of infarct to risk ratio for each treatment group and the mean ± SEM was plotted as a bar chart. The infarct size determination was randomised and blinded.

4.3.5 Analysis of miRNA expression profiles

The miRNA was isolated from left ventricular tissue using the *mir*Vana™ miRNA Isolation Kit from Ambion (UK). The miRNA quantity and quality were measured by NanoDrop from Nanoid Technology (USA). A total of 500 ng miRNA was reverse transcribed into cDNA using primers specific for housekeeping reference RNA U6 snRNA and target miRNAs: hsa-miR-155, hsa-miR-15a, hsa-miR-16-1, rno-miR-1, hsa-miR-27a, hsa-miR-133a or hsa-miR-133b (please note all human hsa-miRNAs assays are compatible with rat samples) from Applied Biosystems (USA) using the MicroRNA Reverse Transcription Kit from Applied Biosystems (USA) according to the manufacturer's instructions. The reverse transcription quantitative PCR reaction was performed with the following setup: 16 °C for 30 min, 42°C for 30 min and

85 °C for 5 min and ∞ at 4°C. The qRT-PCR was performed using the TaqMan Universal PCR Master Mix II (no UNG) from Applied Biosystems (USA) protocol on the 7500 HT Real Time PCR sequence detection system from Applied Biosystems (USA). A 20µl reaction mixture containing 100 ng cDNA, specific primer assays mentioned above from Applied Biosystems (USA) and the TaqMan Universal PCR Master Mix was used in the qRT-PCR reaction in triplicates. A non-template control was included in all experiments. The real time PCR reaction was performed using the program: 1) 2 minutes at 50°C, 2) 10 minutes at 95°C, 3) 15 seconds at 95°C, 4) 1 minute at 60°C. Steps 3) and 4) were repeated 40 times.

Analysis of qRT-PCR data of miRNAs were performed using the Ct values for U6 snRNA as reference for the comparison of the relative amount of miRNAs (rno-miR-1, hsa-miR-27a, hsa-miR-133a and hsa-miR-133b). The relative amount of each of the miRNA was calculated using the formula: $X_0/R_0=2^{CTR-CTX}$, where X_0 is the original amount of target miRNA, R_0 is the original amount of U6 snRNA, CTR is the CT value for U6 snRNA, and CTX is the CT value for the target miRNAs (rno-miR-1, hsa-miR-27a, hsa-miR-133a and hsa-miR-133b) (Sandhu, Ansar and Edvinsson 2010). Averages of the Ct values for each sample group (control, Sunitinib, Sunitinib+NQDI-1 and NQDI-1 alone, treated hearts) and each individual primer set were calculated and bar charts were plotted with mean ± SEM. The mean of the control group was set as 1 for all miRNAs.

4.3.6 Measurement of MKK7 mRNA expression

Total mRNA was extracted from left ventricular tissue using The Ambion MicroPoly (A) Purist kit from Ambion (USA). Extracted mRNA was processed directly to cDNA by reverse transcription using Reverse Transcription Kit from Applied Biosystems (USA) with the

respective primers for MKK7 (MKK7 forward primer: CCCCGTAAAATCACAAAGAAAATCC and MKK7 reverse primer: GGCGGACACACACTCATAAAACAGA) and GAPDH (GAPDH Forward primer: GAACGGGAAGCTCACTGG and GAPDH Reverse primer: GCCTGCTTCACCACCTTCT) according to the instructions from the manufacturer Invitrogen (UK). The reverse transcription PCR reaction was performed with the following setup: 16 °C for 30 minutes, 42°C for 30 minutes and 85 °C for 5 minutes. The qRT-PCR reactions were performed with the iTaq Universal SYBR Green Supermix from BioRad (UK), GAPDH and MKK7 mRNA primer sets on the 7500 HT Real Time PCR machine from Applied Biosystems (USA) using the program: 1) 2 minutes at 50°C, 2) 10 minutes at 95°C, 3) 15 seconds at 95°C, 4) 1 minute at 60°C. Steps 3) and 4) were repeated 40 times.

Analysis of qRT-PCR data of MKK7 mRNA was performed using the Ct values for GAPDH mRNA as reference for the comparison of the relative amount of MKK7 mRNA. This was calculated using the following formula: $X_0/R_0=2^{CTR-CTX}$, where X_0 is the original amount of target mRNA, R_0 is the original amount of GAPDH mRNA, CTR is the CT value for GAPDH mRNA, and CTX is the CT value for the target MKK7 mRNA. Averages of the Ct values for each sample group (control, Sunitinib, Sunitinib+NQDI-1 and NQDI-1 alone, treated hearts) and each individual primer set were calculated and bar charts were plotted with mean ± SEM. The mean of the control group was set as 1 for MKK7 mRNA.

4.3.7 Western blot detection of ASK1, MKK7 and JNK

A total 50 ± 5 mg of the frozen left ventricular tissue was lysed in lysis buffer (NaCl 0.1 M, Tris base 10 µM, EDTA 1 mM, sodium pyrophosphate 2 mM, NaF 2 mM, β-glycaophosphate 2 mM, 4-(2-Aminoethyl) benzenesulfonyl fluoride hydrochloride (AEBSF), (0.1 mg/ml, 1/1.5

of protease cocktail tablet), pH 7.6) using a IKA Overtechnical T25homogeniser at 11,000 RPM. The supernatants were measured for protein content using NanoDrop from Nanoid Technology (USA). Then 80 µg of protein was loaded to a pre-made gel (4–15 % Mini-PROTEAN® TGX™ Gel for MKK7, any KDa Mini-PROTEAN® TGX™ Gel for JNK and 8-20 % Mini-PROTEAN® TGX™ Gel for ASK1 (BioRad, UK)) and separated by electrophoresis at 200 V and 50 mA for 60 minutes.

Following separation, the proteins were transferred to the Bond-P polyvinylidene difluoride (PVDF) membrane from BioRad (UK) by using the Trans-Blot Turbo transfer system from BioRad (UK) and probed for the phosphorylated forms Phospho(Thr^{845})-ASK1 (p-ASK1), Phospho(Ser^{271}/Thr^{275})-MKK7 (p-MKK7) and Phospho(Thr^{183}/Tyr^{185}) -SAPK/JNK (p-JNK), and total forms of ASK1(Thr^{845}), MKK7(Ser^{271}/Thr^{275}) and JNK(Thr^{183}/Tyr^{185}). The p-MKK7 and p-JNK blots were stripped by boiling and the PVDF membrane was used for total MKK7 and total JNK analysis, respectively. According to recommendations from Abcam (UK) total ASK1 analysis had to be performed on a separate Western blot, as the stripping procedure would remove total ASK1 protein. The relative changes in the p-ASK1, p-MKK7 and p-JNK protein levels were measured and corrected for differences in protein loading as established by probing for total ASK1, MKK7 and JNK respectively.

For Western blot analysis, phosphorylated protein levels were normalised to total protein levels in order to correlate for unequal loading of protein and differential blot transfer and to identify the level of active vs inactive protein levels. Results were expressed as a percentage of the density of phosphorylated protein relative to the density of total protein using Image Lab 4.1 from BioRad (UK).

4.3.8 Analysis of p-MKK7 levels by flow cytometry

4.3.8.1 Cardiomyocyte isolation

Rats were sacrificed by cervical dislocation (schedule 1 Home Office procedure) and the hearts were rapidly excised and placed into ice-cold KH buffer. Hearts were mounted onto a modified Langendorff apparatus and perfused with a modified KH buffer (described in 2.10) oxygenated and maintained at 37°C and a pH of 7.4. Once the heart had stabilised, the collagenase buffer (described in section 2.10) was administered 10 mins later to the heart at a rate of 7.5 ml/min for approximately 7 mins with a peristatic pump. The heart was then detached from the apparatus. The atria were removed and discarded. The ventricles were chopped and mechanically digested in the collagenase buffer.

Nylon mesh was used to filter cells from undigested tissue into restoration buffer (described in section 2.10).

4.3.8.2 Cardiomyocyte preparation for Flow cytometry

A suspension of 1 x 10^5 cells per well were aliquoted into a 24 well plate and incubated with control, increasing concentrations of Sunitinib (10-0.001 µM), NQDI-1 (2.5 µM), co-treatment of Sunitinib (1 µM) with NQDI-1 (2.5 µM). The cells were then incubated at 37 °C at normoxic conditions in the Nuaire DH autoflow CO_2 air jacketed incubator (Caerphilly, UK) for 2 hrs.

The cells were washed with PBS and then fixed with 3% formaldehyde in PBS and incubated for 10 mins at 37 °C. The cells were then washed with PBS and permeabilised with 90% ice

cold methanol and incubated on ice for 30 mins. The cells were stored at -20 °C until required.

The methanol was removed, the cells were washed with incubation buffer and blocked incubation buffer for 10 mins with incubation buffer. The cells were then incubated with phosphor-MKK7 antibody at a 1:100 concentration and a fluorescent conjugated secondary antibody (Alexa flour@ 488 conjugated secondary antibody) (1:100) was added. Cells were incubated in the dark for 1 hour at room temperature.

The cells were then washed with incubation buffer twice and resuspended in PBS. Samples were analysed using flow cytometry on the FL1 channel and 10000 cells were counted (FACS, Becton Dickinson, Oxford, UK).

For the flow cytometry data, values were normalised to the respective untreated control, which was represented as 1.

4.3.9 Assessment of HL60 cell viability in the presence if Sunitinib with and without NQDI-1

4.3.9.1 HL60 cell culture

The HL60 cell line were maintained in in RPMI 1640 medium supplemented with L-Glutamine (2 mM) and 10 % heat-inactivated FBS and antibiotics mix at 37 °C in a humidified incubator under 5 % CO_2/95 % air. Cells were split in a 1:5 ratio every 2-3 days. Cells were incubated with Control, increasing concentrations of Sunitinib (1 nM – 10 µM), Sunitinib (0.1 – 10 µM) + NQDI-1 (2.5 µM) 0r increasing concentrations of NQDI-1 (0.2-200 µM) for 24 h.

Both Sunitinib and NQDI-1 were dissolved in dimethyl sulfoxide (DMSO) and the DMSO concentration was < 0.05 % (v/v) during the *in vitro* studies.

4.3.9.2 Cell viability assessed by MTT assay

Cells were plated at a cell density of 10^5 cells/ml in 96-well plates and the above indicated concentration of the drug was added. The plate was then incubated at 37°C for 24hrs. After drug incubation, 50 µl of 3-(4, 5-Dimethylthiazol-2-yl)-2, 5-Diphenyltetrazolium Bromide (MTT) solution (5 mg MTT/ml H_2O) was added and the cells were incubated for a further 24 h. Next, 50 µl of DMSO was added to each well and mixed by pipetting to release reduced MTT crystals from the cells. Relative cell viability was obtained by scanning with an ELISA reader (Anthos Labtech AR 2001 Multiplate Reader, *Anthos Labtec* Instruments, Austria) with a 490 nm filter. Results were expressed as a percentage of viable cells relative to untreated cells/control. Experiments were performed in triplicates and repeated ≥ 3 times. For the determination of cell viability by the MTT assay. The mean absorbance of each treatment group was obtained. This was used to calculate the percentage of the mean absorbance of the control group.

4.3.10 Data analysis and statistics

Results are presented as mean ± standard error of the mean (SEM). The significance of all data sets were measured by the IBM SPSS program (USA) or GraphPad Prism version 5 (USA) as described in the figure legends. The following groups were compared during ANOVA analysis: Control versus Sunitinib (*A)*, Control versus Sunitinib+NQDI-1 (B), NQDI-1, Control verses NQDI-1 (C) and Sunitinib versus Sunitinib+NQDI-1 (D). P-values <0.05 were considered statistically significant.

4.4 Results

4.4.1 Sunitinib treatment impairs heart function and induces cardiac injury

The effect of Sunitinib (1μM) administration on haemodynamic parameters (HR, LVDP and CF) and myocardial infarction was investigated (Tables 4.1-4.3, Figures 4.1 i-iii, and Figure 4.2). The hearts were stabilised for a period of 20 minutes, followed by 125 minutes of drug perfusion.

The LVDP (mmHg) and HR (beats per min) raw data did not demonstrate any significant differences (Table 4.1). The CF (ml/min/g) raw data observed a significant decrease in Sunitinib+NQDI-1 treated hearts compared to both control and Sunitinib alone, between time points 65 and 125 mins.

When the haemodynamic parameters were normalised to the stabilisation period, administration of Sunitinib (1μM) caused a significant reduction of LVDP (% stabilisation period) at 50 min (Control: 101.65 ± 7.23 %; Sunitinib: 83.84 ± 5.04 %, $p<0.05$), compared to control. Sunitinib also reduced HR (% stabilisation period) at 95 mins (Control: 85.27 ± 3.50 %; Sunitinib: 68.53 ± 4.05 %, $p<0.05$) for the rest of the time course, compared with non-treated controls (Figures 4.1 A-C) (Tables 0.3-0.5 of the appendices).

Administration of Sunitinib (1μM) for 125 minutes resulted in a significant increase in infarct size compared with non-treated controls (Control: 7.81 ± 1.16 %; Sunitinib: 41.02 ± 1.23 %, $p<0.001$) (Figure. 4.2). This demonstrated that Sunitinib treatment of the Langendorff perfused hearts causes a drastic increase in cardiac injury. An effect of Sunitinib (1μM) (1

μM) on cardiac function is also observed with a reduction of LVDP and HR, during administration of Sunitinib for 125 mins.

Table 4.1: Left ventricular developed Pressure (mmHg) raw data values obtained during a 125 minute of langendorff perfusion.

Groups: control (n=9), Sunitinib (1 μM) (n=9), Sunitinib (1 μM) + NQDI-1 (2.5 μM) (n=9) or NQDI-1 (2.5 μM) alone (n=11). Data expressed at mean ± S.E.M. One-way repeated measures ANOVA, Tukey post hoc.

Time	**Control**	**Sunitinib**	**Sunitinib + NQDI-1**	**NQDI-1**
0	112.15 ± 3.09	113.21 ± 3.14	132.21 ± 11.30	123.01 ± 8.58
5	123.77 ± 2.96	138.17 ± 8.01	136.06 ± 12.00	124.49 ± 8.04
10	119.93 ± 2.90	131.19 ± 7.22	135.83 ± 13.24	126.58 ± 9.52
15	116.01 ± 3.04	122.76 ± 8.44	139.27 ± 13.98	124.44 ± 7.99
20	116.98 ± 3.46	112.67 ± 5.98	132.64 ± 11.80	123.95 ± 9.83
25	112.87 ± 3.58	112.12 ± 4.99	130.58 ± 12.07	116.44 ± 8.82
30	115.84 ± 3.50	106.30 ± 5.56	121.41 ± 11.34	113.36 ± 8.48
35	113.97 ± 4.49	106.92 ± 3.87	120.27 ± 8.78	112.15 ± 8.76
50	110.06 ± 6.35	96.97 ± 5.89	111.55 ± 7.92	104.61 ± 8.33
65	107.63 ± 7.18	92.67 ± 4.65	102.22 ± 7.83	98.41 ± 8.23
80	101.16 ± 5.24	91.29 ± 4.23	99.72 ± 7.20	90.24 ± 8.25
95	98.19± 2.23	92.83 ± 5.48	95.96 ± 7.39	84.48 ± 6.14
110	93.20 ± 2.76	84.55 ± 4.01	91.66 ± 7.52	84.67 ± 6.74
125	92.71 ± 2.31	80.16 ± 3.97	93.26 ± 9.06	82.45 ± 7.50

Table 4.2: Heart rate (bpm) raw data values obtained during a 125 minute of langendorff perfusion. Groups: control (n=9), Sunitinib (1 µM) (n=9), Sunitinib (1 µM) + NQDI-1 (2.5 µM) (n=9) or NQDI-1 (2.5 µM) alone (n=11). Data expressed at mean ± S.E.M. Statistics: A (p<0.05) vs control. One-way repeated measures ANOVA, Tukey post hoc.

Time	Control	Sunitinib	Sunitinib + NQDI-1	NQDI-1
0	262.22 ± 6.80	275.56 ± 7.93	297.78 ± 9.15	274.55 ± 8.41
5	257.78 ± 6.56	271.11 ± 9.91	292.22 ± 8.80	264.55 ± 8.98
10	256.67 ± 7.29	262.22 ± 8.06	295.56 ± 9.54[A]	258.18 ± 6.76
15	256.67 ± 6.85	255.56 ± 7.31	287.78 ± 10.12	263.64 ± 7.39
20	256.67 ± 6.85	250.00 ± 7.50	277.78 ± 11.15	271.82 ± 11.03
25	262.22 ± 7.86	256.67 ± 9.35	273.33 ± 10.90	265.45 ± 12.28
30	262.22 ± 8.06	248.89 ± 7.59	266.67 ± 11.32	265.45 ± 13.52
35	271.11 ± 7.80	255.56 ± 7.31	268.89 ± 11.10	270.00 ± 13.56
50	256.67 ± 7.71	250.00 ± 7.91	261.11 ± 12.56	274.55 ± 12.36
65	257.78 ± 8.62	254.44 ± 8.86	255.56 ± 10.17	265.45 ± 9.73
80	255.56 ± 9.86	250.00 ± 6.61	267.78 ± 13.20	258.18 ± 11.90
95	261.11 ± 7.99	248.89 ± 7.80	258.89 ± 17.45	250.00 ± 10.77
110	263.33 ± 9.68	252.22 ± 7.45	250.00 ± 15.41	248.18 ± 11.03
125	265.56 ± 9.20	245.56 ± 6.15	245.56 ± 15.52	246.36 ± 13.44

Table 4.3: Coronary flow (ml/min/g) raw data values obtained during a 125 minute of langendorff perfusion.

Groups: control (n=9), Sunitinib (1 µM) (n=9), Sunitinib (1 µM) + NQDI-1 (2.5 µM) (n=9) or NQDI-1 (2.5 µM) alone (n=11). Data expressed at mean ± S.E.M. Statistics: A (p<0.05) vs control; B (p<0.05) vs Sunitinib. One-way repeated measures ANOVA, Tukey post hoc.

Time	**Control**	**Sunitinib**	**Sunitinib + NQDI-1**	**NQDI-1**
0	8.06 ± 0.58	7.29 ± 0.42	6.10 ± 0.80	7.47 ± 0.37
5	7.57 ± 0.52	7.68 ± 0.38	6.18 ± 0.82	7.34 ± 0.47
10	7.33 ± 0.55	7.93 ± 0.59	5.91 ± 0.87	7.40 ± 0.42
15	7.10 ± 0.47	7.67 ± 0.65	5.75 ± 0.75	7.34 ± 0.42
20	7.34 ± 0.56	7.36 ± 0.50	5.85 ± 0.83	7.25 ± 0.38
25	7.23 ± 0.48	7.21 ± 0.47	5.87 ± 0.88	7.13 ± 0.37
30	7.18 ± 0.52	6.79 ± 0.52	5.58 ± 0.85	7.03 ± 0.40
35	7.13 ± 0.48	6.91 ± 0.53	5.45 ± 0.90	6.97 ± 0.35
50	6.90 ± 0.54	6.81 ± 0.56	4.84 ± 0.93	6.59 ± 0.38
65	6.93 ± 0.66	6.59 ± 0.58	4.51 ± 0.85^{A}	6.55 ± 0.34
80	6.47 ± 0.56	6.43 ± 0.51	4.35 ± 0.85	6.18 ± 0.36
95	6.46 ± 0.53	6.31 ± 0.57	4.06 ± 0.62^{AB}	5.97 ± 0.37
110	6.21 ± 0.58	6.12 ± 0.57	3.89 ± 0.61^{AB}	5.79 ± 0.36
125	6.11 ± 0.58	5.93 ± 0.56	3.89 ± 0.62^{A}	5.70 ± 0.32

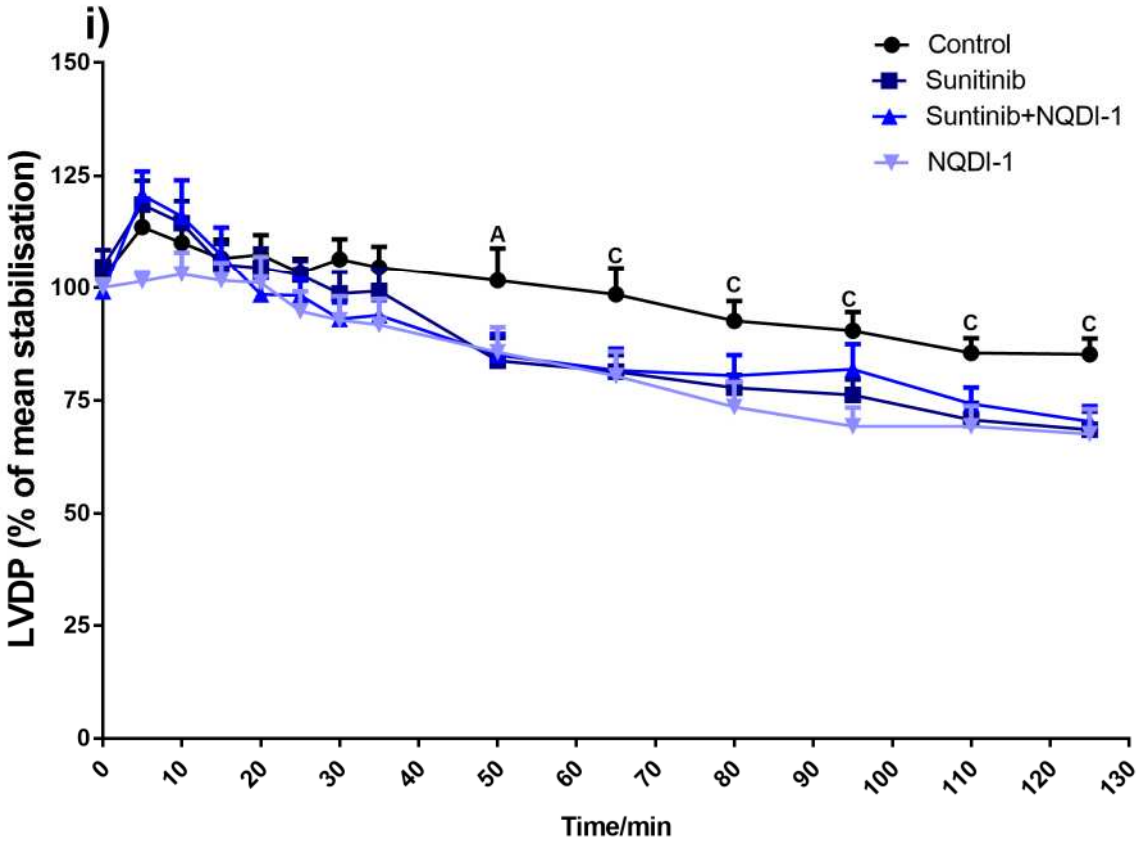
i)
LVDP (% of mean stabilisation)
Time/min
Control
Sunitinib
Suntinib+NQDI-1
NQDI-1
A
C
C
C
C
C

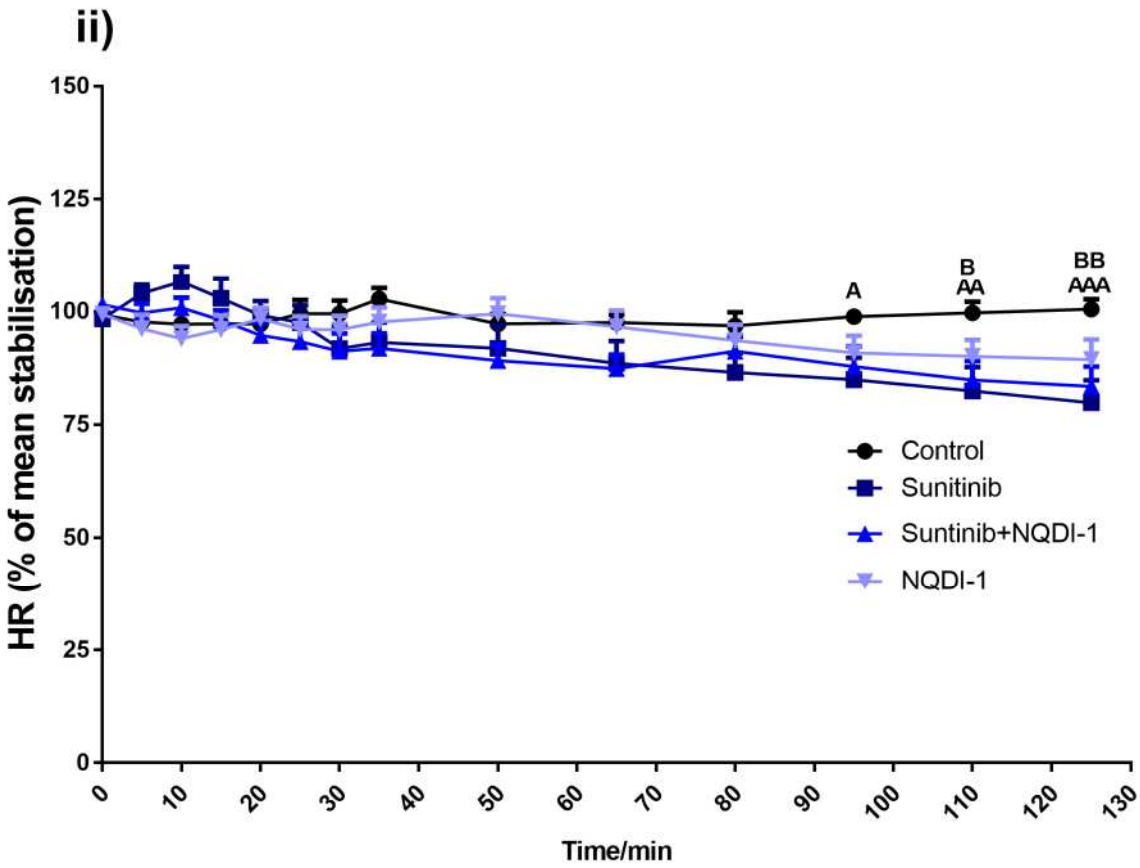
ii)
HR (% of mean stabilisation)
Time/min
Control
Sunitinib
Suntinib+NQDI-1
NQDI-1
A
B
AA
BB
AAA

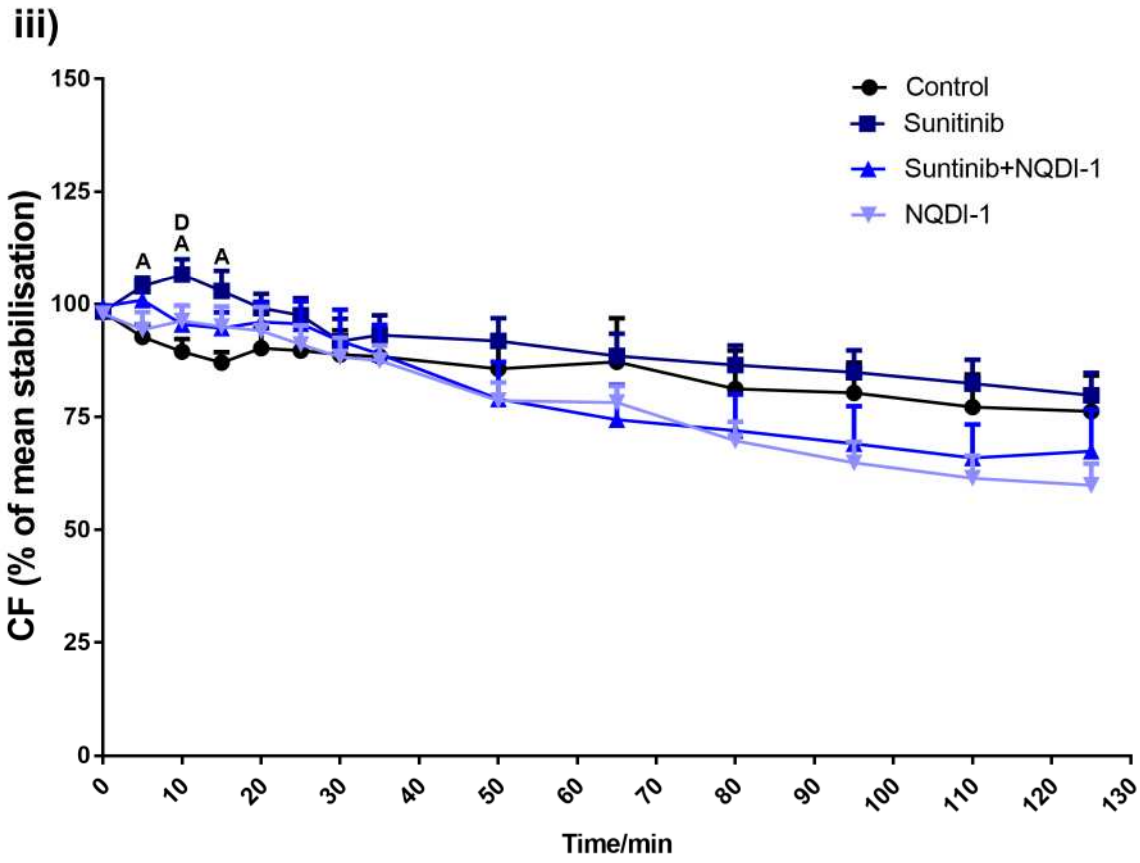

Figure 4.1: Haemodynamic data. The effect of Sunitinib and the co-administration of ASK1 inhibitor NQDI-1 on relative haemodynamic data.

Haemodynamic effects are presented as a percentage of the mean stabilisation period for each parameter to allow clear comparison across drug groups. i) LVDP, ii) HR, and iii) CF. Groups: Control, Sunitinib (1 µM*), Sunitinib (1* µM*) +NQDI-1 (2.5* µM*) and NQDI-1 (2.5* µM*) (n=9-11 per group). Groups were assessed for statistical significance at each time point using* One-way repeated measures ANOVA, Tukey post hoc. *Control versus Sunitinib (A = p<0.05), Control versus Sunitinib+NQDI-1 (B = p<0.05), Control versus NQDI-1 (C = p<0.05, CC = p<0.01), or Sunitinib vs Sunitinib+NQDI-1 (D = p<0.05).*

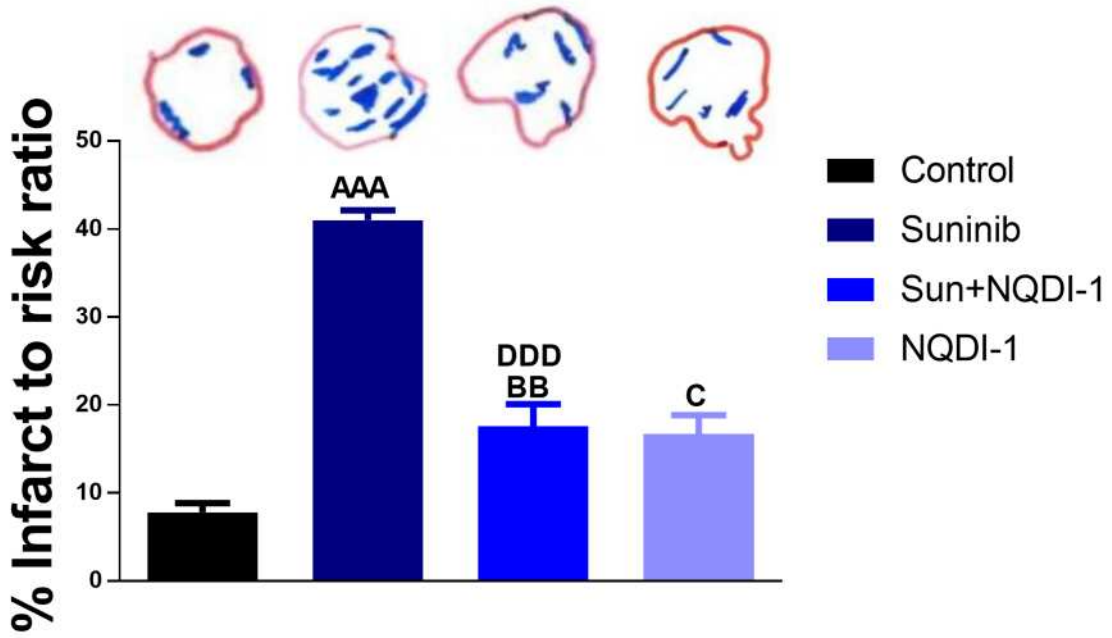

Figure 4.2: The hearts were drug perfused with Sunitinib (1 µM) and/or NQDI-1 (2.5 µM) for 125 min in an isolated Langendorff heart model.

This establishes that Sunitinib-induced cardiotoxicity is reduced by ASK1 inhibitor NQDI-1. Groups: Control, Sunitinib (1 µM), Sunitinib (1 µM) and NQDI-1 (2.5 µM), and NQDI-1 (2.5 µM) (n=6 per group). Groups were assessed for statistical significance at each time point using one-way ANOVA. Control versus Sunitinib (AAA = p<0.001), Control versus Sunitinib+NQDI-1 (BB = p<0.01), Control versus NQDI-1 (C = p<0.05), or Sunitinib vs Sunitinib+NQDI-1 (DDD = p<0.001).

4.4.2 Sunitinib and NQDI-1 co-treatment alleviated cardiac injury

The effect of ASK1 inhibition by NQDI-1 on cardiac function and infarction was investigated.

Co-administration of Sunitinib with NQDI-1 significantly decreased infarct size compared with Sunitinib treated hearts (Sunitinib: 41.02 ± 1.23 %; Sunitinib + NQDI-1: 17.54 ± 2.97 %, p<0.001). Administration of NQDI-1 mono therapy for 125 minutes of perfusion significantly

increased infarct size compared with control hearts (Control: 7.81 ± 1.16 %; NQDI-1: 16.68 ± 2.66 %, $p<0.05$) (Figure 4.2).

However, the hearts perfused with NQDI-1 alone also showed a significant decrease in LVDP (% stabilisation period) when compared to control hearts at time points from 65 mins until the experiment ended (e.g. 125 mins: Control: 85.27 ± 3.50 %; NQDI-1: 67.57 ± 5.54 %, $p<0.05$), (Figure 4.1i and table 0.3 of the appendices).

The HR (% stabilisation period) was significantly decreased at time point 110 mins and onwards in hearts treated with Sunitinib (1 μM) with and without the ASK1 inhibitor NQDI-1 (2.5 μM) when compared to control perfused hearts NQDI-1 did not significantly reduce HR compared to control, however a tendency for a decrease in HR was observed (figure 4.1ii and 0.4 of the appendices).

CF (% stabilisation period) was not altered by NQDI-1 treatment alone. Co-administration of NQDI-1 with Sunitinib only decreased the CF at time point 10 mins, when compared to the Sunitinib treated hearts (Control: 89.46 ± 2.81 %; Sunitinib+NQDI-1: 95.50 ± 3.48 %, $p<0.05$) (Figures 4.1 iii and table 0.5 of the appendices).

4.4.3 Sunitinib treatment modulates expression of miRNAs involved in cardiac injury

The expression of cardiac injury specific miRNAs during Sunitinib-induced cardiotoxicity was determined by qRT-PCR assessment. The miRNAs miR-1, miR-27a, miR-133a and miR-133b have been shown to produce differential expression patterns during the progression of heart failure (Akat et al. 2014, Tijsen, Pinto and Creemers 2012). The ratio of target miRNA

normalised to U6 was set to 1 in the control group for easier comparison of miRNA ratio values between the various drug therapy groups. There was a significant increase in miR-133a when hearts were perfused with Sunitinib (1 µM) compared to control hearts (Ratio of target miRNA normalised to U6 in Sunitinib treated hearts: miR-133a: 535.78 ± 61.27, $p<0.001$) (Figure 4.3iii). Co-administration of NQDI-1 (2.5 µM) along with Sunitinib reversed this miR-133a expression trend by decreasing the miR-133a expression when compared to Sunitinib perfused hearts (Ratio of target miRNA normalised to U6 in Sunitinib and NQDI-1 treated hearts: miR-133a: 52.76 ± 25.83, $p<0.001$) (Figure 4.3iii). Hearts perfused with NQDI-1 alone, showed an increase in miR-1, miR-27a and miR-133b expression compared to control hearts (Ratio of target miRNA normalised to U6 in NQDI-1 treated hearts: miR-1: 32.33 ± 16.47, $p<0.01$; miR-27a: 11.72 ± 2.86, $p<0.001$; miR-133b: 167.85 ± 58.16, $p<0.001$). The expression of miR-1, miR-27a, miR-133a and miR-133b was increased in the Sunitinib and NQDI-1 co-treated hearts when compared to Sunitinib perfused hearts (miR-1: $p<0.05$; miR-27a: $p<0.01$; miR-133a: $p<0.001$; miR-133b: $p<0.01$) (Figure 4.3 i-iV).

The results from the miRNA qRT-PCR analysis show there is a similar expression pattern for miR-1, miR-27 and miR-133b, while miR-133a has its own pattern. Perfusion of hearts with Sunitinib (1 µM) increases miR-133a expression when compared to control hearts. This indicates a complex alteration of these cardiac injury miRNAs by Sunitinib and ASK1 specific inhibitor NQDI-1. This could indicate an interaction between the ASK1/MKK7 pathway and Sunitinib in respect to the expression of cardiotoxicity linked miRNAs during cardiac injury.

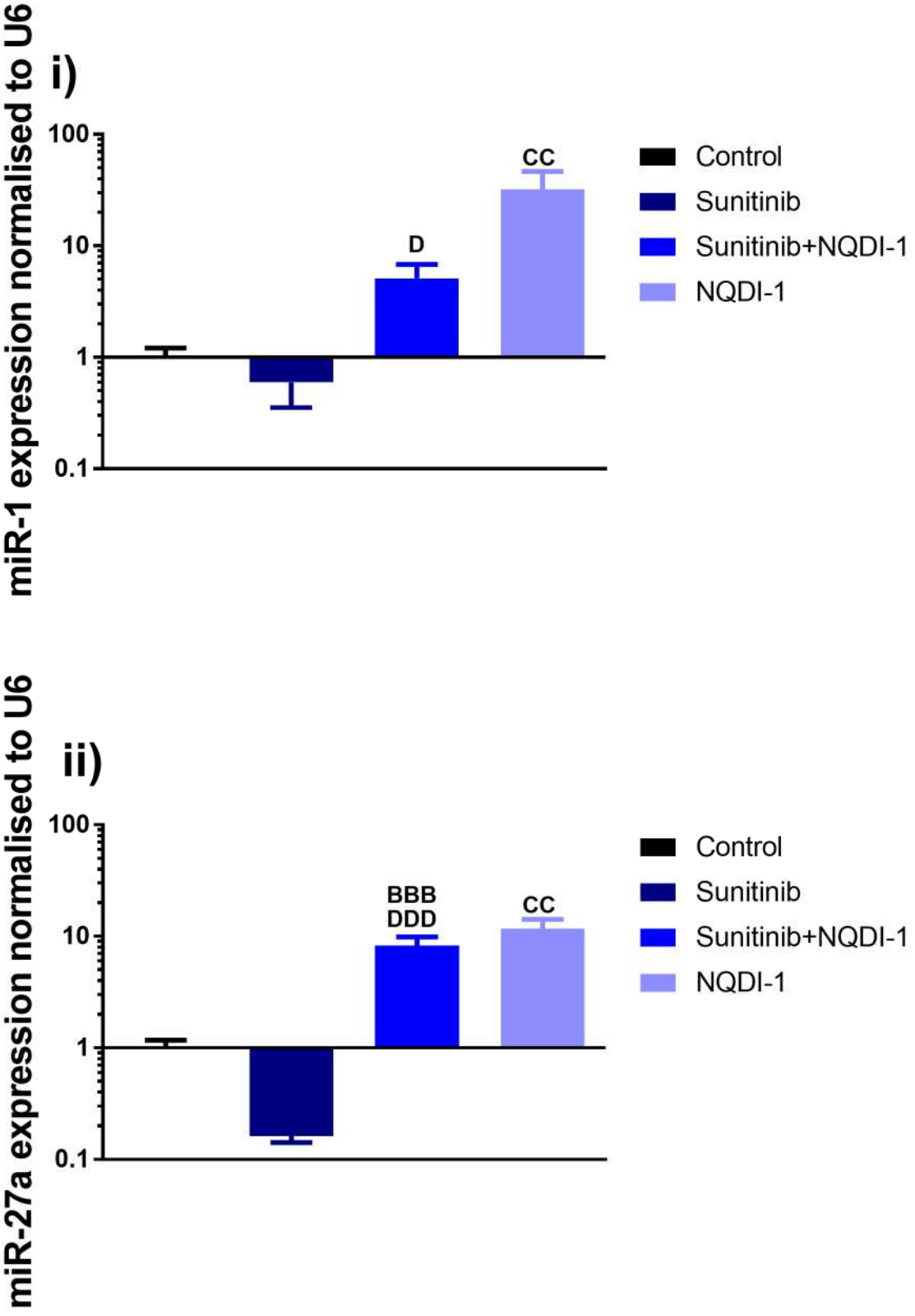
i)
miR-1 expression normalised to U6
100
10
1
0.1
D
CC
Control
Sunitinib
Sunitinib+NQDI-1
NQDI-1
ii)
miR-27a expression normalised to U6
100
10
1
0.1
BBB
DDD
CC
Control
Sunitinib
Sunitinib+NQDI-1
NQDI-1

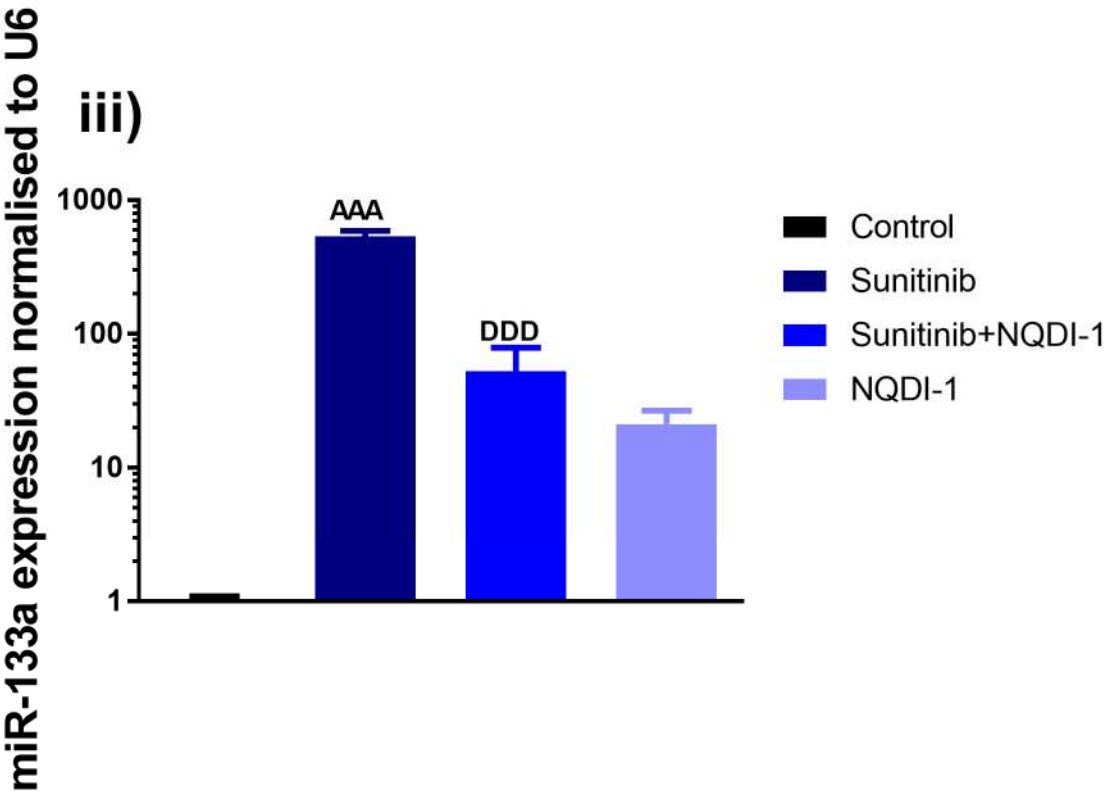
iii)
miR-133a expression normalised to U6
1000
100
10
1
AAA
DDD
Control
Sunitinib
Sunitinib+NQDI-1
NQDI-1

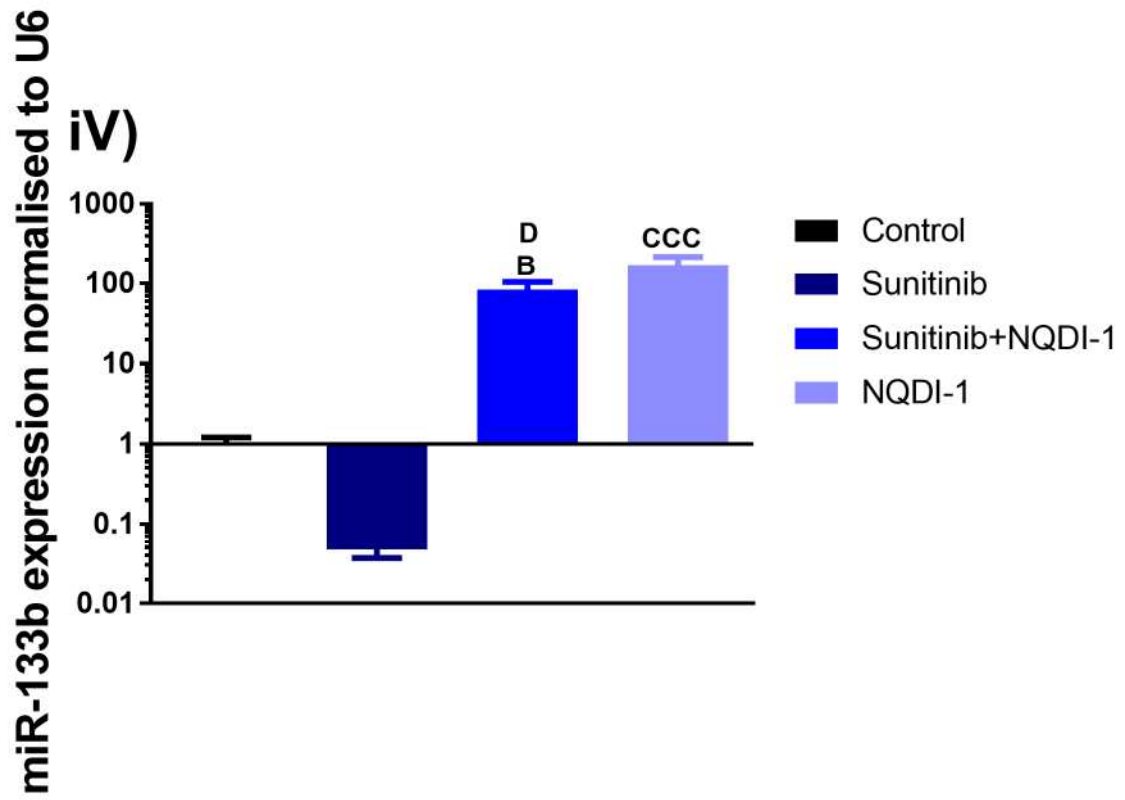

Figure 4.3: The effect of Sunitinib (1 µM) and the co-administration of ASK1 inhibitor, NQDI-1 (2.5 µM), on the expression of cardiotoxicity linked miRNAs following 125 minute drug perfusion in an isolated heart Langendorff model.

The qRT-PCR results are shown as the ratio of target miRNA normalised to U6 with control group miRNA ratio set as 1 of miRNAs i) miR-1, ii) miR-27a, iii) miR-133a and iV) miR-133b. The ratio of target miRNA normalised to U6 is presented on a log scale. Groups: Control (n=6 for miR-1, miR-27a and miR-133a; n=5 for miR-133b), Sunitinib (1 µM) (n=6 for miR-1 and miR-27a; n=5 for miR-133a and miR-133b), Sunitinib (1 µM) and NQDI-1 (2.5 µM) (n=6 for miR-1, miR-27a, miR-133a and miR-133b), and NQDI-1 (2.5 µM) (n=4 for miR-1, miR-27a, miR-133a and miR-133b). Groups were assessed for statistical significance at each time point using one-way ANOVA. Control versus Sunitinib (AAA = p<0.001), Control versus Sunitinib+NQDI-1 (B = p<0.05, BBB = p<0.001), Control versus NQDI-1 (C = p<0.05), or Sunitinib vs Sunitinib+NQDI-1 (D = p<0.05, DD = p<0.01, and DDD = p<0.001).

4.4.4 MKK7 mRNA expression profile is altered by ASK1 inhibitor NQDI-1

Previous studies have demonstrated an inhibitory effect of Sunitinib on MAPK signalling (Aparicio-Gallego et al. 2011). However, the involvement of MKK7 in Sunitinib's mechanism of action has not been directly investigated. We therefore investigate the effect of Sunitinib treatment on MKK7, and whether Sunitinib has an inhibitory effect on the MKK7/JNK pathway.

The level of MKK7 expression after Langendorff perfusion with Sunitinib was assessed at a transcriptional level by MKK7 mRNA qRT-PCR analysis. The ASK1 specific inhibitor, NQDI-1 in the presence and absence of Sunitinib was investigated to establish the effect inhibition of the ASK1/MKK7/JNK has on Sunitinib-induced cardiotoxicity. We also question whether changes in MKK7 mRNA levels could be linked to the level of myocardial damage detected by infarct size measurement.

The ratio of MKK7 mRNA normalised to GAPDH was set to 1 in the control group for easier comparison of GAPDH normalised MKK7 mRNA values between the discussed drug therapy groups. The qRT-PCR analysis of MKK7 mRNA revealed that co-administration of NQDI-1 (2.5 µM) with Sunitinib (1 µM) caused a significant increase in MKK7 mRNA expression compared to Sunitinib treatment alone (Ratio of MKK7 mRNA normalised to GAPDH. Sunitinib: 0.12 ± 0.03; Sunitinib + NQDI-1: 1.18 ± 0.65, $p<0.05$) (Figure 4.4). The decrease in MKK7 mRNA levels in the Sunitinib perfused hearts, compared to control hearts was not significant, but a clear trend was observed. If the data from groups control and Sunitinib were compared using a Student's t-test the decline in MKK7 mRNA in Sunitinib treated hearts was statistically significant with $p=0.0043$.

These MKK7 mRNA qRT-PCR results clearly demonstrate that Sunitinib treatment shows a tendency to decrease the MKK7 mRNA, and co-administration of ASK1 specific inhibitor NQDI-1 restores the MKK7 mRNA level observed in control treated heart. This could indicate a complex regulation system where Sunitinib-induced cardiac injury in directly linked with the ability of Sunitinib to reduced MKK7 expression at transcriptional level, which is counteracted by the ASK1 specific inhibitor NQDI-1.

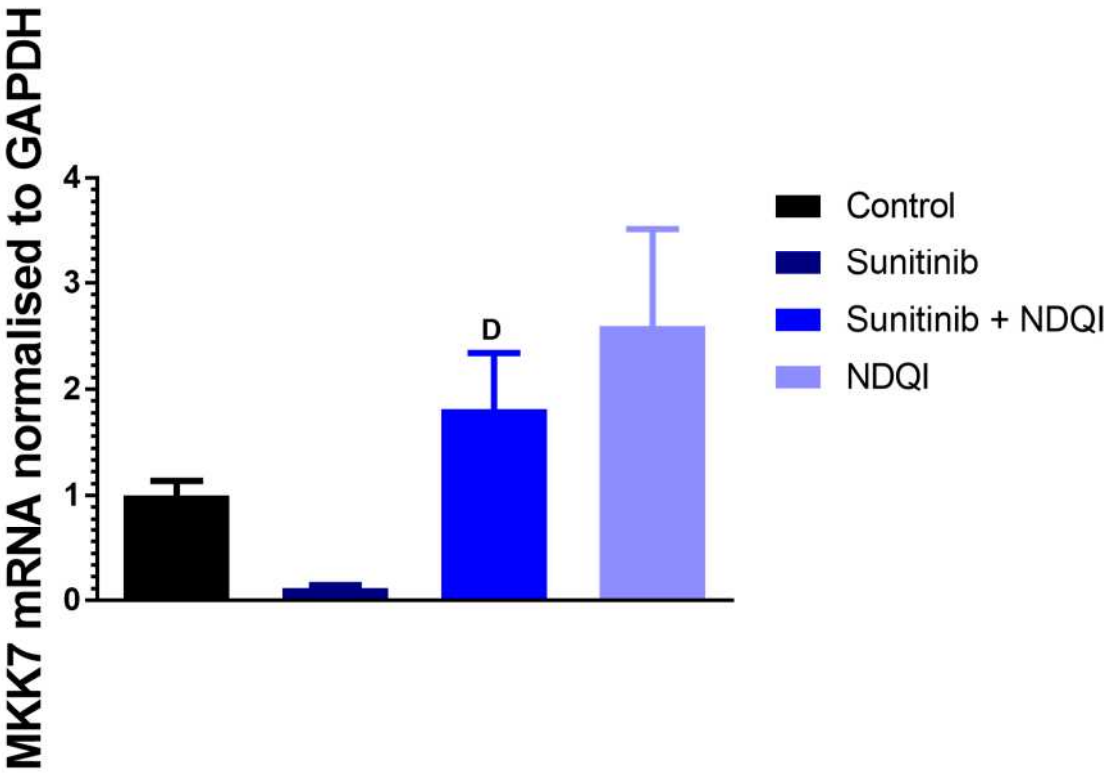

Figure 4.4: MKK7 mRNA expression levels.

The qRT-PCR assessment of MKK7 mRNA expression levels in an isolated heart Langendorff model. The qRT-PCR results are shown as the ratio of MKK7 mRNA normalised to GAPDH with control group ratio set as 1. Groups: Control (n=5), Sunitinib (1 µM) (n=6), Sunitinib (1 µM) and NQDI-1 (2.5 µM) (n=3), and NQDI-1 (2.5 µM) (n=3). Groups were assessed for statistical significance at each time point using one-way ANOVA. Control versus Sunitinib+NQDI-1 (D = p<0.05).

4.4.5 Changes in p-MKK7 levels in response to Sunitinib and the co-treatment of Sunitinib with NQDI-1

To identify the effect of Sunitinib treatment on MKK7 phosphorylation levels, cardiomyocytes were treated with increasing concentrations (1nM-10µM) of Sunitinib and the level of p-MKK7 was measured by flow cytometry (Figure 4.5). Flow cytometric analysis revealed that p-MKK7 levels decreased in a dose-dependent manner. There were significant reductions in p-MKK7 at 10 µM (48.00 ± 11.00 %, $p<0.05$) and 1 µM (65.76 ± 11.32 %, $p<0.05$) concentrations, compared to control (100.00 ± 0.74 %). This dose response gives an IC_{50} of 0.74 µM.

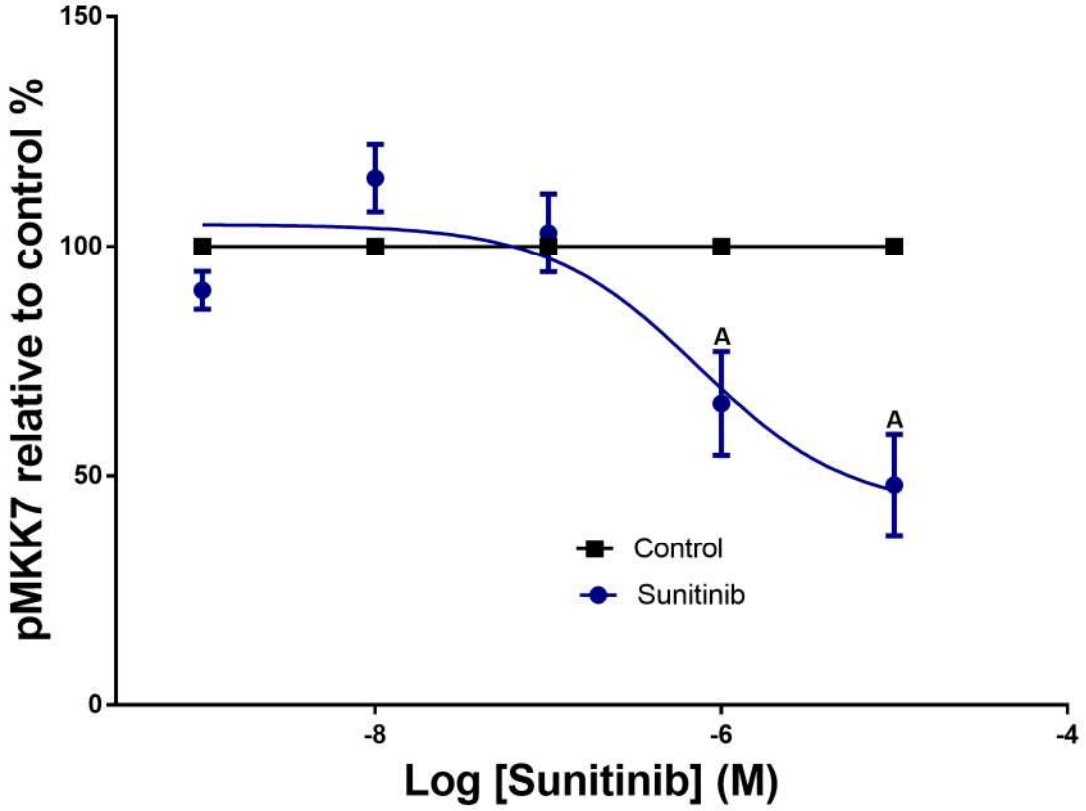

Figure 4.5: Concentration response curve of increasing concentrations of Sunitinib (10µM-1nM) compared to control (n=2). Statistics: Students T-test Control vs Sunitinib: A = p<0.05.

The effect of the ASK1 inhibitor, NQDI-1 on p-MKK7 levels were determined by flow cytometry. A single concentration of 2.5 µM was used alone and in combination with Sunitinib (1 µM). The combination of Sunitinib with NQDI-1 significantly increased the level of MKK7 phosphorylation 1.4 fold compared to control and 2.14 fold compared to Sunitinib (1 µM) alone ($p<0.05$). There is a tendency for a decrease in p-MKK7 levels with a concentration of 1 µM Sunitinib. NQDI-1 alone did not have an effect on p-MKK7 levels (Figure 4.6).

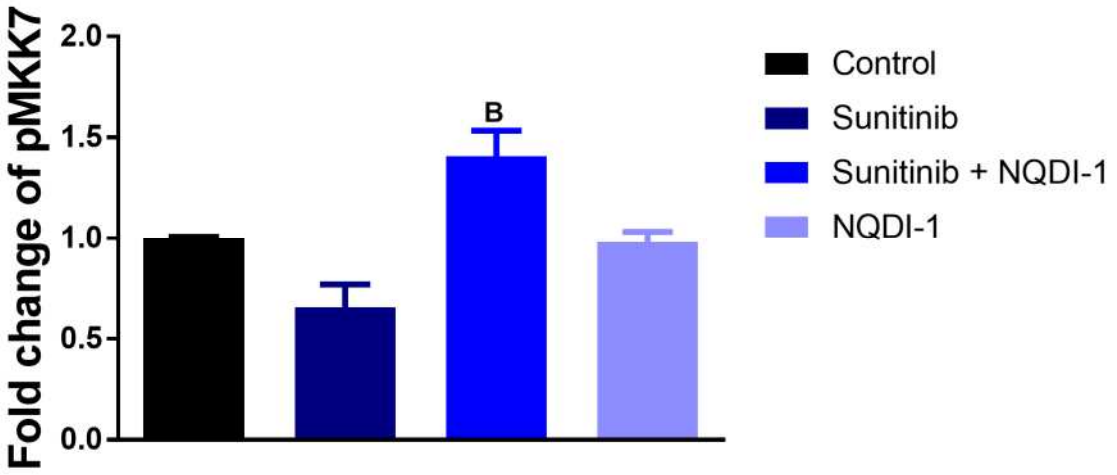

Figure 4.6: The effect of Sunitinib (1 µM), NQDI-1 (2.5 µM) and the co-treatment of Sunitinib (1 µM) with NQDI-1 (2.5 µM.

Data shows the fold change in pMKK7 levels (Control=1). Data presented as mean ± S.E.M. Statistics: One-way ANOVA comparing: Control versus Sunitinib, Control versus Sunitinib+NQDI-1, Control versus NQDI-1, or Sunitinib vs Sunitinib+NQDI-1. *(B = p<0.05 Sunitinib+NQDI-1 verses control).*

4.4.6 ASK1/MKK7/JNK pathway involved in Sunitinib-induced cardiotoxicity

As explained previously, the aim of this chapter was to investigate the effect of Sunitinib treatment on MKK7 and to identify a link between changes in MKK7 phosphorylation levels and Sunitinib-induced cardiotoxicity. Here we also investigated the role of cardiotoxic Sunitinib therapy on the ASK1/MKK7/JNK pathway and how the cyto-protective ASK1 specific agent, NQDI-1 effects the ASK1/MKK7/JNK protein phosphorylation levels (Nomura et al. 2013). Following Langendorff perfusion of Sunitinib and NQDI-1, p-ASK1, p-MKK7 and p-JNK levels were measured by Western blot analysis. The ratio of p-ASK1, p-MKK7 and p-JNK normalised to their total protein was set to 1 in the control group for easier comparison of phosphorylated protein levels normalised to their total protein level values between the discussed drug therapy groups.

Western blot analysis demonstrated a significant decrease in p-ASK1, p-MKK7 and p-JNK levels after Sunitinib treatment, when compared to control (density of phosphorylated protein normalised to total protein: p-ASK1: Control: 1.00± 0.10 and Sunitinib: 0.43 ± 0.08 $p<0.001$; p-MKK7: Control: 1.00 ± 0.08 and Sunitinib: 0.43 ± 0.07, $p<0.001$; p-JNK: Control: 1.00 ± 0.06 and Sunitinib: 0.53 ± 0.06, $p<0.001$) (Figure 4.7i-iii). Co-administration with NQDI-1 restored this decrease in p-ASK1, p-MKK7 and p-JNK levels and increased them to levels which surpassed control levels (density of phosphorylated protein normalised to total protein: p-ASK1: Sunitinib + NQDI-1: 1.33 ± 0.09, $p<0.001$; p-MKK7: Sunitinib + NQDI-1: 0.69 ± 0.03, $p<0.05$; p-JNK: 1.15 ± 0.06, $p<0.001$) (Figure 4.7iii). The p-ASK1, p-MKK7 and p-JNK levels were decreased in NQDI-1 treated hearts compared to control hearts (density of phosphorylated protein normalised to total protein: p-ASK1: NQDI-1: 0.53 ± 0.05, $p<0.01$; p-MKK7: NQDI-1: 0.33 ± 0.05, $p<0.001$; p-JNK: 0.67 ± 0.06, $p<0.01$) (Figures 4.7 i-iii).

These Western blot results show that Sunitinib decreased the phosphorylation of the ASK1/MKK7/JNK pathway proteins. As Sunitinib demonstrated a strong tendency to decrease MKK7 mRNA it could be possible that the decreased MKK7 phosphorylation is regulated at the transcriptional level, which is then affecting the post-transcriptional MKK7 phosphorylation levels. Interestingly, Sunitinib demonstrates an inhibiting effect throughout all 3 links of the ASK1/MKK7/JNK pathway. Co-administration of NQDI-1 is counteracting the Sunitinib inhibiting effect on the phosphorylation level throughout the ASK1/MKK7/JNK pathway. These results show a clear indication of Sunitinib interacting with ASK1, MKK7 and JNK at post-translational level and MKK7 gene expression at pre-transcriptional level.

i)

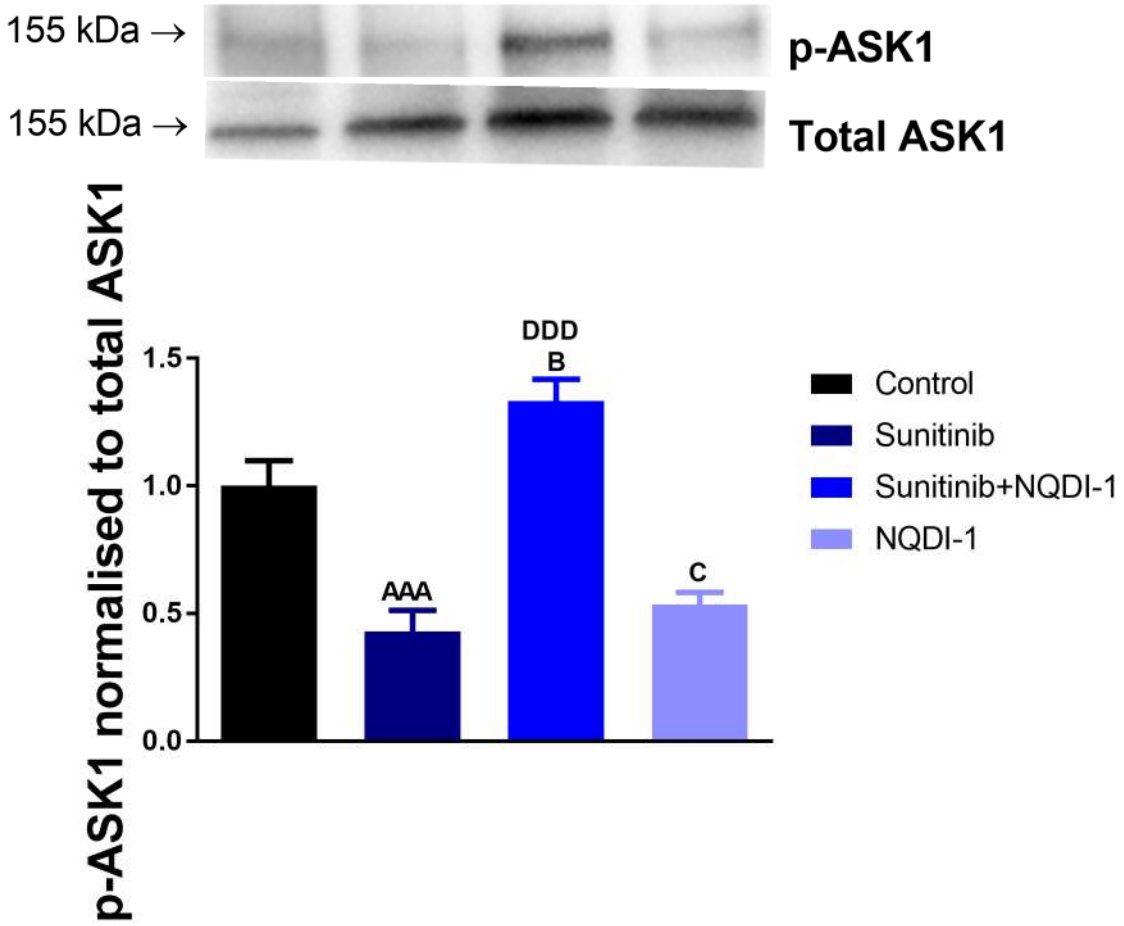
155 kDa →
p-ASK1
155 kDa →
Total ASK1
p-ASK1 normalised to total ASK1
1.5
1.0
0.5
0.0
AAA
DDD
B
C
Control
Sunitinib
Sunitinib+NQDI-1
NQDI-1

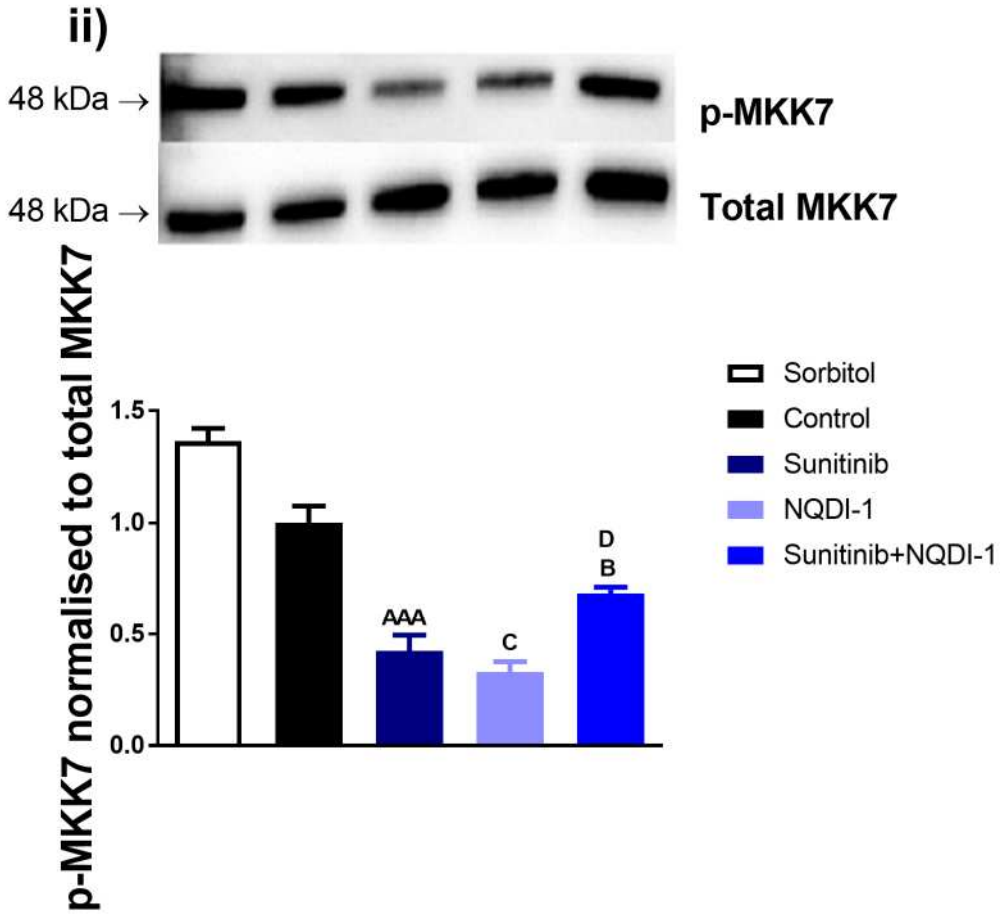
ii)
48 kDa →
48 kDa →
p-MKK7
Total MKK7
p-MKK7 normalised to total MKK7
1.5
1.0
0.5
0.0
AAA
C
D
B
Sorbitol
Control
Sunitinib
NQDI-1
Sunitinib+NQDI-1

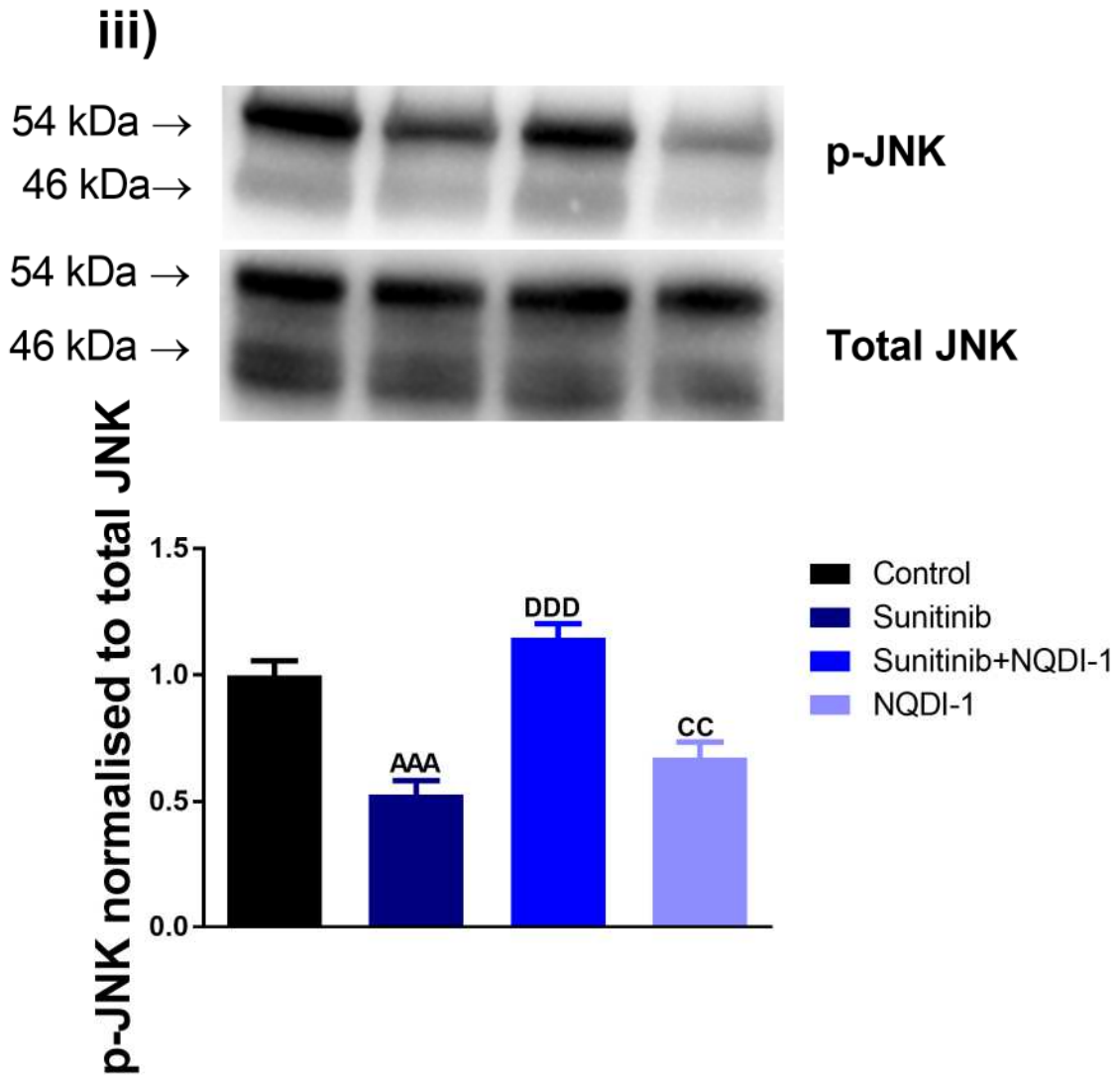

Figure 4.7: Western blot assessment.

i) p-ASK1, ii) p-MKK7, and iii) p-JNK phosphorylation levels in an isolated heart Langendorff model. Sorbitol was included as a positive control in p-MKK7 Western blot analysis (n=4). Groups: Control (n=6 for p-ASK1; n=4 for p-MKK7 and p-JNK), Sunitinib (1 µM) (n=5 for p-ASK1; n=4 for p-MKK7 and p-JNK), Sunitinib (1 µM) and NQDI-1 (2.5 µM) (n=6 for p-ASK1; n=4 for p-MKK7 and p-JNK) and NQDI-1 (2.5 µM) (n=5 for p-ASK1; n=4 for p-MKK7 and p-JNK). Groups were assessed for statistical significance at each time point using one-way ANOVA. Control versus Sunitinib (AAA = p<0.001), Control versus Sunitinib+NQDI-1 (B = p<0.05 and BB = p <0.01), Control versus NQDI-1 (C = P<0.05 and CC = P<0.01), or Sunitinib vs Sunitinib+NQDI-1 (D = p<0.05 and DDD = P<0.001).

4.4.7 Cancer cell viability in response to Sunitinib with and without NQDI-1

The effect of Sunitinib treatment on cell viability was examined in HL60 cells. The HL60 cells were treated with Sunitinib for 24 hrs and then the level of mitochondrial metabolic-activity inhibition was measured with the MTT assay. As shown in Figure 4.8, Sunitinib showed a pronounced decrease in metabolic activity and a dose-dependent decrease in cell viability. Sunitinib significantly reduces cell viability at 1 nM (82.62 ± 6.55 %, $p<0.05$), 0.1 µM (85.94 ± 3.80 %, $p<0.05$), 0.5 µM (83.94 ± 3.86 %, $p<0.05$), 1 µM (77.28 ± 6.58 %, $p<0.05$), 5 µM (58.61 ± 4.44 % $p<0.001$) and 10 µM (47.14 ± 6.77 %, $p<0.001$) concentrations of Sunitinib. The IC_{50} value was 6.16 µM.

The co-administration of NQDI-1 (2.5 µM) to increasing concentrations of Sunitinib (1 nM - 10 µM) enhanced the Sunitinib induced reductions in cell viability. Specifically, co-treatment of Sunitinib with NQDI-1 reduced cell viability at 1 µM (59.58 ± 6.30 %, $p<0.001$), 5 µM (36.62 ± 6.52 %, $p<0.0001$) and 10 µM (15.10 ± 2.31 %, $p< 0.0001$) concentrations of Sunitinib with NQDI-1 (2.5 µM) compared to Sunitinib alone. The IC_{50} value for Sunitinib plus NQDI-1 was 1.76 µM (Figure 4.8i).

For all the concentrations of Sunitinib in the absence and presence of NQDI-1 used produced significant reductions in cell viability compared to control.

Interestingly, increasing concentrations of NQDI-1 alone (0.2-200 µM) only significantly reduced cell viability at very high concentrations (Figure 4.8ii). Reductions in cell viability were significant at 100 µM (55.44 ± 12.39 %, $p<0.05$), 200 µM (33.15± 9.67 %, $p<0.001$) (Figure 4.8 i-ii). The IC_{50} value for NQDI-1 produced by the MTT assay was 130.8 µM.

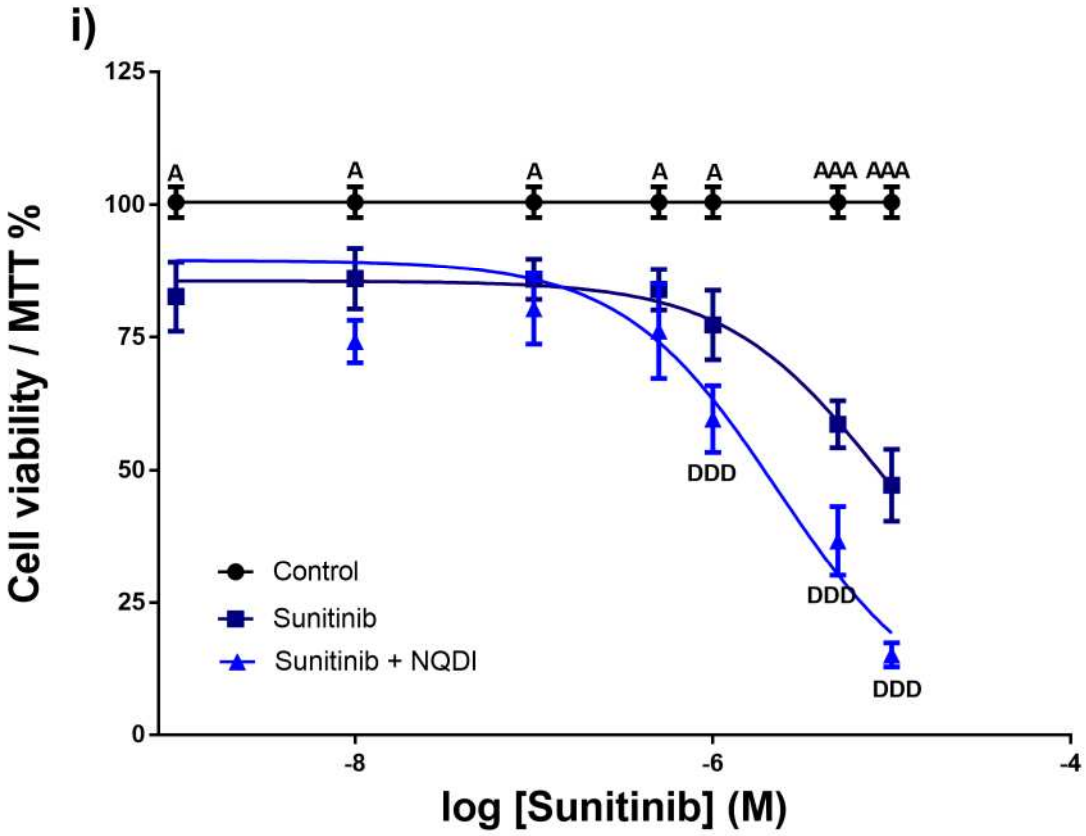
i)
Cell viability / MTT %
125
100
75
50
25
0
A
A
A
A
A
AAA
AAA
DDD
DDD
DDD
Control
Sunitinib
Sunitinib + NQDI
-8
-6
-4
log [Sunitinib] (M)

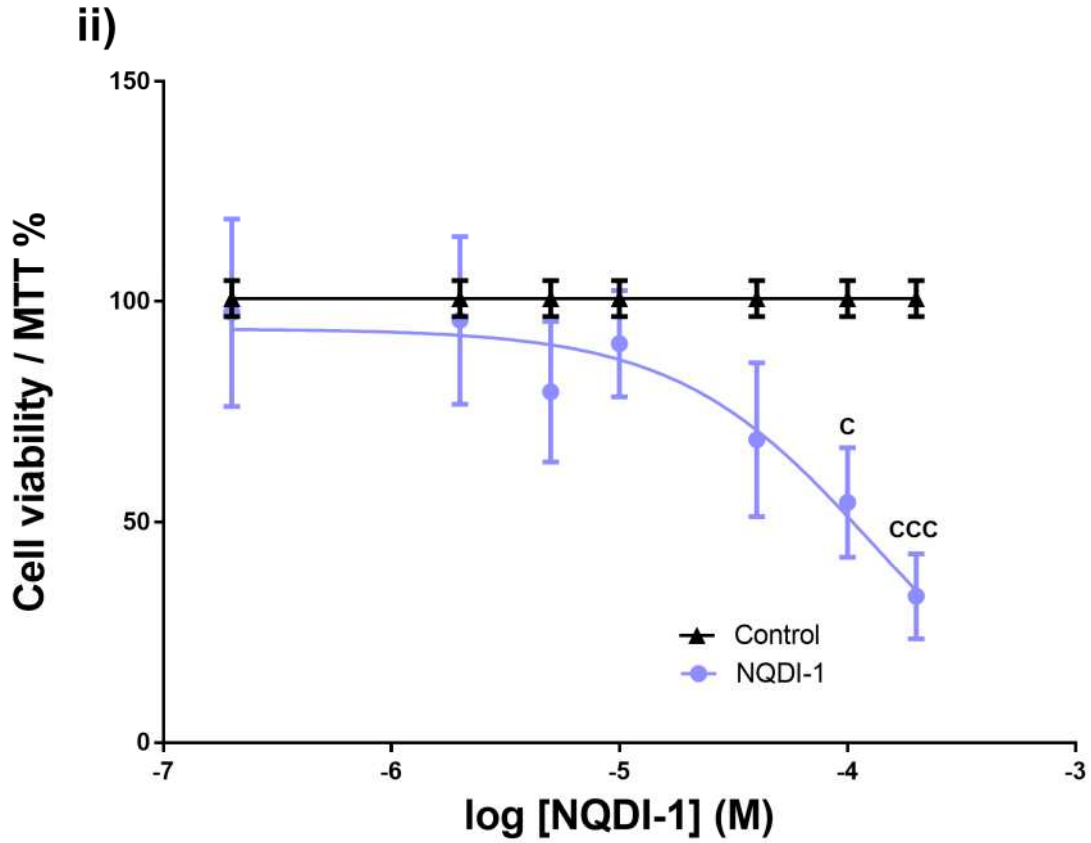

Figure 4.8: Cell viability of HL60 cells.

HL60 cells (10^5 cells/ml) incubated for 24 hours with control (n=4) or with increasing concentrations of i) Sunitinib (0.1 – 10 µM) (n=4) or Sunitinib (0.1 – 10 µM) + NQDI-1 (2.5 µM) (n=3) or ii) NQDI-1 (0.2 µM – 200 µM) (n=3). Statistics: Control compared to Sunitinib (A = p<0.05, AAA = p<0.0001); Control compared to NQDI-1 (C = p<0.05, CCC = p<0.001). Sunitinib vs Sunitinib + NQDI-1 (D = p<0.05).

4.5 Discussion

4.5.1 Sunitinib-induced cardiotoxicity is attenuated by ASK1 specific inhibitor NQDI-1

Heart failure associated with anti-cancer treatment has been investigated extensively (Khakoo et al. 2008); however, the underlying mechanism of Sunitinib-induced cardiotoxicity is still unclear. Determining cellular pathways involved in Sunitinib-induced cardiotoxicity could help to develop therapies which could prevent the potential development of heart failure associated with Sunitinib treatment (Khakoo et al. 2008).

As in chapter 3, data presented in this chapter confirms that Sunitinib causes drug-induced myocardial injury via an increase in infarct size and decline in haemodynamic parameters, including HR (% stabilisation period) and LVDP (% stabilisation period). These observations are in accordance with other studies investigating Sunitinib-induced cardiotoxicity, which also identified significant decrease in left ventricular function and HR in animals (Henderson et al. 2013, Mooney et al. 2015). In addition, left ventricular dysfunction has also been identified in patients undergoing Sunitinib chemotherapy (Di Lorenzo et al. 2009). Sunitinib treatment can produce electrophysiological disturbances and an increased pro-arrhythmic relative risk of developing QT interval prolongation (Ghatalia et al. 2015, Schmidinger et al. 2008). Several studies demonstrate the ability of Sunitinib to block hERG channels and cause irregular contractions (Doherty et al. 2013, Guo et al. 2013).

Modulation of ASK1 and its downstream targets MKK7 and JNK has previously been associated with the regulation of cardiomyocyte survival, apoptosis, hypertrophic remodelling and intracellular signalling associated with heart failure (Mitchell et al. 2006).

Therefore, we hypothesised that successful modulation of the ASK1/MKK7/JNK pathway would produce an effective cardioprotective treatment against Sunitinib induced cardiotoxicity.

As there are currently no commercially available selective inhibitors of MKK7, we targeted ASK1, the upstream kinase of MKK7, as a surrogate inhibitor. The ASK1 specific inhibitor NQDI-1 resulted in abrogation of the some cardiotoxic effects of Sunitinib. This chapter therefore, demonstrated the potential role that this kinase and the ASK1/MKK7/JNK pathway could play in protecting the heart from Sunitinib-induced cardiotoxicity. These observations are in accordance with other studies that have implicated the involvement of ASK1 in cardioprotection in other mammalian models (Boehm et al. 2015, Hao et al. 2016, He et al. 2003). Inhibition of ASK1 with thioredoxin results in reduction of infarct size compared to ischaemic/reperfusion control hearts (Zhang et al. 2007, Gerczuk et al. 2012, Huang et al. 2015).

ASK1 signalling pathway is facilitated through two main routes: either (i) MKK4/7 and JNK, or (ii) MKK3/6 and p38 (Ichijo et al. 1997). As mentioned in the introduction, the study by Izumiya *et al.* 2003 demonstrated the importance of ASK1 during angiotensin II induced hypertension and cardiac hypertrophy in mice, as ASK1 knockout mice failed develop to cardiac hypertrophy and remodelling through both JNK and p38 (Izumiya et al. 2003). In another study by Yamaguchi *et al.* 2003 knockout of ASK1 in mice was also linked to cardioprotection through the JNK pathway, as coronary artery ligation or thoracic transverse aortic constriction in ASK1 deficient hearts showed no morphological or histological defects. Both left ventricular end-diastolic and end-systolic ventricular dimensions were increased less than WT mice, and the decreases in fractional shortening in both experimental models

were less when compared with WT mice (Yamaguchi et al. 2003). However, in a study by Taniike *et al.* 2008 when ASK1 knockout mice were subjected to mechanical stress, it resulted in exaggerated heart growth and hypertrophy through the p38 pathway (Taniike et al. 2008). It is worth noting that attenuation of ASK1 by NQDI-1 during normoxic conditions and Sunitinib treatment could have affected the MKK3/6 and p38 signalling pathway, which could have led to the cardiotoxicity that was observed during this study. Where, Sunitinib-induced reduction of the haemodynamic parameters, LVDP and HR which were not attenuated by NQDI-1 co-administration. NQDI-1 alone, increased infarct size, in addition to reducing LVDP and HR.

NQDI-1 has demonstrated strong selectivity for ASK1. However, as NQDI-1 is a relatively new compound there is limited data which profiles the protein interactions of NQDI-1. It is therefore possible that NQDI-1 may interact with other signalling molecules (Nomura et al. 2013). In the presence of 25 µM NQDI-1 the residual activity of ASK1 is reduced to 12.5 % using the ɣ-32P-ATP *in vitro* kinase assay model (Nomura et al. 2013). By using the same model, Volynetys and colleagues determined the residual activity of the tyrosine protein kinase fibroblast growth factor receptor 1 (FGFR1) which was measured to be 44 % after 25 µM NQDI-1 exposure (Volynets et al. 2011). FGFR1 is a key component involved in *in vivo* cardiomyocyte proliferation during early stage heart development (Seyed and DiMario 2008). Furthermore, FGFR1 is an essential regulator of coronary vascular development through Hedgehog signalling activation, which in the adult heart leads to increased coronary vessel density (Lavine et al. 2006). It is therefore be possible that NQDI-1 has an inhibitory effect on FGFR1 in the treated hearts of our study and thereby exerting an increase in infarct size and haemodynamic dysfunction, in comparison to the control.

Further studies are required to unravel the underlying mechanisms associated with the cardiac tissue injury and haemodynamic responses observed upon NQDI-1 stimuli to assess if p38 and/or FGFR1 are involved. Also, other concentrations of NQDI-1 treatment of hearts should be investigated, as lower concentrations of NQDI-1 most could cause fewer cardiac adverse effects.

4.5.2 Profiling cardiac injury linked miRNAs

MicroRNAs have been shown to have important roles in tissue formation and function in response to injury and disease. The miRNAs miR-1, miR-27a, miR-133a and miR-133b have been shown to produce differential expression patterns during the progression of heart failure (Akat et al. 2014, Tijsen, Pinto and Creemers 2012). Here we investigate the altered expression profiles of miRNAs miR-1, miR-27a, miR-133a and miR-133b after Sunitinib-induced cardiotoxicity with or without the ASK1 inhibitor NQDI-1. A reduction in hERG potassium channels expression causes the delayed myocyte repolarisation attributed to a long QT interval and interestingly the 3' untranslated region of hERG potassium channel transcripts have a partial complimentary miR-133a target site (Xiao et al. 2007). The current study shows an increase in miR-133a expression following Sunitinib treatment, which was attenuated with NQDI-1 co-administration. This could imply that miR-133a overexpression inhibits the h*ERG* potassium channel, which would have a negative impact on the electrophysiological response (Xu et al. 2007). Over expression of miR-133a has also been shown to have negative effects on cardiomyocyte proliferation and survival (Liu et al. 2008) and hence HR, which confirms the results from the current study.

In the heart, miR-1 and miR-133 maintain the heart beat rhythm by regulating the cardiac conduction system (Kim 2013). Furthermore, miR-1 and miR-133 are downregulated during cardiac hypertrophy in both mouse and human models. *In vitro* studies have shown that the overexpression of miR-133 inhibits cardiac hypertrophy, whereas inhibition of miR-133 induces more pronounced hypertrophy (Care et al. 2007). In addition, a decreased in cardiac expression of miR-133b is sufficient to induce hypertrophic gene expression (Sucharov, Bristow and Port 2008). In support of these studies our analysis shows that the miR-133b expression is increased during NQDI-1 mono-therapy and co-administration hearts, thus protecting the heart against hypotrophy/cardiac damage development, which is the same pattern as we observe in the infarct to risk analysis.

The miR-27a expression has been observed to downregulate FOXO-1 protein, a transcription factor which regulates genes involved in the apoptotic response, cell cycle, and cellular metabolism (Guttilla and White 2009). Moreover, miR-27a is down-regulated in coronary sinus samples of heart failure patients (Marques et al. 2016). The increase in miR-27a expression found in this study during NQDI-1 hearts support the findings from these studies as the link increased miR-27 expression to reduced apoptosis, which was observe in the infarct to risk analysis.

4.5.3 Sunitinib treatment suppresses the ASK1/MKK7/JNK pathway

MKK7 has been shown to provide a role in protecting the heart from hypertrophic remodelling and cardiomyocytes apoptosis during stress and therefore the transition into heart failure (Mitchell et al. 2006). Studies by Liu *et al*. (2011) revealed the importance of MKK7 by demonstrating that deprivation of MKK7 in cardiomyocytes provokes heart failure

in mice when exposed to pressure overload (Liu et al. 2011). In addition to this, it has been shown that inhibition and specific knockout of MKK7 increases the sensitivity of hepatocytes to TNF-α-induced apoptosis (Jia et al. 2015). Treatment with Sunitinib in rat hearts down regulates both mRNA and phosphorylated protein levels of MKK7. These studies suggest an important role of MKK7 in the maintenance of heart homeostasis and an upregulation of MKK7 demonstrates an upregulation of genes known to be upregulated during cardiac hypertrophy and heart failure.

MKK7 contains an ATP binding domain which could be inhibited by the ATP analogue, Sunitinib (Roskoski 2007, Shukla et al. 2009, Song et al. 2013). Also, a study by Karaman et al. 2008 demonstrated that Sunitinib did not have a preference of tyrosine kinases over serine/threonine kinases (Karaman et al. 2008). It is therefore possible that Sunitinib has an inhibitory effect on the serine/threonine MKK7/JNK signal transduction pathway. With reduced MKK7 activity demonstrating an incline towards cardiomyocyte damage, and a reversal of anti-tumour effects of chemotherapy, it would be interesting to assess both the changes in expression levels and levels of phosphorylated MKK7 in the presence of Sunitinib. It may therefore be possible to identify a link between MKK7 expression and TKI induced cardiotoxicity.

ASK1 has multiple phosphorylation sites. The Akt/protein kinas B complex binds to and phosphorylates Ser^{83} of ASK1, resulting in the inhibition of ASK1-mediated apoptosis (Kim et al. 2001), the 14-3-3 interacts with phosphorylated Ser^{967} of ASK1 to block the function of ASK1 (Zhang, Chen and Fu 1999), protein phosphatase 5 dephosphorylates Thr^{845} within the activation loop of ASK1 and thereby inhibits ASK1-mediated apoptosis (Morita et al. 2001), while Ser^{1034} phosphorylation suppresses ASK1 proapoptotic function (Fujii et al. 2004).

ASK1 undergoes auto-phosphorylation at the Thr^{845} (Tobiume, Saitoh and Ichijo 2002). It has been proposed that auto-phosphorylation at Thr^{845} is increased in response to H_2O_2 treatment, due to H_2O_2 preventing thioredoxin from complexing with ASK1. This suggests that ASK1 activation is due to oxidative stress (Tobiume, Saitoh and Ichijo 2002). It is possible that auto-phosphorylation increased when Sunitinib was combined with NQDI-1, which led to the increased levels of p-ASK1 identified by western blot analysis.

An increase in p-ASK1 could indicate increased levels of oxidative stress, with potential to reduce cardiac function and generated a level of infarct when NQDI-1 was administered alone, compared to control.

Attenuation of ASK1/MKK7 by the specific inhibitor NQDI-1 reduced infarct size compared to Sunitinib treatment alone. In this study, the ASK1 Thr^{845} phosphorylation site was investigated. However, in future studies it would be interesting to investigate the ASK1 Ser^{967} phosphorylation, as phosphorylation at this site has been linked to cytoprotection (Kim et al. 2009).

Co-treatment of Sunitinib and NQDI-1 increased p-MKK7 levels compared to Sunitinib treated hearts, restoring them to the levels observed in control hearts. This could suggest that a level of p-MKK7 is required to prevent damage to the heart. To illustrate this upregulation of TGF-β has been found in compensatory hypertrophy, myocardial remodelling and heart failure (Rosenkranz 2004). However, if MKK7 is removed entirely from the JNK pathway cardiomyocyte damage ensues (Liu et al. 2011). Tang *et al*. (2012) demonstrated that by causing an upregulation of MKK7 in hepatoma cells, by Alpinetin treatment, it was possible to arrest cells in the G0/G1 phase of the cell cycle. However, by inhibiting MKK7 the anti-tumour effect of the δ-opioid receptor agonist cis-diammined

dichloridoplatinum was reversed (Tang et al. 2012). This suggests that use of an MKK7 agonist may both enhance anti-cancer properties of chemotherapy agents, as well as initiating levels of apoptosis as the cell cycle is arrested.

Many JNK knock out models have been used to determine the role of JNK in the development of cardiac dysfunction. Kaiser *et al*. (2005) demonstrated the importance of JNK in ischemia-reperfusion injury. They showed that a reduction in JNK activity in the heart resulted in a reduced level of cardiac injury and cellular apoptosis. The same study demonstrated an increase in JNK activity by using mouse models overexpressing MKK7 in the heart, and this caused a significant protection against ischaemia-reperfusion injury (Kaiser et al. 2005). This highlights the complexity of JNK signalling. In this study, a significant decrease in JNK phosphorylation was identified when hearts were treated with Sunitinib. In addition, NQDI-1 treatment had a tendency to increase in JNK phosphorylation. It has been established that a reduction in JNK activation is associated with cardiac hypertrophy and cardiovascular dysfunction (Pan et al. 2014). The reduction in JNK activation caused by the treatment of Sunitinib could also explain the increased infarct size and irregularities found in the haemodynamic data.

The findings of this chapter contradict previous studies, for example Wang *et al*. 1998 investigated the role of MKK7 in cardiac hypertrophy in neonatal myocytes (Wang et al. 1998). Transgenic neonatal rat cardiomyocytes expressing wild type MKK7 and a constitutively active mutant of MKK7 were created. This study demonstrated JNK specific activation by MKK7 and showed the key role of the JNK pathway in cardiac hypertrophy as cells infected with the constitutively active form of MKK7 adopted characteristic features of myocardial stress (Wang et al. 1998). Contrastingly, we show a dose-dependent decline in p-

MKK7 levels in cardiomyocytes and a decrease in levels of ASK1/MKK7/JNK signal transduction pathway when hearts are treated with Sunitinib compared to control. This decrease is attenuated by the co-treatment with NQDI-1 in both cardiomyocytes and in LV tissue. Also, in cardiomyocytes p-MKK7 levels are significantly increased by the co-treatment of Sunitinib (1 μM) with NQDI-1 (2.5 μM). This could suggest that there is an increased level of ASK1 auto-phosphorylation and this has increased the levels of p-MKK7 as Sunitinib concentrations increase. This altered pattern in ASK1/MKK7/JNK pathway phosphorylation suggests that Sunitinib has a direct effect on part of the ASK1/MKK7/JNK pathway.

This study highlights the pharmacological potential of the ASK1/MKK7/JNK pathway and in particular the cardioprotective role of ASK1 inhibitor NQDI-1 during Sunitinib-induced cardiotoxicity.

4.5.4 The anti-cancer properties of Sunitinib were enhanced by NQDI-1 treatment.

It is well established that Sunitinib achieves anti-tumour effects by inhibiting tyrosine kinases such as VEGFR and PDGFR which have been over-expressed in cancer cells (Krause and Van Etten 2005). Sunitinib has previously been shown to directly inhibit the survival and proliferation of a variety of cancer cells, including leukaemia cells (Ilyas et al. 2016).

This study demonstrated a dose dependant decline in the cell viability of HL60 cells when treated with Sunitinib. This produced an IC_{50} value of 6.16 μM. The data presented are in line with existing data on Sunitinib's anti-proliferative effect on HL60 cells. Sunitinib has previously been shown to reduce the level of HL60 cell survival in a dose dependant manor using a cell-titre blue reagent proliferation assay. This produced an IC_{50} value of 5.7 μM after

48 hrs of Sunitinib treatment (Ilyas et al. 2016). Another group performed an MTT assay on a variety of acute myelogenous leukaemia cell lines and found Sunitinib to have an IC_{50} values between 0.007-13 µM (Hu et al. 2008).

To investigate the anti-proliferative effect of inhibition of the MKK7 pathway, HL60 cells were treated with Sunitinib in co-treatment with NQDI-1 and NQDI-1 alone. NQDI-1 is a selective inhibitor for ASK1, the upstream regulator of MKK7. Previous studies have shown ASK1 to have a crucial role in a variety of organ systems. However, ASK1 has also been shown to promote tumorigenesis in gastric cancer and promote the proliferation of cancer cells in skin cancer (Hayakawa et al. 2012, Iriyama et al. 2009).

Inhibition of ASK1 with the specific ASK1 inhibitor, K811 has been shown to prevent cell proliferation in gastric cancer cell lines and reduce the size of xenograft tumours (Hayakawa et al. 2012). Recently, Luo et al. 2016, investigated the involvement of ASK1 in pancreatic tumour cell (PANC1) proliferation (Luo et al. 2016). The knock-down of ASK1 in mice with pancreatic tumours reduced tumour growth, suggesting that ASK1 has an important role in pancreatic tumorigenesis. The same group also demonstrated a dose-dependent inhibition of PANC1 when cells were treated with NQDI-1 at concentrations of 10 and 30 µM. However, the inhibition of ASK1 did not increase levels of apoptosis.

This study has shown that increasing concentrations of NQDI-1 (0.2-200 µM) significantly reduce the level of viable HL60 cells at 100 and 200 µM. This could suggest that ASK1 is expressed at different levels in different cell types, as a higher concentration was required in HL60 cells compared to PANC1 cells to reduce proliferation. Interestingly, the increasing concentrations of Sunitinib with 2.5 µM NQDI-1 enhanced the level of Sunitinib-induced reduction in HL60 cell proliferation. The reason for this is not yet clear. Further investigation

into this is required to investigate the changes induced by Sunitinib on HL60 cell death pathways.

As mentioned before NQDI-1 blocks FGFR-1 (Volynets et al. 2011). In cancer cells FGFR1 inhibitors have shown to elicit direct anti-tumour effects. The FGFR-1 inhibitors being investigated in clinical trials for their anti-tumour qualities effecting various cancer types include AZD4547, BGJ398, Debio-1347 and Dovitinib (Katoh 2016). The apoptotic effect of NQDI-1 we are observing in HL60 cells can therefore be a direct consequence of FGFR-1 inhibition.

4.6 Conclusion

In conclusion, this chapter demonstrates the potential of NQDI-1 to protect against a level of cardiac injury through inhibition of the ASK1/MKK7/JNK transduction pathway. Identifying the involvement of this pathway in Sunitinib-induced cardiotoxicity could possibly lead to development of cardioprotective adjunct therapy during drug-induced cardiac injury. NQDI-1 was observed to be partially cardioprotective as it reduced the Sunitinib-induced infarct size, and in addition it increased the apoptotic effect of Sunitinib in HL60 cells. A drug which is cardioprotective against Sunitinib-induced toxicity and also enhances the anti-cancer abilities of Sunitinib would be an ideal candidate for future drug development projects.

NQDI-1 has demonstrated some of the desired characteristics of a potential cardioprotective drug candidate. However, in contrast to the hypothesis, NQDI-1 did not effectively attenuate Sunitinib-induced changes to LVDP, HR and miRNA levels. Therefore, alternative cardioprotective compounds should be investigated, such as IB-MECA.

5. Sunitinib-induced cardiotoxicity is attenuated by A3 adenosine receptor activation

5.1 Abstract

Sunitinib is an anti-cancer tyrosine kinase inhibitor (TKI) associated with severe cardiotoxic adverse effects. Using a rat Langendorff heart model, the involvement of Protein Kinase C alpha (PKCα), MKK7 and JNK in Sunitinib-induced cardiotoxicity. The human acute myeloid leukaemia 60 (HL60) cell line was used to assess the involvement of PKCα in cancer cell survival. The cardioprotective and anti-cancer properties of the A_3 adenosine receptor (A3AR) agonist 2-Chloro-N6-(3-iodobenzyl)-adenosine-5'-N-methyluronamide (IB-MECA) (1nM) were investigated.

The cardiac effect of Sunitinib (1μM) and IB-MECA (1nM) treatment was measured through haemodynamic and infarct size assessment. Myocardial injury associated microRNAs (miR-1, miR-27a, miR-133a and miR-133b) and cancer associated microRNAs (miR-15a, miR-16-1 and miR-155) were profiled by qRT-PCR in the cardiac tissue and HL60 cells, while phosphorylated MKK7 (p-MKK7), JNK (p-JNK) and PKCα (p-PKCα) levels were measured by Western Blot analysis. The cytotoxic effect of Sunitinib (0.1 – 10 μM) and IB-MECA (10 nM – 10 μM) on HL60 cells was assessed using the methylthiazolyldiphenyl-tetrazolium bromide (MTT) assay technique.

Sunitinib treatment increased infarct size and decreased Left ventricular developed pressure (LVDP) and Heart rate (HR). Co-treatment of IB-MECA attenuated Sunitinib-induced myocardial injury. IB-MECA did not alter the anti-cancer effect of Sunitinib in HL60

cells. The expression signature of myocardial injury and cancer associated microRNAs in HL60 cells and cardiac tissue showed an altered expression profile when treated with Sunitinib in the absence and presence of IB-MECA.

p-PKCα levels were increased by Sunitinib treatment in cardiac tissue and HL60 cells, plus co-administration of IB-MECA attenuated this increase in the cardiac tissue. The combined therapy of Sunitinib and IB-MECA did not reduce Sunitinib's cytotoxicity in HL60 cells.

Sunitinib inhibited the MKK7-JNK pathway, however IB-MECA attenuated the decrease in p-MKK7 and p-JNK levels, returning them back to levels similar to controls.

This study reveals that A3AR activation by IB-MECA attenuates Sunitinib-induced cardiotoxicity without interfering with the anti-cancer efficacy of Sunitinib. Findings in this study suggest that PKCα is involved in Sunitinib induced cardiotoxicity and may also be a tumour suppressor. Both A3AR and PKCα pathways could therefore play key roles as cardioprotective adjunctive therapy during TKI-induced cardiotoxicity.

5.2 Introduction

Sunitinib belongs to the tyrosine kinase inhibitor family and is used to treat various cancer forms, such as renal cell carcinoma, gastrointestinal stromal tumours and colorectal cancers (Le Tourneau, Raymond and Faivre 2007). Sunitinib inhibits cancer specific cellular signalling by targeting the adenosine 5'-triphosphate (ATP) binding site of multiple receptor tyrosine kinases involved in tumour angiogenesis and tumour cell proliferation, including platelet-derived growth factor (PDGFR) and vascular endothelial growth factor (VEGFR). Attenuation

of PDGFR and VEGFR signalling by Sunitinib is a powerful tumour treatment as both tumour vascularisation is reduced and cancer cell apoptosis is initiated (Mendel et al. 2003).

Sunitinib displays a lack of kinase selectivity, resulting in the cardiotoxic effects (Hasinoff and Patel 2010, Hasinoff, Patel and O'Hara 2008, Krause and Van Etten 2005). Cardiotoxic adverse effects of TKIs therapy include: asymptomatic QT prolongation, reduction in left ventricular ejection fraction (LVEF), acute coronary syndromes, myocardial infarction and symptomatic congestive heart failure (Chu et al. 2007, Force, Krause and Van Etten 2007, Kerkelä et al. 2006, Khakoo et al. 2008).

Sunitinib has multiple kinase targets; however, many unexpected off-targets have also been identified (Karaman et al. 2008). Sunitinib inactivates the adenosine monophosphate-activated protein kinase (AMPK), which is crucial for cell survival after hypoxia, causing cardiomyocyte death and hypertrophy (Force, Krause and Van Etten 2007). AMPK has the potential to inhibit the activation of protein kinase C (PKC) (Ceolotto et al. 2007). PKC is involved in the negative regulation of cardiac contractility (Braz et al. 2004). Braz *et al.* 2004 demonstrated that over expression of PKCα produces hypo-contractility, which is associated with cardiomyopathy (Braz et al. 2004).

The A_3 adenosine receptor (A3AR), agonist IB-MECA has been shown to have powerful cardioprotective effects against cardiac damage caused by hypoxia, ischemia/reperfusion injury and anti-cancer treatment with Doxorubicin (Carr et al. 1997, Emanuelov et al. 2010, Maddock et al. 2002, Maddock et al. 2003, Shneyvays et al. 2002, Tracey et al. 1997). IB-MECA has been shown to reduce the level of ischemia and infarct size in the heart by reducing abnormal Ca^{2+} levels and the accumulation of free radicals. It has been suggested that the cardioprotection generated by IB-MECA is mediated through the PKC pathway

(Auchampach et al. 1997), as inhibition of the PKC pathway has been shown to produce cardioprotective results by reducing apoptosis (Rakkar and Bayraktutan 2016, Thuc et al. 2012).

Furthermore, Sunitinib has potent mitogen activated protein kinase (MAPK) inhibitor properties (Faivre et al. 2007, Fenton et al. 2010). MAPKs have vital stress signalling roles within the heart (Rose, Force and Wang 2010). In particular, mitogen activated kinase kinase 7 (MKK7) and c-Jun N-terminal kinase (JNK) have been shown to be heavily involved in cardiac hypertrophy and cardiomyocyte cell death in response to stress (Wang et al. 1998).

Interestingly, adenosine signalling can activate MKK7 and JNK (Melani et al. 2009). Also, the activation of A3AR has been shown to activate MAPK signalling (Abbracchio et al. 2001, Schulte and Fredholm 2003). Therefore, we investigated whether Sunitinib has an inhibitory effect on MKK7 and JNK phosphorylation specifically and whether, the use of the A3AR agonist, IB-MECA can attenuate the inhibition of the MKK7-JNK pathway and produce a cardioprotective effect.

In addition, miR-1, miR-27, miR-133a and miR-133b have been linked to myocardial injury (Ai et al. 2010, D'Alessandra et al. 2010, Sandhu and Maddock 2014, Wang et al. 2010, Yang et al. 2007). While, the expression of miRNA miR-155 and the miR-15a-miR-16-1 cluster have been associated with cancer development (Calin et al. 2002, Faraoni et al. 2009).

This study investigated the ability of the A3AR agonist, IB-MECA to reduce the level of Sunitinib-induced cardiotoxicity in Langendorff heart experiments and miRNAs associated with cardiotoxicity profiles were measured. The intracellular signalling proteins: MKK7, JNK and PKCα were assessed to determine their involvement in the cardioprotection elicited by

IB-MECA. Furthermore, the anti-cancer properties of IB-MECA and determined whether co-administration of IB-MECA with Sunitinib affected the anti-cancer/apoptotic effect of Sunitinib in HL60 cells, were assessed. Plus, microRNA associated with cancer were also profiled.

5.2.1 Hypothesis

Activation of the A3 adenosine receptor with IB-MECA will protect against the adverse effects of Sunitinib treatment on the isolated-Langendorff-perfused heart. In addition, the anti-cancer properties of Sunitinib will not be affected by adjunct therapy IB-MECA.

5.3 Materials and methods

5.3.1 Cell line and reagents

The HL60 cell line (Human promyelocytic leukaemia cells) was obtained from European Collection of Cell Culture (England). RPMI 1640 medium was purchased from Sigma Aldrich (US) and the medium supplements L-Glutamine, HEPES and antibiotics mix (100 U/ml penicillin and 100 μg/ml of streptomycin) were from Invitrogen (UK), while foetal bovine serum (FBS) was from Biosera (UK).

Formaldehyde was purchased from Fisher Scientific (US). Protease inhibitor cocktail was purchased from Roche (UK). Sunitinib malate and 2, 3, 5-triphenyltetrazolium chloride (TTC) was purchased from Sigma Aldrich (US) and IB-MECA was purchased from Tocris Bioscience (UK). Antibodies anti-PKC α (phospho T497) p-PKC α and total PKC were from Abcam (UK), while glyceraldehyde 3-phosphate dehydrogenase (GAPDH) (14C10), Phospho-MKK7 (Ser271/Thr275), Total MKK7, Phospho-ASK1 (Thr 845), Phospho-SAPK/JNK

(Thr183/Tyr185), Total SAPK/JNK rabbit mAb antibodies and anti-rabbit linked IgG antibody conjugated to horseradish peroxidase were from Cell Signalling (UK). RNAlater, Ambion mirVana miRNA Isolation Kit, Applied Biosystems MicroRNA Reverse Transcription Kit, TaqMan Universal PCR Master Mix II (uracil N-Glycosylase not included), Applied Biosystems primers assays (U6, hsa-miR155, hsa-miR-15a, hsa-miR-16-1, rno-miR-1, hsa-miR-27a, hsa-miR-133a and hsa-miR-133b) were purchased from Life Technologies (US).

5.3.2 Animals and Ethics

Adult male Sprague-Dawley rats (300-350 g in body weight); were purchased from Charles River UK Ltd (UK) and housed suitably, received humane care and had free access to standard diet according to "The Guidance on the Operation of the Animals (Scientific Procedures) Act of 1986". Animals were selected at random for all treatment groups and the collected tissue was blinded for infarct size assessment. The experiments were performed after approval of the protocol by the Coventry University Ethics Committee. All efforts were made to minimize animal suffering and to reduce the number of animals used in the experiments.

5.3.3 Langendorff perfused model using rat hearts

Rats were sacrificed by cervical dislocation (Schedule 1 Home Office procedure) and the hearts were rapidly excised and placed into ice-cold Krebs Henseleit (KH) buffer (118.5 mM NaCl, 25 mM $NaHCO_3$, 4.8 mM KCl, 1.2 mM $MgSO_4$, 1.2 mM KH_2PO_4, 1.7 mM $CaCl_2$, and 12 mM glucose, pH=7.4). The hearts were mounted onto the Langendorff system and retrogradely perfused with KH buffer. The pH of the KH buffer was maintained at 7.4 by gassing continuously with 95 % O_2 and 5 % CO_2 and maintained at 37 ± 0.5 °C using a water-

jacketed organ chamber. The left atrium was removed and a latex iso-volumic balloon was carefully introduced into the left ventricle and inflated up to 5-10 mmHg. Functional recordings (LVDP and HR) were taken via a physiological pressure transducer and data recorded using Powerlab, AD Instruments Ltd. (UK). Coronary flow (CF) was measured by collecting and measuring the volume of perfusate for 1 min, thereafter it was disposed of. All haemodynamic parameters were measured at 5 min intervals for the first 35 mins and then 15 min intervals until the end of the experiment at 125 mins. In the graphical representation of the haemodynamic data Time 0 is the end point of the stabilisation period. Haemodynamic effects are presented as a percentage of the mean stabilisation period for each parameter to allow clear comparison across drug groups.

Each Langendorff study was conducted for 145 min: a 20 min stabilisation period and 125 min of drug or control perfusion in normoxic conditions. Hearts were included in the study with a HR between 225-325 beats per min, a LVDP between 80-150 mmHg and a CF between 3.5-12.0 ml/g (weight of the rat heart) during the stabilisation period. Sunitinib malate (1 μM) was administered throughout the perfusion period in the presence or absence of IB-MECA (1 nM). The concentration of 1 μM Sunitinib was chosen in line with the clinically relevant study by Goodman *et al.* 2007, where patients suffering from Imatinib refractory or intolerant gastrointestinal stromal tumour, and patients with metastatic renal cell carcinoma where treated with Sunitinib. The steady state blood concentrations of Sunitinib was reported to be in the range of 0.1 – 1.0 μM (Goodman et al. 2007, Henderson et al. 2013). The dose of 1 nM IB-MECA was chosen in line with previous *in vitro* studies by Maddock *et al.* 2002 (Maddock, Mocanu and Yellon 2002).

Langendorff perfused hearts treated with control were recorded as control group (KHB). The hearts were then weighed and either stored at -20 °C for 2,3,5-Triphenyl-2H-tetrazolium chloride (TTC) staining or the left ventricular (LV) tissue was dissected free and immersed in RNAlater for qRT-PCR or snap frozen by liquid nitrogen for Western blot analysis.

5.3.4 Infarct size analysis

Frozen whole hearts were sliced into approximately 2 mm thick transverse sections and incubated in 0.1 % TTC solution in phosphate buffer (2 ml of 100 mM $NaH_2PO_4.2H_2O$ and 8 ml of 100 mM NaH_2PO_4, pH 7.4) at 37 °C for 15 min and fixed in 10 % formaldehyde (Fisher Scientific, UK) for 4 h. The risk zone and infarct areas were traced onto acetate sheets. The tissue at risk stained red and infarct tissue appeared pale. The acetate sheet was scanned and ImageTool from UTHSCSA (USA) software was used to measure the area of infarct and the area of risk. The infarct to risk size was calculated (Infarct size (%) = (Area of infarct / Total area of heart slice) X 100) for each individual slice, and an average was taken of all of the slices from each heart to give the percentage infarct size of the whole heart. The mean of infarct to risk ratio for each treatment group and the mean ± SEM was plotted as a bar chart. The infarct size determination was randomised and blinded.

5.3.5 Human acute myeloid leukaemia HL60 cell studies

5.3.5.1 HL60 cell culture

The HL60 cell line were maintained in RPMI 1640 medium supplemented with L-Glutamine (2 mM) and 10 % heat-inactivated FBS and antibiotics mix at 37 °C in a humidified incubator under 5 % CO_2/95 % air. Cells were counted with nucleoCounter (Chemometec, Denmark)

and split in a 1:5 ratio every 2-3 days. Cells were incubated with: vehicle (Control) or increasing concentrations of: Sunitinib (0.1 – 10 µM), Sunitinib (0.1 – 10 µM) + IB-MECA (1nM) or IB-MECA (0.01 nM – 10 µM) for 24 h. Both Sunitinib and IB-MECA were dissolved in dimethyl sulfoxide (DMSO) and the DMSO concentration was < 0.05 % (v/v) during the *in vitro* studies.

5.3.5.2 Cell viability assessed by MTT assay

HL60 cells were incubated in 100 µl of RPMI media in 96-well plates with the above indicated concentration of the drugs for 24 h at an initial cell density of 10^5 cells/ml. After each period of incubation 30 µl of 3-(4, 5-dimethylthiazol-2-yl)-2, 5-diphenyltetrazolium bromide (MTT) solution (5 mg MTT/ml PBS) was added and cells incubated for a further 24 h, thus to make sure that the HL60 cells in suspension had adequate time to interact with the diluted MTT solution. A volume of 100 µl of DMSO was added to each culture and mixed by pipetting to release reduced MTT crystals from the cells. Relative cell viability was obtained by scanning with an ELISA reader (Anthos Labtech AR 2001 Multiplate Reader, *A*nthos Labtec Instruments, Austria) with a 480 nm filter. Results were expressed as a percentage of viable cells relative to untreated cells/control. Experiments were performed in triplicates and repeated ≥ 4 times. Cells treated with drugs were normalised against untreated cells, and IC50 values were calculated using the GraphPad prism program.

5.3.6 Western blot analysis for p-PKCα and p-MKK7 in heart tissue and p-PKCα in HL60 cells

5.3.6.1 Protein preparation of HL60 cells

$5x10^6$ cells were incubated for 24 h with: Control, Sunitinib (7 µM), Sunitinib (7 µM) + IB-MECA (1 nM) or IB-MECA (1 nM). A concentration 7 µM Sunitinib was chosen to reflect the IC_{50} determined during the MTT assay. After treatment cells were harvested and washed with ice-cold phosphate buffered saline (PBS). The cell pellet was dissolved in ice-cold Protein Lysis Buffer (25 mM HEPES, 100 mM NaCl, 1 mM EDTA, 10 % v/v Glycerol, 1 % (v/v) Triton X-100, pH 7.4) and cells were lysed by homogenising with a syringe needle. After centrifugation at 14,000 rpm for 30 min at 4°C the supernatant was collected and the amount of protein extracted from cells was detected using NanoDrop-1000 (NanoDrop Products, USA) measuring the absorbance at 260nm.

5.3.6.2 Protein preparation of Langendorff perfused heart samples

A total 45-55 mg of the frozen left ventricular tissue was lysed in lysis buffer (NaCl 0.1 M, Tris base 10 µM, EDTA 1 mM, sodium pyrophosphate 2 mM, NaF 2 mM, β-glycaophosphate 2 mM, 4-(2-Aminoethyl) benzenesulfonyl fluoride hydrochloride (AEBSF) (0.1 mg/ml, 1/1.5 of protease cocktail tablet, pH 7.6) using a IKA Overtechnical T25 homogeniser (UK) at 11,000 RPM. The supernatants were measured for protein content using NanoDrop from Nanoid Technology (USA).

5.3.6.3 Western blot analysis of HL60 cells and Langendorff perfused heart samples

A total of 60 µg of protein was loaded to Any kDa Mini-Protean TGX Gel from BioRad (UK) and separated at 200 V for 60 min. After separation, the proteins were transferred to the Bond-P polyvinylidene difluoride membrane from BioRad (UK) by using the Trans-Blot Turbo transfer system from BioRad (UK) and probed for phosphorylated PKCα and Total PKC. The membranes were stripped by boiling and the PVDF membrane was used for total PKC. The relative changes in the p-PKCα protein levels were measured and corrected for differences in protein loading as established by probing for total PKC.

For p-MKK7 80 µg of protein was loaded on to 4–15 % Mini-Protean TGX and p-JNK 80 µg of protein was loaded on to Any KDa Mini-Protean TGX measurement, from BioRad (UK) and separated at 200 V for 60 minutes. After separation, the proteins were transferred to the Bond-P polyvinylidene difluoride membrane from BioRad (UK) by using the Trans-Blot Turbo transfer system from BioRad (UK) and probed for the phosphorylated form Phospho(Ser^{271}/Thr^{275})-MKK7 (p-MKK7), Phospho(Thr^{183}/Tyr^{185}) -SAPK/JNK (p-JNK), and the total forms of MKK7 and JNK. The p-MKK7 blots were stripped by boiling and the PVDF membrane was used for total.

Phosphorylated antibody levels were normalised to total antibody levels in order to correlate for unequal loading of protein and differential blot transfer and to identify the level of active vs inactive protein levels. Results were expressed as a percentage of the density of phosphorylated protein relative to the density of total protein using Image Lab 4.1 from BioRad (UK). The phosphorylated antibody levels determination was randomised and blinded.

5.3.7 Real-time PCR assessment of miRNAs associated with myocardial injury and cancer in HL60 cells and heart tissue

5.3.7.1 Extraction of miRNA from HL60 cells and Langendorff perfused heart samples

The HL60 cells were cultured in 6-well plates - each well containing 10^6 cells - for 24 h with: Control, Sunitinib (7 µM), Sunitinib (7 µM) + IB-MECA (1nM) or IB-MECA (1nM). Langendorff perfused hearts were treated for 125 min with: Control, Sunitinib (1 µM), Sunitinib (1 µM) + IB-MECA 1nM or IB-MECA (1 nM). After treatment miRNA from cells/tissue was extracted with the mirVana miRNA Isolation Kit (Ambion, USA) according to the manufacturer´s instructions. The miRNA quantity and quality were detected by NanoDrop-1000 (NanoDrop Products, USA) measuring the absorbance at 260nm and 280 nm to ensure high RNA quality.

5.3.6.2 Real time PCR of HL60 cells and Langendorff perfused samples

A total of 500 ng miRNA was reverse transcribed into cDNA using primers specific for housekeeping reference RNA U6 snRNA and target miRNAs: hsa-miR-155, hsa-miR-15a, hsa-miR-16-1, hsa-miR-1, rno-miR-1, hsa-miR-27a, hsa-miR-133a or hsa-miR-133b (all human hsa-miRNAs assays are compatible with rat samples as well) using the MicroRNA Reverse Transcription Kit according to the manufacturer's instructions. The reverse transcription PCR reaction was performed with the following setup: 1) 16 °C for 30 min, 2) 42°C for 30 min, 3) 85 °C for 5 min and 4) ∞ at 4°C. The qRT-PCR was performed using the TaqMan Universal PCR Master Mix II (no UNG) protocol on the 7500 HT Real Time PCR sequence detection system from Applied Biosystems (USA). A 20 µl reaction mixture containing 100 ng cDNA, specific primer assays mentioned and the TaqMan Universal PCR Master Mix II (no UNG)

was used in the qRT-PCR reaction in triplicates. A non-template control was included in all experiments. The real time PCR reaction was performed using the program: 1) 2 min at 50°C, 2) 10 min at 95°C, 3) 15 s at 95°C, 4) 1 minute at 60°C. Steps 3) and 4) were repeated 39 times.

The microRNAs data analysis was calculated using the formula $X_0/R_0=2^{CTR-CTX}$, where X_0 is the original amount of target microRNAs (hsa-miR-155, hsa-miR-15a, hsa-miR-16-1, hsa-miR-1, rno-miR-1, hsa-miR-27a, hsa-miR-133a or hsa-miR-133b), R_0 is the original amount of U6 snRNA, CTR is the CT value for U6 snRNA, and CTX is the CT value for the target microRNAs (hsa-miR-155, hsa-miR-15a, hsa-miR-16-1, hsa-miR-1, rno-miR-1, hsa-miR-27a, hsa-miR-133a or hsa-miR-133b). Each individual primer set were calculated and bar charts were plotted with mean ± SEM. The mean of the control group was set as 1 for the miRNA study.

5.3.7 Statistical analysis

Results are presented as mean ± standard error of the mean (SEM). Significance of all data sets were measured the IBM SPSS program (USA) or GraphPad Prism version 5 (USA) as described in the figure legends. The following groups were compared during ANOVA analysis: Control versus Sunitinib, control versus Sunitinib + IB-MECA, control versus IB-MECA or Sunitinib versus Sunitinib + IB-MECA. P-values <0.05 were considered statistically significant.

5.4 Results

5.4.1 Sunitinib treatment injures the heart dramatically and results in decreased cardiac haemodynamic parameters HR and LVDP.

To characterise the level of Sunitinib induced cardiotoxicity in the presence and absence of cardioprotective IB-MECA, the Langendorff perfused heart model was used. Hearts were perfused with: Control, Sunitinib (1 μM), Sunitinib (1 μM) ± IB-MECA (1 nM), or IB-MECA (1 nM) and haemodynamic data was collected: LVDP, HR and CF measurements. The hearts were stabilised for a period of 20 min, followed by 125 min of drug perfusion (Tables 5.1-5.3, Figure 5.1i-iii).

The LVDP (mmHg) raw data demonstrated significant increases in LVDP in the IB-MECA group compared to control at time points 0-10 mins (Table 5.1). The HR (beats per min) and CF (ml/min/g) raw data did not demonstrate any significant differences (Tables 5.2 and 5.3).

When the haemodynamic parameters were normalised the stabilisation period, haemodynamic assessment detected significant decreases in LVDP (% stabilisation period) throughout the 125 min perfusion of Sunitinib (1 μM), compared to control, at time points at time points: 30, 50, and 125 mins (Figure 5.1i and Table 5.1 of the appendices). While, Sunitinib + IB-MECA treatment had a tendency to attenuate the Sunitinib-induced decline in LVDP at time point 20 min (Figure 5.1i and Table 0.6 of the appendices).

There was also a significant decline in HR (% stabilisation period) in the Sunitinib treatment group compared to control at time points 30, 35, 110 and 125 mins (Figure 5.1ii). However, at time points 110 and 125 minutes Sunitinib + IB-MECA treatment also produced significant

declines in HR compared to control. The specific time points where significant reductions in HR are listed in Table 0.7 of the appendices.

CF (both raw data and % stabilisation period) was not significantly affected by Sunitinib, IB-MECA or Sunitinib + IB-MECA treatment compared to control (Figure 5.1iii).

Administration of Sunitinib (1 μM) for 125 min resulted in a significant increase in infarct size compared with non-treated hearts (Control: 8.47 ± 0.67 %; Sunitinib: 43.02 ± 3.15 %, $p<0.001$) (Figure 5.2). This demonstrated that Sunitinib treatment resulted in a drastic increase in cardiac injury and there is also an effect on the cardiac function of the heart as observed by a reduction in HR and LVDP.

Table 5.1: Left ventricular developed Pressure (mmHg) raw data values obtained during a 125 minute of langendorff perfusion.

Groups: control (n=8), Sunitinib (1 µM) (n=9), Sunitinib (1 µM) + IB-MECA (1 nM) (n=9) or IB-MECA (1 nM) alone (n=9). Data expressed at mean ± S.E.M. Statistics: A (p<0.05), AA (p<0.01) vs control. One-way repeated measures ANOVA, Tukey post hoc.

Time	Control	Sunitinib	Sunitinib + IB-MECA	IB-MECA
0	110.59 ± 4.13	114.05 ± 3.75	116.88 ± 3.09	138.59 ± 2.77^{AA}
5	120.75 ± 3.15	140.31 ± 7.73	123.33 ± 3.65	143.43 ± 3.92^{A}
10	118.40 ± 4.42	130.20 ± 9.31	125.26 ± 4.43	146.07 ± 6.15^{AA}
15	118.97 ± 5.03	117.49 ± 9.63	119.66 ± 5.07	139.93 ± 5.25
20	115.22 ± 4.68	111.27 ± 7.77	119.83 ± 4.67	136.17 ± 5.31
25	111.45 ± 3.83	112.66 ± 6.62	110.23 ± 5.67	129.16 ± 7.18
30	115.33 ± 5.56	104.75 ± 7.19	110.46 ± 5.91	123.07 ± 4.58
35	110.29 ± 5.14	106.12 ± 5.08	108.31 ± 7.19	126.07 ± 4.99
50	107.36 ± 6.95	94.67 ± 7.44	102.83 ± 7.69	116.80 ± 3.61
65	99.80 ± 6.84	88.98 ± 4.94	97.57 ± 6.98	106.61 ± 5.42
80	96.43 ± 4.03	87.41 ± 4.29	91.65 ± 4.86	101.16 ± 6.08
95	98.78 ± 3.97	87.86 ± 5.61	91.37 ± 4.19	99.59 ± 8.97
110	91.51 ± 3.70	81.35 ± 4.42	89.26 ± 3.55	96.33 ± 10.56
125	93.55 ± 2.20	76.94 ± 4.12	87.01 ± 3.41	95.62 ± 10.34

Table 5.2: Heart rate (bpm) raw data values obtained during a 125 minute of langendorff perfusion. Groups: control (n=8), Sunitinib (1 µM) (n=9), Sunitinib (1 µM) + IB-MECA (1 nM) (n=9) or IB-MECA (1 nM) alone (n=9). Data expressed at mean ± S.E.M. One-way repeated measures ANOVA, Tukey post hoc.

Time	Control	Sunitinib	Sunitinib + IB-MECA	IB-MECA
0	281.67 ± 17.53	280.00 ± 9.72	287.00 ± 11.55	262.86 ± 16.62
5	280.00 ± 17.44	275.71 ± 12.44	284.00 ± 11.57	254.29 ± 14.31
10	283.33 ± 22.74	265.71 ± 10.24	274.00 ± 14.67	258.57 ± 14.23
15	285.00 ± 25.42	255.71 ± 9.68	277.00 ± 12.38	258.57 ± 14.61
20	286.67 ± 24.93	252.86 ± 9.64	268.00 ± 15.38	258.57 ± 15.71
25	283.33 ± 25.09	261.43 ± 11.41	270.00 ± 15.07	257.14 ± 14.85
30	285.00 ± 24.78	252.86 ± 8.73	260.00 ± 14.99	255.71 ± 17.46
35	293.33 ± 23.44	261.43 ± 7.97	260.00 ± 15.48	260.00 ± 13.74
50	288.33 ± 25.83	250.00 ± 10.54	262.00 ± 15.70	271.43 ± 11.16
65	285.00 ± 23.79	252.86 ± 11.48	254.00 ± 11.78	270.00 ± 11.30
80	276.67 ± 26.33	251.43 ± 7.97	244.00 ± 8.49	267.14 ± 8.07
95	266.67 ± 17.81	255.71 ± 8.12	244.00 ± 8.20	260.00 ± 14.53
110	278.33 ± 22.17	258.57 ± 7.97	242.00 ± 9.00	248.57 ± 20.06
125	280.00 ± 20.40	250.00 ± 6.67	241.00 ± 12.32	254.29 ± 21.19

Table 5.3: Coronary Flow (ml/min/g) raw data values obtained during a 125 minute of langendorff perfusion.

Groups: control (n=8), Sunitinib (1 µM) (n=9), Sunitinib (1 µM) + IB-MECA (1 nM) (n=9) or IB-MECA (1 nM) alone (n=9). Data expressed at mean ± S.E.M. One-way repeated measures ANOVA, Tukey post hoc.

Time	Control	Sunitinib	Sunitinib + IB-MECA	IB-MECA
0	8.06 ± 0.51	7.19 ± 0.48	7.24 ± 0.54	8.58 ± 0.67
5	7.70 ± 0.44	7.68 ± 0.34	7.26 ± 0.62	8.43 ± 0.69
10	7.69 ± 0.51	7.94 ± 0.72	7.19 ± 0.70	8.36 ± 0.63
15	7.71 ± 0.58	7.63 ± 0.84	7.38 ± 0.75	819 ± 0.59
20	7.57 ± 0.64	7.22 ± 0.62	7.25 ± 0.76	8.01 ± 0.54
25	7.44 ± 0.63	7.03 ± 0.57	6.90 ± 0.70	7.85 ± 0.63
30	7.43 ± 0.65	6.49 ± 0.59	7.00 ± 0.69	7.71 ± 0.61
35	7.37 ± 0.66	6.64 ± 0.62	6.83 ± 0.72	7.64 ± 0.58
50	7.08 ± 0.63	6.57 ± 0.65	6.55 ± 0.75	7.32 ± 0.59
65	6.67 ± 0.58	6.22 ± 0.61	6.28 ± 0.79	7.26 ± 0.56
80	6.44 ± 0.56	6.07 ± 0.54	6.17 ± 0.68	6.90 ± 0.55
95	6.37 ± 0.49	6.04 ± 0.62	6.24 ± 0.78	6.31 ± 0.48
110	5.80 ± 0.58	5.85 ± 0.65	5.87 ± 0.77	6.09 ± 0.56
125	5.68 ± 0.46	5.67 ± 0.61	5.48 ± 0.70	5.60 ± 0.55

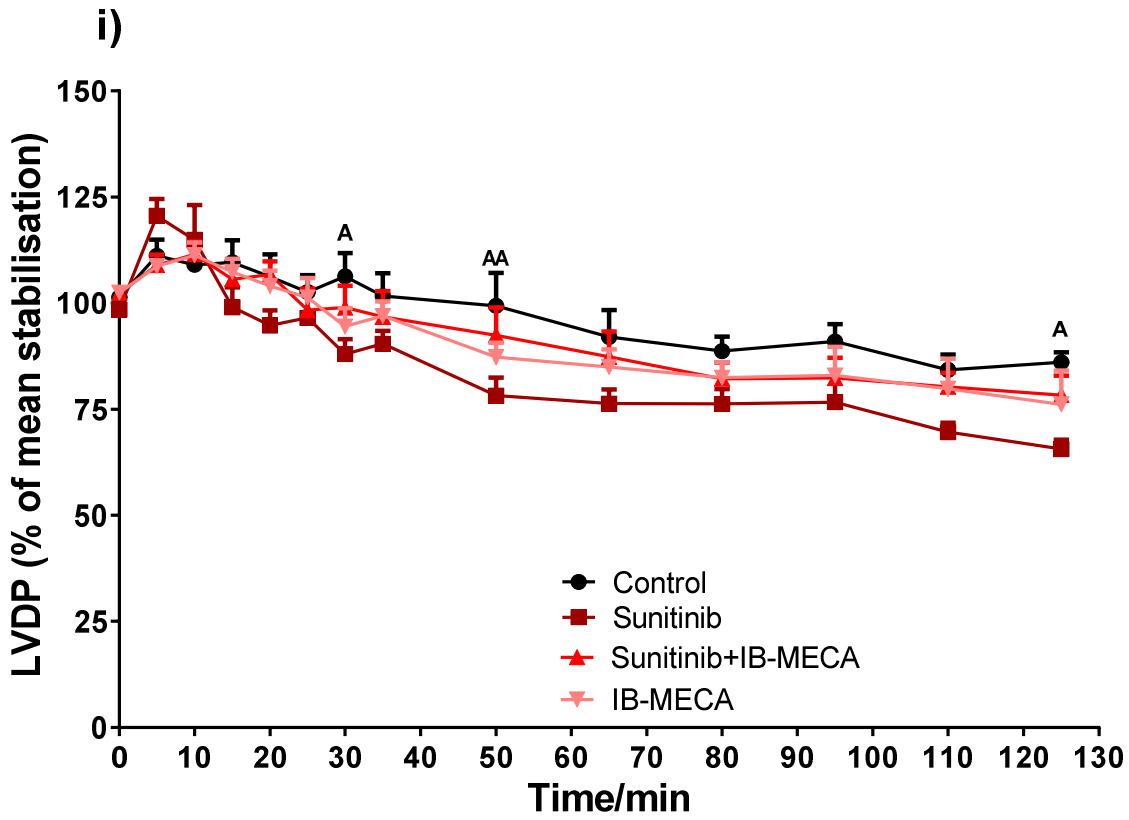
i)
LVDP (% of mean stabilisation)
150
125
100
75
50
25
0
0 10 20 30 40 50 60 70 80 90 100 110 120 130
Time/min
A
AA
A
Control
Sunitinib
Sunitinib+IB-MECA
IB-MECA

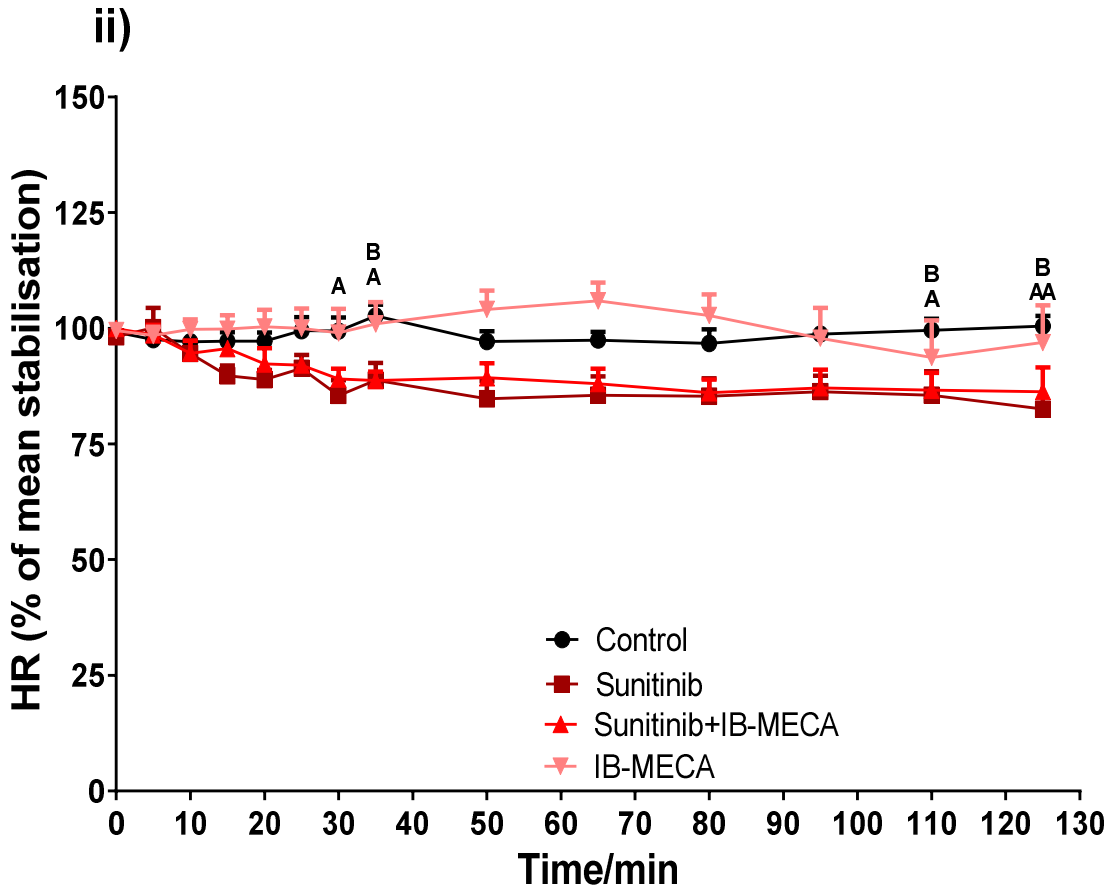
ii)
HR (% of mean stabilisation)
150
125
100
75
50
25
0
0 10 20 30 40 50 60 70 80 90 100 110 120 130
Time/min
A
B
A
B
A
B
AA
Control
Sunitinib
Sunitinib+IB-MECA
IB-MECA

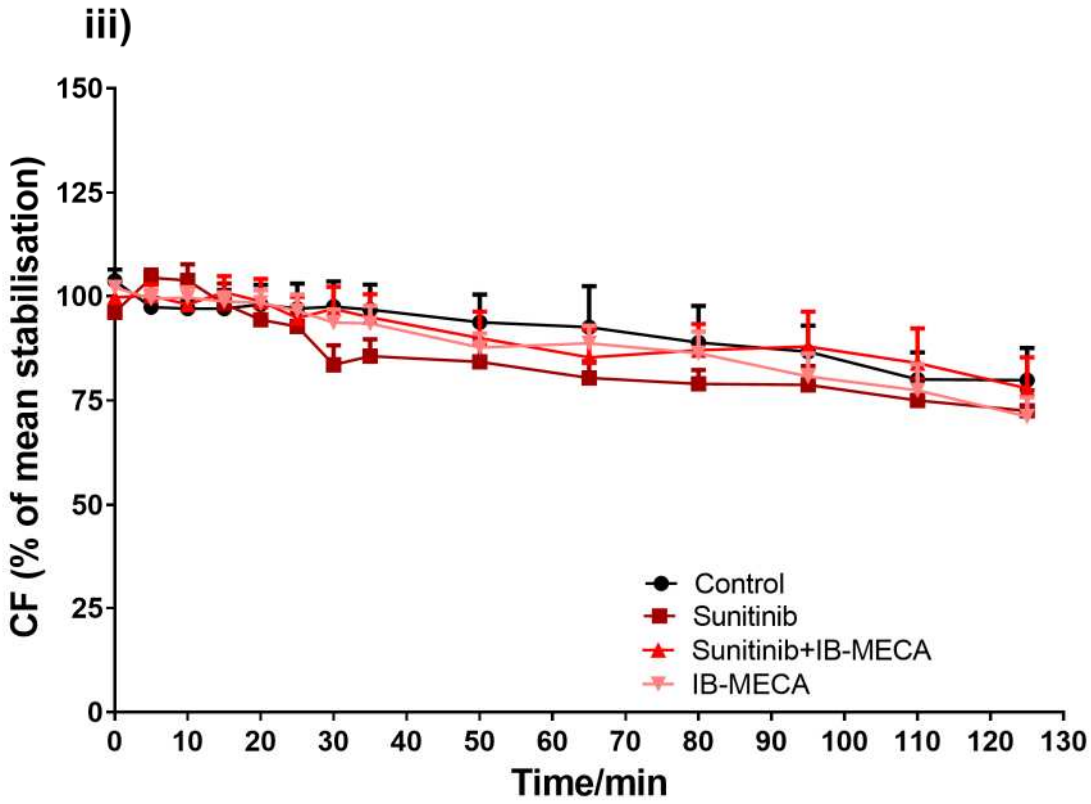

Figure 5.1: Representation of haemodynamic data collected during Langendorff experiments over time relative to the stabilisation period.

*Drug treatment groups: Control (n=8), Sunitinib (1µM) (n=9), Sunitinib (1µM) + IB-MECA (1nM) (n=9) and IB-MECA (1nM) (n=9). i) Change in LVDP (mmHg), ii) Heart Rate (HR) and iii) Coronary flow (CF) (ml). Data expressed as mean ± S.E.M. Statistics: * = p<0.05. Groups compared during One-way repeated measures ANOVA, Tukey post hoc. Comparing: Control versus Sunitinib (A), Control versus Sunitinib + IB-MECA (B), Control versus IB-MECA (C) and Sunitinib versus Sunitinib + IB-MECA (D).*

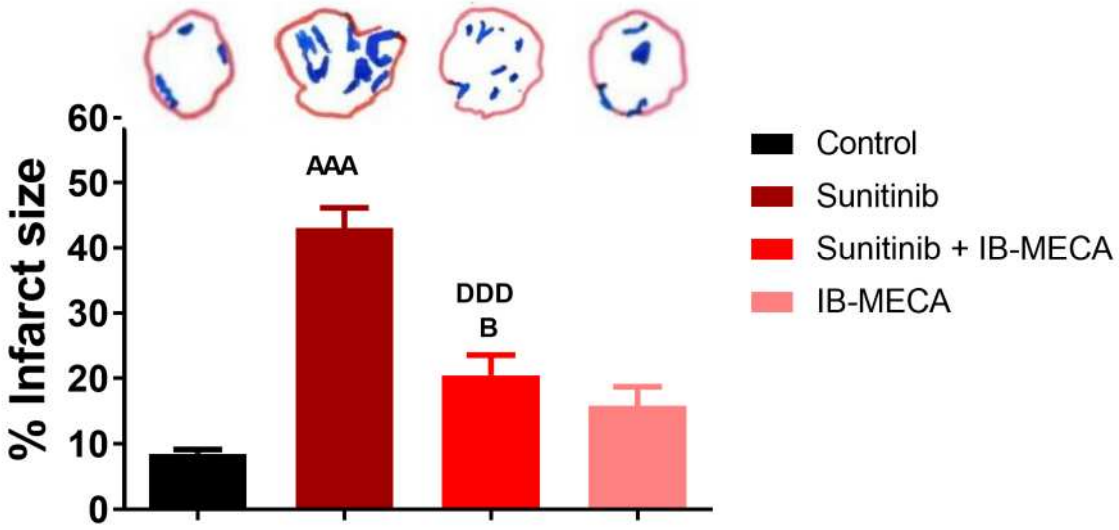

Figure 5.2: Representation of infarct size.

Drug treatment groups: Control, Sunitinib (1 µM), Sunitinib (1 µM) + IB-MECA and IB-MECA (1 nM) (n=5). One-Way ANOVA statistical analysis: control vs Sunitinib AAA = p<0.001, control vs Sunitinib + IB-MECA B= P<0.05 and Sunitinib vs Sunitinib + IB-MECA DDD= p<0.001.

5.4.2 Sunitinib-mediated cardiotoxicity is reduced by A3AR agonist IB-MECA

The effect of the A3AR agonist on cardiac function and infarction was investigated. IB-MECA significantly counteracted Sunitinib's effect on left ventricular developed pressure and coronary flow, although it could not protect against the bradycardic effect of Sunitinib. In addition, IB-MECA treatment alone did not induce any significant change in all studied parameters as compared to the control group (Figure 5.2).

Co-administration of Sunitinib with IB-MECA significantly decreased infarct size compared to Sunitinib treated hearts (Sunitinib: 43.02 ± 3.15 %; Sunitinib + IB-MECA: 20.46 ± 3.13 %, p<0.001). Administration of IB-MECA alone did not significantly affect infarct size compared

to control (Control: 8.47 ± 0.67 %; IB-MECA (13.80 ± 3.40 %, $p<0.05$) (Figure 5.2). This demonstrates that IB-MECA is effective in attenuating Sunitinib induced cardiac injury.

5.4.3 The miRNAs associated with myocardial injury: miR-1, miR-27a, miR-133a and miR-133b in heart tissue

The expression of miRNAs associated with cardiac injury were analysed in left ventricular heart tissue, collected after Langendorff perfusion with Sunitinib in the absence or presence of IB-MECA (Figure 5.3). There was a tendency for a decrease in miR-1 (Figure 5.3i) and miR-27a (Figure 5.3ii). Plus, miR-133b (Figure 5.3iV) tended to increase, while miR-133a (Figure 5.3iii) was significantly increased by Sunitinib treatment, compared to control.

Co-administration of Sunitinib with IB-MECA significantly increased miR-27a 6.60 fold ($p<0.001$) (Figure 5.3ii), miR-133a 5.07 fold ($p<0.001$) (Figure 5.3iii) and miR-133b 23.38 fold ($p<0.001$) (Figure 5.3iV), compared to control hearts. There was also a tendency for Sunitinib + IB-MECA treatment to increase in miR-1 (Figure 5.3i), compared to control group, however this increase was not significant.

All of the cardiac injury associated miRNAs expression levels were significantly increased after treatment with Sunitinib + IB-MECA compared to Sunitinib alone. Co-administration of IB-MECA with Sunitinib increased miR-1 7.98 fold ($p<0.05$) (Figure 5.3i), miR-27a 16.5 fold ($p<0.01$) (Figure 5.3ii), miR-133a 1.88 fold ($p<0.001$) (Figure 5.3iii) and miR-133b 4.96 fold ($p<0.01$) (Figure 5.3iV), compared to hearts treated with Sunitinib alone.

There was a clear increase in all miRNAs in the Sunitinib + IB-MECA group compared to all of the drug treatment groups.

The miRNA levels were not altered in hearts treated with IB-MECA alone compared to control hearts in any of the microRNAs investigated (Figure 5.3).

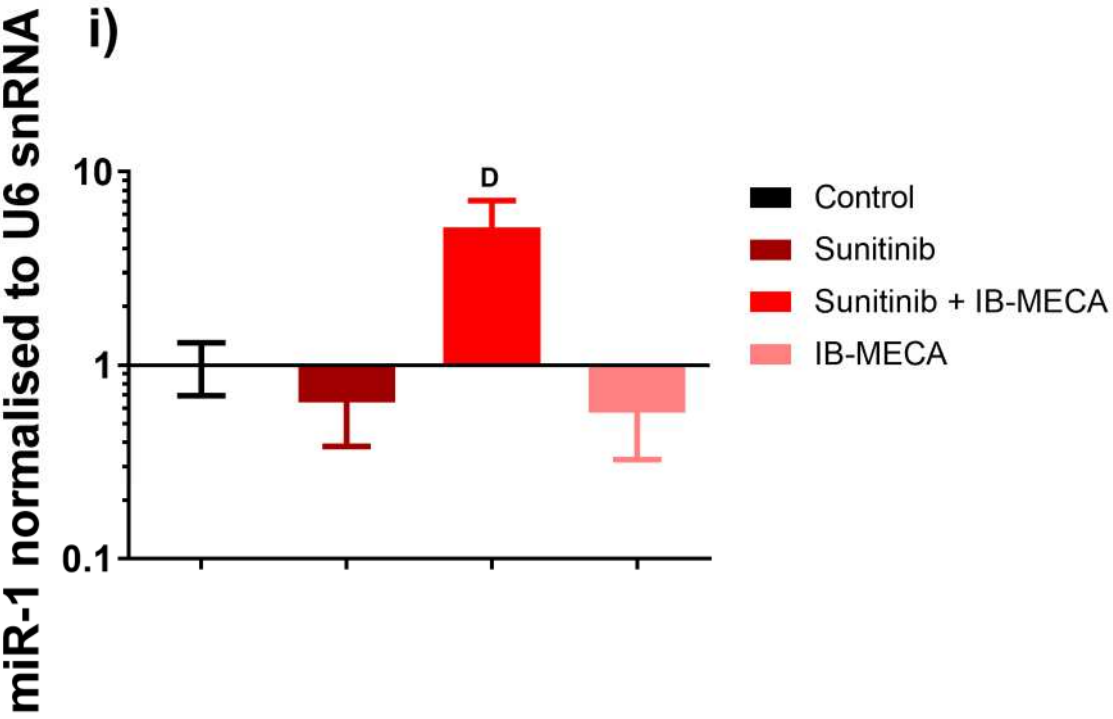

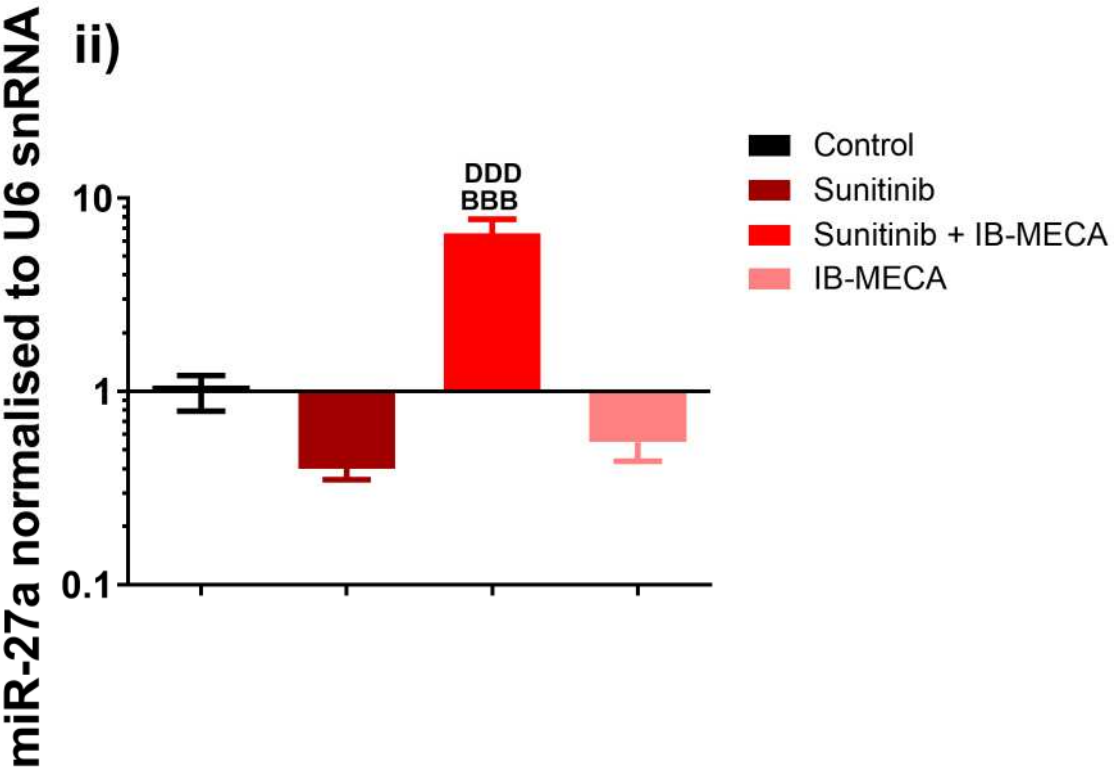
ii)
miR-27a normalised to U6 snRNA
10
1
0.1
DDD
BBB
Control
Sunitinib
Sunitinib + IB-MECA
IB-MECA

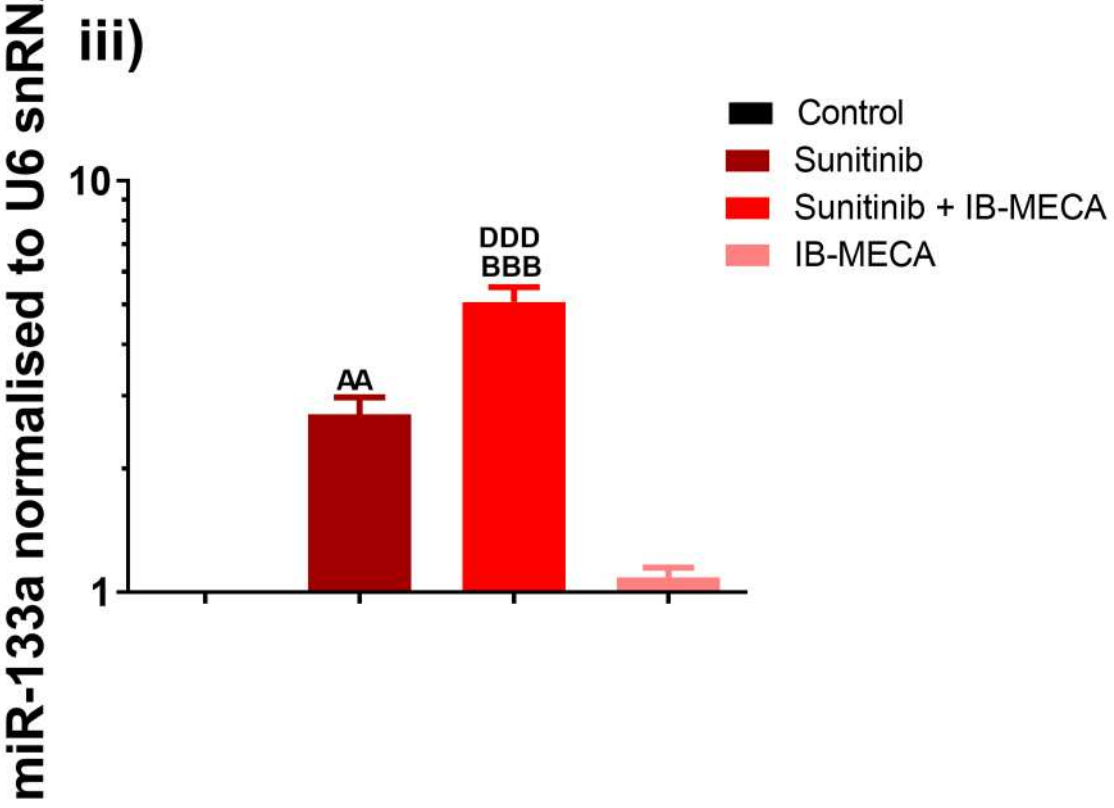
iii)
miR-133a normalised to U6 snRNA
10
1
AA
DDD
BBB
Control
Sunitinib
Sunitinib + IB-MECA
IB-MECA

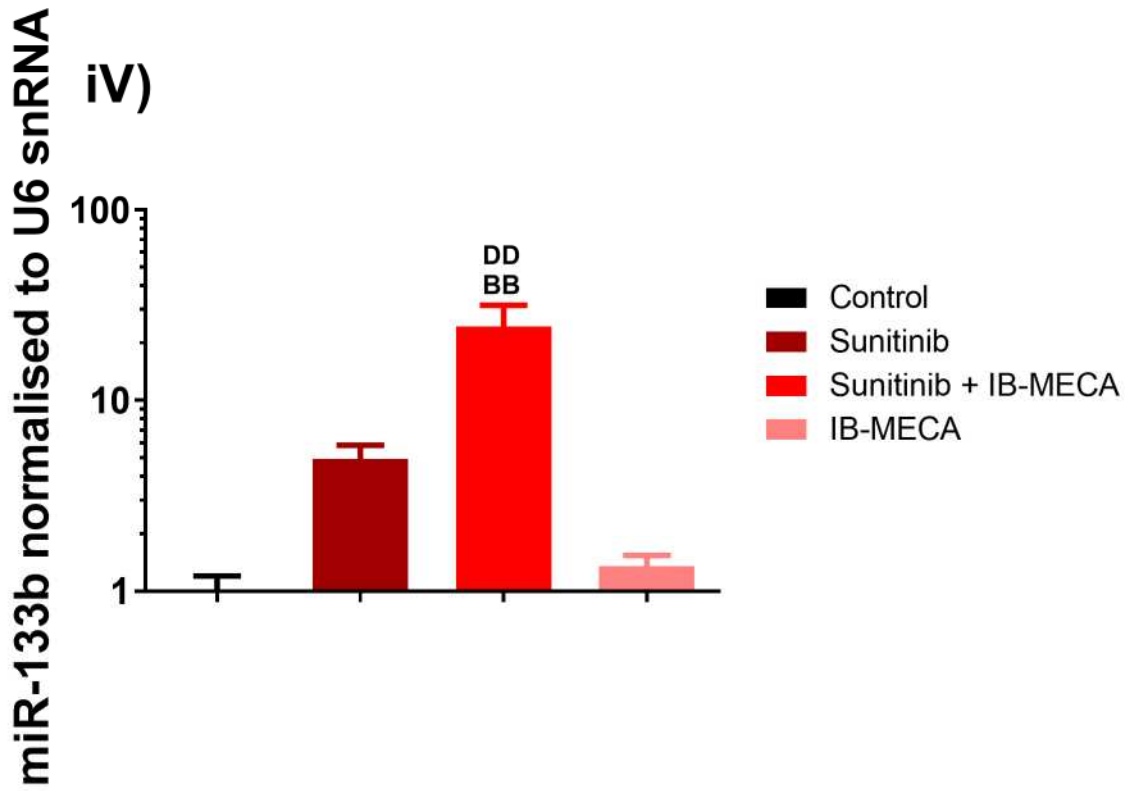

Figure 5.3: qRT-PCR analysis of Langendorff hearts (n = 5-6).

Treated with Control, Sunitinib (1 µM), Sunitinib (1 µM) + IB-MECA (1 nM) or IB-MECA (1 nM), showing miRNA expression of (i) miR-1, (ii) miR-27a, (iii) miR-133a and (iV) miR-133b. One-Way ANOVA statistical analysis: Control versus Sunitinib (AA = p<0.01), Control versus Sunitinib + IB-MECA (BB = p<0.01, BBB = P<0.001) and Control versus IB-MECA (C) and Sunitinib versus Sunitinib + IB-MECA (D = P<0.05, DD = p<0.01, DDD = P<0.001).

5.4.4 IB-MECA protects against Sunitinib-induced cardiotoxicity in Langendorff perfused hearts through MKK7-JNK and PKCα signalling pathways

MKK7 is an important stress regulating protein in the heart (Liu et al. 2011). Previously, we have shown that the MKK7 pathway is down regulated by Sunitinib treatment (chapter 3

and 4). This was confirmed by western blot analysis of Control, Sunitinib (1 µM), Sunitinib (1 µM) + IB-MECA (1nM). Sunitinib significantly reduces the p-MKK7 levels (Control: 1.00 ± 0.05; Sunitinib: 0.35 ± 0.07, p<0.001). Co-treatment of Sunitinib with IB-MECA significantly attenuated this decrease in p-MKK7 levels (Sunitinib: 0.35 ± 0.07; Sunitinib + IB-MECA = 0.75 ± 0.06, p<0.01).

Levels of p-MKK7 were not significantly altered after treatment with Sunitinib + IB-MECA and IB-MECA alone groups, compared to control.

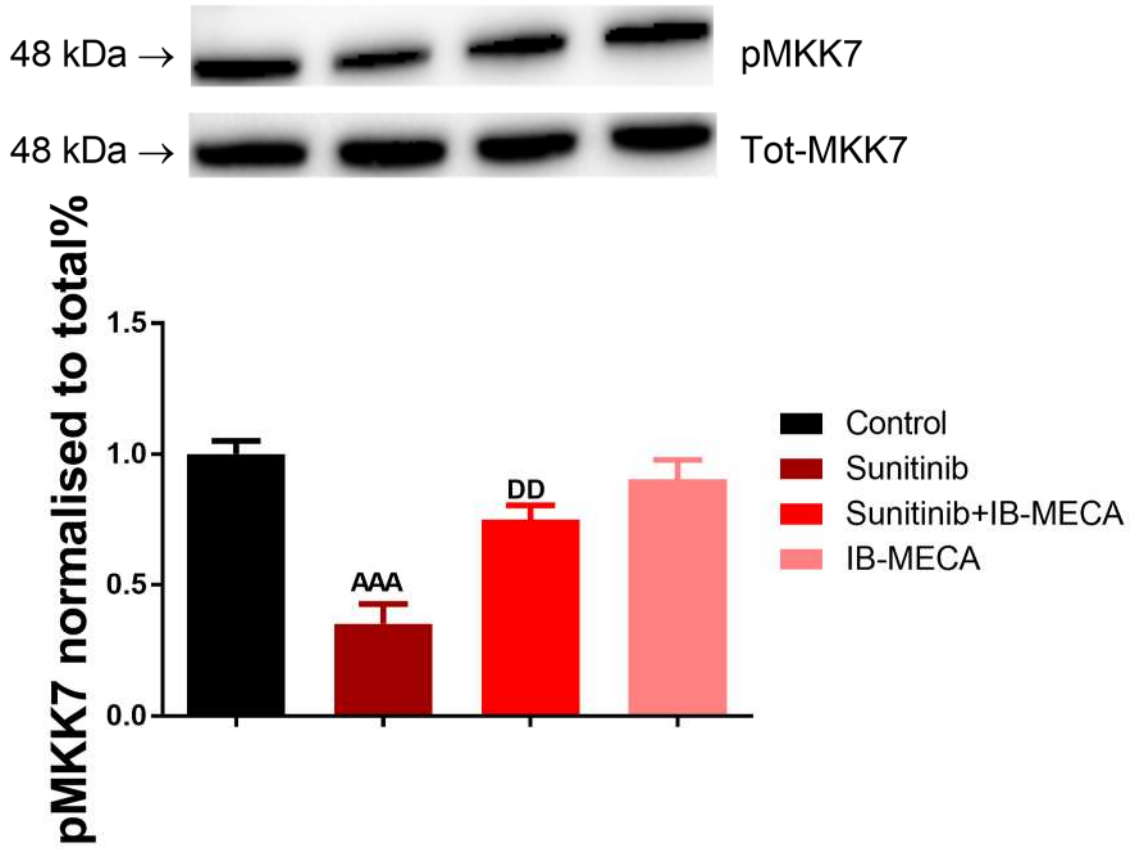

Figure 5.4: Western blot assessment of p-MKK7 levels in an isolated heart Langendorff model (n = 4). Statistics: Control versus Sunitinib (AAA = p<0.001), Sunitinib versus Sunitinib + IB-MECA (DD = P<0.01).

JNK is activated by MKK7 (Dhanasekaran and Reddy 2008). When activated, JNK interacts with the transcription factor c-Jun (Dérijard et al. 1994). This interaction results in a number of biological processes including cell proliferation, differentiation, apoptosis and cell survival (Chang and Karin 2001). As with MKK7, activation of JNK occurs in response to inflammatory cytokines and cellular stresses. JNKs can also be activated by growth factors and G protein coupled receptors (O'Hayre, Degese and Gutkind 2014). In the heart, JNK signalling has been shown to be affected by ischemia reperfusion injury and hypertrophy, however the exact role of JNK in the heart is controversial (Singh et al. 2016).

Here, significant reductions in JNK phosphorylation levels when hearts are treated with Sunitinib (1 μM) (Sunitinib = 0.34 ± 0.05, Control = 1.00 ± 0.03, $p<0.001$), was found (Figure 5.4).

The addition of IB-MECA to Sunitinib attenuated this decrease in JNK phosphorylation, returning p-JNK levels to levels similar to control (Sunitinib = 0.34 ± 0.05, Sunitinib + IB-MECA = 0.81 ± 0.08, $p<0.01$).

IB-MECA alone treatment did not significantly alter p-JNK levels.

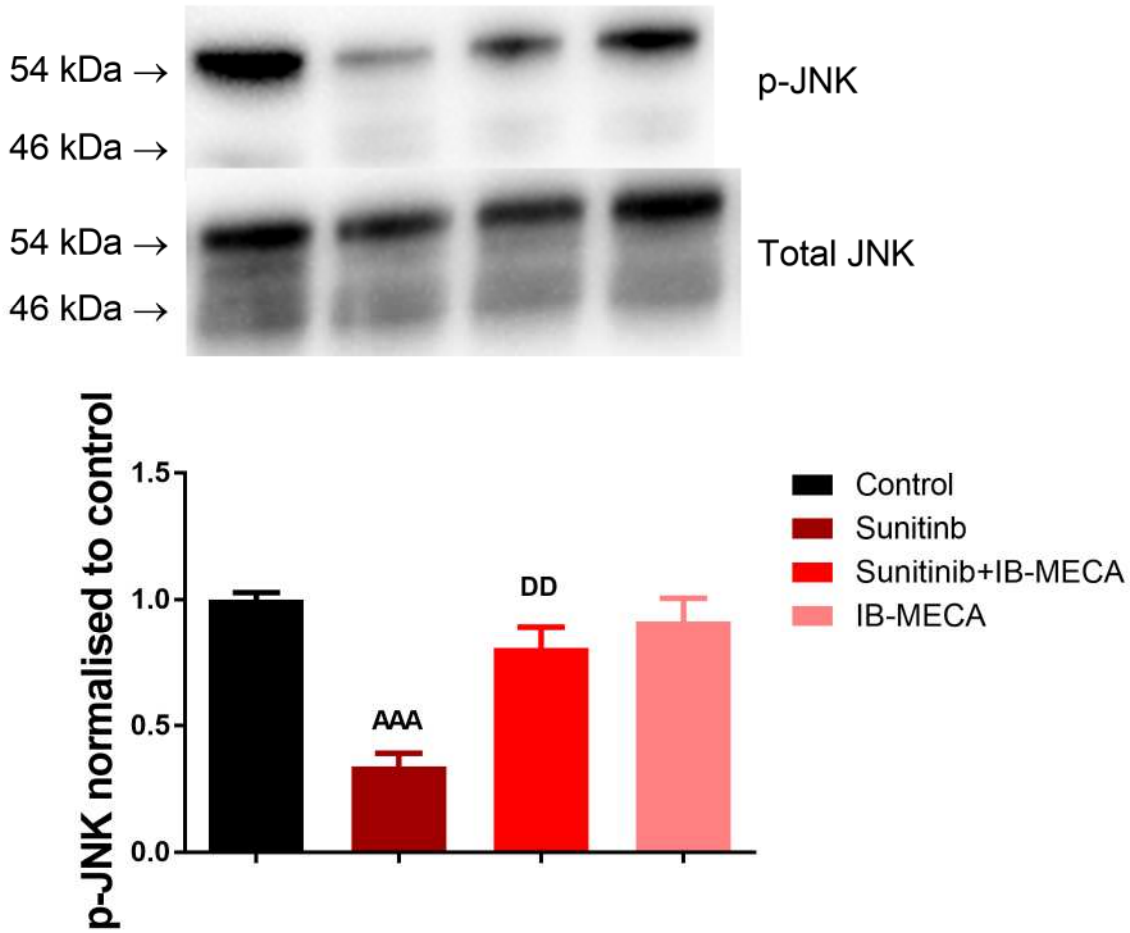

Figure 5.5: Western blot assessment of p-JNK levels in an isolated heart Langendorff model (n = 3). Statistics: Control versus Sunitinib (AAA = p<0.001), Sunitinib versus Sunitinib + IB-MECA (DD = P<0.001).

PKCα has been previously shown to negatively regulate heart contraction (Braz et al. 2004, Lange et al. 2016). We investigated whether PKCα signalling contributed to Sunitinib induced cardiotoxicity. PKCα phosphorylation was significantly increased 1.68 fold in the Sunitinib (1µM) treatment group compared to control ($p<0.05$). IB-MECA significantly attenuated the increase in PKCα when co-administered with Sunitinib by 0.9 fold ($p<0.001$) (Figure 5.7i). The p-PKCα levels were normalised to total PKCα.

i)

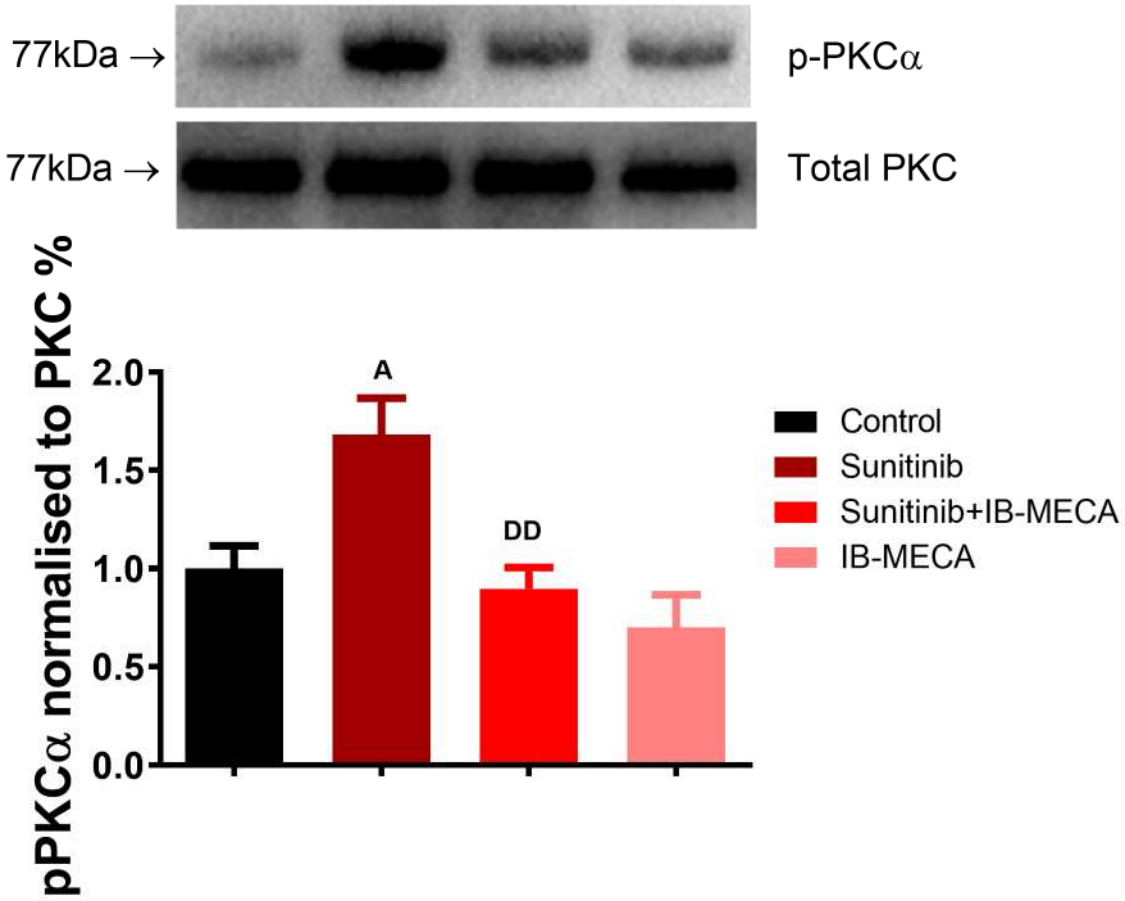
77kDa →
p-PKCα
77kDa →
Total PKC
pPKCα normalised to PKC %
2.0
1.5
1.0
0.5
0.0
A
DD
Control
Sunitinib
Sunitinib+IB-MECA
IB-MECA

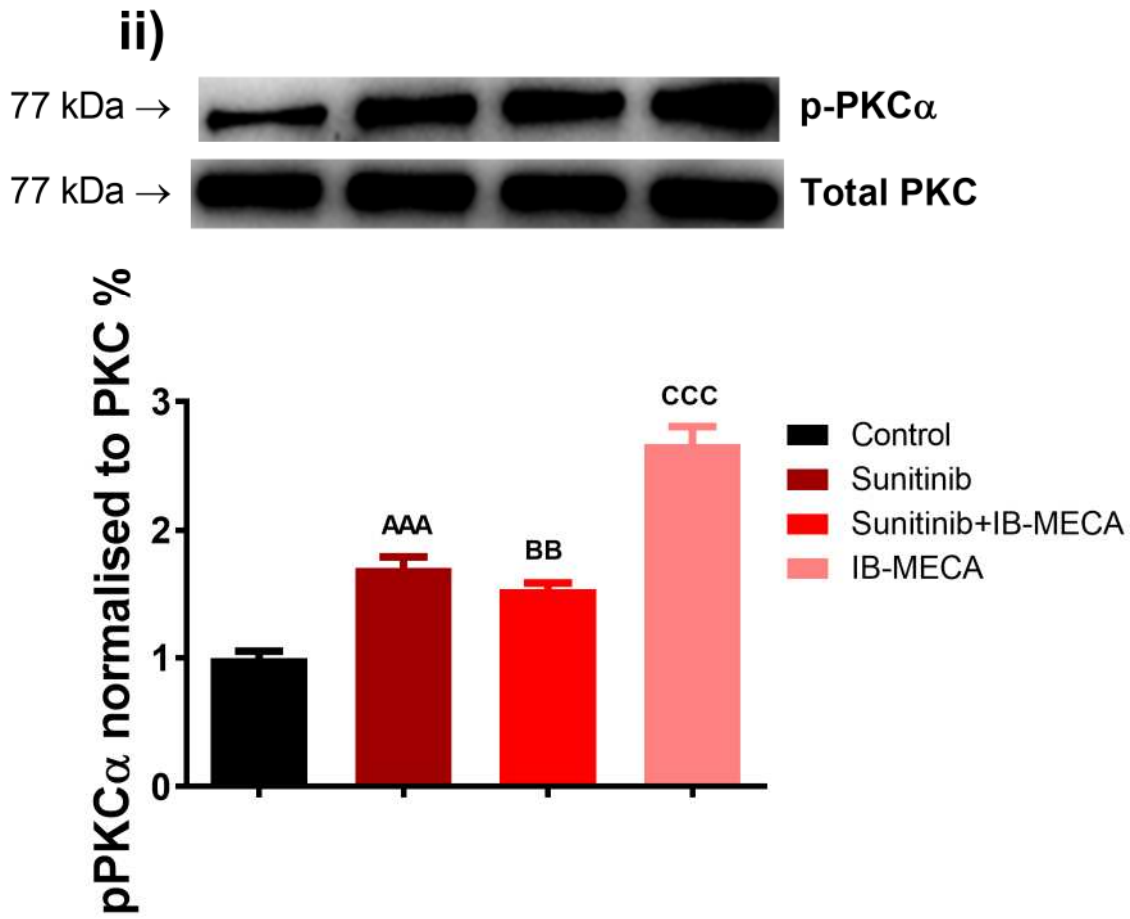

Figure 5.6: Western blot analysis showing fold change in p-PKC α.

(i) Langendorff perfused heart tissue samples of groups: Control, Sunitinib (1 µM), Sunitinib (1 µM) + IB-MECA (1 nM) and IB-MECA (1 nM) normalised to total PKC (n=6). (ii) p-PKCα western blots of HL60 cell sample groups: Control, Sunitinib (7 µM), Sunitinib (7 µM) + IB-MECA (1 nM) and IB-MECA (1 nM) normalised to total PKC (n=5). Statistical analysis: Control versus Sunitinib (A = p<0.05, AAA = p<0.001), Control versus Sunitinib + IB-MECA (BB = p<0.01), Control versus IB-MECA (CCC = p<0.001) and Sunitinib versus Sunitinib + IB-MECA (DD = p<0.01).

5.4.5 Sunitinib and IB-MECA cause an Up-regulation of PKCα in HL60 cells

PKCα has been shown to have a crucial role in cancer progression (Antal et al. 2015). The level of p-PKCα expression was determined after 24 hours of treatment with: Control,

Sunitinib (7 µM), Sunitinib (7 µM) ± IB-MECA (1 nM) and IB-MECA (1 nM). The p-PKCα levels in HL60 cells were significantly increased by administration of Sunitinib (7 µM) alone 1.7 fold ($p<0.001$) and by IB-MECA (1 nM) alone 2.67 fold ($p<0.001$), compared to Control. The co-treatment of Sunitinib with IB-MECA also demonstrated a significant increase in p-PKCα levels compared to control. Interestingly, the combination of Sunitinib and IB-MECA did not attenuate the increase in PKCα phosphorylation, compared to Sunitinib (Figure 5.7ii).

5.4.6 IB-MECA does not interfere the anti-cancer property of Sunitinib

To investigate the anti-cancer properties of Sunitinib in combination with the cardioprotective agent, IB-MECA, HL60 cells were incubated with: Control or increasing concentrations of Sunitinib (0.1 – 10 µM), Sunitinib (0.1 – 10 µM) + 1 nM IB-MECA or IB-MECA (0.01 nM – 10 µM). Cell viability was measured using the MTT assay method after 24 h of treatment. Addition of Sunitinib to the HL60 cells significantly decreased cell viability in a dose dependent manner ($p<0.001$) (Figure 5.5i). The cell viability was decreased significantly from 102.0 ± 1.4 % in control to 43.2 ± 6.3 % ($n=5-7$, $p<0.001$) when 10 µM Sunitinib was added to the cell culture. Co-administration of 1 nM IB-MECA did not attenuate the decrease in cell viability produced by Sunitinib treatment. The dose-response curve produced IC_{50}-values of: Sunitinib: 8.4 ± 1.3 and Sunitinib + 1 nM IB-MECA: 7.0 ± 1.6). Administration of IB-MECA alone to HL60 cells did not have any impact on cell viability at low doses. However, addition of a high dose of 10 µM IB-MECA did decrease the cell viability significantly. Cell viability decreased significantly from 102.0 ± 1.4 % in control to 72.1 ± 17.5 % ($p<0.001$) when treated with 10 µM IB-MECA (Figure 5.5ii).

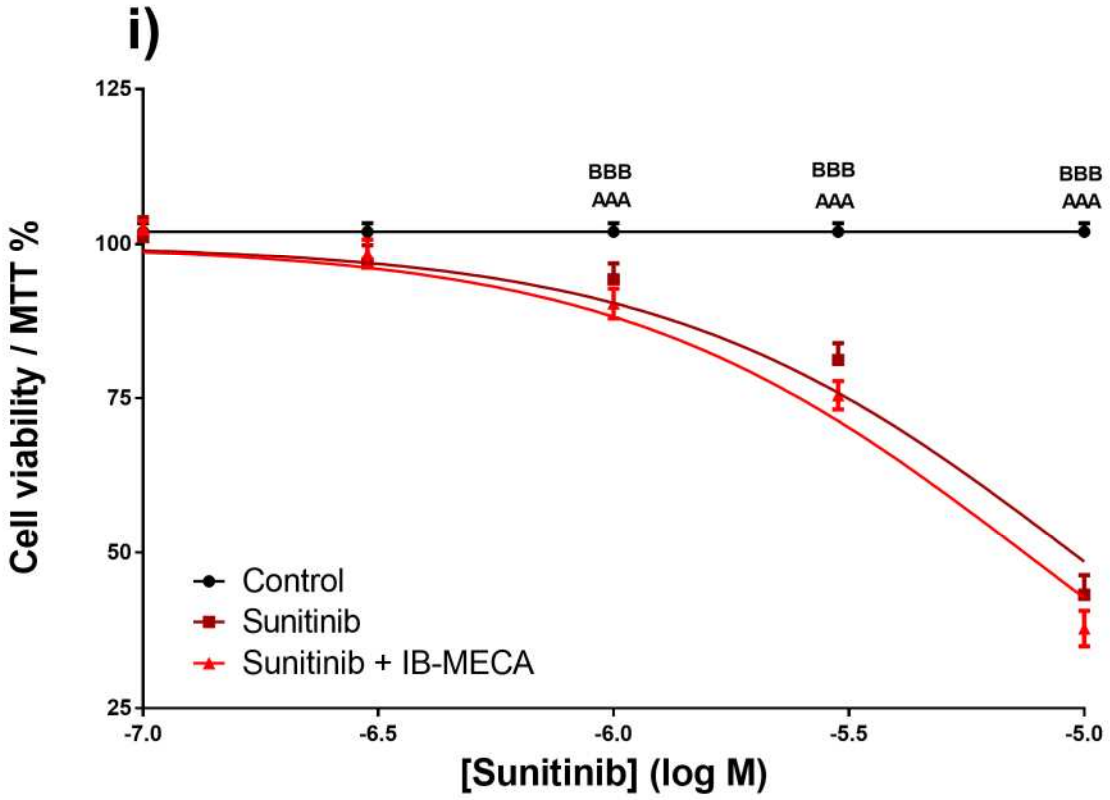
i)
125
100
75
50
25
Cell viability / MTT %
BBB
AAA
BBB
AAA
BBB
AAA
Control
Sunitinib
Sunitinib + IB-MECA
-7.0
-6.5
-6.0
-5.5
-5.0
[Sunitinib] (log M)

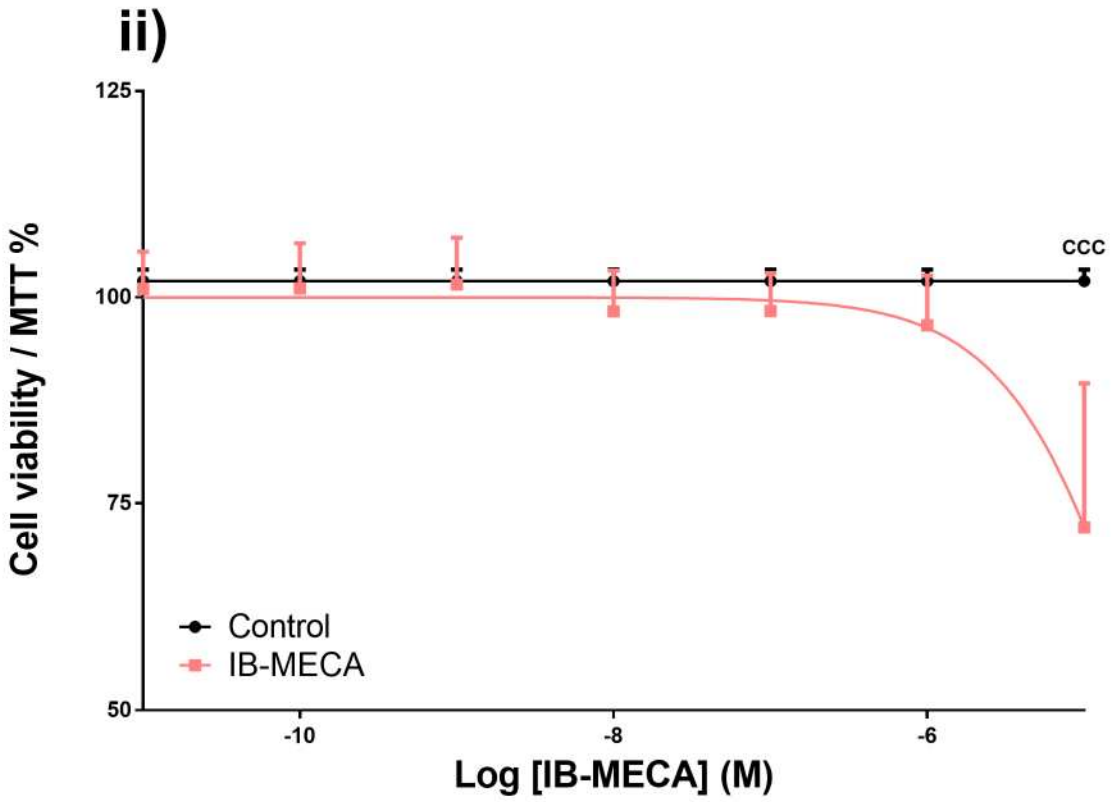

Figure 5.7: Cell viability in % of HL60 cells.

HL60 cells (10^5 cells/ml) incubated for 24 hours with control (Control) (n=7) or with increasing concentrations of i) Sunitinib (0.1 – 10 µM) (n=5) or Sunitinib (0.1 – 10 µM) + IB-MECA (1 nM) (n=6) or ii) IB-MECA (0.01 nM – 10 µM) (n=6). Statistics: Control versus Sunitinib (AAA = p<0.001), Control versus Sunitinib + IB-MECA (BBB = p<0.001) and Control verses IB-MECA (CCC = p<0.001).

5.4.7 microRNAs associated with apoptosis and cancer development: miR-15a, miR-16-1 and miR-155

Treatment of HL60 cells with Sunitinib in the absence and presence of IB-MECA altered the expression of miRNAs associated with apoptosis and cancer development (Figure 5.6i-iii). The qRT-PCR analysis of miR-15a showed a slight increase in miR-15a expression in HL60 cells treated with Sunitinib (1.4 fold) and Sunitinib ± IB-MECA (1.5 fold), compared to

Control. While, HL60 cells treated with IB-MECA alone produced a significant (0.4 fold) decrease in miR-15a expression compared to Control treated HL60 cells (Figure 5.6i).

The expression of miR-16-1 was slightly increased (3.6 fold) in Sunitinib treated HL60 cells compared to control. Also, the co-administration of Sunitinib with IB-MECA significantly increased the miR-16-1 expression further 7.7 fold ($p<0.05$), compared to Sunitinib treated HL60 cells. Treatment with IB-MECA showed a significant 46.8 fold increase ($p<0.001$) in miR-16-1 expression compared to Control treated HL60 cells (Figure 5.6ii). The levels of miR-155 was increased with a 2.3 fold in Sunitinib treated HL60 cells and co-administration of IB-MECA did not alter this increase. Treating the HL60 cells with IB-MECA showed a significant 82.2 fold increase ($p<0.001$) in miR-155 expression compared to Control (Figure 5.6iii).

The expression of the miRNAs involved in apoptosis and cancer development were also analysed in left ventricular heart tissue, collected after Langendorff perfusion with control, and Sunitinib, IB-MECA and Sunitinib + IB-MECA (Figure 5.6iV-Vi). There was a tendency for a decrease in miR-15a expression in both Sunitinib alone and IB-MECA alone treatment groups compared to control. Co-administration of IB-MECA with Sunitinib upregulated miR-15a expression significantly (71.3 fold) compared to Sunitinib (Figure 5.6iV).

The miR-16-1 expression profile showed no significant changes in miR-16-1 levels in Sunitinib and IB-MECA alone groups. However, co-administration of Sunitinib with IB-MECA significantly increased the miR-16-1 expression 5.7 fold (Figure 5.6V). The miRNA, miR-155 demonstrated a tendency for a reduction in expression in response to Sunitinib treatment, compared to control. There was also a significant 712.7 fold increase in miR-155 levels in the Sunitinib + IB-MECA co-treatment group compared to hearts treated with Sunitinib (Figure 5.6Vi).

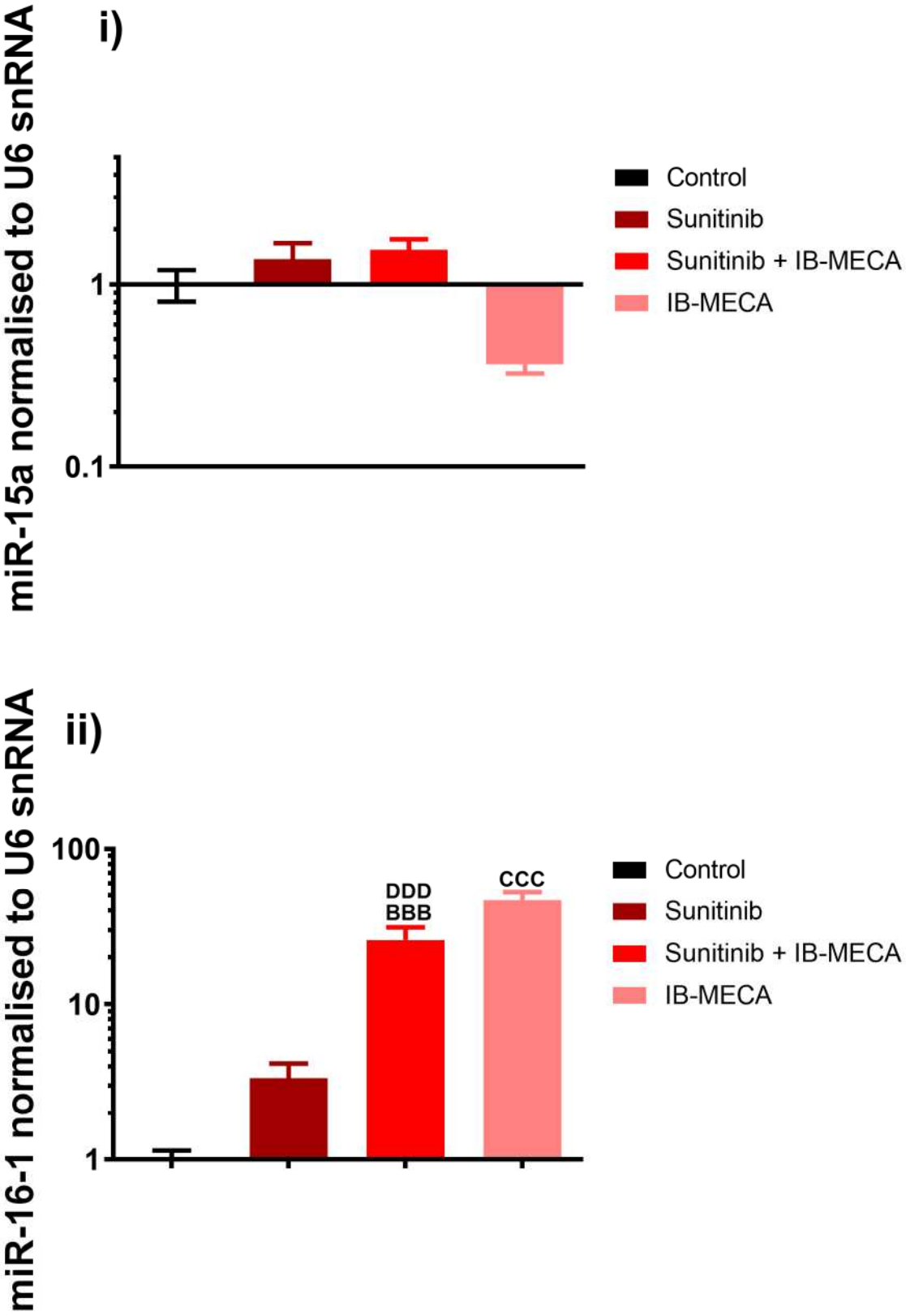
i)
miR-15a normalised to U6 snRNA
1
0.1
Control
Sunitinib
Sunitinib + IB-MECA
IB-MECA
ii)
miR-16-1 normalised to U6 snRNA
100
10
1
DDD
BBB
CCC
Control
Sunitinib
Sunitinib + IB-MECA
IB-MECA

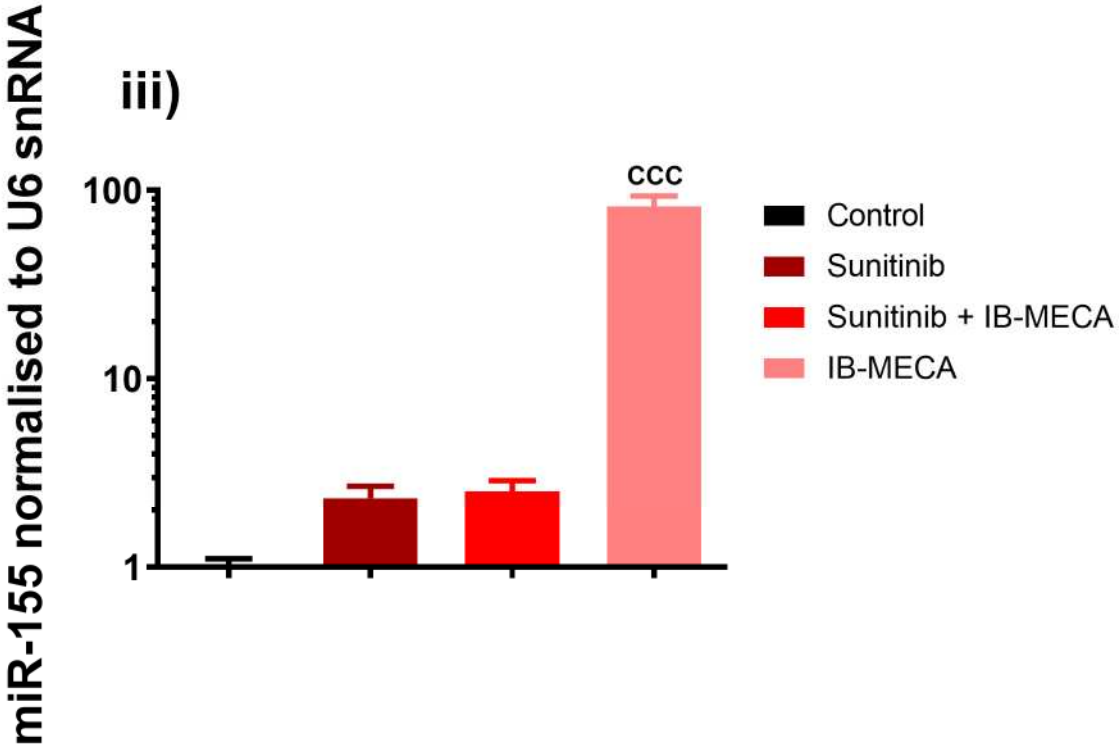
iii)
miR-155 normalised to U6 snRNA
100
10
1
ccc
Control
Sunitinib
Sunitinib + IB-MECA
IB-MECA

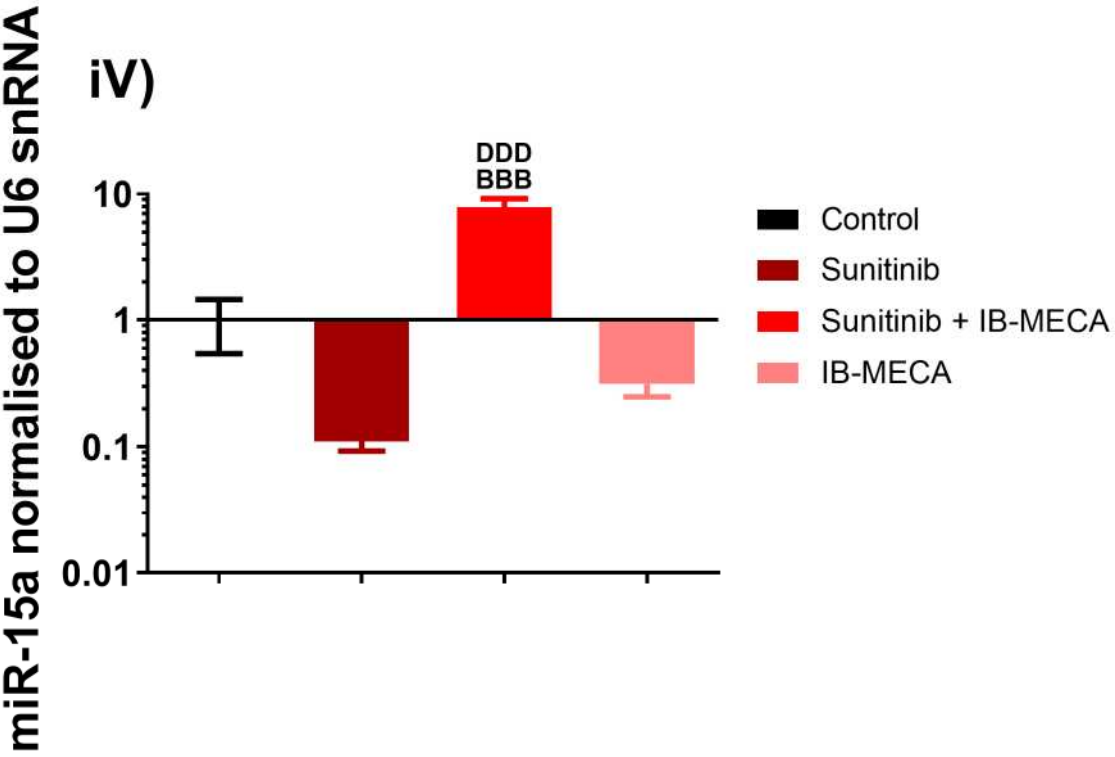
iV)
miR-15a normalised to U6 snRNA
DDD
BBB
10
1
0.1
0.01
Control
Sunitinib
Sunitinib + IB-MECA
IB-MECA

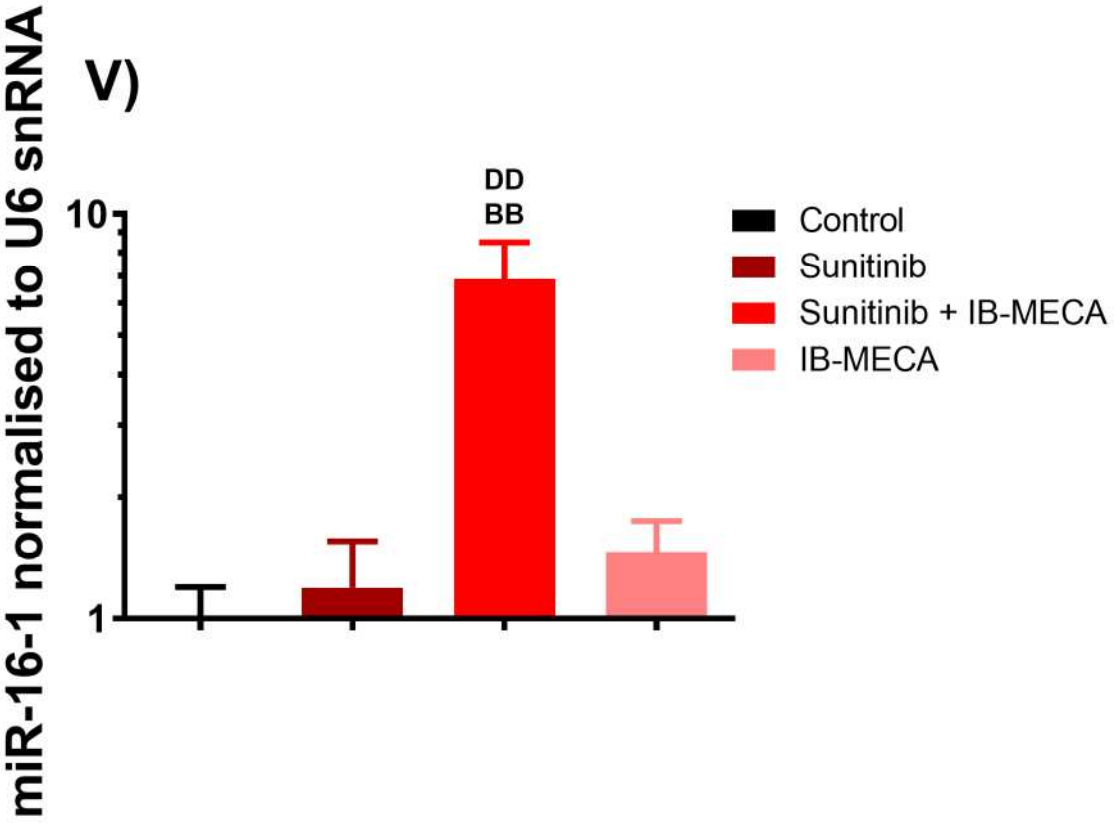
V)
miR-16-1 normalised to U6 snRNA
DD
BB
10
1
Control
Sunitinib
Sunitinib + IB-MECA
IB-MECA

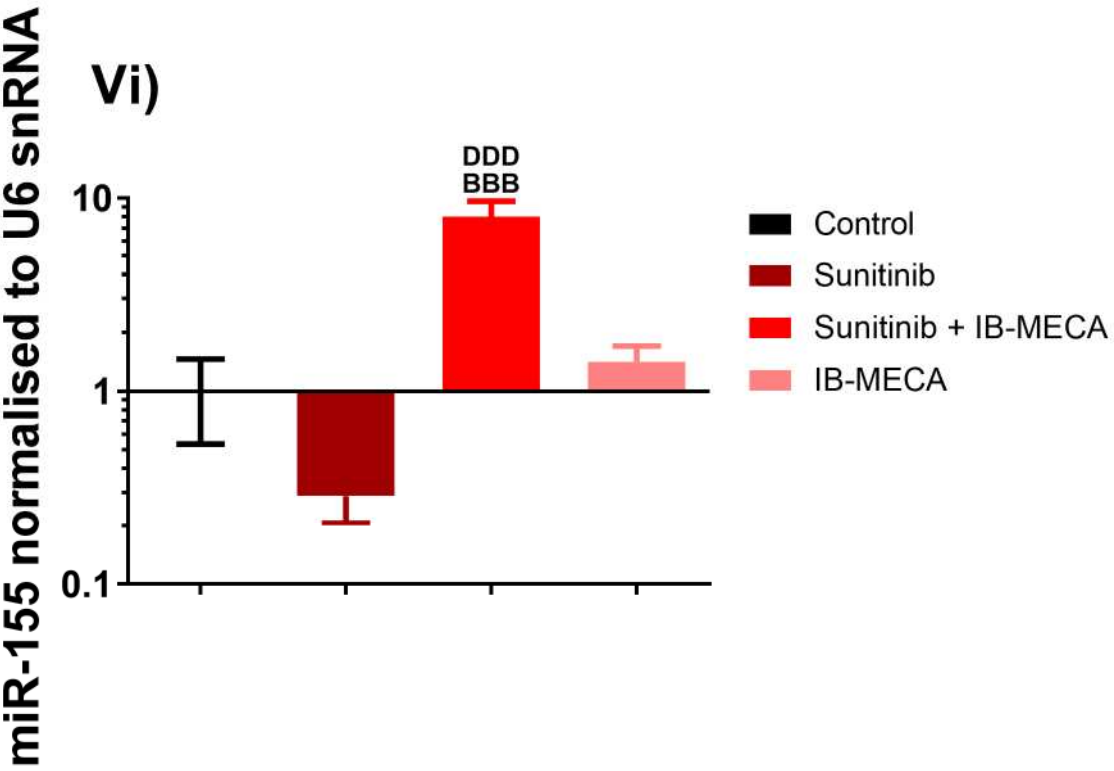

Figure 5.8: qRT-PCR analysis of HL60 cells (n=6).

Treated with: Control, Sunitinib (7 µM) Sunitinib (7 µM) with IB-MECA (1 nM) and IB-MECA (1 nM), showing miRNA expression of (i) miR-15a, (ii) miR-16-1 and (iii) miR-155. qRT-PCR analysis of Langendorff hearts (n=5-6) treated with: Control, Sunitinib (1 µM), Sunitinib (1 µM) with IB-MECA (1 nM) or IB-MECA (1 nM) showing miRNA expression of (iv) miR-15a, (v) miR-16-1 and (vi) miR-155. One-Way ANOVA statistical analysis: Control versus Sunitinib (A = $p<0.05$), Control versus Sunitinib + IB-MECA (BB = $p<0.01$, BBB = $p<0.001$) Control versus IB-MECA (CCC = $p<0.001$) and Sunitinib versus Sunitinib + IB-MECA (DD = $p<0.01$, DDD = $p<0.001$).

5.5 Discussion

5.5.1 Sunitinib induces cardiotoxicity in Langendorff perfused hearts

Sunitinib has very effective antineoplastic activity; however adverse cardiac events have

been reported in the clinic. In some cases, the cardiotoxic effects of Sunitinib led to congestive heart failure or even sudden death (Khakoo et al. 2008, Uraizee, Cheng and Moslehi 2011). The mechanism of Sunitinib's cardiotoxic action is thought to function through both the on-target inhibition of VEGF, receptors for platelet-derived growth factor, c-KIT and fms-like tyrosine kinase-3, and also the off-target inhibition of various other kinases essential in the maintenance of cardiac function (de Jesus-Gonzalez et al. 2012, Force and Kolaja 2011, Ghoreschi, Laurence and O'Shea 2009).

In this study, the cardiotoxic impact of Sunitinib (1 µM) and the cardioprotective effect of IB-MECA (1 nM) were measured during a 125 min Langendorff heart perfusion. The level of infarction caused by Sunitinib and the co-treatment of Sunitinib with IB-MECA was determined. Infarct size was significantly increased in hearts treated with 1 µM Sunitinib, compared to control hearts. This was also found in chapters 3 and 4, plus this is in accordance with other studies investigating the level of cardiotoxicity induced by Sunitinib. Existing evidence supports that Sunitinib treatment could result in left ventricular dysfunction and even heart failure in patients (Chu et al. 2007, Di Lorenzo et al. 2009, Henderson et al. 2013, Mooney et al. 2015).

Chu et al. (2007) demonstrated that Sunitinib induces mitochondrial injury and cardiomyocyte apoptosis or necrosis, which resulted in symptoms of heart failure in 11% of patients studied (Chu et al. 2007). In addition, Force et al. suggest that inhibition of ribosomal S6 Kinase is responsible for Sunitinib induced cardiotoxicity as activates the intrinsic apoptotic pathway and causes ATP depletion (Force, Krause and Van Etten 2007). Loss of large numbers of myocytes within the heart reduces the efficiency of heart function

and leads to the symptoms of heart failure in patients (Mughal, Dhingra and Kirshenbaum 2012).

Loss of cardiac function can be identified by a reduction in haemodynamic parameters. In this study, haemodynamic parameters (LVDP, HF and CF) of rat hearts treated with Sunitinib, A3AR IB-MECA and the co-treatment of Sunitinib and IB-MECA were measured. After Sunitinib treatment there was a significant decrease in LVDP and HR compared to control. This is in accordance with other studies investigating the level of cardiotoxicity induced by Sunitinib (Henderson et al. 2013, Mooney et al. 2015). Chu et al. demonstrated a reduction in LVEF in patients treated with Sunitinib (Chu et al. 2007). Another characteristic indicator of cardiac injury is ventricular arrhythmia. Bello et al. demonstrated a dose dependent effect on QT interval and increased risk of ventricular arrhythmias in patients treated with Sunitinib by electrocardiogram assessment (Bello et al. 2009). This has been associated with Sunitinib's inhibitory effect on AMPK and hERG, which leads to a reduction in cardiomyocyte depolarisation and repolarisation, which alters the beat pattern of the heart (Doherty et al. 2013). This study shows that Sunitinib produces cardiotoxic effects in rat hearts which results in left ventricular dysfunction, bradicardia and cardiomyocyte death. This supports existing evidence that Sunitinib treatment could result in left ventricular dysfunction and even heart failure in patients (Di Lorenzo et al. 2009).

5.5.2 IB-MECA attenuates Sunitinib induced cardiotoxicity

It is well established that A3AR stimulation produces cardioprotective results (Carr et al. 1997, McIntosh and Lasley 2012). In rat hearts, IB-MECA has shown to be beneficial for ischaemia (Hochhauser et al. 2007). IB-MECA has been shown to have powerful

cardioprotective effects against cardiac damage caused by hypoxia, ischaemia/reperfusion injury and anti-cancer treatment with Doxorubicin (Shneyvays et al. 2002).

In this chapter, the A3AR selective agonist IB-MECA attenuated Sunitinib-induced cardiac injury. The infarct size generated by Sunitinib treatment alone was significantly decreased by the co-administration of IB-MECA.

The key cardioprotective functions mediated by IB-MECA to reduced ischaemia and infarct size are suggested to be through mitochondrial K_{ATP} (mtK_{ATP}) activation and reduces the level of ATP catabolism, which increases the O_2 consumption and ATP production in mitochondria (Lipshultz et al. 2013, Sandhu and Maddock 2014). IB-MECA also inhibits mitochondrial swelling due to Ca^{2+} and prevents mitochondrial permeability transition pore (mtPTP) opening, through the inactivation of glycogen synthase kinase 3β (GSK3β) (Park et al. 2006).

As previously mentioned, Sunitinib treatment reduces ATP levels in cardiomyocytes and produces mitochondrial dysfunction, which leads to high levels of apoptosis and necrosis in cardiomyocytes (Force, Krause and Van Etten 2007, Will et al. 2008). In a study by Emanuelov *et al*. 2010 Doxorubicin treatment lead to left ventricular dysfunction due to mitochondrial dysfunction and increased Ca^{2+} in the cytosol and mitochondria, causing a negative effect on contractility. Co-administration of IB-MECA attenuated the harmful effect of Doxorubicin by reducing Ca^{2+} overload in cardiomyocytes and restoring the function of the mitochondria (Emanuelov et al. 2010). Therefore, IB-MECA may have attenuated Sunitinib induced cardiotoxicity by inhibiting ATP, Ca^{2+} and mitochondrial dysfunction. However, by carrying out similar experiments to Emanuelov et al. it will be possible to

identify whether cardioprotection by IB-MECA elevates Sunitinib-induced cardiotoxicity through a similar mechanism.

We show through activation of A3AR it is possible to protect the heart from the extensive damage caused by Sunitinib, thus highlighting A3AR, IB-MECA has noticeable cardioprotective abilities. However, the decrease in HR by Sunitinib alone was not attenuated by co-administration with IB-MECA. This highlights that further studies are required to determine why reductions in infarct size and LVDP by Sunitinib are attenuated by IB-MECA, but HR is not.

However, the co-treatment of Sunitinib and IB-MECA did not significantly alter the haemodynamic parameters LVDP (after 20 minutes) and CF (for the whole drug perfusion) compared to control. Perhaps an increase in IB-MECA concentration and/or IB-MECA pre-treatment would improve the levels of protection against Sunitinib induced cardiotoxicity. Tracy et al. demonstrated a post-occlusion, dose-dependent increase in LVDP and HR with the pre-treatment of IB-MECA (1 nM - 50 nM) in rabbit hearts (Tracey et al. 1998).

Finally, the haemodynamic parameters and level of heart tissue infarction were not altered by IB-MECA treatment alone. Therefore, IB-MECA did not produce cardiotoxicity when administered alone.

5.5.3 miRNA expression profiles are altered by Sunitinib and IB-MECA treatment

miRNA profiling is progressively becoming an important screening tool to identify miRNAs that are responsive to drugs and environmental factors. In particular, the cardiac injury

associated miRNAs miR-1, miR-27a, miR-133a and miR-133b have been linked to cardiotoxicity (Sandhu and Maddock 2014).

Both miR-1 and miR-133 regulate heart development and are dysregulated in patients with cardiac hypertrophy and heart failure (Care et al. 2007, Chen, Kerkela and Force 2008). Plus, mir-1, mi-133a and miR-133b are dysregulated in patients with cardiac hypertrophy, myocardial infarction and heart failure (Bostjancic et al. 2010). The miRNA miR-133a has a partial complimentary target site in the 3'UTR region of ether-a-go-go gene and a reduction in ether-a-go-go levels can cause the delayed myocyte repolarisation attributed to a long QT interval (Xiao et al. 2007). And miR-27a is important in the regulation of contractility within the heart (Nishi et al. 2011).

In the present study, a significant increase in miR-133a was detected after Sunitinib treatment alone, compared to control. Previous studies measuring the levels of miR-133a in blood have shown significant increases of miR-133a in cases of myocardial infarction (Widera et al. 2011). This increase in miR-133a has also been suggested as a predictor for risk of death following acute coronary syndrome (Eitel et al. 2012).

There was also a tendency for an increase in miR-133b levels in response to Sunitinib treatment, compared to control. Wang et al. (2013) found elevated levels of miR-133b detected in plasma after heart transplantation. This increase has been suggested as strong predictor of heart injury after transplantation as miR-133b was shown to be more sensitive than detecting elevated levels of cardiac troponin (cTnI), a well-established marker for cardiac injury (Wang et al. 2013).

Furthermore, miR1 and miR-27a levels were not significantly altered by Sunitinib compared to control. However, there is a tendency for a decrease in miR-27a levels. In chapter 3 miR-27a levels are significantly decreased after Sunitinib treatment, compared to control. An evaluation of circulating miRNAs in patients with acute myocardial infarction revealed miR-27a plasma levels to be significantly lower than that of healthy controls (Ovchinnikova et al. 2015). This suggests that elevated levels of miR-133a and miR-133b, and low levels of miR-27a could indicated Sunitinib-induced cardiotoxicity.

IB-MECA treatment alone did not alter any of the cardiac injury associated miRNAs assessed. This suggests that IB-MECA alone does not caused cardiac injury at a molecular level.

Interestingly, this study reveals an increase in miR-27a expression in Sunitinib + IB-MECA treated hearts when compared to Sunitinib, and both miR-133a and miR-133b are increased in Sunitinib + IB-MECA treated hearts when compared to Sunitinib. The expression of miR-1 was not altered when the hearts were treated with Sunitinib or IB-MECA. The increase in miR-27a, miR-133a and miR-133b in the co-treatment group indicates that the combination of Sunitinib and IB-MECA induces stress at a cellular miRNA level, however, in the perfused heart tissue IB-MECA does attenuate Sunitinib-induced cardiotoxicity. Further investigations to unravel the difference in miR-27a, miR-133a and miR-133b expression levels during Sunitinib and IB-MECA treatment are required in order to clarify this. This could be carried out by assessing the effect of Sunitinib and IB-MECA treatment on the predicted protein targets of these miRNAs.

5.5.4 Sunitinib inhibits MKK7/JNK signalling and this inhibition was blocked through activation of the A3AR by IB-MECA

MKK7 and JNK are stress signalling proteins of a MAPK pathway (Ho et al. 2006). This pathway regulates essential in processes within cells, such as apoptosis, proliferation and cell survival (Wada et al. 2004). Such processes are of high interest in the heart as the heart is highly susceptible to toxicity and injury (Kalogeris et al. 2012). We have shown that Sunitinib produces detrimental effects on cardiac function and structure. Understanding the signalling pathways involved in Sunitinib-induced cardiotoxicity and the cardioprotection exerted by IB-MECA could lead to the production of effective agents which can attenuate Sunitinib-induced cardiotoxicity.

Here we have shown that phosphorylation levels of both MKK7 and JNK are significantly reduced in left ventricular tissue by Sunitinib. This is in accordance with previous data showing the potent inhibiting effect Sunitinib has on MAPKs (Faivre et al. 2007, Fenton et al. 2010).

Inhibition of MKK7 activity has been shown to have adverse effects on the heart. Liu et al., (2011) demonstrated that mice developed characteristic symptoms of heart failure after the deletion of MKK7 and pressure overload to the heart in mice (Liu et al. 2011). This highlights the importance of MKK7 in the development of heart failure. Also, Chowdhury et al., demonstrated that under hypertrophic stress the level of MKK7 phosphorylation is decreased, which has a direct effect on a number of key potassium channel genes. This results in delayed repolarisation which lead to ventricular arrhythmias (Chowdhury et al. 2017). Therefore, decrease in p-MKK7 levels in response to Sunitinib treatment could be

linked to irregular regulation of potassium channels within the left ventricular myocytes and this may have resulted in the decline in HR and LVDP. However, the relationship between MKK7 activation and potassium channels needs to be investigated for a conclusion to be drawn.

Furthermore, Sunitinib is an anti-angiogenic agent. In endothelial cells, JNK phosphorylation levels have been shown to be high during angiogenesis, suggesting that JNK is involved in angiogenesis (Ramo et al. 2014, Roskoski 2007). Inhibition of JNK has previously been shown to reduce endothelial cell proliferation and angiogenesis (Uchida et al. 2008). Disruption of angiogenesis in the heart can cause contractile dysfunction and impaired cardiac growth, which contributes to the progression of heart failure (Shiojima et al. 2005).

Direct inhibition of JNK has also been shown to lead to apoptosis. In cardiomyocytes, JNK inhibitory mutants which reduced levels of p-JNK and have been shown to cause a significant increase in NO-mediated and ischaemia-reperfusion induced apoptosis (Andreka et al. 2001, Dougherty et al. 2002). Loss of JNK activity through targeted disruption of the gene encoding MEK kinase 1 resulted in a greater apoptotic response when embryonic stem cells were under hyperosmolar stress (Yujiri et al. 1998). This suggests that JNK produces anti-apoptotic effects.

Interestingly, in our study, the co-treatment of an A3AR agonist, IB-MECA attenuated Sunitinib-induced inhibition of both MKK7 and JNK phosphorylation back to levels similar to control hearts. Adenosine receptors have been shown to activate MAPK signalling pathways through the recruitment of Rho-family GTPases (Abbracchio et al. 2001, Schulte and Fredholm 2003). In the heart, the administration of adenosine was shown to increase levels of MAPK proteins such as JNK during ischaemia reperfusion (Haq, Clerk and Sugden 1998).

IB-MECA has been shown to induce cardioprotective effects through an increase in the activation of many signalling pathways including: PKC-δ, NF-κβ, iNOS, MAPK/ERK and Akt/PI3 (Hussain et al. 2014)

Contrastingly, other studies have demonstrated increased p-MKK7 and p-JNK levels in response to stresses in the heart (Cook, Sugden and Clerk 1999) . There has been much controversy over the exact mechanism of the MKK7-JNK signalling pathway, many groups have shown upregulation to occur as a result of cytotoxicity/injury. Whereas other groups have shown downregulation of the MKK7-JNK pathway to be associated with cellular dysfunction and hypertrophy in the heart. Generally, greater signalling of MKK7 or JNK has been linked to heart disease with ventricular remodelling, while inhibition of JNK is associated with hypertrophic stress and different disease phenotypes (Haq, Clerk and Sugden 1998).

MAPK signalling is very complex and much information on the regulation of MAPKs is yet to be discovered. It could be possible that the MKK7-JNK pathway is activated by several routes. Potentially, Sunitinib could inhibit the predominant MKK7-JNK activation route. Whereas the A3AR could activate the MKK7-JNK pathway via a less potent route. Further investigation into drug-protein interactions and the functional properties are required to know this for certain.

Furthermore, in chapter 4, elevations in ASK1/MKK7/JNK phosphorylation were found in Sunitinib + NQDI-1 treated hearts, which also produced declines in haemodynamic function and increased infarct size compared to control. Therefore, these findings suggest a balance of MKK7-JNK activation is found in healthy tissue and this balance is required to reduce cardiac injury in response to Sunitinib treatment.

5.5.5 PKC is involved in Sunitinib-induced cardiotoxicity and Sunitinib's anti-cancer properties

PKCα is a stress signalling which has been shown to have a pro-apoptotic effect in the heart (Steinberg 2004). PKC is regulated by many membrane-bound receptors, such as receptor tyrosine kinases and adenosine receptors (Lemmon and Schlessinger 2010, Parker and Murray-Rust 2004). Elevated levels of the protein PKCα in cardiomyocytes contribute to the onset of cardiomyopathy, which can lead to heart failure (Lange et al. 2016).

The present study identified an increase in p-PKCα levels in hearts treated with Sunitinib (1 μM) compared to control. This suggests that PKCα is involved in Sunitinib-induced cardiotoxicity, as co-administration with IB-MECA attenuated this increase in p-PKCα. Previous studies have linked the TKI, Imatinib, with increased levels of PKC phosphorylation in the heart (Steinberg 2004). This suggests that PKC is involved in TKI induced cardiotoxicity.

Interestingly an increase in PKC phosphorylation and a decrease in AMPK phosphorylation has been associated with myocardial infarction (Kong et al. 2012). Kong et al. demonstrated that in controls and groups with low levels of infarction both AMPK and PKC phosphorylation remain at a similar level. This group suggested that myocardial infarction directly correlates with an increase in PKC phosphorylation and not AMPK phosphorylation (Kong et al. 2012). This was confirmed in the results of the present study where Sunitinib, a known inhibitor of AMPK, has also been shown to significantly increase infarct size also significantly increases PKCα phosphorylation.

Furthermore, Braz et al., 2004 revealed that by deleting the PKC gene in mice it was possible to protect against heart failure during pressure overload (Braz et al. 2004). AMPK has also been shown to inhibit activation of PKC (Ceolotto et al. 2007). We demonstrate a significant decrease in PKCα phosphorylation with the co-administration of Sunitinib with IB-MECA compared to Sunitinib alone treatment. This could suggest that IB-MECA protects the heart against Sunitinib-induced cardiotoxicity by inhibiting PKC phosphorylation induced by Sunitinib. It is also possible that IB-MECA raised AMPK levels, however, this was not investigated in this study.

5.5.5.1 PKC signalling in HL60 cells

A3AR receptors have been shown to be differentially expressed in various tissue types (Zhou et al. 1992). In cancer cells A3ARs are linked to G_i protein, adenylate cyclase (AC) and G_q protein, phospholipase C-γ (PLC_γ). A3AR cause inhibition of AC, reduces cAMP production and inhibits PKA. A3AR also activates of PLC_γ, which increases inositol 1, 4, 5-trisphosphate (IP3) and diacylglycerol production which activates PKC (Tsuchiya and Nishizaki 2015). PKC has been shown to have an important role in cancer progression (Atten et al. 2005, Kazi, Kabir and Rönnstrand 2013). Interestingly, in many cancers PKC regulation is low due to the presence of a loss of PKC function mutation (Antal et al. 2015).

In the present study, the phosphorylation levels of PKCα were measured in HL60 cells treated with Control, Sunitinib (7 μM), Sunitinib (7 μM) + IB-MECA (1 nM) and IB-MECA (1 nM) alone. Phosphorylation levels of PKCα were significantly increased in all groups compared to control. Our findings are in agreement with previous findings published in Teng *et al.* 2013 where treatment of HL60 cells with 0.1-1 μM Sunitinib resulted in increased phosphorylation of PKCα in a Sunitinib dose dependent manner. This increase in p-PKCα was

shown to facilitate Sunitinib-induced G1 cell cycle arrest and increased pro-apoptotic molecule levels. This was confirmed by the addition of the PKCα specific inhibitor Go6976 which attenuated both the increased PKCα phosphorylation and abolished AML differentiation (Teng et al. 2013).

In the present study, addition of IB-MECA to HL60 cells significantly increased p-PKCα expression levels. Previously, IB-MECA has been shown to increase p-PKC levels in macrophages (Forte et al. 2011). Activation of PKCα has been to inhibit the growth of pancreatic tumours (Detjen et al. 2000). Whereas, inhibition of PKCα promotes proliferation and cell survival (Scaglione-Sewell et al. 1998). In addition, PKCα is known to suppress non-small cell lung cancer (NSCLC) cell cycle progression (Oliva et al. 2008), colon cell proliferation (Gwak et al. 2009) and repress Kirsten rat sarcoma viral oncogene homolog (KRAS) tumorigenesis (Hill et al. 2014). It is therefore believed that PKCα is a tumour suppressor (Antal et al. 2015).

There was an increase in p-PKCα levels detected in HL60 cells and a decrease in heart tissue treated with IB-MECA alone compared to control. This could be due to the differential expression of PKC and A3AR in cardiac myocytes and cancer cells. This could allow for a successful adjunct therapy, such as IB-MECA, which is both cardioprotective and exhibit anti-cancer effects.

These findings indicate that IB-MECA attenuates Sunitinib induced cardiac injury through a reduction in p-PKCα levels compared to Sunitinib in heart tissue. Interestingly, in HL60 cells Sunitinib alone and Sunitinib co-treatment with IB-MECA increase p-PKCα levels compared to control. IB-MECA alone increases p-PKCα levels further, highlighting the anti-cancer properties of IB-MECA.

5.5.6 A3AR activation by IB-MECA does not alter the anti-cancer properties of Sunitinib

A3AR activation plays a key role in adenosine-induced inhibition of tumour cell proliferation (Fishman et al. 2000). This study demonstrated a concentration dependent decline in HL60 cell viability with Sunitinib and IB-MECA. A study by Fishman *et al.* 2002 showed that melanoma cells treated with 0.01 µM IB-MECA resulted in inhibition of cell proliferation through the Wnt pathway (Fishman et al. 2002). Furthermore, studies by the team of Sang Kook Lee have shown the adenosine analogue thio-Cl0IB-MECA to inhibit HL60 cell proliferation and A549 human lung cancer cells (thio-Cl0IB-MECA dose up to 25 µM for HL60 and 20 µM for A549) through G_0/G_1 cell cycle arrest and in higher concentrations induce apoptosis (thio-Cl0IB-MECA dose up to 50 µM for HL60 and 80 µM for A549 cells) (Kim et al. 2008, Lee et al. 2005), and again the involvement of Wnt pathway was implicated in adenosine-induced proliferation inhibition.

It is imperative to assess the effects of adjunct therapies, aiming to reduce the cardiotoxic effect, on the anti-tumour effects. Many cardioprotective strategies fail to demonstrate beneficial effects in clinical or in vivo settings as they interfere or reduce with the anti-cancer effects and thereby reduce the clinical utility (Granger 2006).

Collectively, our data shows that co-treatment with the A3AR agonist IB-MECA can ameliorate the cardiotoxic effects of Sunitinib without affecting its anticancer properties. These finding warrant further investigations in the relevant animal models of cancer.

5.5.7 Cancer specific miRNA expression profiles alter with Sunitinib and IB-MECA treatment

5.5.7.1 miR-15a and miR16-1

The tumour suppressor miRNAs miR-15a and miR-16-1 are involved in the regulation of multiple myeloma cell proliferation processes. This is achieved by the blocking of AKT serine/threonine-protein-kinase, ribosomal-protein-S6, MAPKs and NF-κβ -activator MAP3KIP3 (Roccaro et al. 2009). The miR-15a/16 cluster has been proposed as a potential biomarker for poor patient survival rate in colorectal cancer tissue, where the expression of miR-15a and miR-16-1 is downregulated when compared with adjacent colorectal mucosa (Xiao et al. 2014). In gastric adenocarcinoma miR-15a and miR-16-1 expression is downregulated, and ectopic expression of miR-15a and miR-16-1 suppress cell proliferation through G_0/G_1 cell cycle arrest (Kang et al. 2015).

However, in a recent study by Papadopuolos *et al.* 2015, renal cancer Caki-1 cells were treated with 2 µM of Sunitinib and the expression of the miR-15a/16 cluster was quantified. After 36 and 48 h of Sunitinib treatment the Caki-1 cells showed an increase in miR-15a expression and after 24 and 48 h a decrease in miR-16 expression was observed when compared to Caki-1 cell not treated with Sunitinib (time point 0 h) (Papadopoulos, Yousef and Scorilas 2015). In our study exposing HL60 cells to 7 µM of Sunitinib for 24 hours we observe a tendency for an increase in miR-16-1 expression, but no significant change was identified in miR-15a expression. This could suggest that Sunitinib could increase cellular apoptosis by increasing the expression of miR-16-1, though further investigation is still required to determine whether Sunitinib induces apoptosis in HL60 cells.

The role of miR-15a and miR-16-1 in HL60 cells during IB-MECA treatment seems complex as the miR-15a expression is decreased while the miR-16-1 is increased when compared to Control. In the perfused heart tissue both miR-15a and miR-16-1 levels increase with Sunitinib and IB-MECA co-treatment compared to Sunitinib alone, indicating a potential role for miR-15a and miR-16-1 in Sunitinib-induced injured cardiac tissue. Hullinger et al. 2012 previously demonstrated that miR-15 is linked to cardioprotection (Hullinger et al. 2012).

Interestingly, von Brendenstein et al. found the expression of miR-15a to be inversely linked with PKCα, as PKCα translocates to the nucleus in malignant renal tumours and binds the pri-miRNA-15a directly and thereby supress the expression of miR-15a (von Brandenstein et al. 2012). Therefore, an increase in p-PKCα should result in a decrease in miR-15a levels. However, the present study did not fully demonstrate this. In HL60 cells, there was a significant increase in p-PKCα levels in cells treated with Sunitinib, the co-treatment of Sunitinib with IB-MECA and IB-MECA alone. However, in HL60 cells there was a tendency for an increase in miR-15a expression levels with Sunitinib and the co-treatment of Sunitinib with IB-MECA. Interestingly, IB-MECA treatment on HL60 cells did produce reduced the level of miR-15a expression. This suggests that IB-MECA (concentration of 1 nM) could enhance HL60 cell proliferation at a through the suppression of miR-15a. However, phosphorylation levels of PKCα, a tumour suppressor were significantly increased after IB-MECA treatment. This suggests that in HL60 cells there is not an inverse relationship between PKCα and miR-15a. However, it would be interesting to investigate this in a renal cell carcinoma line.

Plus, in perfused heart tissue, a similar pattern to von Brendenstein et al. was found when hearts were treated with Sunitinib alone and IB-MECA alone, in both cases p-PKCα levels were increased and miR-15a levels had a tendency for a reduction. However, administration

of Sunitinib in co-treatment with IB-MECA did not follow this pattern as both p-PKCα and miR-15a levels were significantly increased. As previously hypothesised, perhaps the combination of Sunitinib and IB-MECA produces miRNA detection false positives in heart tissue or potentially there could be dysfunctional miRNA regulation occurring.

5.5.7.2 miR-155

The oncogene miR-155 was the first miRNA transcript shown to possess tumour-promoting activity (Eis et al. 2005) and miR-155 has been linked to diverse tumour types including B-cell lymphoma, and breast, lung and pancreatic adenocarcinoma (Eis et al. 2005, Iorio et al. 2005, Lee et al. 2007, Yanaihara et al. 2006). A case study by Merhautova *et al*. 2015 found that expression levels of miR-155 was decreased and linked to Sunitinib resistance development in metastatic renal cell carcinoma (Merhautova et al. 2015). In our study, there was a tendency for an increase in miR-155 expression in HL60 cells with all of the drug treatment groups, compared to Control. However, only IB-MECA alone treatment produced a significant increase. This could suggest that IB-MECA reduces Sunitinib resistance.

Furthermore, Kluiver *et al.* 2006, found the expression of mature miR-155 from primary miR-155 (pri-miR-155) in both Hodgkin's lymphoma cell lines and normal lymphoid tonsillar B cells was strongly linked to activation by PKC (Kluiver et al. 2006). pri-miR-155 possesses oncogenic abilities in lymphoma and leukaemia by associating with the oncogene c myc (Tam et al. 2002). In the present study, IB-MECA increased phosphorylation levels of PKCα and also increased miR-155 levels. This and the pattern identified between p-PKCα and miR-15a could suggest that IB-MECA (1 nM) treatment may enhance HL60 cell proliferation and that PKCα may not be involved in HL60 cell death, as IB-MECA did not reduce cell viability at a concentration of 1 nM. It is possible that complex signalling in HL60 cells results in a

reduction in cell viability in response to Sunitinib alone and Sunitinib in co-treatment with IB-MECA.

Furthermore, in perfused heart tissue treated with Sunitinib and IB-MECA increased expression of miR-155 when compared to Sunitinib treatment alone. The miR-155 has been shown to have a key role in cardiac hypertrophy (Sayed et al. 2007, Seok et al. 2014). Most research investigating miR-155 in relation to cardiac injury suggests that circulating levels are increased in response to myocardial infarction (Corsten et al. 2012, Matsumoto et al. 2012). Contrastingly, we show a tendency for a decrease in miR-155 in response to Sunitinib treatment. Plus, this study shows an increase in miR-155 levels in response to the co-treatment of Sunitinib with IB-MECA. This increase in miR-155 suggests that the combination therapy causes some level of cardiac damage, which was established through infarct size assessment and a decline in HR. However, miR-155 levels were reduced in hearts treated with Sunitinib alone. This could suggest that miR-155 is not involved in Sunitinib induced cardiotoxicity. This study highlights that miRNA signalling is very complex and many factors contribute changes miRNA in profiles. More in-depth investigation is required to generate a succinct conclusion.

5.6 Conclusion

As hypothesised this study reveals that A3AR activation improves myocardial survival by attenuating Sunitinib-induced myocardial injury without interfering with the anti-tumour efficacy of Sunitinib. Investigating the specific A3AR associated signalling pathways and miRNAs involved in Sunitinib-induced cardiotoxicity, as well as further investigating PKC and the MKK7 pathway signalling, could be important in the development of adjunctive cardioprotective chemotherapy treatment.

6. General Discussion

6.1 Summary of thesis findings

This thesis identified the level of Sunitinib-induced cardiotoxicity in 3 month, 12 month and 24 month Sprague-Dawely rat hearts, using the *ex vivo* Langendorff heart technique. Then, investigated the involvement of cardiac injury specific miRNAs and the stress-signalling protein MKK7 in Sunitinib-induced cardiotoxicity. Following this, the cardioprotective properties of the adjunct agents: NQDI-1 and IB-MECA were assessed. The effect NQDI-1 and IB-MECA exerted on these cardiac injury specific miRNAs and proteins of the MKK7 pathway were then measured. Next, the anti-cancer properties of Sunitinib in co-treatment with the adjunct therapies was measured by MTT assay and cancer specific miRNA expression levels in HL60 cells. Following this, the involvement of the signalling protein PKCα was investigated after treatment with Sunitinib in the presence or absence of the adjunct therapies, in both left ventricular tissue and HL60 cells.

Overall, the results from this thesis indicated that Sunitinib treatment causes adverse effects on the haemodynamic properties and the tissue of the heart. This was demonstrated by the *ex vivo* Langendorff perfused heart model. In Langendorff perfused, 3, 12 and 24 month old Sprague-Dawely rat hearts, Sunitinib induced significant declines in LVDP and increased infarct size, after 125 minute perfusion with 1 μM Sunitinib compared to control hearts of the same age group. The 3 and 12 month group also produced significant declines in HR during Sunitinib treatment. The cardiotoxic effects of Sunitinib detected in this thesis were expected as Sunitinib is known to cause adverse cardiovascular events. It has been postulated that Sunitinib produces adverse cardiovascular events through both on-target

inhibition of VEGF, PDGFR, c-KIT and FLT-3; and also off-target inhibition of various other kinases essential in the maintenance of cardiac function (Force and Kolaja 2011, Telli et al. 2008).

Previously, the level of cellular dysfunction induced by Sunitinib was demonstrated by Cohen et al. in human stem cell derived cardiomyocytes (Cohen et al. 2011). Cohen et al. (2011) found Sunitinib-induced cardiotoxic responses such as cellular ATP depletion, release of lactate dehydrogenase and induction of apoptosis in a dose-dependent manner. In addition to this, Rainer et al. (2012) showed that Sunitinib decreased sarcomere shortening, intracellular Ca^{2+} levels and an increase in ROS generation in isolated human myocardium (Rainer et al. 2012). As well as this, concentrations of 1 and 10 μg/ml Sunitinib produced significant decreases in developed force in isolated human myocardium after 30 minutes of treatment (Rainer et al. 2012). This implies that decreases in myocardium contraction developed force could be linked to the clinical cases of Sunitinib-induced impairment of left ventricular function (Chu et al. 2007).

These studies are in accordance with the data established in this thesis, as we have demonstrated Sunitinib-induced increases in infarct size and declines in LVDP, which could have resulted from the suggested increased levels of ROS and apoptosis by Cohen and Rainer et al. ROS has previously been shown to induce apoptosis (Simon, Haj-Yehia and Levi-Schaffer 2000), however, interestingly, ROS has also been implicated in the impairment of cardiac contractile function by altering Ca^{2+} cycling (Katori et al. 2006). Perhaps, Sunitinib induced ROS generation could have been responsible for the declines in LVDP identified in this thesis. Future studies should investigate this by the use of a ROS detection kit such as the CellROX kit by ThermoFisher, which uses cell-permeant reagents which when oxidised

by ROS produce a colour (either deep red, orange or green depending on the kit purchased) which can be detected by a plate reader. This would identify the level of ROS generated by Sunitinib treatment in cardiomyocytes.

Overall, the 24 month group produced the largest reduction in LVDP levels in response to Sunitinib treatment. This was an expected outcome as declines in myocardial function are associated with ageing (Linton et al. 2015). The heart has a high-energy demand and through ageing essential cellular processes including autophagy become dysfunctional (Peart et al. 2014). This leads to an accumulation of impaired cellular machinery, such as mitochondria. The loss of functioning mitochondria reduces the level of ATP available for cardiomyocytes and reduces heart function, both of which have been linked to age associated heart failure (Moyzis, Sadoshima and Gustafsson 2015). It is likely that Sunitinib caused a further depletion in ATP levels in aged hearts through the inhibition of AMPK which lead to a decline in left ventricular function (Force, Krause and Van Etten 2007). Younger hearts have more efficient autophagy mechanisms and cell death pathways, which prevent the accumulation of dysfunctional mitochondrial and protein signalling (Zhao et al. 2010). Therefore, data from this thesis could be a result of the aged rat heart experiencing enhanced levels of dysfunctional cell death pathways. This may have reduced the level of stress induced apoptosis and therefore produced the smallest level of infarction of all the age groups tested. Investigations which determine Sunitinib-induced changes in cell death pathway, autophagy and mitochondria function, in models of ageing are required to confirm this. Future studies should consider using an apoptosis/ necrosis detection assay, such as terminal deoxynucleotidyl transferase dUTP nick end labelling (TUNEL), which labels double-strand DNA breaks generated during apoptosis (Loo et al. 2011). There are also

commercially available kits used for the detection of autophagy, for example, an autophagy detection kit by Abcam labels autophagic vacuoles with a fluorescent dye.

Another explanation could be that aged animals have a reduced healing ability, due to lower levels of myofibroblasts in their heart tissue compared to younger animals. This reduction in myofibroblasts reduces the ability of the heart to form collagen-based scaring or fibrosis, response to ischaemia-reperfusion injury, which resulted in a smaller infarct size compared to younger animals (Bujak et al. 2008). However, with this reduced level of infarct the older animals still developed more sever cardiac complications that their younger counterparts. This was thought to be due to lack of tensile strength where tissue injury had occurred, compared to younger animals (Bujak et al. 2008).

In addition, significant declines in HR were found in the 3 month and the 12 month groups during Sunitinib treatment compared to their control groups. This was expected as Henderson et al. (2013) showed a dose-dependent decline in HR (Henderson et al. 2013). Plus, several studies have reported the inhibitory effect of Sunitinib on hERG ion channels (Cohen et al. 2011, Doherty et al. 2013). Inhibition of hERG has been implicated in long QT syndrome in patients and bradycardia (Gintant 2011). In addition, Cohen et al. (2011) also found a reduction in cardiomyocyte beat rate followed by the prolongation of field-potential duration at concentrations as low as 1 μM Sunitinib. This reduction in beat rate and field-potential duration was believed to resemble QT-prolongation, which is a known clinical cardiotoxic response to Sunitinib in patients (Shah, Morganroth and Shah 2013), (Bello et al. 2009). Cohen et al. (2011) demonstrated that this prolongation of field-potential could have occurred due to reductions in Na^+ and Ca^{2+} cycling and the inhibition of hERG voltage-gated ion channel (Cohen et al. 2011). Also, as previously mentioned, at a cellular level, Sunitinib

has been shown to block the cardiac hERG channel which is associated with long QT syndrome (Doherty et al. 2013). Therefore, the decline in HR associated with the Sunitinib treatment of 3 and 12 month rat hearts was an expected result.

However, in this thesis, Sunitinib treatment did not induce a decline in HR in the 24 month group. This could be due the 24 month group having a much lower heart rate at baseline than in the control hearts, as shown in chapter 3. Commonly, ageing of the heart has been associated with an accumulation of compensatory cardiomyocyte remodelling in the heart. Over time, the heart enlarges in response to increase in haemodynamic load, neuro-hormonal and pro-hypertrophic signalling (Gosse 2005). Remodelling fundamentally begins with molecular changes, such as altered cell growth regulation and protein expression. This results in impairment of myocardial performance and causes a lower heart rate (Lupón et al. 2015). Therefore, Sunitinib treatment may not have affected HR because the HR was already low at baseline. In addition, as n=3 for the control 24 month group, there may have been a high amount of variation in the HR data. Therefore, it would be important to repeat this experiment, increase the n-number and investigate whether HR is altered in response to Sunitinib treatment in aged animals, when there is a lower level of variation.

However, there were no significant differences in CF compared to control in any of the age groups. Interestingly, previous studies, such as Henderson et al. (2013) demonstrated a dose-dependent declines in CF in response to Sunitinib perfusion under ischaemic conditions (Henderson et al. 2013). Perhaps, if ischaemic conditions were used in the future our data would better reflect that of published data.

TTC staining revealed that 3 month rat hearts were more susceptible to tissue infarction following Sunitinib treatment. The 12 month group and the 24 month group also produced a

significant increase in infarct size, however, their infarct sizes were significantly lower than the 3 month group's. This could have occurred due to higher levels of reversible myocardial damage found in the 3 month and 12 month group by TTC staining. Younger tissue has been shown to be vulnerable to Sunitinib induced toxicity (Oeffinger et al. 2006). However, these effects were shown to diminish over time (Dubois et al. 2011). It has been suggested that younger animals have the ability to tolerate significantly larger infarct sizes without producing left ventricular dysfunction and other symptoms of coronary heart failure compared to aged animals (Gould et al. 2002).

In addition, the 24 month age group produced a significantly smaller infarct size compared to the 12 month group. As previously mentioned, this could be due to a lack of functioning cell death pathways. Future studies should consider using an apoptosis/ necrosis detection assay or an autophagy detection such as those previously mentioned (Barth et al. 2010, Krysko et al. 2008).

In addition to identifying changes in the haemodynamic properties of the heart during and after Sunitinib treatment, real-time PCR was used to quantify the expression patterns of miRNAs associated with myocardial injury (miR-1, miR-27a, miR-133a and miR-133b) in response to Sunitinib Langendorff perfusion. A significant decrease in miR-27a, but significant increases in miR-133a and miR-133b were found in 3 month old animals treated with Sunitinib compared to control. In contrast to our study, Rainer et al. (2012) carried out microarray analysis of miRNAs associated with cardiac damage from HL-1 cells (a mouse cardiac muscle cell line) (Rainer et al. 2012). During this study, Rainer et al. investigated both miR-1 and miR-133b and many other miRNAs which were not assessed in this thesis. They did not find any changes in miRNA expression levels in response to Sunitinib (0.1 and 1 μM)

treatment. We identified that the expression pattern of miR-1 was not altered by Sunitinib treatment in any age group tested, which is in accordance with the findings of Rainer et al. However, we did find miR-133b levels to change in response to Sunitinib treatment. To our knowledge no other group has investigated cardiac injury specific miRNA in response to Sunitinib treatment. Therefore, only limited comparisons can be made. Our findings suggest that changes to the level of cardiac specific miRNAs miR-27, miR-133a and miR-133b could indicate Sunitinib-induced cardiotoxicity.

Interestingly, data from this thesis found that miR-133a and miR-133b expression pattern varies in the respective age groups. Other studies have shown changes in miRNA expression patterns to be associated with ageing (Chen et al. 2010). This highlights the different mechanisms which occur in the heart of rats at different ages. This suggests that age could affect how the heart responds to Sunitinib treatment. However, a more detailed investigation into miRNA expression patterns, perhaps considering additional miRNAs associated with cardiac injury, such as those listed by Chen et al. 2017 (Chen et al. 2017). It would also be interesting to investigate the targets of the miRNAs to test if the miRNA levels correlate with the regulation of target proteins in response to Sunitinib treatment.

Moreover, this study identified changes in MKK7 mRNA and protein phosphorylation levels in response to Sunitinib perfusion. MKK7 is a stress signalling molecule which is responsible for the regulation of a variety of vital cellular processes (Wada et al. 2004). The 3 month group showed a decrease in both MKK7 mRNA and p-MKK7 levels compared to control. Liu et al. increased the susceptibility of mice to heart failure by knocking out the MKK7 gene specifically in the heart (Liu et al. 2011). The inhibitory effect of Sunitinib on MKK7 in 3 month rats may have been responsible for the increased level of infarct size demonstrated

by TTC staining compared to the older groups assessed. However, further investigation is required to identify whether MKK7 directly effects tissue necrosis. Studies using siRNA which target MKK7 and over expression of MKK7 in cardiomyocytes treated with Sunitinib should provide an insight into this.

The 12 month group treated with Sunitinib did not have an altered level of MKK7 mRNA. However, p-MKK7 levels were significantly increased compared to control. Increased levels of activated MKK7 have been previously shown to increase levels of cellular apoptosis and produce characteristic phenotypes of cardiac hypertrophy and cardiomyopathy (Mitchell et al. 2006, Wang et al. 1998). This increase in p-MKK7 could be responsible for the increased level of cardiac dysfunction identified by decreases in LVDP and HR and the significant increase in infarct size compared to control.

The 24 month group treated with Sunitinib showed an increase in MKK7 mRNA but a significant decrease in p-MKK7 levels compared to control. An increase in MKK7 mRNA suggests an increase in total MKK7 protein levels. However, we did not see a difference in total MKK7 levels between the age groups. This could suggest degradation of MKK7 protein is occurring due to dysfunctional protein degradation in the aged hearts, as MKK7 mRNA levels were altered. Dysfunctional protein regulation and signalling is associated with ageing (Martinez-Vicente, Sovak and Cuervo 2005). It is possible that dysfunctional protein regulation could have resulted in cardiac remodelling which gave the lower baseline HR in the 24 month group. Sunitinib treatment may have caused myocardial damage and a reduction in LVDP to the 24 month rat hearts because of the reduction in p-MKK7. However, this does not explain why the 24 month group had a smaller infarct size. Perhaps other signalling pathways are involved in Sunitinib-induced cardiotoxicity in ageing models.

Further studies into cellular signalling and Sunitinib-induced cell death, such as those previously described are required to fully characterise the differences in cardiotoxicity identified in this study.

In summary, the first results chapter of this thesis (chapter 3) has shown that Sunitinib at a concentration of 1µM produces significant cardiotoxic responses in the isolated rat heart Langendorff perfusion model and by changes in cardiac injury specific miRNAs.

Chapter 3 also demonstrated the involvement of MKK7 in Sunitinib-induced cardiotoxicity. Therefore, potential cardioprotective adjunct therapies, as well as, intracellular proteins and cardiac injury specific miRNAs were subsequently investigated.

Small molecule inhibitors of MKK7 are not commercially available. Therefore, for the first investigation into adjunct therapy we used an ASK1 inhibitor, NQDI-1 (Chapter 4). ASK1 is an upstream regulator of MKK7. This project demonstrated that NQDI-1 reduced the level of infarct generated by Sunitinib. However, the reduction in the haemodynamic properties of the heart induced by Sunitinib were not attenuated. In previous studies, NQDI-1 has been shown to attenuate ischaemic injury in kidneys and the brain (Eter 2013, Hao et al. 2016). However, the exact mechanism of protection has not been established and NQDI-1 has not been previously studied in the heart. Previous studies, have however, investigated the level of cardioprotection generated through inhibition of ASK1. It has been found that inhibition of ASK1 or the deletion of the ASK1 gene reduces levels of apoptosis and non-apoptotic cardiomyocyte cell death (Liu et al. 2009, Liu and Min 2002, Watanabe et al. 2005). Therefore, the attenuation of Sunitinib-induced heart tissue infarction by NQDI-1 could be due to inhibition of ASK1 mediated cell death. However, to confirm this, further investigation into the cellular mechanisms responsible for the cardioprotection exhibited by

NQDI-1 is required. Future studies should consider investigating other ASK1 inhibitors (Fujisawa 2017) along-side apoptosis detection assays to identify whether this is an effective method for cardioprotection against Sunitinib-induced cardiotoxicity (Krysko et al. 2008).

In addition, the pharmacodynamic properties of NQDI-1 have not previously been investigated. Future investigation into the effect of NQDI-1 on cardiomyocyte repolarisation and its effect on ion channels are required to determine if NQDI-1 has a direct impact on cardiac functions such as HR and LVDP. The use of a variety of concentrations of NQDI-1 should also be investigated, as lower concentrations of NQDI-1 may provide a more satisfactory level of cardioprotection.

Unexpectedly, NQDI-1 treatment increased levels of MKK7 mRNA levels, phosphorylation levels of: MKK7, ASK1 and JNK, when co-administered with Sunitinib. This suggests that the combination of Sunitinib and NQDI-1 has an unknown effect on the MKK7 pathway at a transcriptional, translational and post-translational level. It could be possible that the two drugs interact with each other, and prevent the inhibition MKK7 transcription and the proteins of the MKK7 pathway. As previous studies have not investigated the effect of NQDI-1 on MKK7 and cardioprotection, further investigation is necessary.

To obtain a greater understanding of the involvement of the MKK7 pathway in Sunitinib induced cardiotoxicity, a variety of agonists and antagonists of the MKK7 pathway should be used in future work.

Due to the limitations of NQDI-1 as a cardioprotective agent identified in this thesis, such as NQDI-1 was unable to attenuate Sunitinib-induced LVDP decline; a second cardioprotective agent was investigated. IB-MECA had previously been shown to alleviate the adverse

cardiovascular effects of Doxorubicin (Emanuelov et al. 2010). Therefore IB-MECA was chosen to determine whether Sunitinib-induced cardiotoxicity could be attenuated (chapter 5). Data from this thesis revealed that IB-MECA successfully reduced infarct size, attenuated the reduction in LVDP and HR. Altered: the expression profiles of miRNAs associated with cardiotoxicity, as well as the phosphorylation levels of MKK7, JNK and PKCα. Phosphorylation of MKK7, JNK and PKCα were returned to levels similar to control hearts. As mentioned in chapter 1, Sunitinib has an inhibitory effect on MAPK signalling pathways (Faivre et al. 2007). This was confirmed when the phosphorylation levels of the proteins of the MKK7 pathway were significantly reduced in response to Sunitinib treatment, which suggests that Sunitinib inhibits this pathway. However, biochemical investigations into protein-protein interactions and drug binding are required to determine whether Sunitinib directly interacts with the proteins of the MKK7/JNK/ASK1 pathway.

Interestingly, adenosine receptors also have the ability to initiate the regulation of MAPK and PKC signalling pathways. The use of an A3 adenosine receptor agonist has been previously shown to regulate these pathways (Borea et al. 2015). The cardioprotective effect of IB-MECA could have been generated through the initiation of MAPK and PKC signalling regulation, returning the protein phosphorylation levels back to control levels. However, the results in this thesis do not provide a clear explanation as to why cardioprotection occurs. Investigations into apoptosis, ROS generation and pathways involved in cardiac hypertrophy and cardiac injury should be considered in future work to identify the exact mechanism of cardioprotection by IB-MECA (Seddon et al. 2007).

PKCα involvement in response to stresses in the heart is more established than the MKK7 pathway. Previous studies identified that an increase in PKCα phosphorylation indicated

cellular stresses which may lead to apoptosis (Braz et al. 2004), data from this thesis confirms this. PKCα phosphorylation levels were increased by Sunitinib treatment. However, numerous isozymes of PKC have also been shown to be involved in cardiac function (Budas, Churchill and Mochly-Rosen 2007). Further studies into other PKC isozymes and the level of apoptosis generated by Sunitinib should be investigated.

Furthermore, data in this thesis revealed that expression levels of miRNA involved in myocardial injury and cancer changed in response to Sunitinib, NQDI-1 and IB-MECA treatment. However, the miRNA expression patterns did not clearly identify the role of these miRNAs in Sunitinib induced cardiotoxicity, plus the role of miRNA levels during cardioprotection by NQDI-1 and IB-MECA is unclear. An explanation for this could be that each of the miRNAs investigated have many targets (Thum et al. 2007). Therefore, it is difficult to determine which miRNA-mRNA interactions occur during the myocardial injury generated by Sunitinib and the cardioprotection by NQDI-1 and IB-MECA. Future work, should investigate a larger panel of miRNAs and use methods of miRNA inhibition or activation to act as positive and negative controls. This would provide a clearer indication of miRNAs which could act as predictors on Sunitinib induced cardiotoxicity.

In addition, this thesis investigated the anti-cancer properties of Sunitinib and the named adjunct therapies by assessing the cell viability of a cancer cell line (HL60 cell). The MTT assay demonstrated that Sunitinib has a negative effect on the cell viability the HL60 cancer cell line. As Sunitinib is an anti-cancer therapy, this result was expected. Sunitinib has previously been shown to induce G1 cell cycle arrest and apoptosis in acute myeloid leukaemia using the trypan blue staining method to identify viable cells (Teng et al. 2013). Sunitinib induces leukaemia cell growth arrest and apoptosis through the inhibition of FLT3,

which is commonly over expressed in cases of acute myelogenous leukaemia (Nishioka et al. 2009).

ASK1 inhibitor, NQDI-1 decreased the level of viable cells compared to control at high concentrations. ASK1 has previously been shown to have oncogenic properties (Luo et al. 2016). Inhibition of ASK1 by high concentrations of NQDI-1 may have resulted in the reduction in cell viability detected compared to control.

NQDI-1 also decreased the number of viable cells when co-treated with Sunitinib, compared to Sunitinib alone. The combination of NQDI-1 enhanced the anti-cancer properties of Sunitinib in HL60 cells. This could be through the inhibition of oncogenic ASK1 (Luo et al. 2016). Luo et al. (2016) demonstrated that ASK1 is over expressed in pancreatic cancer cells and ASK1 promotes proliferation and stimulates tumorigenic capacity. However, many studies have concluded that activation of ASK1 is required to induce cancer cell apoptosis (Park et al. 2016, Zhang et al. 2016). Findings in this thesis confirm that inhibition of ASK1 enhances Sunitinib-induced reductions in HL60 cell viability. However, due to the controversial findings in the literature, further investigation is required to determine the exact mechanism which caused NQDI-1 to increase Sunitinib's anti-cancer properties and to identify whether these enhanced anti-cancer properties would occur in patients treated with Sunitinib.

Similarly, IB-MECA decreased the number of viable cells compared to control. This was an expected result as A3AR agonists have been previously shown to induce apoptosis in HL60 cells (Kohno et al. 1996). However, the exact mechanism of IB-MECAs ability to reduce HL60 cell viability needs to be further investigated. In co-treatment with Sunitinib, IB-MECA did

not increase the number of viable cells, compared to Sunitinib alone. Therefore, IB-MECA did not enhance or diminish Sunitinib's anti-cancer properties.

The MTT assay involves the reduction of tetrazolium into formazan by dehydrogenases which occur in mitochondria. This suggests that the MTT assay is measuring mitochondrial activity. Therefore, the MTT assay reflects the metabolic activity of living cells (Gerlier and Thomasset 1986). There is a potential for negative data as viable cells can have low metabolic rates. Therefore, to accurately assess cell viability, a more appropriate technique for measuring cell viability, such as trypan blue staining, which only stains the cells with damaged cell membranes and are therefore not viable. Therefore, additional studies which investigate apoptosis and necrosis should be carried out to confirm our data.

Finally, this thesis investigated the effect of Sunitinib treatment on the expression patterns of miRNAs associated with cancer (miR-15a, miR-16-1 and miR-155) in both cancer cells and cardiac tissue. The same miRNAs responded differently to Sunitinib ± IB-MECA and IB-MECA alone in the HL60 cancer cell line and rat left ventricular cardiac tissue. IB-MECA alone demonstrated cancer properties through the altering of miRNA profiles. For example, the increase in miR-155 is related to tumour promoting pathways (Eis et al. 2005). However, IB-MECA treatment alone caused a significant decrease in HL60 cell viability. The investigation of miRNA associated with cancer demonstrate that the anti-cancer properties of Sunitinib and IB-MECA alone are unclear. Future studies should clarify this by the use of specific miRNA inhibitors, siRNAs and models of miRNA overexpression.

6.2 Study limitations and future prospects

6.2.1 The use of Sprague-Dawley rats as models of ageing

The rodents used in this thesis did not suffer from comorbidities such as diabetes or hypertension and are therefore less likely to develop cardiovascular events compared to elderly human patients (Dai and Rabinovitch 2009). A more accurate model of ageing, such as a model with a comorbidity common in humans is required to properly reflect the toxicity of Sunitinib in elderly patients. Though, this study highlights through successful ageing, the small population who surpass the standard life expectancy, without comorbitities, could have a lower incidence of cardiotoxicity than younger patients (Capitanio et al. 2016).

6.2.2 Sunitinib induced cardiotoxicity and adjunct therapy

Sunitinib does cause cardiotoxicity, however, further investigation is required to establish the exact mechanism of Sunitinib induced cardiotoxicity and the cardioprotective action of NQDI-1 and IB-MECA. The current study observed a significant reduction in the haemodynamic function of the heart following Sunitinib administration. This study is very limited as it only demonstrates that decline in haemodynamic function could be due to the loss of functional cardiomyocytes, as demonstrated by TTC staining. This is very simplistic, as there are many contributing factors which may have resulted in a Sunitinib-induced reduction in HR and LVDP. Therefore, investigation into Sunitinib's ability to inhibit ion channels such as hERG, calcium signalling and ATP regulation within cardiomyocytes, is required to identify if Sunitinib has a direct effect on heart contraction and therefore HR and LVPD.

Also, in the three age groups assessed, differing levels of Sunitinib-induced cardiotoxicity were experienced. It is important to investigate this further to identify whether ageing can elicit a protective response in the heart by measuring changes to cell survival mechanisms over time in an aging model.

Additionally, this research demonstrated that Sunitinib does not alter CF. However, Sunitinib has been shown to induce vasoconstriction which in the clinic can lead to hypertension (Kappers et al. 2012). This highlights that a further parameter is required to measure the effect of Sunitinib on the vasculature of the heart. The use of technology such as video capillary microscopy with frame-to-frame analysis or laser Doppler anemometry could be used to identify changes in flow velocity of coronary flow. This would give a more refined technique to determine the effect of Sunitinib on CF and predict hypertension of the heart.

Moreover, only one concentration of Sunitinib and of each of adjunct therapies investigated was used in the Langendorff study. The reason for this was to reduce the number of animals used for this project. According to the National Centre for the Replacement, Refinement and Reduction of Animals in research (NC3Rs) if animal experimentation data is publicly available, an experiment should not be repeated. Therefore, after a review of existing literature, 1 µM of Sunitinib, 2.5 µM of NQDI-1 and 1nM of IB-MECA was used (Volynets et al. 2011, Henderson et al. 2013, Maddock, Mocanu and Yellon 2002, Doherty et al. 2013). However, this is a limitation as a dose response of each compound would have produced a suitable IC_{50} value, giving an optimal concentration of each drug. To limit the number of animals used for a dose response, assessment of cardiomyocyte viability could be used in the future to establish ideal drug concentrations for both measurement of cardiotoxicity and cardioprotection of Sunitinib and adjunct therapies.

6.2.3 Using the Langendorff system

The use of an acute Langendorff perfusion experiment allows an indication to the potential adverse cardiovascular side effects of Sunitinib and whether adjunct therapies could reduce cardiotoxic effects (Guo, Dong and Guthrie 2009).

However, as the Langendorff uses an isolated heart, it is difficult to predict if the same response would be found *in vivo* or in the clinic (Bell, Mocanu and Yellon 2011). Denervation and the absence of peripheral factors, such as hormones, reduces the ability for this technique to mimic physiological conditions *in vivo*. This could be compensated for by the addition of neurotransmitters and other factors, in a controlled manor to the perfusion buffer.

In physiological conditions, the blood is in a constant state of homeostasis in regard to oxygen and nutrient contents. The oxygen supply is closely monitored by chemoreceptors located on the carotid body (Prabhakar and Semenza 2015). Detection of changes in oxygen levels results in the induction of neuronal transduction signals which regulate breathing. However, the Langendorff is unable to simulate this response. It is therefore important to use Langendorff experiments to initially predict cardiotoxicity. *In vivo* models should be used to give a more physiologically relevant model of Sunitinib induced cardiotoxicity. However, the Krebs-Henseleit buffer (KHB) used for Langendorff isolated heart perfusion has a low oxygen carrying capacity. A PO_2 of >500mmhg is required to adequately oxygenate the heart. In this project the O_2 levels were not monitored, but the solution was continuously gassed. Closer monitoring of O_2 levels could help reduce variation between Langendorff experiments and also represent physiological conditions more accurately.

Also, the KHB has low oncotic pressure as it does not contain proteins which mimic plasma proteins. It has been shown that low oncogenic pressure and oxygen-carrying capacity of KHB results in high CF levels, which severely limits the coronary reserve. This means CF values from Langendorff experiments do not reflect normal physiological CF rates.

The metabolism of the heart is also altered by the use of KHB. KHB uses glucose as its main metabolic substrate, whereas the heart uses mostly fatty acids for oxidative metabolism. Addition of fatty acids and proteins such as albumin to the perfusate buffer would allow the buffer to better represent physiological conditions. As a result of KHB variation from blood plasma, myocardial function reduces by approximately 10 % per hour (Bell, Mocanu and Yellon 2011).

In addition to this, the experiments using the Langendorff technique in this thesis were found to produce infarction (<10 %). This is a limitation of the Langendorff technique as healthy control subjects receiving a placebo in the clinic or *in vivo,* would not produce cardiac damage. The main reported causes of cardiac ischaemia or infarction in control hearts during the Langendorff isolated heart assay are warm ischaemia or exposure to air during the dissection and isolation process (Olejnickova et al. 2015). The animal has ceased breathing during the dissection process and as the heart utilises oxygen at a rapid rate, hypoxia can occur in its tissue. To reduce this the heart was submerged in ice cold KHB, which reduces the rate of respiration in the heart (Bell, Mocanu and Yellon 2011). However, a small level of ischaemia is inevitable. The heart is also vulnerable to contusion injuries during the dissection and cannulation stages of the assay, which have the potential to result in infarction.

As well as this, the use of the crystalloid KHB increases the likelihood of hypoxia during perfusion. Schenkman et al. 1999 reported that the use of KHB can reduce arterial PO_2 levels from 600 to 100 mmHg, which resulted in declines in LVDP and also myoglobin O_2 saturation (Schenkman et al. 1999). In addition, it has been shown that while bubbling KHB with 95% O_2 and 5% CO_2 produces an initial PO_2 of >450 mmHg, this is not sustainable as KHB has a very low oxygen-carrying capacity (Schenkman et al. 2003). This was shown to result in heart O_2 saturation levels of lower than 72 %, where in physiological conditions this is approximately 90% (Schenkman et al. 2003). The lack of KHB's O_2-carrying ability has the potential to induce hypoxic mechanisms within the heart which have been shown to result in tissue infarction during Langendorff perfusion (Zhao et al. 2010).

Furthermore, this project only investigated the acute dosing of Sunitinib via a 125 minute Langendorff perfusion. In the clinic, Sunitinib can be administered for many weeks at a time. Using a longer Langendorff perfusion times for Sunitinib treatment would be more relevant as it would allow the cardiotoxic side effects to manifest over time.

It is important to note that the Langendorff isolated heart model is ideal for producing a preliminary prediction as to whether a compound may produce adverse cardiovascular effects at the preclinical stages of drug development. However, *In vivo* studies are required to give insight into the effect of whole body physiology. Also, animal studies are more relevant to clinical conditions as dosing can mimic that of the clinic. Therefore, it is important that *in vivo* studies are carried out in the future to determine the level of clinical relevance the data presented in this thesis possesses.

6.3 Concluding remarks

In conclusion, the results within this thesis have produced novel data, which identified that Sunitinib caused cardiotoxicity in all age groups. Also, the current data highlighted that cellular signalling mechanisms produced by Sunitinib-induced cardiotoxicity are very complex. Inhibition of the MKK7 pathway and activation of PKC could be involved in Sunitinib-induced cardiotoxicity. However, MKK7 signalling was altered by ageing. The use of miRNAs as markers for Sunitinib-induced cardiac injury and anti-cancer capabilities were inconclusive. However, both NQDI-1 and IB-MECA possess promising cardioprotective properties and did not diminish the anti-cancer properties of Sunitinib.

Importantly, the first results chapter of this thesis (chapter 3) has shown that Sunitinib at a concentration of 1µM produces significant cardiotoxic responses in the isolated rat heart Langendorff perfusion model and by changes in cardiac injury specific miRNAs. To our knowledge, no other study has compared the cardiotoxic effects of Sunitinib treatment in different age group. The majority of published clinical studies have investigated the occurrence of Sunitinib-induced cardiotoxicity in patients with an average age of above 54 years old (Chu et al. 2007, Khakoo et al. 2008, and Telli et al. 2008). In addition, other studies have solely concentrated on one age group. For example, DuBois et al. (2008) investigated the pharmacokinetic properties of Sunitinib in paediatric patients aged 10-20 years. This group found the pharmacokinetic properties of Sunitinib to be comparable to that of adults. However, DuBois et al. also found that 17% of the Sunitinib treated paediatric patients developed cardiotoxic effects and required treatment for cardiac symptoms (DuBois et al. 2008). Very few studies have investigated the cardiotoxic side effects Sunitinib produces, which could be due to only 1.5% of patients receiving Sunitinib treatment are

paediatric or young adults (Prakash et al. 2005). Perhaps the occurrence of juvenile Sunitinib-induced cardiotoxicity is under reported because of this. This thesis revealed for the first time that Sunitinib produces different cardiac responses in different age groups and cardiac injury specific miRNA expression patterns. This implies that patients of different age groups may benefit from the monitoring of different cardiac symptoms during Sunitinib chemotherapy and also different levels of cardioprotective adjunct therapy. It is therefore important that further research is conducted to investigate the cardiotoxic effect of Sunitinib treatment in patients of all ages, so that effective monitoring and cardioprotective treatment can be developed and eventually administered in the future.

Chapter 3 also demonstrated the involvement of MKK7 in Sunitinib-induced cardiotoxicity. Sunitinib produced an inhibitory effect on the p-MKK7 levels of the 3 month group. As a MKK7 is a stress signalling molecule, it is likely that inhibition of MKK7 by Sunitinib enhances the level of cardiomyocyte cell death. This could have resulted due to the additional cardiotoxic properties of Sunitinib, such as Sunitinib's ability to reduce cellular ATP levels and induce apoptosis (Cohen et al. 2011). Liu et al. (2011) demonstrated that deprivation of MKK7 in cardiomyocytes lead to heart failure following pressure over load (Liu et al. 2011). Perhaps, this could explain why the 3 month group produced the largest infarct size, as the 12 month and 24 month groups did not experience inhibition of MKK7. The involvement of MKK7 in Sunitinib-induced cardiotoxicity has not been previously investigated therefore, further studies which investigate the differences in MKK7 signalling between different age groups could be important for determining the exact mechanisms of Sunitinib-induced cardiotoxicity. It is likely, that much more complicated mechanisms occur during Sunitinib

treatment. It would therefore be interesting to investigate additional cellular signalling pathways.

Furthermore, this thesis revealed that the adjunct therapies NQDI-1 and IB-MECA both demonstrated a level of cardioprotection. NQDI-1 attenuated Sunitinib-induced infarction and IB-MECA attenuated both Sunitinib-induced infarction and declines in haemodynamic function. However, NQDI-1 did not attenuate Sunitinib-induced declines in haemodynamic function. As NQDI-1 is a relatively new compound, there are no published studies which investigate interactions with other proteins. It could be possible that NQDI-1 has off target interactions which may have resulted in the declines in LVDP and HR identified in this thesis. Perhaps other inhibitors of ASK1 would produce and more effective level of cardioprotection against Sunitinib-induced cardiotoxicity. Thioredoxin is a potent endogenous inhibitor of ASK1, perhaps the use of thioredoxin or its analogues could provide more effective cardioprotection and reduce the haemodynamic side effects of Sunitinib (Satoh et al. 2007). Interestingly, both NQDI-1 and IB-MECA were able to significantly reduce inhibition of MKK7 by Sunitinib. NQDI-1 was not expected to increase MKK7 levels as it is an inhibitor of the upstream regulator of MKK7, ASK1 (Volynets et al. 2011). In addition, both ASK1 and JNK phosphorylation levels are increased by co-treatment of NQDI-1 with Sunitinib. This could suggest that other pathways may activate MKK7 or it may support the idea that NQDI-1 has off-target effects. IB-MECA on the other hand was expected to increase MKK7 levels as A3 adenosine receptors have previously been shown to activate MAPK signalling pathways (Merighi et al. 2006). This thesis suggests that it could be possible, that both NQDI-1 and IB-MECA produced a cardioprotective effect by returning p-MKK7 levels back to control levels.

In addition, in this thesis PKCα was shown to be involved in both Sunitinib-induced cardiotoxicity and Sunitinib's ability to reduce cancer cell viability (Chapter 5). Levels of PKCα were significantly increased by Sunitinib treatment in both left ventricular tissue and HL60 cells. To our knowledge, the involvement of PKCα in Sunitinib-induced cardiotoxicity has not been investigated before. However, an increase in PKCα has been previously associated with heart failure (Braz et al. 2004). Therefore, this increase in p-PKCα by Sunitinib further implies that Sunitinib has the ability to cause adverse effects in the heart. Interestingly, co-treatment with the cardioprotective IB-MECA and Sunitinib returned increased p-PKCα levels back to control levels. This suggest that PKCα could be involved in IB-MECA's ability to provide cardioprotection. Investigations into inhibitors of PKCα could provide further evidence of PKCα's involvement in Sunitinib induce cardiotoxicity and IB-MECA's cardioprotection.

Furthermore, activation of PKC has been shown to produce apoptosis in HL60 cells (Bang, Park and Kang 2001). Therefore, Sunitinib may also produce anti-cancer effects through mechanisms involving PKCα.

Finally, the ability of Sunitinib to reduce HL60 cell viability was not inhibited by either NQDI-1 or IB-MECA. Maintaining anti-cancer properties is a desirable property of a cardioprotective adjunct therapy against Sunitinib-induced cardiotoxicity. This is because Sunitinib has the important role in treating many forms of cancer. A cardioprotective therapy which does not reduce Sunitinib's anti-cancer properties will allow Sunitinib to effectively treat cancer and protect the heart from Sunitinib-induced cardiac injury at the same time. It would therefore, be important to assess the effect of both NQDI-1 and IB-

MECA on Sunitinib's anti-cancer ability in other cell lines, such as a renal cell cancer cell line to establish whether NQDI-1 and IB-MECA's anti-cancer properties are universal.

In this thesis, IB-MECA has demonstrated a higher level of cardioprotection against Sunitinib-induced cardiotoxicity compared to NQDI-1. Therefore, IB-MECA has been shown to have potential to act as an adjunct therapy in the clinic. However, this would need to be confirmed with chronic *in vivo* studies. Additionally, investigations into Sunitinib and IB-MECA therapy should be further investigated in human tissue and cells to further strengthen the data presented in this thesis.

References

Abbracchio, M. P., Camurri, A., Ceruti, S., Cattabeni, F., Falzano, L., Giammarioli, A. M., Jacobson, K. A., Trincavelli, L., Martini, C., Malorni, W., and Fiorentini, C. (2001) 'The A3 Adenosine Receptor Induces Cytoskeleton Rearrangement in Human Astrocytoma Cells Via a Specific Action on Rho Proteins.' *Annals of the New York Academy of Sciences*, *939*(1), 63-73.

Abbracchio, M. P., Brambilla, R., Ceruti, S., Kim, H. O., von Lubitz, D. K., Jacobson, K. A., and Cattabeni, F. (1995) 'G Protein-Dependent Activation of Phospholipase C by Adenosine A3 Receptors in Rat Brain'. *Molecular Pharmacology* 48 (6), 1038-1045

Abedi, H., Aghaei, M., Panjehpour, M., and Hajiahmadi, S. (2014) 'Mitochondrial and Caspase Pathways are Involved in the Induction of Apoptosis by IB-MECA in Ovarian Cancer Cell Lines'. *Tumor Biology* 35 (11), 11027-11039

Aggarwal, S., Kamboj, J., and Arora, R. (2013) 'Chemotherapy-Related Cardiotoxicity'. *Therapeutic Advances in Cardiovascular Disease* 7 (2), 87-98

Ai, J., Zhang, R., Li, Y., Pu, J., Lu, Y., Jiao, J., Li, K., Yu, B., Li, Z., Wang, R., Wang, L., Li, Q., Wang, N., Shan, H., Li, Z., and Yang, B. (2010) 'Circulating microRNA-1 as a Potential Novel Biomarker for Acute Myocardial Infarction'. *Biochemical and Biophysical Research Communications* 391 (1), 73-77

Akat, K. M., Moore-McGriff, D., Morozov, P., Brown, M., Gogakos, T., Correa Da Rosa, J., Mihailovic, A., Sauer, M., Ji, R., Ramarathnam, A., Totary-Jain, H., Williams, Z., Tuschl, T., and Schulze, P. C. (2014) 'Comparative RNA-Sequencing Analysis of Myocardial and Circulating Small RNAs in Human Heart Failure and their Utility as Biomarkers'. *Proceedings of the National Academy of Sciences of the United States of America* 111 (30), 11151-11156

Anderson, P. G., Bishop, S. P., and Peterson, J. T. (2006) 'Chapter 26- Cardiovascular Research, in American College of Laboratory Animal Medicine' in The Laboratory Rat (Second Edition). Ed by Suckow, M. A., Weisbroth , S. H. and Franklin, C. L, Academic Press, Burlington, 773-802

Andreka, P., Zang, J., Dougherty, C., Slepak, T. I., Webster, K. A., and Bishopric, N. H. (2001) 'Cytoprotection by Jun Kinase during Nitric Oxide-Induced Cardiac Myocyte Apoptosis'. *Circulation Research* 88 (3), 305-312

Antal, C., Hudson, A., Kang, E., Zanca, C., Wirth, C., Stephenson, N., Trotter, E., Gallegos, L., Miller, C., Furnari, F., Hunter, T., Brognard, J., and Newton, A. (2015) 'Cancer-Associated Protein Kinase C Mutations Reveal Kinase's Role as Tumor Suppressor'. *Cell* 160 (3), 489-502

Aparicio-Gallego, G., Blanco, M., Figueroa, A., Garcia-Campelo, R., Valladares-Ayerbes, M., Grande-Pulido, E., and Anton-Aparicio, L. (2011) 'New Insights into Molecular Mechanisms of Sunitinib-Associated Side Effects'. *Molecular Cancer Therapeutics* 10 (12), 2215-2223

Arand, J. and Sage, J. (2017) 'G1 Cyclins Protect Pluripotency'. *Nature Cell Biology* 19 (3), 149-150

Ardehali, A. and Ports, T. A. (1990) 'Myocardial Oxygen Supply and Demand Cardiovascular' *Chest*, *98*(3), 699-705.

Ashour, A. E., Sayed-Ahmed, M. M., Abd-Allah, A. R., Korashy, H. M., Maayah, Z. H., Alkhalidi, H., Mubarak, M., and Alhaider, A. (2012) 'Metformin Rescues the Myocardium from Doxorubicin-Induced Energy Starvation and Mitochondrial Damage in Rats'. *Oxidative Medicine and Cellular Longevity* 2012

Atkinson, H. H., Rosano, C., Simonsick, E. M., Williamson, J. D., Davis, C., Ambrosius, W. T., Rapp, S. R., Cesari, M., Newman, A. B., Harris, T. B., Rubin, S. M., Yaffe, K., Satterfield, S., Kritchevsky, S. B., and Health ABC study (2007) 'Cognitive Function, Gait Speed Decline, and Comorbidities: The Health, Ageing and Body Composition Study'. *The Journals of Gerontology.Series A, Biological Sciences and Medical Sciences* 62 (8), 844-850

Atten, M. J., Godoy-Romero, E., Attar, B. M., Milson, T., Zopel, M., and Holian, O. (2005) 'Resveratrol Regulates Cellular PKC A and Δ to Inhibit Growth and Induce Apoptosis in Gastric Cancer Cells'. *Investigational New Drugs* 23 (2), 111-119

Auchampach, J. A., Rizvi, A., Qiu, Y., Tang, X., Maldonado, C., Teschner, S., and Bolli, R. (1997) 'Selective Activation of A3 Adenosine Receptors with N6-(3-Iodobenzyl)Adenosine-5'-N-Methyluronamide Protects Against Myocardial Stunning and Infarction without Hemodynamic Changes in Conscious Rabbits'. *Circulation Research* 80 (6), 800-809

Azizi, M., Chedid, A., and Oudard, S. (2008) 'Home Blood-Pressure Monitoring in Patients Receiving Sunitinib'. *N Engl J Med* 358 (1), 95-97

Babiarz, J. E., Ravon, M., Sridhar, S., Ravindran, P., Swanson, B., Bitter, H., Weiser, T., Chiao, E., Certa, U., and Kolaja, K. L. (2011) 'Determination of the Human Cardiomyocyte mRNA and miRNA Differentiation Network by Fine-Scale Profiling'. *Stem Cells and Development* 21 (11), 1956-1965

Baek, D., Villén, J., Shin, C., Camargo, F. D., Gygi, S. P., and Bartel, D. P. (2008) 'The Impact of microRNAs on Protein Output'. *Nature* 455 (7209), 64-71

Bagga, S., Bracht, J., Hunter, S., Massirer, K., Holtz, J., Eachus, R., and Pasquinelli, A. E. (2005) 'Regulation by Let-7 and Lin-4 miRNAs Results in Target mRNA Degradation'. *Cell* 122 (4), 553-563

Bang, O., Park, J., and Kang, S. (2001) 'Activation of PKC but Not of ERK is Required for Vitamin E-Succinate-Induced Apoptosis of HL-60 Cells'. *Biochemical and Biophysical Research Communications* 288 (4), 789-797

Bartel, D. P. (2004) 'MicroRNAs: Genomics, Biogenesis, Mechanism, and Function'. *Cell* 116 (2), 281-297

Barth, S., Glick, D., and Macleod, K.F. (2010) 'Autophagy: assays and artifacts'. *The Journal of pathology 221*(2), 117-124.

Bell, R. M., Mocanu, M. M., and Yellon, D. M. (2011) 'Retrograde Heart Perfusion: The Langendorff Technique of Isolated Heart Perfusion'. *Journal of Molecular and Cellular Cardiology* 50 (6), 940-950

Bello, C. L., Mulay, M., Huang, X., Patyna, S., Dinolfo, M., Levine, S., Van Vugt, A., Toh, M., Baum, C., and Rosen, L. (2009) 'Electrocardiographic Characterization of the QTc Interval in Patients with Advanced Solid Tumors: Pharmacokinetic- Pharmacodynamic Evaluation of Sunitinib'. *Clinical Cancer Research* 15 (22), 7045-7052

Bernstein, E., Kim, S. Y., Carmell, M. A., Murchison, E. P., Alcorn, H., Li, M. Z., Mills, A. A., Elledge, S. J., Anderson, K. V., and Hannon, G. J. (2003) 'Dicer is Essential for Mouse Development'. *Nature Genetics* 35 (3), 215-217

Bhojani, N., Jeldres, C., Patard, J., Perrotte, P., Suardi, N., Hutterer, G., Patenaude, F., Oudard, S., and Karakiewicz, P. I. (2008) 'Toxicities Associated with the Administration of Sorafenib, Sunitinib, and Temsirolimus and their Management in Patients with Metastatic Renal Cell Carcinoma'. *European Urology* 53 (5), 917-930

Blume-Jensen, P. and Hunter, T. (2001) 'Oncogenic Kinase Signalling'. *Nature* 411 (6835), 355-365

Boehm, M., Kojonazarov, B., Ghofrani, H. A., Grimminger, F., Weissmann, N., Liles, J. T., Budas, G. R., Seeger, W., and Schermuly, R. T. (2015) 'Effects of Apoptosis Signal-Regulating Kinase 1 (ASK1) Inhibition in Experimental Pressure Overload-Induced Right Ventricular Dysfunction'. *European Respiratory Journal* 46 (suppl 59), PA4913

Bonci, D., Coppola, V., Musumeci, M., Addario, A., Giuffrida, R., Memeo, L., D'Urso, L., Pagliuca, A., Biffoni, M., Labbaye, C., Bartucci, M., Muto, G., Peschle, C., and De Maria, R. (2008) 'The miR-15a-miR-16-1 Cluster Controls Prostate Cancer by Targeting Multiple Oncogenic Activities'. *Nature Medicine* 14 (11), 1271-1277

Borea, P. A., Varani, K., Vincenzi, F., Baraldi, P. G., Tabrizi, M. A., Merighi, S., and Gessi, S. (2015) 'The A3 Adenosine Receptor: History and Perspectives'. *Pharmacological Reviews* 67 (1), 74-102

Borg, C., Terme, M., Taieb, J., Menard, C., Flament, C., Robert, C., Maruyama, K., Wakasugi, H., Angevin, E., Thielemans, K., Le Cesne, A., Chung-Scott, V., Lazar, V., Tchou, I., Crepineau, F., Lemoine, F., Bernard, J., Fletcher, J. A., Turhan, A., Blay, J. Y., Spatz, A.,

Emile, J. F., Heinrich, M. C., Mecheri, S., Tursz, T., and Zitvogel, L. (2004) 'Novel Mode of Action of C-Kit Tyrosine Kinase Inhibitors Leading to NK Cell-Dependent Antitumor Effects'. *The Journal of Clinical Investigation* 114 (3), 379-388

Bostjancic, E., Zidar, N., Stajer, D., and Glavac, D. (2010) 'MicroRNAs miR-1, miR-133a, miR-133b and miR-208 are Dysregulated in Human Myocardial Infarction'. *Cardiology* 115 (3), 163-169

Botelho, S. F., Martins, M. A. P., Vieira, L. B., and Reis, A. M. M. (2016) 'Postmarketing Safety Events Relating to New Drugs Approved in Brazil between 2003 and 2013: A Retrospective Cohort Study'. *The Journal of Clinical Pharmacology, 57*(4), 493-499.

Brand, M.D. and Nicholls, D.G. (2011) 'Assessing mitochondrial dysfunction in cells'. *Biochemical Journal*, *435*(2), 297-312.

Braz, J. C., Gregory, K., Pathak, A., Zhao, W., Sahin, B., Klevitsky, R., Kimball, T. F., Lorenz, J. N., Nairn, A. C., and Liggett, S. B. (2004) 'PKC-Alpha Regulates Cardiac Contractility and Propensity Toward Heart Failure'. *Nature Medicine* 10 (3), 248-254

Brookes, P. S., Yoon, Y., Robotham, J. L., Anders, M., and Sheu, S. (2004) 'Calcium, ATP, and ROS: A Mitochondrial Love-Hate Triangle'. *American Journal of Physiology-Cell Physiology* 287 (4), C817-C833

Brunello, A., Basso, U., Sacco, C., Sava, T., De Vivo, R., Camerini, A., Barile, C., Roma, A., Maruzzo, M., Falci, C., and Zagonel, V. (2012) 'Safety and Activity of Sunitinib in Elderly Patients (=70 Years) with Metastatic Renal Cell Carcinoma: A Multicenter Study'. *Annals of Oncology, 24*(2), 336-342

Budas, G. R., Churchill, E. N., and Mochly-Rosen, D. (2007) 'Cardioprotective Mechanisms of PKC Isozyme-Selective Activators and Inhibitors in the Treatment of Ischemia-Reperfusion Injury'. *Pharmacological Research* 55 (6), 523-536

Bujak, M., Kweon, H. J., Chatila, K., Li, N., Taffet, G., and Frangogiannis, N. G. (2008) 'Ageing-Related Defects are Associated with Adverse Cardiac Remodeling in a Mouse Model of Reperfused Myocardial Infarction*' Journal of the American College of Cardiology*, *51*(14), 1384-1392.

Bunkoczi, G., Salah, E., Filippakopoulos, P., , F., O., Müller, S., Sobott, F., Parker, S. A., Zhang, F., Min, W., Turk, B. E., and Knappemail, S. (2007) 'Structural and Functional Characterization of the Human Protein Kinase ASK1'. - *Structure* 15 (10), 1215-1226

Buoncervello, M., Marconi, M., Carè, A., Piscopo, P., Malorni, W. and Matarrese, P. (2017) 'Preclinical models in the study of sex differences'. *Clinical Science. 131*(6) 449-469

Burgess, M. R., Skaggs, B. J., Shah, N. P., Lee, F. Y., and Sawyers, C. L. (2005) 'Comparative Analysis of Two Clinically Active BCR-ABL Kinase Inhibitors Reveals the Role of Conformation-Specific Binding in Resistance'. *Proceedings of the National Academy of Sciences of the United States of America* 102 (9), 3395-3400

Calin, G. A. and Croce, C. M. (2006) 'MicroRNA Signatures in Human Cancers'. *Nature Reviews Cancer* 6 (11), 857-866

Calin, G. A., Ferracin, M., Cimmino, A., Di Leva, G., Shimizu, M., Wojcik, S. E., Iorio, M. V., Visone, R., Sever, N. I., Fabbri, M., Iuliano, R., Palumbo, T., Pichiorri, F., Roldo, C., Garzon, R., Sevignani, C., Rassenti, L., Alder, H., Volinia, S., Liu, C. -., Kipps, T. J., Negrini, M., and Croce, C. M. (2005) 'A microRNA Signature Associated with Prognosis and Progression in Chronic Lymphocytic Leukemia'. *New England Journal of Medicine* 353 (17), 1793-1801

Calin, G. A., Dumitru, C. D., Shimizu, M., Bichi, R., Zupo, S., Noch, E., Aldler, H., Rattan, S., Keating, M., Rai, K., Rassenti, L., Kipps, T., Negrini, M., Bullrich, F., and Croce, C. M. (2002) 'Frequent Deletions and Down-Regulation of Micro- RNA Genes miR15 and miR16 at 13q14 in Chronic Lymphocytic Leukemia'. *Proceedings of the National Academy of Sciences* 99 (24), 15524-15529

Cao, Y. (2013) 'Multifarious Functions of PDGFs and PDGFRs in Tumor Growth and Metastasis'. *Trends in Molecular Medicine* 19 (8), 460-473

Capitanio, D., Leone, R., Fania, C., Torretta, E., and Gelfi, C. (2016) 'Sprague Dawley Rats: A Model of Successful Heart Ageing'. *EuPA Open Proteomics* 12, 22-30

Cardinale, D. and Cipolla, C. M. (2016) 'Chemotherapy-Induced Cardiotoxicity: Importance of Early Detection'. *Expert Review of Cardiovascular Therapy* 14 (12), 1297-1299

Cardinale, D., Colombo, A., Sandri, M. T., Lamantia, G., Colombo, N., Civelli, M., Martinelli, G., Veglia, F., Fiorentini, C., and Cipolla, C. M. (2006) 'Prevention of High-Dose Chemotherapy-Induced Cardiotoxicity in High-Risk Patients by Angiotensin-Converting Enzyme Inhibition'. *Circulation* 114 (23), 2474-2481

Care, A., Catalucci, D., Felicetti, F., Bonci, D., Addario, A., Gallo, P., Bang, M., Segnalini, P., Gu, Y., and Dalton, N. D. (2007) 'MicroRNA-133 Controls Cardiac Hypertrophy'. *Nature Medicine* 13 (5), 613-618

Carlsson, J., Yoo, L., Gao, Z., Irwin, J. J., Shoichet, B. K., and Jacobson, K. A. (2010) 'Structure-Based Discovery of A2A Adenosine Receptor Ligands'. *Journal of Medicinal Chemistry* 53 (9), 3748-3755

Carmeliet, P. (2005) 'Angiogenesis in Life, Disease and Medicine'. *Nature* 438 (7070), 932

Carmeliet, P. and Jain, R. K. (2000) 'Angiogenesis in Cancer and Other Diseases'. *Nature* 407 (6801), 249-257

Carr, C. S., Hill, R. J., Masamune, H., Kennedy, S. P., Knight, D. R., Tracey, W. R., and Yellon, D. M. (1997) 'Evidence for a Role for both the Adenosine A1 and A3 Receptors in Protection of Isolated Human Atrial Muscle Against Simulated Ischaemia'. *Cardiovascular Research* 36 (1), 52-59

Casanova, E., Garate, C., Ovalle, S., Calvo, P., and Chinchetru, M. A. (1996) 'Identification of Four Splice Variants of the Mouse Stress-Activated Protein Kinase JNK/SAPK [Alpha]-Isoform.'. *Neuroreport* 7 (7), 1320-1324

Ceolotto, G., Gallo, A., Papparella, I., Franco, L., Murphy, E., Iori, E., Pagnin, E., Fadini, G. P., Albiero, M., Semplicini, A., and Avogaro, A. (2007) 'Rosiglitazone Reduces Glucose-Induced Oxidative Stress Mediated by NAD(P)H Oxidase Via AMPK-Dependent Mechanism'. *Arteriosclerosis, Thrombosis, and Vascular Biology* 27 (12), 2627-2633

Chang, L. and Karin, M. (2001) 'Mammalian MAP Kinase Signalling Cascades'. *Nature* 410 (6824), 37-40

Chen, C., Ponnusamy, M., Liu, C., Gao, J., Wang, K., and Li, P. (2017) 'MicroRNA as a Therapeutic Target in Cardiac Remodeling'. *BioMed research international*, *2017*.

Chen, J. F., Murchison, E. P., Tang, R., Callis, T. E., Tatsuguchi, M., Deng, Z., Rojas, M., Hammond, S. M., Schneider, M. D., Selzman, C. H., Meissner, G., Patterson, C., Hannon, G. J., and Wang, D. Z. (2008) 'Targeted Deletion of Dicer in the Heart Leads to Dilated Cardiomyopathy and Heart Failure'. *Proceedings of the National Academy of Sciences of the United States of America* 105 (6), 2111-2116

Chen, J., Zou, A., Splawski, I., Keating, M. T., and Sanguinetti, M. C. (1999b) 'Long QT Syndrome-Associated Mutations in the Per-Arnt-Sim (PAS) Domain of HERG Potassium Channels Accelerate Channel Deactivation'. *The Journal of Biological Chemistry* 274 (15), 10113-10118

Chen, L., Chiou, G., Chen, Y., Li, H., and Chiou, S. (2010) 'microRNA and Aging: A Novel Modulator in Regulating the Aging Network'. *Aging Research Reviews* 9, Supplement, S59-S66

Chen, M. H., Kerkela, R., and Force, T. (2008) 'Mechanisms of Cardiac Dysfunction Associated with Tyrosine Kinase Inhibitor Cancer Therapeutics'. *Circulation* 118 (1), 84-95

Chen, Z., Seimiya, H., Naito, M., Mashima, T., Kizaki, A., Dan, S., Imaizumi, M., Ichijo, H., Miyazono, K., and Tsuruo, T. (1999a) 'ASK1 Mediates Apoptotic Cell Death Induced by Genotoxic Stress.' *Oncogene* 18 (1), 173-180

Cheng, G. (2015) 'Circulating miRNAs: Roles in Cancer Diagnosis, Prognosis and Therapy'. *Advanced Drug Delivery Reviews* 81, 75-93

Cheng, H. and Force, T. (2010) 'Molecular Mechanisms of Cardiovascular Toxicity of Targeted Cancer Therapeutics'. *Circulation Research* 106 (1), 21-34

Chetty, R., Stepner, M., Abraham, S., Lin, S., Scuderi, B., Turner, N., Bergeron, A., and Cutler, D. (2016) 'The Association between Income and Life Expectancy in the United States, 2001-2014'. *Jama* 315 (16), 1750-1766

Chiusa, M., Hool, S., Truetsch, P., Djafarzadeh, S., Jakob, S. M., Seifriz, F., Scherer, S. J., Suter, T. M., Zuppinger, C., and Zbinden, S. (2012) 'Cancer Therapy Modulates VEGF Signaling and Viability in Adult Rat Cardiac Microvascular Endothelial Cells and Cardiomyocytes'. *Journal of Molecular and Cellular Cardiology* 52 (5), 1164-1175

Chowdhury, S. K., Liu, W., Zi, M., Li, Y., Wang, S., Tsui, H., Prehar, S., Castro, S., Zhang, H., Ji, Y., Zhang, X., Xiao, R., Zhang, R., Lei, M., Cyganek, L., Guan, K., Millar, C. B., Liao, X., Jain, M. K., Boyett, M. R., Cartwright, E. J., Shiels, H. A., and Wang, X. (2017) 'Stress-Activated Kinase Mitogen-Activated Kinase Kinase-7 Governs Epigenetics of Cardiac Repolarization for Arrhythmia Prevention'. *Circulation* 135 (7), 683-699

Christensen, J. G. (2007) 'A Preclinical Review of Sunitinib, a Multitargeted Receptor Tyrosine Kinase Inhibitor with Anti-Angiogenic and Antitumour Activities'. *Annals of Oncology : Official Journal of the European Society for Medical Oncology* 18 Suppl 10, x3-10

Chu, T. F., Rupnick, M. A., Kerkela, R., Dallabrida, S. M., Zurakowski, D., Nguyen, L., Woulfe, K., Pravda, E., Cassiola, F., and Desai, J. (2007) 'Cardiotoxicity Associated with Tyrosine Kinase Inhibitor Sunitinib'. *The Lancet* 370 (9604), 2011-2019

Ciriello, G., Miller, M. L., Aksoy, B. A., Senbabaoglu, Y., Schultz, N., and Sander, C. (2013) 'Emerging Landscape of Oncogenic Signatures Across Human Cancers'. *Nature Genetics* 45 (10), 1127-1133

Cohen, J., Babiarz, J., Abrams, R., Guo, L., Kameoka, S., Chiao, E., Taunton, J., and Kolaja, K. (2011) 'Use of Human Stem Cell Derived Cardiomyocytes to Examine Sunitinib Mediated Cardiotoxicity and Electrophysiological Alterations'. *Toxicology and Applied Pharmacology* 257 (1), 74-83

Cook, S. A., Sugden, P. H., and Clerk, A. (1999) 'Activation of C-Jun N-Terminal Kinases and p38-Mitogen-Activated Protein Kinases in Human Heart Failure Secondary to Ischaemic Heart Disease'. *Journal of Molecular and Cellular Cardiology* 31 (8), 1429-1434

Corsten, M. F., Papageorgiou, A., Verhesen, W., Carai, P., Lindow, M., Obad, S., Summer, G., Coort, S. L., Hazebroek, M., van Leeuwen, R., Gijbels, M. J., Wijnands, E., Biessen, E. A., De Winther, M. P., Stassen, F. R., Carmeliet, P., Kauppinen, S., Schroen, B., and Heymans, S. (2012) 'MicroRNA Profiling Identifies microRNA-155 as an Adverse Mediator of Cardiac Injury and Dysfunction during Acute Viral Myocarditis'. *Circulation Research* 111 (4), 415-425

Costinean, S., Zanesi, N., Pekarsky, Y., Tili, E., Volinia, S., Heerema, N., and Croce, C. M. (2006) 'Pre-B Cell Proliferation and Lymphoblastic Leukemia/High-Grade Lymphoma in Eμ-miR155 Transgenic Mice'. *Proceedings of the National Academy of Sciences* 103 (18), 7024-7029

Cristofanilli, M., Charnsangavej, C., and Hortobagyi, G. N. (2002) 'Angiogenesis Modulation in Cancer Research: Novel Clinical Approaches'. *Nature Reviews Drug Discovery* 1 (6), 415-426

Dai, D. -. and Rabinovitch, P. S. (2009) 'Cardiac Ageing in Mice and Humans: The Role of Mitochondrial Oxidative Stress'. *Trends in Cardiovascular Medicine* 19 (7), 213-220

Dai, D., Rabinovitch, P. S., and Ungvari, Z. (2012) 'Mitochondria and Cardiovascular Ageing'. *Circulation Research* 110 (8), 1109-1124

D'Alessandra, Y., Devanna, P., Limana, F., Straino, S., Di Carlo, A., Brambilla, P. G., Rubino, M., Carena, M. C., Spazzafumo, L., De Simone, M., Micheli, B., Biglioli, P., Achilli, F., Martelli, F., Maggiolini, S., Marenzi, G., Pompilio, G., and Capogrossi, M. C. (2010) 'Circulating microRNAs are New and Sensitive Biomarkers of Myocardial Infarction'. *European Heart Journal* 31 (22), 2765-2773

Davis, R. J. (2000) 'Signal Transduction by the JNK Group of MAP Kinases'. *Cell* 103 (2), 239-252

de Jesus-Gonzalez, N., Robinson, E., Moslehi, J., and Humphreys, B. D. (2012) 'Management of Antiangiogenic Therapy-Induced Hypertension'. *Hypertension* 60 (3), 607-615

Dérijard, B., Hibi, M., Wu, I., Barrett, T., Su, B., Deng, T., Karin, M., and Davis, R. J. (1994) 'JNK1: A Protein Kinase Stimulated by UV Light and Ha-Ras that Binds and Phosphorylates the C-Jun Activation Domain' *Cell*, *76*(6), 1025-1037

Detjen, K. M., Brembeck, F. H., Welzel, M., Kaiser, A., Haller, H., Wiedenmann, B., and Rosewicz, S. (2000) 'Activation of Protein Kinase Calpha Inhibits Growth of Pancreatic Cancer Cells Via p21(Cip)-Mediated G(1) Arrest'. *Journal of Cell Science* 113 (Pt 17) (Pt 17), 3025-3035

Dhanasekaran, D. N., Kashef, K., Lee, C. M., Xu, H., and Reddy, E. P. (2007) 'Scaffold Proteins of MAP-Kinase Modules'. *Oncogene* 26 (22), 3185-3202

Dhanasekaran, D. N. and Reddy, E. P. (2008) 'JNK Signaling in Apoptosis'. *Oncogene* 27 (48), 6245-6251

Di Lorenzo, G., Autorino, R., Bruni, G., Cartenì, G., Ricevuto, E., Tudini, M., Ficorella, C., Romano, C., Aieta, M., Giordano, A., Giuliano, M., Gonnella, A., De Nunzio, C., Rizzo, M., Montesarchio, V., Ewer, M., and De Placido, S. (2009) 'Cardiovascular Toxicity Following Sunitinib Therapy in Metastatic Renal Cell Carcinoma: A Multicenter Analysis'. *Annals of Oncology* 20 (9), 1535-1542

Dirix, L., Maes, H., and Sweldens, C. (2007) 'Treatment of Arterial Hypertension (AHT) Associated with Angiogenesis Inhibitors'. *Annals of Oncology* 18 (6), 1121-1122

Doenst, T., Nguyen, T. D., and Abel, E. D. (2013) 'Cardiac Metabolism in Heart Failure: Implications Beyond ATP Production'. *Circulation Research* 113 (6), 709-724

Doherty, K. R., Wappel, R. L., Talbert, D. R., Trusk, P. B., Moran, D. M., Kramer, J. W., Brown, A. M., Shell, S. A., and Bacus, S. (2013) 'Multi-Parameter in Vitro Toxicity Testing of Crizotinib, Sunitinib, Erlotinib, and Nilotinib in Human Cardiomyocytes'. *Toxicology and Applied Pharmacology* 272 (1), 245-255

Dong, S., Cheng, Y., Yang, J., Li, J., Liu, X., Wang, X., Wang, D., Krall, T. J., Delphin, E. S., and Zhang, C. (2009) 'MicroRNA Expression Signature and the Role of MicroRNA-21 in the Early Phase of Acute Myocardial Infarction' 284 (43), 29514-29525

Dougherty, C. J., Kubasiak, L. A., Prentice, H., Andreka, P., Bishopric, N. H., and Webster, K. A. (2002) 'Activation of C-Jun N-Terminal Kinase Promotes Survival of Cardiac Myocytes After Oxidative Stress'. *Biochemical Journal* 362 (3), 561-571

DuBois, S., Shusterman, S., Ingle, A., Baruchel, S., Stempak, D., Sun, J., Ivy, S., Glade-Bender, J., Blaney, S., and Adamson, P. (2008) 'A Pediatric Phase I Trial and Pharmacokinetic (PK) Study of Sunitinib: A Children's Oncology Group Phase I Consortium Study'. *Journal of Clinical Oncology* 26 (15_suppl), 3561-3561

Dubois, S. G., Shusterman, S., Ingle, A. M., Ahern, C. H., Reid, J. M., Wu, B., Baruchel, S., Glade-Bender, J., Ivy, P., Grier, H. E., Adamson, P. C., and Blaney, S. M. (2011) 'Phase I and Pharmacokinetic Study of Sunitinib in Pediatric Patients with Refractory Solid Tumors: A Children's Oncology Group Study'. *Clinical Cancer Research : An Official Journal of the American Association for Cancer Research* 17 (15), 5113-5122

Eaton, G., Zhang, Q., Diallo, C., Matsuzawa, A., Ichijo, H., Steinbeck, M., and Freeman, T. (2014) 'Inhibition of Apoptosis Signal-Regulating Kinase 1 Enhances Endochondral Bone Formation by Increasing Chondrocyte Survival'. *Cell Death & Disease* 5 (11), e1522

Eis, P. S., Tam, W., Sun, L., Chadburn, A., Li, Z., Gomez, M. F., Lund, E., and Dahlberg, J. E. (2005) 'Accumulation of miR-155 and BIC RNA in Human B Cell Lymphomas'. *Proceedings of the National Academy of Sciences of the United States of America* 102 (10), 3627-3632

Eitel, I., Adams, V., Dieterich, P., Fuernau, G., de Waha, S., Desch, S., Schuler, G., and Thiele, H. (2012) 'Relation of Circulating MicroRNA-133a Concentrations with Myocardial Damage and Clinical Prognosis in ST-Elevation Myocardial Infarction.' *American heart journal*, *164*(5), 706-714

Ekhteraei Tousi, S., Mohammad Soltani, B., Sadeghizadeh, M., Hoseini, S., and Soleimani, M. (2013) 'Hsa-miR-133b Expression Profile during Cardiac Progenitor Cell Differentiation and its Inhibitory Effect on Srf Expression'. *Modares Journal of Medical Sciences: Pathobiology* 16 (1), 1-9

Emanuelov, A. K., Shainberg, A., Chepurko, Y., Kaplan, D., Sagie, A., Porat, E., Arad, M., and Hochhauser, E. (2010) 'Adenosine A3 Receptor-Mediated Cardioprotection Against Doxorubicin-Induced Mitochondrial Damage'. *Biochemical Pharmacology* 79 (2), 180-187

Eter, E. E. (2013) 'NQDI 1, an Inhibitor of ASK1 Attenuates Acute Ischemic Renal Injury by Modulating Oxidative Stress and Cell Death.' 11 (3), 179-186

Ewer, M. S., Suter, T. M., Lenihan, D. J., Niculescu, L., Breazna, A., Demetri, G. D., and Motzer, R. J. (2014) 'Cardiovascular Events among 1090 Cancer Patients Treated with Sunitinib, Interferon, Or Placebo: A Comprehensive Adjudicated Database Analysis Demonstrating Clinically Meaningful Reversibility of Cardiac Events'. *European Journal of Cancer* 50 (12), 2162-2170

Faivre, S., Demetri, G., Sargent, W., and Raymond, E. (2007) 'Molecular Basis for Sunitinib Efficacy and Future Clinical Development'. *Nature Reviews Drug Discovery* 6 (9), 734-745

Faivre, S., Delbaldo, C., Vera, K., Robert, C., Lozahic, S., Lassau, N., Bello, C., Deprimo, S., Brega, N., Massimini, G., Armand, J. P., Scigalla, P., and Raymond, E. (2006) 'Safety, Pharmacokinetic, and Antitumor Activity of SU11248, a Novel Oral Multitarget Tyrosine Kinase Inhibitor, in Patients with Cancer'. *Journal of Clinical Oncology : Official Journal of the American Society of Clinical Oncology* 24 (1), 25-35

Faraoni, I., Antonetti, F. R., Cardone, J., and Bonmassar, E. (2009) 'miR-155 Gene: A Typical Multifunctional microRNA'. *Biochimica Et Biophysica Acta (BBA) - Molecular Basis of Disease* 1792 (6), 497-505

Fenton, M. S., Marion, K. M., Salem, A. K., Hogen, R., Naeim, F., and Hershman, J. M. (2010) 'Sunitinib Inhibits MEK/ERK and SAPK/JNK Pathways and Increases Sodium/Iodide Symporter Expression in Papillary Thyroid Cancer'. *Thyroid* 20 (9), 965-974

Fernald, K. and Kurokawa, M. (2013) 'Evading Apoptosis in Cancer'. *Trends in Cell Biology* 23 (12), 620-633

Ferrara, N. and Kerbel, R. S. (2005) 'Angiogenesis as a Therapeutic Target'. *Nature* 438 (7070), 967-974

Fima, E., Shtutman, M., Libros, P., Missel, A., Shahaf, G., Kahana, G., and Livneh, E. (2001) 'PKC [Eta] Enhances Cell Cycle Progression, the Expression of G1 Cyclins and p21 in MCF-7 Cells'. *Oncogene* 20 (46), 6794

Fishman, P., Bar-Yehuda, S., Barer, F., Madi, L., Multani, A. S., and Pathak, S. (2001) 'The A3 Adenosine Receptor as a New Target for Cancer Therapy and Chemoprotection'. *Experimental Cell Research* 269 (2), 230-236

Fishman, P., Madi, L., Bar-Yehuda, S., Barer, F., Del Valle, L., and Khalili, K. (2002) 'Evidence for Involvement of Wnt Signaling Pathway in IB-MECA Mediated Suppression of Melanoma Cells'. *Oncogene* 21 (25), 4060-4064

Fishman, P., Bar-Yehuda, S., Ohana, G., Pathak, S., Wasserman, L., Barer, F., and Multani, A. S. (2000) 'Adenosine Acts as an Inhibitor of Lymphoma Cell Growth: A Major Role for the A3 Adenosine Receptor'. *European Journal of Cancer* 36 (11), 1452-1458

Foglia, M. J. and Poss, K. D. (2016) 'Building and Re-Building the Heart by Cardiomyocyte Proliferation'. *Development (Cambridge, England)* 143 (5), 729-740

Foltz, I. N., Gerl, R. E., Wieler, J. S., Luckach, M., Salmon, R. A., and Schrader, J. W. (1998) 'Human Mitogen-Activated Protein Kinase Kinase 7 (MKK7) is a Highly Conserved C-Jun N-Terminal Kinase/Stress-Activated Protein Kinase (JNK/SAPK) Activated by Environmental Stresses and Physiological Stimuli'. *Journal of Biological Chemistry* 273 (15), 9344-9351

Force, T., Krause, D. S., and Van Etten, R. A. (2007) 'Molecular Mechanisms of Cardiotoxicity of Tyrosine Kinase Inhibition'. *Nat Rev Cancer* 7 (5), 332-344

Force, T. and Kolaja, K. L. (2011) 'Cardiotoxicity of Kinase Inhibitors: The Prediction and Translation of Preclinical Models to Clinical Outcomes'. *Nature Reviews Drug Discovery* 10 (2), 111-126

Forte, G., Sorrentino, R., Montinaro, A., Pinto, A., and Morello, S. (2011) 'Cl-IB-MECA Enhances TNF-A Release in Peritoneal Macrophages Stimulated with LPS'. *Cytokine* 54 (2), 161-166

Fredholm, B. B., IJzerman, A. P., Jacobson, K. A., Linden, J., and Muller, C. E. (2011) 'International Union of Basic and Clinical Pharmacology. LXXXI. Nomenclature and Classification of Adenosine Receptors--an Update'. *Pharmacological Reviews* 63 (1), 1-34

Fredriksson, R., Lagerstrom, M. C., Lundin, L. G., and Schioth, H. B. (2003) 'The G-Protein-Coupled Receptors in the Human Genome Form Five Main Families. Phylogenetic Analysis, Paralogon Groups, and Fingerprints'. *Molecular Pharmacology* 63 (6), 1256-1272

Fujii, K., Goldman, E. H., Park, H. R., Zhang, L., Chen, J., and Fu, H. (2004) 'Negative Control of Apoptosis Signal-Regulating Kinase 1 through Phosphorylation of Ser-1034'. *Oncogene* 23 (29), 5099-5104

Fujis awa, T. (2017) ‘Therapeutic application of apoptosis signal-regulating kinase 1 inhibitors’ *Advances in Biological* 66, 85-90

Fulda, S. and Debatin, K. (2006) 'Extrinsic Versus Intrinsic Apoptosis Pathways in Anticancer Chemotherapy'. *Oncogene* 25 (34), 4798

Gerczuk, P. Z., Breckenridge, D. G., Liles, J. T., Budas, G. R., Shryock, J. C., Belardinelli, L., Kloner, R. A., and Dai, W. (2012) 'An Apoptosis Signal-Regulating Kinase 1 Inhibitor Reduces Cardiomyocyte Apoptosis and Infarct Size in a Rat Ischemia-Reperfusion Model'. *Journal of Cardiovascular Pharmacology* 60 (3), 276-282

Gerlier, D. and Thomasset, N. (1986) 'Use of MTT Colorimetric Assay to Measure Cell Activation'. *Journal of Immunological Methods* 94 (1-2), 57-63

Gershoni, J. M. and Palade, G. E. (1982) 'Electrophoretic Transfer of Proteins from Sodium Dodecyl Sulfate-Polyacrylamide Gels to a Positively Charged Membrane Filter'. *Analytical Biochemistry* 124 (2), 396-405

Gharanei, M., Hussain, A., Janneh, O., and Maddock, H. (2013) 'Attenuation of Doxorubicin-Induced Cardiotoxicity by Mdivi-1: A Mitochondrial Division/Mitophagy Inhibitor'. *PloS One* 8 (10), e77713

Ghatalia, P., Je, Y., Kaymakcalan, M., Sonpavde, G., and Choueiri, T. (2015) 'QTc Interval Prolongation with Vascular Endothelial Growth Factor Receptor Tyrosine Kinase Inhibitors'. *British Journal of Cancer* 112 (2), 296-305

Ghoreschi, K., Laurence, A., and O'Shea, J. J. (2009) 'Selectivity and Therapeutic Inhibition of Kinases: To be Or Not to be?'. *Nature Immunology* 10 (4), 356-360

Gidlöf, O., Smith, J. G., Miyazu, K., Gilje, P., Spencer, A., Blomquist, S., and Erlinge, D. (2013) 'Circulating Cardio-Enriched microRNAs are Associated with Long-Term Prognosis Following Myocardial Infarction'. *BMC Cardiovascular Disorders* 13 (1), 1

Gintant, G. (2011) 'An Evaluation of hERG Current Assay Performance: Translating Preclinical Safety Studies to Clinical QT Prolongation.' *Pharmacology & therapeutics*, *129*(2), 109-119

Goel, H. L. and Mercurio, A. M. (2013) 'VEGF Targets the Tumour Cell'. *Nature Reviews Cancer* 13 (12), 871-882

Gonzalvez, F. and Ashkenazi, A. (2010) 'New Insights into Apoptosis Signaling by Apo2L/TRAIL'. *Oncogene* 29 (34), 4752-4765

Good, M. C., Zalatan, J. G., and Lim, W. A. (2011) 'Scaffold Proteins: Hubs for Controlling the Flow of Cellular Information'. *Science* 332 (6030), 680-686

Goodman, V. L., Rock, E. P., Dagher, R., Ramchandani, R. P., Abraham, S., Gobburu, J. V., Booth, B. P., Verbois, S. L., Morse, D. E., Liang, C. Y., Chidambaram, N., Jiang, J. X., Tang, S., Mahjoob, K., Justice, R., and Pazdur, R. (2007) 'Approval Summary: Sunitinib for the Treatment of Imatinib Refractory Or Intolerant Gastrointestinal Stromal Tumors and Advanced Renal Cell Carcinoma'. *Clinical Cancer Research : An Official Journal of the American Association for Cancer Research* 13 (5), 1367-1373

Gosse, P. (2005) 'Left Ventricular Hypertrophy as a Predictor of Cardiovascular Risk'. *Journal of Hypertension* 23, S27-S33

Gould, K. E., Taffet, G. E., Michael, L. H., Christie, R. M., Konkol, D. L., Pocius, J. S., Zachariah, J. P., Chaupin, D. F., Daniel, S. L., Sandusky, G. E.,Jr, Hartley, C. J., and Entman, M. L. (2002) 'Heart Failure and Greater Infarct Expansion in Middle-Aged Mice: A Relevant Model for Postinfarction Failure'. *American Journal of Physiology.Heart and Circulatory Physiology* 282 (2), H615-21

Gouspillou, G., Scheede-Bergdahl, C., Spendiff, S., Vuda, M., Meehan, B., Mlynarski, H., Archer-Lahlou, E., Sgarioto, N., Purves-Smith, F. M., and Konokhova, Y. (2015) 'Anthracycline-Containing Chemotherapy Causes Long-Term Impairment of Mitochondrial Respiration and Increased Reactive Oxygen Species Release in Skeletal Muscle'. *Scientific Reports* 5

Granger, C. B. (2006) 'Prediction and Prevention of Chemotherapy-Induced Cardiomyopathy: Can it be done?'. *Circulation* 114 (23), 2432-2433

Grossmann, M., Premaratne, E., Desai, J., and Davis, I. D. (2008) 'Thyrotoxicosis during Sunitinib Treatment for Renal Cell Carcinoma'. *Clinical Endocrinology* 69 (4), 669-672

Gschwind, A., Fischer, O. M., and Ullrich, A. (2004) 'The Discovery of Receptor Tyrosine Kinases: Targets for Cancer Therapy'. *Nature Reviews.Cancer* 4 (5), 361

Guellich, A., Mehel, H., and Fischmeister, R. (2014) 'Cyclic AMP Synthesis and Hydrolysis in the Normal and Failing Heart'. *Pflügers Archiv-European Journal of Physiology* 466 (6), 1163-1175

Gundewar, S., Calvert, J. W., Jha, S., Toedt-Pingel, I., Ji, S. Y., Nunez, D., Ramachandran, A., Anaya-Cisneros, M., Tian, R., and Lefer, D. J. (2009) 'Activation of AMP-Activated Protein Kinase by Metformin Improves Left Ventricular Function and Survival in Heart Failure'. *Circulation Research* 104 (3), 403-411

Guo, L., Dong, Z., and Guthrie, H. (2009) 'Validation of a Guinea Pig Langendorff Heart Model for Assessing Potential Cardiovascular Liability of Drug Candidates'. *Journal of Pharmacological and Toxicological Methods* 60 (2), 130-151

Guo, L., Coyle, L., Abrams, R. M., Kemper, R., Chiao, E. T., and Kolaja, K. L. (2013) 'Refining the Human iPSC-Cardiomyocyte Arrhythmic Risk Assessment Model'. *Toxicological Sciences : An Official Journal of the Society of Toxicology* 136 (2), 581-594

Gupta, R. and Maitland, M. L. (2011) 'Sunitinib, Hypertension, and Heart Failure: A Model for Kinase Inhibitor-Mediated Cardiotoxicity'. *Current Hypertension Reports* 13 (6), 430-435

Gupta, S., Barrett, T., Whitmarsh, A. J., Cavanagh, J., Sluss, H. K., Derijard, B., and Davis, R. J. (1996) 'Selective Interaction of JNK Protein Kinase Isoforms with Transcription Factors'. *The EMBO Journal* 15 (11), 2760-2770

Guttilla, I. K. and White, B. A. (2009) 'Coordinate Regulation of FOXO1 by miR-27a, miR-96, and miR-182 in Breast Cancer Cells'. *Journal of Biological Chemistry* 284 (35), 23204-23216

Gwak, J., Jung, S., Kang, D., Kim, E., Kim, D., Chung, Y., Shin, J., and Oh, S. (2009) 'Stimulation of Protein Kinase C-A Suppresses Colon Cancer Cell Proliferation by Down-Regulation of B-Catenin'. *Journal of Cellular and Molecular Medicine* 13 (8b), 2171-2180

Hagström, L., Henein, M. Y., Karp, K., Waldenström, A., and Lindqvist, P. (2016) 'Impact of Age and Sex on Normal Left Heart Structure and Function'. *Clinical Physiology and Functional Imaging*

Hahn, H. S., Marreez, Y., Odley, A., Sterbling, A., Yussman, M. G., Hilty, K. C., Bodi, I., Liggett, S. B., Schwartz, A., and Dorn, G. W.,2nd (2003) 'Protein Kinase Calpha Negatively Regulates Systolic and Diastolic Function in Pathological Hypertrophy'. *Circulation Research* 93 (11), 1111-1119

Hahn, V. S., Lenihan, D. J., and Ky, B. (2014) 'Cancer Therapy-Induced Cardiotoxicity: Basic Mechanisms and Potential Cardioprotective Therapies'. *Journal of the American Heart Association* 3 (2), e000665

Hambleton, M., York, A., Sargent, M. A., Kaiser, R. A., Lorenz, J. N., Robbins, J., and Molkentin, J. D. (2007) 'Inducible and Myocyte-Specific Inhibition of PKCalpha Enhances Cardiac Contractility and Protects Against Infarction-Induced Heart Failure'. *American Journal of Physiology.Heart and Circulatory Physiology* 293 (6), H3768-71

Hanahan, D. and Weinberg, R. A. (2011) 'Hallmarks of Cancer: The Next Generation'. *Cell* 144 (5), 646-674

Hancock, S. L., Tucker, M. A., and Hoppe, R. T. (1993) 'Factors Affecting Late Mortality from Heart Disease After Treatment of Hodgkin's Disease'. *Jama* 270 (16), 1949-1955

Hao, H., Li, S., Tang, H., Liu, B., Cai, Y., Shi, C., and Xiao, X. (2016) 'NQDI-1, an Inhibitor of ASK1 Attenuates Acute Perinatal Hypoxic-Ischemic Cerebral Injury by Modulating Cell Death'. *Molecular Medicine Reports* 13 (6), 4585-4592

Haq, S. E. A., Clerk, A., and Sugden, P. H. (1998) 'Activation of Mitogen-Activated Protein Kinases (p38-MAPKs, SAPKs/JNKs and ERKs) by Adenosine in the Perfused Rat Heart'. *FEBS Letters* 434 (3), 305-308

Hare, J. M. (2001) 'Oxidative Stress and Apoptosis in Heart Failure Progression'. *Circulation Research* 89 (3), 198-200

Hartmann, J. T., Haap, M., Kopp, H., and Lipp, H. (2009) 'Tyrosine Kinase Inhibitors-a Review on Pharmacology, Metabolism and Side Effects'. *Current Drug Metabolism* 10 (5), 470-481

Hasinoff, B. B. and Patel, D. (2010) 'Mechanisms of Myocyte Cytotoxicity Induced by the Multikinase Inhibitor Sorafenib'. *Cardiovascular Toxicology* 10 (1), 1-8

Hasinoff, B. B., Patel, D., and O'Hara, K. A. (2008) 'Mechanisms of Myocyte Cytotoxicity Induced by the Multiple Receptor Tyrosine Kinase Inhibitor Sunitinib'. *Molecular Pharmacology* 74 (6), 1722-1728

Hayakawa, Y., Hirata, Y., Sakitani, K., Nakagawa, H., Nakata, W., Kinoshita, H., Takahashi, R., Takeda, K., Ichijo, H., and Maeda, S. (2012) 'Apoptosis Signal-regulating Kinase-1

Inhibitor as a Potent Therapeutic Drug for the Treatment of Gastric Cancer'. *Cancer Science* 103 (12), 2181-2185

He, B., Xiao, J., An-Jing Ren, Yu-Feng Zhang, Zhang, H., Chen, M., Xie, B., Xiao-Gang Gao, and Ying-Wei Wang (2011) 'Role of miR-1 and miR-133a in Myocardial Ischemic Postconditioning'. *Journal of Biomedical Science* 18 (1), 22-31

He, X., Liu, Y., Sharma, V., Dirksen, R. T., Waugh, R., Sheu, S., and Min, W. (2003) 'ASK1 Associates with Troponin T and Induces Troponin T Phosphorylation and Contractile Dysfunction in Cardiomyocytes'. *The American Journal of Pathology* 163 (1), 243-251

Heinrich, M. C., Maki, R. G., Corless, C. L., Antonescu, C. R., Harlow, A., Griffith, D., Town, A., McKinley, A., Ou, W., and Fletcher, J. A. (2008) 'Primary and Secondary Kinase Genotypes Correlate with the Biological and Clinical Activity of Sunitinib in Imatinib-Resistant Gastrointestinal Stromal Tumor'. *Journal of Clinical Oncology* 26 (33), 5352-5359

Heinrich, M. C., Rubin, B. P., Longley, B. J., and Fletcher, J. A. (2002) 'Biology and Genetic Aspects of Gastrointestinal Stromal Tumors: KIT Activation and Cytogenetic Alterations'. *Human Pathology* 33 (5), 484-495

Heldin, C. (1995) 'Dimerization of Cell Surface Receptors in Signal Transduction'. *Cell* 80 (2), 213-223

Henderson, K. A., Borders, R. B., Ross, J. B., Huwar, T. B., Travis, C. O., Wood, B. J., Ma, Z. J., Hong, S. P., Vinci, T. M., and Roche, B. M. (2013) 'Effects of Tyrosine Kinase Inhibitors on Rat Isolated Heart Function and Protein Biomarkers Indicative of Toxicity'. *Journal of Pharmacological and Toxicological Methods* 68 (1), 150-159

Hengartner, M. O. (2000) 'The Biochemistry of Apoptosis'. *Nature* 407 (6805), 770

Hicklin, D. J. and Ellis, L. M. (2005) 'Role of the Vascular Endothelial Growth Factor Pathway in Tumor Growth and Angiogenesis'. *Journal of Clinical Oncology : Official Journal of the American Society of Clinical Oncology* 23 (5), 1011-1027

Hikoso, S., Ikeda, Y., Yamaguchi, O., Takeda, T., Higuchi, Y., Hirotani, S., Kashiwase, K., Yamada, M., Asahi, M., and Matsumura, Y. (2007) 'Progression of Heart Failure was Suppressed by Inhibition of Apoptosis Signal-Regulating Kinase 1 Via Transcoronary Gene Transfer'. *Journal of the American College of Cardiology* 50 (5), 453-462

Hill, K., Erdogan, E., Khoor, A., Walsh, M., Leitges, M., Murray, N. R., and Fields, A. P. (2014) 'Protein Kinase Cα Suppresses Kras-Mediated Lung Tumor Formation through Activation of a p38 MAPK-TGFβ Signaling Axis'. *Oncogene* 33 (16), 2134-2144

Ho, D. T., Bardwell, A. J., Grewal, S., Iverson, C., and Bardwell, L. (2006) 'Interacting JNK-Docking Sites in MKK7 Promote Binding and Activation of JNK Mitogen-Activated Protein Kinases'. *The Journal of Biological Chemistry* 281 (19), 13169-13179

Hochhaus, A., O'Brien, S. G., Guilhot, F., Druker, B. J., Branford, S., Foroni, L., Goldman, J. M., Müller, M. C., Radich, J. P., Rudoltz, M., Mone, M., Gathmann, I., Hughes, T. P., and Larson, R. A. (2009) 'Six-Year Follow-Up of Patients Receiving Imatinib for the First-Line Treatment of Chronic Myeloid Leukemia'. *Leukemia* 23 (6), 1054-1061

Hochhauser, E., Leshem, D., Kaminski, O., Cheporko, Y., Vidne, B. A., and Shainberg, A. (2007) 'The Protective Effect of Prior Ischemia Reperfusion Adenosine A1 Or A3 Receptor Activation in the Normal and Hypertrophied Heart'. *Interactive CardioVascular and Thoracic Surgery* 6 (3), 363-368

Holmes, K., Roberts, O. L., Thomas, A. M., and Cross, M. J. (2007) 'Vascular Endothelial Growth Factor Receptor-2: Structure, Function, Intracellular Signalling and Therapeutic Inhibition'. *Cellular Signalling* 19 (10), 2003-2012

Horenstein, M. S., Vander Heide, R. S., and L'Ecuyer, T. J. (2000) 'Molecular Basis of Anthracycline-Induced Cardiotoxicity and its Prevention'. *Molecular Genetics and Metabolism* 71 (1–2), 436-444

Hu, S., Niu, H., Minkin, P., Orwick, S., Shimada, A., Inaba, H., Dahl, G. V., Rubnitz, J., and Baker, S. D. (2008) 'Comparison of Antitumor Effects of Multitargeted Tyrosine Kinase Inhibitors in Acute Myelogenous Leukemia'. *Molecular Cancer Therapeutics* 7 (5), 1110-1120

Huang, Q., Zhou, H. J., Zhang, H., Huang, Y., Hinojosa-Kirschenbaum, F., Fan, P., Yao, L., Belardinelli, L., Tellides, G., Giordano, F. J., Budas, G. R., and Min, W. (2015) 'Thioredoxin-2 Inhibits Mitochondrial ROS Generation and ASK1 Activity to Maintain Cardiac Function'. *Circulation* 114

Hubbard, S. R., Wei, L., Ellis, L., and Hendrickson, W. A. (1994) 'Crystal Structure of the Tyrosine Kinase Domain of the Human Insulin Receptor'. *Nature* 372 (6508), 746-754

Hullinger, T. G., Montgomery, R. L., Seto, A. G., Dickinson, B. A., Semus, H. M., Lynch, J. M., Dalby, C. M., Robinson, K., Stack, C., Latimer, P. A., Hare, J. M., Olson, E. N., and van Rooij, E. (2012) 'Inhibition of miR-15 Protects Against Cardiac Ischemic Injury'. *Circulation Research* 110 (1), 71-81

Hussain, A., Gharanei, A. M., Nagra, A. S., and Maddock, H. L. (2014) 'Caspase Inhibition Via A3 Adenosine Receptors: A New Cardioprotective Mechanism Against Myocardial Infarction'. *Cardiovascular Drugs and Therapy* 28 (1), 19-32

Hutson, T., Bukowski, R., Rini, B., Gore, M., Larkin, J., Figlin, R., Barrios, C., Escudier, B., Lin, X., and Fly, K. (2014) 'Efficacy and Safety of Sunitinib in Elderly Patients with Metastatic Renal Cell Carcinoma'. *British Journal of Cancer* 110 (5), 1125-1132

Hwang, H., Kloner, R. A., Dai, W., Simkhovich, B. Z., Kleinman, M. T., Poole, W. K., and McDonald, S. A. (2010) 'Isolated Heart Preparation'. In Comprehensive Toxicology (Second Edition). Ed by McQueen, C. A. Oxford: Elsevier, Oxford. 149-159Ichijo, H., Nishida, E., Irie, K., ten Dijke, P., Saitoh, M., Moriguchi, T., Takagi, M., Matsumoto, K.,

Miyazono, K., and Gotoh, Y. (1997) 'Induction of Apoptosis by ASK1, a Mammalian MAPKKK that Activates SAPK/JNK and p38 Signaling Pathways'. *Science (New York, N.Y.)* 275 (5296), 90-94

Ilyas, A. M., Ahmed, Y., Gari, M., Alqahtani, M. H., Kumosani, T. A., Al-Malki, A. L., Abualnaja, K. O., Albohairi, S. H., Chaudhary, A. G., and Ahmed, F. (2016) 'Sunitinib Reduces Acute Myeloid Leukemia Clonogenic Cells in Vitro and has Potent Inhibitory Effect on Sorted AML ALDH Cells'. *Open Journal of Blood Diseases* 6 (01), 9

Inoue, S., Browne, G., Melino, G., and Cohen, G. (2009) 'Ordering of Caspases in Cells Undergoing Apoptosis by the Intrinsic Pathway'. *Cell Death & Differentiation* 16 (7), 1053-1061

Iorio, M. V., Ferracin, M., Liu, C. G., Veronese, A., Spizzo, R., Sabbioni, S., Magri, E., Pedriali, M., Fabbri, M., Campiglio, M., Menard, S., Palazzo, J. P., Rosenberg, A., Musiani, P., Volinia, S., Nenci, I., Calin, G. A., Querzoli, P., Negrini, M., and Croce, C. M. (2005) 'MicroRNA Gene Expression Deregulation in Human Breast Cancer'. *Cancer Research* 65 (16), 7065-7070

Iriyama, T., Takeda, K., Nakamura, H., Morimoto, Y., Kuroiwa, T., Mizukami, J., Umeda, T., Noguchi, T., Naguro, I., Nishitoh, H., Saegusa, K., Tobiume, K., Homma, T., Shimada, Y., Tsuda, H., Aiko, S., Imoto, I., Inazawa, J., Chida, K., Kamei, Y., Kozuma, S., Taketani, Y., Matsuzawa, A., and Ichijo, H. (2009) 'ASK1 and ASK2 Differentially Regulate the Counteracting Roles of Apoptosis and Inflammation in Tumorigenesis'. *The EMBO Journal* 28 (7), 843-853

Ishikawa, K., Takenaga, K., Akimoto, M., Koshikawa, N., Yamaguchi, A., Imanishi, H., Nakada, K., Honma, Y., and Hayashi, J. (2008) 'ROS-Generating Mitochondrial DNA Mutations can Regulate Tumor Cell Metastasis'. *Science (New York, N.Y.)* 320 (5876), 661-664

Izarra, A., Moscoso, I., Levent, E., Cañón, S., Cerrada, I., Díez-Juan, A., Blanca, V., Núñez-Gil, I., Valiente, I., Ruíz-Sauri, A., Sepúlveda, P., Tiburcy, M., Zimmermann, W., and Bernad, A. (2014) 'miR-133a Enhances the Protective Capacity of Cardiac Progenitors Cells After Myocardial Infarction'. *Stem Cell Reports* 3 (6), 1029-1042

Izumiya, Y., Shiojima, I., Sato, K., Sawyer, D. B., Colucci, W. S., and Walsh, K. (2006) 'Vascular Endothelial Growth Factor Blockade Promotes the Transition from Compensatory Cardiac Hypertrophy to Failure in Response to Pressure Overload'. *Hypertension (Dallas, Tex.: 1979)* 47 (5), 887-893

Izumiya, Y., Kim, S., Izumi, Y., Yoshida, K., Yoshiyama, M., Matsuzawa, A., Ichijo, H., and Iwao, H. (2003) 'Apoptosis Signal-Regulating Kinase 1 Plays a Pivotal Role in Angiotensin II-Induced Cardiac Hypertrophy and Remodeling'. *Circulation Research* 93 (9), 874-883

Janeway, K. A., Albritton, K. H., Van Den Abbeele, Annick D, D'Amato, G. Z., Pedrazzoli, P., Siena, S., Picus, J., Butrynski, J. E., Schlemmer, M., and Heinrich, M. C. (2009) 'Sunitinib Treatment in Pediatric Patients with Advanced GIST Following Failure of Imatinib'. *Pediatric Blood & Cancer* 52 (7), 767-771

Jang, S., Zheng, C., Tsai, H., Fu, A. Z., Barac, A., Atkins, M. B., Freedman, A. N., Minasian, L., and Potosky, A. L. (2016) 'Cardiovascular Toxicity After Antiangiogenic Therapy in Persons Older than 65 Years with Advanced Renal Cell Carcinoma'. *Cancer* 122 (1), 124-130

Janicke, R. U., Sprengart, M. L., Wati, M. R., and Porter, A. G. (1998) 'Caspase-3 is Required for DNA Fragmentation and Morphological Changes Associated with Apoptosis'. *The Journal of Biological Chemistry* 273 (16), 9357-9360

Jia, B., Guo, M., Li, G., Yu, D., Zhang, X., Lan, K., and Deng, Q. (2015) 'Hepatitis B Virus Core Protein Sensitizes Hepatocytes to Tumor Necrosis Factor-Induced Apoptosis by Suppression of the Phosphorylation of Mitogen-Activated Protein Kinase Kinase 7'. *Journal of Virology* 89 (4), 2041-2051

Jiang, H., Xiao, J., Kang, B., Zhu, X., Xin, N., and Wang, Z. (2016) 'PI3K/SGK1/GSK3β Signaling Pathway is Involved in Inhibition of Autophagy in Neonatal Rat Cardiomyocytes Exposed to Hypoxia/Reoxygenation by Hydrogen Sulfide'. *Experimental Cell Research* 345 (2), 134-140

Jiang, M. T., Moffat, M. P., and Narayanan, N. (1993) 'Age-Related Alterations in the Phosphorylation of Sarcoplasmic Reticulum and Myofibrillar Proteins and Diminished Contractile Response to Isoproterenol in Intact Rat Ventricle'. *Circulation Research* 72 (1), 102-111

Joensuu, H., Trent, J.C. and Reichardt, P. (2011) 'Practical management of tyrosine kinase inhibitor-associated side effects in GIST' *Cancer treatment reviews*, *37*(1), 75-88

Hsieh, C.C., Rosenblatt, J.I. and Papaconstantinou, J. (2003) 'Age-associated changes in SAPK/JNK and p38 MAPK signaling in response to the generation of ROS by 3-nitropropionic acid' *Mechanisms of ageing and development*, *124*(6), 733-746

Kaakeh, Y., Overholser, B. R., Lopshire, J. C., and Tisdale, J. E. (2012) 'Drug-Induced Atrial Fibrillation'. *Drugs* 72 (12), 1617-1630

Kaelin Jr, W. G. (2008) 'The Von Hippel–Lindau Tumour Suppressor Protein: O2 Sensing and Cancer'. *Nature Reviews Cancer* 8 (11), 865-873

Kaiser, R. A., Liang, Q., Bueno, O., Huang, Y., Lackey, T., Klevitsky, R., Hewett, T. E., and Molkentin, J. D. (2005) 'Genetic Inhibition Or Activation of JNK1/2 Protects the Myocardium from Ischemia-Reperfusion-Induced Cell Death in Vivo'. *The Journal of Biological Chemistry* 280 (38), 32602-32608

Kalogeris, T., Baines, C. P., Krenz, M., and Korthuis, R. J. (2012) 'Cell Biology of Ischemia/Reperfusion Injury'. *International Review of Cell and Molecular Biology* 298, 229-317

Kang, W., Tong, J. H., Lung, R. W., Dong, Y., Zhao, J., Liang, Q., Zhang, L., Pan, Y., Yang, W., and Pang, J. C. (2015) 'Targeting of YAP1 by microRNA-15a and microRNA-16-1 Exerts Tumor Suppressor Function in Gastric Adenocarcinoma'. *Molecular Cancer* 14 (1), 1

Kappers, M. H., de Beer, V. J., Zhou, Z., Danser, A. H., Sleijfer, S., Duncker, D. J., van den Meiracker, A. H., and Merkus, D. (2012) 'Sunitinib-Induced Systemic Vasoconstriction in Swine is Endothelin Mediated and does Not Involve Nitric Oxide Or Oxidative Stress'. *Hypertension (Dallas, Tex.: 1979)* 59 (1), 151-157

Karaman, M. W., Herrgard, S., Treiber, D. K., Gallant, P., Atteridge, C. E., Campbell, B. T., Chan, K. W., Ciceri, P., Davis, M. I., and Edeen, P. T. (2008) 'A Quantitative Analysis of Kinase Inhibitor Selectivity'. *Nature Biotechnology* 26 (1), 127-132

Karin, M., Liu, Z., and Zandi, E. (1997) 'AP-1 Function and Regulation'. *Current Opinion in Cell Biology* 9 (2), 240-246

Katoh, M. (2016) 'FGFR Inhibitors: Effects on Cancer Cells, Tumor Microenvironment and Whole-Body Homeostasis (Review)'. *International Journal of Molecular Medicine* 38 (1), 3-15

Katori, T., Donzelli, S., Tocchetti, C. G., Miranda, K. M., Cormaci, G., Thomas, D. D., Ketner, E. A., Lee, M. J., Mancardi, D., and Wink, D. A. (2006) 'Peroxynitrite and Myocardial Contractility: In Vivo Versus in Vitro Effects'. *Free Radical Biology and Medicine* 41 (10), 1606-1618

Kazi, J. U., Kabir, N. N., and Rönnstrand, L. (2013) 'Protein Kinase C (PKC) as a Drug Target in Chronic Lymphocytic Leukemia'. *Medical Oncology* 30 (4), 1-8

Kerkela, R., Woulfe, K. C., Durand, J., Vagnozzi, R., Kramer, D., Chu, T. F., Beahm, C., Chen, M. H., and Force, T. (2009) 'Sunitinib-induced Cardiotoxicity is Mediated by Off-target Inhibition of AMP-activated Protein Kinase'. *Clinical and Translational Science* 2 (1), 15-25

Kerkelä, R., Grazette, L., Yacobi, R., Iliescu, C., Patten, R., Beahm, C., Walters, B., Shevtsov, S., Pesant, S., and Clubb, F. J. (2006) 'Cardiotoxicity of the Cancer Therapeutic Agent Imatinib Mesylate'. *Nature Medicine* 12 (8), 908-916

Khakoo, A. Y., Kassiotis, C. M., Tannir, N., Plana, J. C., Halushka, M., Bickford, C., Trent, J., Champion, J. C., Durand, J., and Lenihan, D. J. (2008) 'Heart Failure Associated with Sunitinib Malate'. *Cancer* 112 (11), 2500-2508

Kim, G. H. (2013) 'MicroRNA Regulation of Cardiac Conduction and Arrhythmias'. *Translational Research* 161 (5), 381-392

Kim, A. H., Khursigara, G., Sun, X., Franke, T. F., and Chao, M. V. (2001) 'Akt Phosphorylates and Negatively Regulates Apoptosis Signal-Regulating Kinase 1'. *Molecular and Cellular Biology* 21 (3), 893-901

Kim, H. J., Jung, K. J., Yu, B. P., Cho, C. G., and Chung, H. Y. (2002) 'Influence of Ageing and Calorie Restriction on MAPKs Activity in Rat Kidney'. *Experimental Gerontology* 37 (8–9), 1041-1053

Kim, I., Shu, C. W., Xu, W., Shiau, C. W., Grant, D., Vasile, S., Cosford, N. D., and Reed, J. C. (2009) 'Chemical Biology Investigation of Cell Death Pathways Activated by Endoplasmic Reticulum Stress Reveals Cytoprotective Modulators of ASK1'. *The Journal of Biological Chemistry* 284 (3), 1593-1603

Kim, S., Min, H., Chung, H., Park, E., Hong, J., Kang, Y., Shin, D., Jeong, L. S., and Lee, S. K. (2008) 'Inhibition of Cell Proliferation through Cell Cycle Arrest and Apoptosis by Thio-Cl-IB-MECA, a Novel A3 Adenosine Receptor Agonist, in Human Lung Cancer Cells'. *Cancer Letters* 264 (2), 309-315

Kishimoto, H., Nakagawa, K., Watanabe, T., Kitagawa, D., Momose, H., Seo, J., Nishitai, G., Shimizu, N., Ohata, S., Tanemura, S., Asaka, S., Goto, T., Fukushi, H., Yoshida, H., Suzuki, A., Sasaki, T., Wada, T., Penninger, J. M., Nishina, H., and Katada, T. (2003) 'Different Properties of SEK1 and MKK7 in Dual Phosphorylation of Stress-Induced Activated Protein Kinase SAPK/JNK in Embryonic Stem Cells'. *The Journal of Biological Chemistry* 278 (19), 16595-16601

Klein, U., Lia, M., Crespo, M., Siegel, R., Shen, Q., Mo, T., Ambesi-Impiombato, A., Califano, A., Migliazza, A., Bhagat, G., and Dalla-Favera, R. (2010) 'The DLEU2/miR-15a/16-1 Cluster Controls B Cell Proliferation and its Deletion Leads to Chronic Lymphocytic Leukemia'. *Cancer Cell* 17 (1), 28-40

Kluiver, J., Haralambieva, E., de Jong, D., Blokzijl, T., Jacobs, S., Kroesen, B., Poppema, S., and van den Berg, A. (2006) 'Lack of BIC and microRNA miR-155 Expression in Primary Cases of Burkitt Lymphoma'. *Genes, Chromosomes and Cancer* 45 (2), 147-153

Knaapen, M.W., Davies, M.J., De Bie, M., Haven, A.J., Martinet, W., and Kockx, M.M. (2001) 'Apoptotic versus autophagic cell death in heart failure'. *Cardiovascular research 51*(2), 304-312.

Kobayashi, K., Maeda, K., Takefuji, M., Kikuchi, R., Morishita, Y., Hirashima, M., and Murohara, T. (2017) 'Dynamics of Angiogenesis in Ischemic Areas of the Infarcted Heart'. *Scientific Reports* 7 (1), 7156

Kohno, Y., Sei, Y., Koshiba, M., Kim, H. O., and Jacobson, K. A. (1996) 'Induction of Apoptosis in HL-60 Human Promyelocytic Leukemia Cells by Adenosine A 3 Receptor Agonists'. *Biochemical and Biophysical Research Communications* 219 (3), 904-910

Kong, S., Liu, J., Yu, X., Lu, Y., and Zang, W. (2012) 'Protection Against Ischemia-Induced Oxidative Stress Conferred by Vagal Stimulation in the Rat Heart: Involvement of the AMPK-PKC Pathway'. *International Journal of Molecular Sciences* 13 (11), 14311-14325

Korff, S., Katus, H. A., and Giannitsis, E. (2006) 'Differential Diagnosis of Elevated Troponins'. *Heart (British Cardiac Society)* 92 (7), 987-993

Koutsoulidou, A., Mastroyiannopoulos, N. P., Furling, D., Uney, J. B., and Phylactou, L. A. (2011) 'Expression of miR-1, miR-133a, miR-133b and miR-206 Increases during Development of Human Skeletal Muscle'. *BMC Developmental Biology* 11 (1), 1

Krause, D. S. and Van Etten, R. A. (2005) 'Tyrosine Kinases as Targets for Cancer Therapy'. *N Engl J Med* 353 (2), 172-187

Kroemer, G. and Levine, B. (2008) 'Autophagic Cell Death: The Story of a Misnomer'. *Nature Reviews Molecular Cell Biology* 9 (12), 1004-1010

Krysko, D.V., Berghe, T.V., D'Herde, K., and Vandenabeele, P. (2008) 'Apoptosis and necrosis: detection, discrimination and phagocytosis'. *Methods 44*(3), 205-221

Kudo, N., Gillespie, J. G., Kung, L., Witters, L. A., Schulz, R., Clanachan, A. S., and Lopaschuk, G. D. (1996) 'Characterization of 5' AMP-Activated Protein Kinase Activity in the Heart and its Role in Inhibiting Acetyl-CoA Carboxylase during Reperfusion Following Ischemia'. *Biochimica Et Biophysica Acta (BBA)-Lipids and Lipid Metabolism* 1301 (1), 67-75

Kudo, N., Barr, A. J., Barr, R. L., Desai, S., and Lopaschuk, G. D. (1995) 'High Rates of Fatty Acid Oxidation during Reperfusion of Ischemic Hearts are Associated with a Decrease in Malonyl-CoA Levels due to an Increase in 5'-AMP-Activated Protein Kinase Inhibition of Acetyl-CoA Carboxylase'. *Journal of Biological Chemistry* 270 (29), 17513-17520

Kuhar, P., Lunder, M. and Drevenšek, G. (2007) 'The role of gender and sex hormones in ischemic–reperfusion injury in isolated rat hearts'. *European journal of pharmacology*. *561*(1), 51-159

Lagranha, C.J., Deschamps, A., Aponte, A., Steenbergen, C. and Murphy, E. (2010) 'Sex differences in the phosphorylation of mitochondrial proteins result in reduced production of reactive oxygen species and cardioprotection in females'. *Circulation research. 106*(11) 1681-1691

Lange, S., Gehmlich, K., Lun, A. S., Blondelle, J., Hooper, C., Dalton, N. D., Alvarez, E. A., Zhang, X., Bang, M., and Abassi, Y. A. (2016) 'MLP and CARP are Linked to Chronic PKC [Alpha] Signalling in Dilated Cardiomyopathy'. *Nature Communications* 7

Langendorff, O. (1895) 'Untersuchungen Am Überlebenden Säugethierherzen'. *Pflügers Archiv European Journal of Physiology* 61 (6), 291-332

Lavine, K. J., White, A. C., Park, C., Smith, C. S., Choi, K., Long, F., Hui, C. C., and Ornitz, D. M. (2006) 'Fibroblast Growth Factor Signals Regulate a Wave of Hedgehog Activation that is Essential for Coronary Vascular Development'. *Genes & Development* 20 (12), 1651-1666

Le Tourneau, C., Raymond, E., and Faivre, S. (2007) 'Sunitinib: A Novel Tyrosine Kinase Inhibitor. A Brief Review of its Therapeutic Potential in the Treatment of Renal

Carcinoma and Gastrointestinal Stromal Tumors (GIST)'. *Therapeutics and Clinical Risk Management* 3 (2), 341

Lee, E. J., Gusev, Y., Jiang, J., Nuovo, G. J., Lerner, M. R., Frankel, W. L., Morgan, D. L., Postier, R. G., Brackett, D. J., and Schmittgen, T. D. (2007) 'Expression Profiling Identifies microRNA Signature in Pancreatic Cancer'. *International Journal of Cancer* 120 (5), 1046-1054

Lee, Y. (2010) 'To Proliferate Or Not to Proliferate'. *Cardiovascular Research* 3 (86), 347-348

Lee, E., Min, H., Chung, H., Park, E., Shin, D., Jeong, L. S., and Lee, S. K. (2005) 'A Novel Adenosine Analog, Thio-Cl-IB-MECA, Induces G0/G1 Cell Cycle Arrest and Apoptosis in Human Promyelocytic Leukemia HL-60 Cells'. *Biochemical Pharmacology* 70 (6), 918-924

Lemmon, M. A. and Schlessinger, J. (2010) 'Cell Signaling by Receptor Tyrosine Kinases'. *Cell* 141 (7), 1117-1134

Lenihan, D. J. and Cardinale, D. M. (2012) 'Late Cardiac Effects of Cancer Treatment'. *Journal of Clinical Oncology* 30 (30), 3657-3664

Leung, C. H., Wang, L., Nielsen, J. M., Tropak, M. B., Fu, Y. Y., Kato, H., Callahan, J., Redington, A. N., and Caldarone, C. A. (2014) 'Remote Cardioprotection by Transfer of Coronary Effluent from Ischemic Preconditioned Rabbit Heart Preserves Mitochondrial Integrity and Function Via Adenosine Receptor Activation'. *Cardiovascular Drugs and Therapy* 28 (1), 7-17

Levy, J., Zhou, D., and Zippin, J. (2016) 'Cyclic Adenosine Monophosphate Signaling in Inflammatory Skin Disease'. *J Clin Exp Dermatol Res* 7 (326), 2

Li, J., Ning, Y., Hedley, W., Saunders, B., Chen, Y., Tindill, N., Hannay, T., and Subramaniam, S. (2002) 'The Molecule Pages Database'. *Nature* 420 (6916), 716-717

Li, X., Liu, M., Sun, R., Zeng, Y., Chen, S., and Zhang, P. (2016) 'Cardiac Complications in Cancer Treatment- a Review'. *Hellenic Journal of Cardiology*

Lin, S. and Gregory, R. I. (2015) 'MicroRNA Biogenesis Pathways in Cancer'. *Nature Reviews Cancer* 15 (6), 321-333

Linton, P., Gurney, M., Sengstock, D., Mentzer Jr., R. M., and Gottlieb, R. A. (2015) 'This Old Heart: Cardiac Ageing and Autophagy'. *Journal of Molecular and Cellular Cardiology* 83, 44-54

Lipshultz, S. E., Lipsitz, S. R., Sallan, S. E., Simbre, V. C., Shaikh, S. L., Mone, S. M., Gelber, R. D., and Colan, S. D. (2002) 'Long-Term Enalapril Therapy for Left Ventricular Dysfunction in Doxorubicin-Treated Survivors of Childhood Cancer'. *Journal of Clinical Oncology* 20 (23), 4517-4522

Lipshultz, S. E., Adams, M. J., Colan, S. D., Constine, L. S., Herman, E. H., Hsu, D. T., Hudson, M. M., Kremer, L. C., Landy, D. C., Miller, T. L., Oeffinger, K. C., Rosenthal, D. N., Sable, C. A., Sallan, S. E., Singh, G. K., Steinberger, J., Cochran, T. R., Wilkinson, J. D., and American Heart Association Congenital Heart Defects Committee of the Council on Cardiovascular Disease in the Young, Council on Basic Cardiovascular Sciences, Council on Cardiovascular and Stroke Nursing, Council on Cardiovascular Radiolo (2013) 'Long-Term Cardiovascular Toxicity in Children, Adolescents, and Young Adults Who Receive Cancer Therapy: Pathophysiology, Course, Monitoring, Management, Prevention, and Research Directions: A Scientific Statement from the American Heart Association'. *Circulation* 128 (17), 1927-1995

Liu, W., Zi, M., Chi, H., Jin, J., Prehar, S., Neyses, L., Cartwright, E. J., Flavell, R. A., Davis, R. J., and Wang, X. (2011) 'Deprivation of MKK7 in Cardiomyocytes Provokes Heart Failure in Mice when Exposed to Pressure Overload'. *Journal of Molecular and Cellular Cardiology* 50 (4), 702-711

Liu, G. S., Richards, S. C., Olsson, R. A., Mullane, K., Walsh, R. S., and Downey, J. M. (1994) 'Evidence that the Adenosine A3 Receptor may Mediate the Protection Afforded by Preconditioning in the Isolated Rabbit Heart'. *Cardiovascular Research* 28 (7), 1057-1061

Liu, N., Bezprozvannaya, S., Williams, A. H., Qi, X., Richardson, J. A., Bassel-Duby, R., and Olson, E. N. (2008) 'microRNA-133a Regulates Cardiomyocyte Proliferation and Suppresses Smooth Muscle Gene Expression in the Heart'. *Genes & Development* 22 (23), 3242-3254

Liu, Q., Sargent, M. A., York, A. J., and Molkentin, J. D. (2009) 'ASK1 Regulates Cardiomyocyte Death but Not Hypertrophy in Transgenic Mice'. *Circulation Research* 105 (11), 1110-1117

Liu, Y. and Min, W. (2002) 'Thioredoxin Promotes ASK1 Ubiquitination and Degradation to Inhibit ASK1-Mediated Apoptosis in a Redox Activity-Independent Manner'. *Circulation Research* 90 (12), 1259-1266

Lu, M., Zhang, Q., Deng, M., Miao, J., Guo, Y., Gao, W., and Cui, Q. (2008) 'An Analysis of Human microRNA and Disease Associations'. *PloS One* 3 (10), e3420

Luo, Y., Gao, S., Hao, Z., Yang, Y., Xie, S., Li, D., Liu, M., and Zhou, J. (2016) 'Apoptosis Signal-Regulating Kinase 1 Exhibits Oncogenic Activity in Pancreatic Cancer'. *Oncotarget* 7 (46), 75155-75164

Luo, X., Lin, H., Pan, Z., Xiao, J., Zhang, Y., Lu, Y., Yang, B., and Wang, Z. (2008) 'Down-Regulation of miR-1/miR-133 Contributes to Re-Expression of Pacemaker Channel Genes HCN2 and HCN4 in Hypertrophic Heart'. *Journal of Biological Chemistry* 283 (29), 20045-20052

Lupón, J., Domingo, M., de Antonio, M., Zamora, E., Santesmases, J., Díez-Quevedo, C., Altimir, S., Troya, M., Gastelurrutia, P., and Bayes-Genis, A. (2015) 'Ageing and Heart

Rate in Heart Failure: Clinical Implications for Long-Term Mortality'. *Mayo Clinic Proceedings* 90 (6), 765-772

MacLellan, W. R. and Schneider, M. D. (2000) 'Genetic Dissection of Cardiac Growth Control Pathways'. *Annual Review of Physiology* 62 (1), 289-320

Maddock, H. L., Gardner, N. M., Khandoudi, N., Bril, A., and Broadley, K. J. (2003) 'Protection from Myocardial Stunning by Ischaemia and Hypoxia with the Adenosine A 3 Receptor Agonist, IB-MECA'. *European Journal of Pharmacology* 477 (3), 235-245

Maddock, H. L., Broadley, K. J., Bril, A., and Khandoudi, N. (2002) 'Effects of Adenosine Receptor Agonists on Guinea-pig Isolated Working Hearts and the Role of Endothelium and NO'. *Journal of Pharmacy and Pharmacology* 54 (6), 859-867

Maddock, H. L., Mocanu, M. M., and Yellon, D. M. (2002) 'Adenosine A(3) Receptor Activation Protects the Myocardium from Reperfusion/Reoxygenation Injury'. *American Journal of Physiology.Heart and Circulatory Physiology* 283 (4), H1307-13

Madhusudan, S. and Ganesan, T. S. (2004) 'Tyrosine Kinase Inhibitors in Cancer Therapy'. *Clinical Biochemistry* 37 (7), 618-635

Mair, J., Morandell, D., Genser, N., Lechleitner, P., Dienstl, F., and Puschendorf, B. (1995) 'Equivalent Early Sensitivities of Myoglobin, Creatine Kinase MB Mass, Creatine Kinase Isoform Ratios, and Cardiac Troponins I and T for Acute Myocardial Infarction'. *Clinical Chemistry* 41 (9), 1266-1272

Marfella, R., Di Filippo, C., Potenza, N., Sardu, C., Rizzo, M. R., Siniscalchi, M., Musacchio, E., Barbieri, M., Mauro, C., Mosca, N., Solimene, F., Mottola, M. T., Russo, A., Rossi, F., Paolisso, G., and D'Amico, M. (2013) 'Circulating microRNA Changes in Heart Failure Patients Treated with Cardiac Resynchronization Therapy: Responders Vs. Non-Responders'. *European Journal of Heart Failure* 15 (11), 1277-1288

Marques, F. Z., Vizi, D., Khammy, O., Mariani, J. A., and Kaye, D. M. (2016) 'The Transcardiac Gradient of cardio-microRNAs in the Failing Heart'. *European Journal of Heart Failure*

Martinez-Vicente, M., Sovak, G., and Cuervo, A. M. (2005) 'Protein Degradation and Ageing'. *Experimental Gerontology* 40 (8–9), 622-633

Matsumoto, M., Roufail, S., Inder, R., Caesar, C., Karnezis, T., Shayan, R., Farnsworth, R. H., Sato, T., Achen, M. G., and Mann, G. B. (2013) 'Signaling for Lymphangiogenesis Via VEGFR-3 is Required for the Early Events of Metastasis'. *Clinical & Experimental Metastasis* 30 (6), 819-832

Matsumoto, S., Sakata, Y., Nakatani, D., Suna, S., Mizuno, H., Shimizu, M., Usami, M., Sasaki, T., Sato, H., Kawahara, Y., Hamasaki, T., Nanto, S., Hori, M., and Komuro, I. (2012) 'A Subset of Circulating microRNAs are Predictive for Cardiac Death After Discharge for Acute Myocardial Infarction'. *Biochemical and Biophysical Research Communications* 427 (2), 280-284

McIntosh, V. J. and Lasley, R. D. (2012) 'Adenosine Receptor-Mediated Cardioprotection: Are all 4 Subtypes Required Or Redundant?'. *Journal of Cardiovascular Pharmacology and Therapeutics* 17 (1), 21-33

Melani, A., Cipriani, S., Vannucchi, M. G., Nosi, D., Donati, C., Bruni, P., Giovannini, M. G., and Pedata, F. (2009) 'Selective Adenosine A2a Receptor Antagonism Reduces JNK Activation in Oligodendrocytes After Cerebral Ischaemia'. *Brain : A Journal of Neurology* 132 (Pt 6), 1480-1495

Mendel, D. B., Laird, A. D., Xin, X., Louie, S. G., Christensen, J. G., Li, G., Schreck, R. E., Abrams, T. J., Ngai, T. J., Lee, L. B., Murray, L. J., Carver, J., Chan, E., Moss, K. G., Haznedar, J. O., Sukbuntherng, J., Blake, R. A., Sun, L., Tang, C., Miller, T., Shirazian, S., McMahon, G., and Cherrington, J. M. (2003) 'In Vivo Antitumor Activity of SU11248, a Novel Tyrosine Kinase Inhibitor Targeting Vascular Endothelial Growth Factor and Platelet-Derived Growth Factor Receptors: Determination of a Pharmacokinetic/Pharmacodynamic Relationship'. *Clinical Cancer Research : An Official Journal of the American Association for Cancer Research* 9 (1), 327-337

Merhautova, J., Hezova, R., Poprach, A., Kovarikova, A., Radova, L., Svoboda, M., Vyzula, R., Demlova, R., and Slaby, O. (2015) 'miR-155 and miR-484 are Associated with Time to Progression in Metastatic Renal Cell Carcinoma Treated with Sunitinib'. *BioMed Research International* 2015, 941980

Merighi, S., Benini, A., Mirandola, P., Gessi, S., Varani, K., Leung, E., MacLennan, S., Baraldi, P. G., and Borea, P. A. (2006) 'Modulation of the Akt/Ras/Raf/MEK/ERK Pathway by A3 Adenosine Receptor'. *Purinergic Signalling* 2 (4), 627-632

Miller, R. A., Chu, Q., Xie, J., Foretz, M., Viollet, B., and Birnbaum, M. J. (2013) 'Biguanides Suppress Hepatic Glucagon Signalling by Decreasing Production of Cyclic AMP'. *Nature* 494 (7436), 256-260

Minden, A. and Karin, M. (1997) 'Regulation and Function of the JNK Subgroup of MAP Kinases'. *Biochimica Et Biophysica Acta (BBA) - Reviews on Cancer* 1333 (2), F85-F104

Mitchell, S., Ota, A., Foster, W., Zhang, B., Fang, Z., Patel, S., Nelson, S. F., Horvath, S., and Wang, Y. (2006) 'Distinct Gene Expression Profiles in Adult Mouse Heart Following Targeted MAP Kinase Activation'. *Physiological Genomics* 25 (1), 50-59

Monsuez, J., Charniot, J., Vignat, N., and Artigou, J. (2010) 'Cardiac Side-Effects of Cancer Chemotherapy'. *International Journal of Cardiology* 144 (1), 3-15

Moon, J. and Park, S. (2014) 'Reassembly of JIP1 Scaffold Complex in JNK MAP Kinase Pathway using Heterologous Protein Interactions' *PloS one*, *9*(5), e96797

Mooney, L., Skinner, M., Coker, S., and Currie, S. (2015) 'Effects of Acute and Chronic Sunitinib Treatment on Cardiac Function and Calcium/Calmodulin-dependent Protein Kinase II'. *British Journal of Pharmacology* 172 (17), 4342-4354

Morganroth, J. (2007) 'Cardiac Repolarization and the Safety of New Drugs Defined by Electrocardiography'. *Clinical Pharmacology & Therapeutics* 81 (1), 108-113

Morita, N., Sovari, A. A., Xie, Y., Fishbein, M. C., Mandel, W. J., Garfinkel, A., Lin, S., Chen, P., Xie, L., Chen, F., Qu, Z., Weiss, J. N., and Karagueuzian, H. S. (2009) 'Increased Susceptibility of Aged Hearts to Ventricular Fibrillation during Oxidative Stress'. *American Journal of Physiology - Heart and Circulatory Physiology* 297 (5), H1594-H1605

Morita, K., Saitoh, M., Tobiume, K., Matsuura, H., Enomoto, S., Nishitoh, H., and Ichijo, H. (2001) 'Negative Feedback Regulation of ASK1 by Protein Phosphatase 5 (PP5) in Response to Oxidative Stress'. *The EMBO Journal* 20 (21), 6028-6036

Motzer, R. J., Michaelson, M. D., Redman, B. G., Hudes, G. R., Wilding, G., Figlin, R. A., Ginsberg, M. S., Kim, S. T., Baum, C. M., DePrimo, S. E., Li, J. Z., Bello, C. L., Theuer, C. P., George, D. J., and Rini, B. I. (2006) 'Activity of SU11248, a Multitargeted Inhibitor of Vascular Endothelial Growth Factor Receptor and Platelet-Derived Growth Factor Receptor, in Patients with Metastatic Renal Cell Carcinoma'. *Journal of Clinical Oncology* 24 (1), 16-24

Moyzis, A. G., Sadoshima, J., and Gustafsson, A. B. (2015) 'Mending a Broken Heart: The Role of Mitophagy in Cardioprotection'. *American Journal of Physiology.Heart and Circulatory Physiology* 308 (3), H183-92

Mughal, W., Dhingra, R., and Kirshenbaum, L. A. (2012) 'Striking a Balance: Autophagy, Apoptosis, and Necrosis in a Normal and Failing Heart'. *Current Hypertension Reports* 14 (6), 540-547

Munzel, T., Gori, T., Keaney, J. F.,Jr, Maack, C., and Daiber, A. (2015) 'Pathophysiological Role of Oxidative Stress in Systolic and Diastolic Heart Failure and its Therapeutic Implications'. *European Heart Journal* 36 (38), 2555-2564

Nako, H., Kataoka, K., Koibuchi, N., Dong, Y., Toyama, K., Yamamoto, E., Yasuda, O., Ichijo, H., Ogawa, H., and Kim-Mitsuyama, S. (2012) 'Novel Mechanism of Angiotensin II-Induced Cardiac Injury in Hypertensive Rats: The Critical Role of ASK1 and VEGF'. *Hypertension Research* 35 (2), 194-200

Narayan, V., Keefe, S. M., Haas, N., Wang, L., Puzanov, I., Putt, M. E., Catino, A., Fang, J., Agarwal, N., Hyman, D., Smith, A. M., Finkelman, B. S., Narayan, H. K., Ewer, S., ElAmm, C., Lenihan, D. J., and Ky, B. (2017) 'Prospective Evaluation of Sunitinib-Induced Cardiotoxicity in Patients with Metastatic Renal Cell Carcinoma'. *Clinical Cancer Research.*

Newton, A. C. (2001) 'Protein Kinase C: Structural and Spatial Regulation by Phosphorylation, Cofactors, and Macromolecular Interactions'. *Chemical Reviews* 101 (8), 2353-2364

Nishi, H., Ono, K., Horie, T., Nagao, K., Kinoshita, M., Kuwabara, Y., Watanabe, S., Takaya, T., Tamaki, Y., Takanabe-Mori, R., Wada, H., Hasegawa, K., Iwanaga, Y., Kawamura, T., Kita, T., and Kimura, T. (2011) 'MicroRNA-27a Regulates Beta Cardiac Myosin Heavy Chain Gene Expression by Targeting Thyroid Hormone Receptor ß1 in Neonatal Rat Ventricular Myocytes'. *Molecular and Cellular Biology* 31 (4), 744-755

Nishioka, C., Ikezoe, T., Yang, J., and Yokoyama, A. (2009) 'Sunitinib, an Orally Available Receptor Tyrosine Kinase Inhibitor, Induces Monocytic Differentiation of Acute Myelogenous Leukemia Cells that is Enhanced by 1, 25-Dihydroxyvitamin D3'. *Leukemia* 23 (11), 2171-2173

Nomura, K., Lee, M., Banks, C., Lee, G., and Morris, B. J. (2013) 'An ASK1-p38 Signalling Pathway Mediates Hydrogen Peroxide-Induced Toxicity in NG108-15 Neuronal Cells'. *Neuroscience Letters* 549 (0), 163-167

O'Hayre, M., Degese, M. S., and Gutkind, J. S. (2014) 'Novel Insights into G Protein and G Protein-Coupled Receptor Signaling in Cancer'. *Current Opinion in Cell Biology* 27, 126-135

Oeffinger, K. C., Mertens, A. C., Sklar, C. A., Kawashima, T., Hudson, M. M., Meadows, A. T., Friedman, D. L., Marina, N., Hobbie, W., and Kadan-Lottick, N. S. (2006) 'Chronic Health Conditions in Adult Survivors of Childhood Cancer'. *New England Journal of Medicine* 355 (15), 1572-1582

O'Farrell, A. M., Abrams, T. J., Yuen, H. A., Ngai, T. J., Louie, S. G., Yee, K. W., Wong, L. M., Hong, W., Lee, L. B., Town, A., Smolich, B. D., Manning, W. C., Murray, L. J., Heinrich, M. C., and Cherrington, J. M. (2003) 'SU11248 is a Novel FLT3 Tyrosine Kinase Inhibitor with Potent Activity in Vitro and in Vivo'. *Blood* 101 (9), 3597-3605

Oka, T., Akazawa, H., Naito, A. T., and Komuro, I. (2014) 'Angiogenesis and Cardiac Hypertrophy: Maintenance of Cardiac Function and Causative Roles in Heart Failure'. *Circulation Research* 114 (3), 565-571

Olejnickova, V., Novakova, M., and Provaznik, I. (2015) 'Isolated heart models: cardiovascular system studies and technological advances'. *Medical & biological engineering & computing 53*(7), 669-678.

Oliva, J. L., Caino, M. C., Senderowicz, A. M., and Kazanietz, M. G. (2008) 'S-Phase-Specific Activation of PKCa Induces Senescence in Non-Small Cell Lung Cancer Cells'. *Journal of Biological Chemistry* 283 (9), 5466-5476

Oliva, S., Cioffi, G., Frattini, S., Simoncini, E. L., Faggiano, P., Boccardi, L., Pulignano, G., Fioretti, A. M., Giotta, F., Lestuzzi, C., Maurea, N., Sabatini, S., Tarantini, L., and Italian Cardio-Oncological Network (2012) 'Administration of Angiotensin-Converting Enzyme Inhibitors and Beta-Blockers during Adjuvant Trastuzumab Chemotherapy for Nonmetastatic Breast Cancer: Marker of Risk Or Cardioprotection in the Real World?'. *The Oncologist* 17 (7), 917-924

Omura, T., Yoshiyama, M., Yoshida, K., Nakamura, Y., Kim, S., Iwao, H., Takeuchi, K., and Yoshikawa, J. (2002) 'Dominant Negative Mutant of C-Jun Inhibits Cardiomyocyte Hypertrophy Induced by Endothelin 1 and Phenylephrine'. *Hypertension* 39 (1), 81-86

Onakpoya, I. J., Heneghan, C. J., and Aronson, J. K. (2016) 'Post-Marketing Withdrawal of 462 Medicinal Products because of Adverse Drug Reactions: A Systematic Review of the World Literature'. *BMC Medicine* 14 (1), 1

Osawa, T. and Shibuya, M. (2013) . *Targeting Cancer Cells Resistant to Hypoxia and Nutrient Starvation to Improve Anti-Angiogeneic Therapy*

Otrock, Z. K., Makarem, J. A., and Shamseddine, A. I. (2007) 'Vascular Endothelial Growth Factor Family of Ligands and Receptors: Review'. *Blood Cells, Molecules, and Diseases* 38 (3), 258-268

Ovchinnikova, E. S., Schmitter, D., Vegter, E. L., Ter Maaten, J. M., Valente, M. A., Liu, L. C., van der Harst, P., Pinto, Y. M., de Boer, R. A., and Meyer, S. (2015) 'Signature of Circulating microRNAs in Patients with Acute Heart Failure'. *European Journal of Heart Failure*, *17*, 119

Pai, V. B. and Nahata, M. C. (2000) 'Cardiotoxicity of Chemotherapeutic Agents'. *Drug Safety* 22 (4), 263-302

Pan, Y., Wang, Y., Zhao, Y., Peng, K., Li, W., Wang, Y., Zhang, J., Zhou, S., Liu, Q., Li, X., Cai, L., and Liang, G. (2014) 'Inhibition of JNK Phosphorylation by a Novel Curcumin Analog Prevents High Glucose-Induced Inflammation and Apoptosis in Cardiomyocytes and the Development of Diabetic Cardiomyopathy'. *Diabetes* 63 (10), 3497-3511

Papadopoulos, E. I., Yousef, G. M., and Scorilas, A. (2015) 'Cytotoxic Activity of Sunitinib and Everolimus in Caki-1 Renal Cancer Cells is Accompanied by Modulations in the Expression of Apoptosis-Related microRNA Clusters and BCL2 Family Genes'. *Biomedicine & Pharmacotherapy* 70, 33-40

Parikh, J.D., Hollingsworth, K.G., Wallace, D., Blamire, A.M. and MacGowan, G.A. (2016) 'Normal age-related changes in left ventricular function: Role of afterload and subendocardial dysfunction.' *International journal of cardiology 223*, 306-312.

Park, G. B., Kim, Y. S., Lee, H., Yang, J. W., Kim, D., and Hur, D. Y. (2016) 'ASK1/JNK-Mediated TAp63 Activation Controls the Cell Survival Signal of Baicalein-Treated EBV-Transformed B Cells'. *Molecular and Cellular Biochemistry* 412 (1-2), 247-258

Park, S. S., Zhao, H., Jang, Y., Mueller, R. A., and Xu, Z. (2006) 'N6-(3-Iodobenzyl)-Adenosine-5'-N-Methylcarboxamide Confers Cardioprotection at Reperfusion by Inhibiting Mitochondrial Permeability Transition Pore Opening Via Glycogen Synthase Kinase 3 Beta'. *The Journal of Pharmacology and Experimental Therapeutics* 318 (1), 124-131

Parker, P. J. and Murray-Rust, J. (2004) 'PKC at a Glance'. *Journal of Cell Science* 117 (Pt 2), 131-132

Pawson, T. (1995) 'Protein Modules and Signalling Networks' *Nature*, *373*(6515), 573

Peart, J. N., Pepe, S., Reichelt, M. E., Beckett, N., See Hoe, L., Ozberk, V., Niesman, I. R., Patel, H. H., and Headrick, J. P. (2014) 'Dysfunctional Survival-Signaling and Stress-Intolerance in Aged Murine and Human Myocardium'. *Experimental Gerontology* 50, 72-81

Pérez, V. I., Bokov, A., Remmen, H. V., Mele, J., Ran, Q., Ikeno, Y., and Richardson, A. (2009) 'Is the Oxidative Stress Theory of Ageing Dead?'. *Biochimica Et Biophysica Acta (BBA) - General Subjects* 1790 (10), 1005-1014

Petrich, B. G. and Wang, Y. (2004) 'Stress-Activated MAP Kinases in Cardiac Remodeling and Heart Failure: New Insights from Transgenic Studies'. *Trends in Cardiovascular Medicine* 14 (2), 50-55

Petrich, B. G., Molkentin, J. D., and Wang, Y. (2003) 'Temporal Activation of C-Jun N-Terminal Kinase in Adult Transgenic Heart Via Cre-loxP-Mediated DNA Recombination'. *FASEB Journal : Official Publication of the Federation of American Societies for Experimental Biology* 17 (6), 749-751

Pfizer Inc. SUTENT® (sunitinib malate) prescribing information. Available from URL:

http://labeling.pfizer.com/showlabeling.aspx?id=607 2017

Poole, A. W., Pula, G., Hers, I., Crosby, D., and Jones, M. L. (2004) 'PKC-Interacting Proteins: From Function to Pharmacology'. *Trends in Pharmacological Sciences* 25 (10), 528-535

Porta, C., Paglino, C., Imarisio, I., Ganini, C., Sacchi, L., Quaglini, S., Giunta, V., and and De Amici, M. (2013) 'Changes in Circulating Pro-Angiogenic Cytokines, Other than VEGF, before Progression to Sunitinib Therapy in Advanced Renal Cell Carcinoma Patients'. *Oncology* 84, 115-122

Porta, C., Gore, M. E., Rini, B. I., Escudier, B., Hariharan, S., Charles, L. P., Yang, L., DeAnnuntis, L., and Motzer, R. J. (2016) 'Long-Term Safety of Sunitinib in Metastatic Renal Cell Carcinoma'. *European Urology* 69 (2), 345-351

Porter, A. C. and Vaillancourt, R. R. (1998) 'Tyrosine Kinase Receptor-Activated Signal Transduction Pathways which Lead to Oncogenesis.'. *Oncogene* 17 (11)

Poulose, N. and Raju, R. (2014) 'Ageing and Injury: Alterations in Cellular Energetics and Organ Function'. *Ageing and Disease* 5 (2), 101-108

Prabhakar, N.R., and Semenza, G.L. (2015) 'Oxygen sensing and homeostasis'. *Physiology 30*(5), 340-348Prakash, S., Sarran, L., Socci, N., DeMatteo, R. P., Eisenstat, J., Greco, A. M., Maki, R. G., Wexler, L. H., LaQuaglia, M. P., Besmer, P., and Antonescu, C. R. (2005) 'Gastrointestinal Stromal Tumors in Children and Young Adults: A Clinicopathologic, Molecular, and Genomic Study of 15 Cases and Review of the Literature'. *Journal of Pediatric Hematology/Oncology* 27 (4), 179-187

Rahman, M. M., Sykiotis, G. P., Nishimura, M., Bodmer, R., and Bohmann, D. (2013) 'Declining Signal Dependence of Nrf2-MafS-regulated Gene Expression Correlates with Ageing Phenotypes'. *Ageing Cell* 12 (4), 554-562

Rainer, P. P., Doleschal, B., Kirk, J. A., Sivakumaran, V., Saad, Z., Groschner, K., Maechler, H., Hoefler, G., Bauernhofer, T., and Samonigg, H. (2012) 'Sunitinib Causes Dose-dependent Negative Functional Effects on Myocardium and Cardiomyocytes'. *BJU International* 110 (10), 1455-1462

Rakkar, K. and Bayraktutan, U. (2016) 'Increases in Intracellular Calcium Perturb Blood–brain Barrier Via Protein Kinase C-Alpha and Apoptosis'. *Biochimica Et Biophysica Acta (BBA) - Molecular Basis of Disease* 1862 (1), 56-71

Ralevic, V. and Burnstock, G. (1998) 'Receptors for Purines and Pyrimidines'. *Pharmacological Reviews* 50 (3), 413-492

Raman, M., Chen, W., and Cobb, M. (2007) 'Differential Regulation and Properties of MAPKs'. *Oncogene* 26 (22), 3100-3112

Ramasamy, S., Velmurugan, G., Rajan, K. S., Ramprasath, T., and Kalpana, K. (2015) 'MiRNAs with Apoptosis Regulating Potential are Differentially Expressed in Chronic Exercise-Induced Physiologically Hypertrophied Hearts'. *PloS One* 10 (3), e0121401

Ramo, K., Sugamura, K., Keaney, J. F., and Davis, R. J. (2014) 'Endothelial JNK is Critically Required for Native Collateral Artery Development', A330-A330

Raschi, E. and De Ponti, F. (2012) 'Cardiovascular Toxicity of Anticancer-Targeted Therapy: Emerging Issues in the Era of Cardio-Oncology'. *Internal and Emergency Medicine* 7 (2), 113-131

Raschi, E., Vasina, V., Ursino, M. G., Boriani, G., Martoni, A., and De Ponti, F. (2010) 'Anticancer Drugs and Cardiotoxicity: Insights and Perspectives in the Era of Targeted Therapy'. *Pharmacology & Therapeutics* 125 (2), 196-218

Reddy, K. B. (2015) 'MicroRNA (miRNA) in Cancer'. *Cancer Cell International* 15 (1), 38

Remko, M., Bohác, A., and Kováciková, L. (2011) 'Molecular Structure, pKa, Lipophilicity, Solubility, Absorption, Polar Surface Area, and Blood Brain Barrier Penetration of some Antiangiogenic Agents'. *Structural Chemistry* 22 (3), 635-648

Révész, D., Verhoeven, J. E., Milaneschi, Y., de Geus, E. J., Wolkowitz, O. M., and Penninx, B. W. (2014) 'Dysregulated Physiological Stress Systems and Accelerated Cellular Ageing'. *Neurobiology of Ageing* 35 (6), 1422-1430

Richards, C. J., Je, Y., Schutz, F. A., Heng, D. Y., Dallabrida, S. M., Moslehi, J. J., and Choueiri, T. K. (2011) 'Incidence and Risk of Congestive Heart Failure in Patients with Renal and Nonrenal Cell Carcinoma Treated with Sunitinib'. *Journal of Clinical Oncology* 29 (25), 3450-3456

Riley, P. R. and Smart, N. (2011) 'Vascularizing the Heart'. *Cardiovascular Research* 91 (2), 260-268

Rini, B. I. (2007) 'Vascular Endothelial Growth Factor-Targeted Therapy in Renal Cell Carcinoma: Current Status and Future Directions'. *Clinical Cancer Research* 13 (4), 1098-1106

Robertson, S. C., Tynan, J. A., and Donoghue, D. J. (2000) 'RTK Mutations and Human Syndromes: When Good Receptors Turn Bad'. *Trends in Genetics* 16 (6), 265-271

Robinson, D. R., Wu, Y. M., and Lin, S. F. (2000) 'The Protein Tyrosine Kinase Family of the Human Genome'. *Oncogene* 19 (49), 5548-5557

Roccaro, A. M., Sacco, A., Thompson, B., Leleu, X., Azab, A. K., Azab, F., Runnels, J., Jia, X., Ngo, H. T., Melhem, M. R., Lin, C. P., Ribatti, D., Rollins, B. J., Witzig, T. E., Anderson, K. C., and Ghobrial, I. M. (2009) 'MicroRNAs 15a and 16 Regulate Tumor Proliferation in Multiple Myeloma'. *Blood* 113 (26), 6669-6680

Rodriguez, A., Vigorito, E., Clare, S., Warren, M. V., Couttet, P., Soond, D. R., Van Dongen, S., Grocock, R. J., Das, P. P., Miska, E. A., Vetrie, D., Okkenhaug, K., Enright, A. J., Dougan, G., Turner, M., and Bradley, A. (2007) 'Requirement of Bic/microRNA-155 for Normal Immune Function'. *Science* 316 (5824), 608-611

Rohacs, T. (2013) 'Regulation of Transient Receptor Potential Channels by the Phospholipase C Pathway'. *Advances in Biological Regulation* 53 (3), 341-355

Roos, W. P. and Kaina, B. (2013) 'DNA Damage-Induced Cell Death: From Specific DNA Lesions to the DNA Damage Response and Apoptosis'. *Cancer Letters* 332 (2), 237-248

Rose, B. A., Force, T., and Wang, Y. (2010) 'Mitogen-Activated Protein Kinase Signaling in the Heart: Angels Versus Demons in a Heart-Breaking Tale'. *Physiological Reviews* 90 (4), 1507-1546

Rosenbaum, D. M., Rasmussen, S. G., and Kobilka, B. K. (2009) 'The Structure and Function of G-Protein-Coupled Receptors'. *Nature* 459 (7245), 356-363

Rosenkranz, S. (2004) 'TGF-ß1 and Angiotensin Networking in Cardiac Remodeling'. *Cardiovascular Research* 63 (3), 423-432

Rosette, C. and Karin, M. (1996) 'Ultraviolet Light and Osmotic Stress: Activation of the JNK Cascade through Multiple Growth Factor and Cytokine Receptors'. *Science (New York, N.Y.)* 274 (5290), 1194-1197

Roskoski Jr., R. (2007) 'Sunitinib: A VEGF and PDGF Receptor Protein Kinase and Angiogenesis Inhibitor'. *Biochemical and Biophysical Research Communications* 356 (2), 323-328

Roskoski, R. (2007) 'Sunitinib: A VEGF and PDGF Receptor Protein Kinase and Angiogenesis Inhibitor'. *Biochemical and Biophysical Research Communications* 356 (2), 323-328

Rowntree, C., Duke, V., Panayiotidis, P., Kotsi, P., Palmisano, G., Hoffbrand, A., and Foroni, L. (2002) 'Deletion Analysis of Chromosome 13q14. 3 and Characterisation of an Alternative Splice Form of LEU1 in B Cell Chronic Lymphocytic Leukemia'. *Leukemia* 16 (7), 1267

Saitoh, M., Nishitoh, H., Fujii, M., Takeda, K., Tobiume, K., Sawada, Y., Kawabata, M., Miyazono, K., and Ichijo, H. (1998) 'Mammalian Thioredoxin is a Direct Inhibitor of Apoptosis Signal-regulating Kinase (ASK) 1'. *The EMBO Journal* 17 (9), 2596-2606

Sandhu, H., Ansar, S., and Edvinsson, L. (2010) 'Comparison of MEK/ERK Pathway Inhibitors on the Upregulation of Vascular G-Protein Coupled Receptors in Rat Cerebral Arteries'. *European Journal of Pharmacology* 644 (1), 128-137

Sandhu, H. and Maddock, H. (2014) 'Molecular Basis of Cancer-Therapy-Induced Cardiotoxicity: Introducing microRNA Biomarkers for Early Assessment of Subclinical Myocardial Injury'. *Clinical Science (London, England : 1979)* 126 (6), 377-400

Satoh, M., Matter, C. M., Ogita, H., Takeshita, K., Wang, C. Y., Dorn, G. W.,2nd, and Liao, J. K. (2007) 'Inhibition of Apoptosis-Regulated Signaling Kinase-1 and Prevention of Congestive Heart Failure by Estrogen'. *Circulation* 115 (25), 3197-3204

Saunders, L. R. and Verdin, E. (2009) 'Cell Biology: Stress Response and Ageing'. *Science* 323 (5917), 1021-1022

Sawyer, D. B., Peng, X., Chen, B., Pentassuglia, L., and Lim, C. C. (2010) 'Mechanisms of Anthracycline Cardiac Injury: Can we Identify Strategies for Cardioprotection?'. *Progress in Cardiovascular Diseases* 53 (2), 105-113

Sawyers, C. (2004) 'Targeted Cancer Therapy'. *Nature* 432 (7015), 294

Sayed, D., Hong, C., Chen, I. Y., Lypowy, J., and Abdellatif, M. (2007) 'MicroRNAs Play an Essential Role in the Development of Cardiac Hypertrophy'. *Circulation Research* 100 (3), 416-424

Scaglione-Sewell, B., Abraham, C., Bissonnette, M., Skarosi, S. F., Hart, J., Davidson, N. O., Wali, R. K., Davis, B. H., Sitrin, M., and Brasitus, T. A. (1998) 'Decreased PKC-Alpha Expression Increases Cellular Proliferation, Decreases Differentiation, and Enhances the Transformed Phenotype of CaCo-2 Cells'. *Cancer Research* 58 (5), 1074-1081

Scheerer, P., Park, J. H., Hildebrand, P. W., Kim, Y. J., Krauß, N., Choe, H., Hofmann, K. P., and Ernst, O. P. (2008) 'Crystal Structure of Opsin in its G-Protein-Interacting Conformation'. *Nature* 455 (7212), 497-502

Schenkman, K.A., Beard, D.A., Ciesielski, W.A., and Feigl, E.O. (2003) 'Comparison of buffer and red blood cell perfusion of guinea pig heart oxygenation' *American Journal of Physiology-Heart and Circulatory Physiology 285*(5) H1819-H1825.

Schenkman, K.A., Marble, D.R., Burns, D.H., and Feigl, E.O. (1999) 'Optical spectroscopic method for in vivo measurement of cardiac myoglobin oxygen saturation'. *Applied spectroscopy 53*(3) 332-338.

Schlessinger, J. (2014) 'Receptor Tyrosine Kinases: Legacy of the First Two Decades'. *Cold Spring Harbor Perspectives in Biology* 6 (3)

Schlessinger, J. (2000) 'Cell Signaling by Receptor Tyrosine Kinases'. *Cell* 103 (2), 211-225

Schmidinger, M., Zielinski, C. C., Vogl, U. M., Bojic, A., Bojic, M., Schukro, C., Ruhsam, M., Hejna, M., and Schmidinger, H. (2008) 'Cardiac Toxicity of Sunitinib and Sorafenib in Patients with Metastatic Renal Cell Carcinoma'. *Journal of Clinical Oncology* 26 (32), 5204-5212

Schramek, D., Kotsinas, A., Meixner, A., Wada, T., Elling, U., Pospisilik, J. A., Neely, G. G., Zwick, R., Sigl, V., Forni, G., Serrano, M., Gorgoulis, V., and Penninger, J. (2011) 'The Stress Kinase MKK7 Couples Oncogenic Stress to p53 Stability and Tumor Suppression'. *Nat Genet* 43 (3), 212-219

Schulte, G. and Fredholm, B. B. (2003) 'Signalling from Adenosine Receptors to Mitogen-Activated Protein Kinases'. *Cellular Signalling* 15 (9), 813-827

Seddon, M., Looi, Y. H., and Shah, A. M. (2007) 'Oxidative stress and redox signalling in cardiac hypertrophy and heart failure'. *Heart 93*(8), 903–907.

Seok, H. Y., Chen, J., Kataoka, M., Huang, Z. P., Ding, J., Yan, J., Hu, X., and Wang, D. Z. (2014) 'Loss of MicroRNA-155 Protects the Heart from Pathological Cardiac Hypertrophy'. *Circulation Research* 114 (10), 1585-1595

Serrano, C., George, S., Valverde, C., Olivares, D., García-Valverde, A., Suárez, C., Morales-Barrera, R., and Carles, J. (2017) 'Novel Insights into the Treatment of Imatinib-Resistant Gastrointestinal Stromal Tumors'. *Targeted Oncology*, 1-12

Seyed, M. and DiMario, J. X. (2008) 'Fibroblast Growth Factor Receptor 1 Gene Expression is Required for Cardiomyocyte Proliferation and is Repressed by Sp3'. *Journal of Molecular and Cellular Cardiology* 44 (3), 510-519

Shah, R. R. and Morganroth, J. (2015) 'Update on Cardiovascular Safety of Tyrosine Kinase Inhibitors: With a Special Focus on QT Interval, Left Ventricular Dysfunction and overall Risk/Benefit'. *Drug Safety* 38 (8), 693-710

Shah, R. R., Morganroth, J., and Shah, D. R. (2013) 'Cardiovascular Safety of Tyrosine Kinase Inhibitors: With a Special Focus on Cardiac Repolarisation (QT Interval)'. *Drug Safety* 36 (5), 295-316

Shantakumar, S., Olsen, M., Vo, T. T., Nørgaard, M., and Pedersen, L. (2016) 'Cardiac Dysfunction among Soft Tissue Sarcoma Patients in Denmark'. *Clinical Epidemiology* 8, 53

Shen, W., Ke, B., and Wu, Q. (2017) 'The Cardioprotective Effects of Metformin in Myocardial Infarction Patients without Diabetes: Current Status and Future Prospects'. *Frontiers in Cardiovascular Medicine* 4, 13

Shioi, T. and Inuzuka, Y. (2012) 'Ageing as a Substrate of Heart Failure'. *Journal of Cardiology* 60 (6), 423-428

Shiojima, I., Sato, K., Izumiya, Y., Schiekofer, S., Ito, M., Liao, R., Colucci, W. S., and Walsh, K. (2005) 'Disruption of Coordinated Cardiac Hypertrophy and Angiogenesis Contributes to the Transition to Heart Failure'. *The Journal of Clinical Investigation* 115 (8), 2108-2118

Shneyvays, V., Mamedova, M. L. K., Leshem, D., Avishag Korkus, A., and Shainberg, A. (2002) 'Insights into the Cardioprotective Function of Adenosine A_1 and A_3 Receptors'. *Exp Clin Cardiol.* 7 (- 2-3), - 138

Shneyvays, V., Mamedova, L., Zinman, T., Jacobson, K., and Shainberg, A. (2001) 'Activation of A3Adenosine Receptor Protects Against Doxorubicin-Induced Cardiotoxicity'. *Journal of Molecular and Cellular Cardiology* 33 (6), 1249-1261

Shneyvays, V., Zinman, T., and Shainberg, A. (2004) 'Analysis of Calcium Responses Mediated by the A3 Adenosine Receptor in Cultured Newborn Rat Cardiac Myocytes'. *Cell Calcium* 36 (5), 387-396

Shojaei, F. (2012) 'Anti-Angiogenesis Therapy in Cancer: Current Challenges and Future Perspectives'. *Cancer Letters* 320 (2), 130-137

Shukla, S., Robey, R. W., Bates, S. E., and Ambudkar, S. V. (2009) 'Sunitinib (Sutent, SU11248), a Small-Molecule Receptor Tyrosine Kinase Inhibitor, Blocks Function of the ATP-Binding Cassette (ABC) Transporters P-Glycoprotein (ABCB1) and ABCG2'. *Drug Metabolism and Disposition: The Biological Fate of Chemicals* 37 (2), 359-365

Siegel, R. L., Miller, K. D., and Jemal, A. (2015) 'Cancer Statistics, 2015'. *CA: A Cancer Journal for Clinicians* 65 (1), 5-29

Silber, J. H., Cnaan, A., Clark, B. J., Paridon, S. M., Chin, A. J., Rychik, J., Hogarty, A. N., Cohen, M. I., Barber, G., and Rutkowski, M. (2004) 'Enalapril to Prevent Cardiac Function Decline in Long-Term Survivors of Pediatric Cancer Exposed to Anthracyclines'. *Journal of Clinical Oncology* 22 (5), 820-828

Simon, H., Haj-Yehia, A., and Levi-Schaffer, F. (2000) 'Role of Reactive Oxygen Species (ROS) in Apoptosis Induction'. *Apoptosis* 5 (5), 415-418

Simonis, G., Briem, S. K., Schoen, S. P., Bock, M., Marquetant, R., and Strasser, R. H. (2007) 'Protein Kinase C in the Human Heart: Differential Regulation of the Isoforms in Aortic

Stenosis Or Dilated Cardiomyopathy'. *Molecular and Cellular Biochemistry* 305 (1-2), 103-111

Singh, R. M., Mourouzis, I., Singh, J., and Pantos, C. (2016) 'Kinase Signalling and Cardiac Remodelling: A Review'. *World Heart Journal* 8 (1), 29

Skrzypiec-Spring, M., Grotthus, B., Szeląg, A., and Schulz, R. (2007) 'Isolated Heart Perfusion According to Langendorff—Still Viable in the New Millennium' *Journal of pharmacological and toxicological methods*, *55*(2), 113-126

Song, J., Cheon, S. Y., Lee, W. T., Park, K. A., and Lee, J. E. (2015) 'The Effect of ASK1 on Vascular Permeability and Edema Formation in Cerebral Ischemia'. *Brain Research* 1595, 143-155

Song, N. R., Lee, E., Byun, S., Kim, J. E., Mottamal, M., Park, J. H., Lim, S. S., Bode, A. M., Lee, H. J., Lee, K. W., and Dong, Z. (2013) 'Isoangustone A, a Novel Licorice Compound, Inhibits Cell Proliferation by Targeting PI3K, MKK4, and MKK7 in Human Melanoma'. *Cancer Prevention Research (Philadelphia, Pa.)* 6 (12), 1293-1303

Srivastava, D. (2006) 'Making Or Breaking the Heart: From Lineage Determination to Morphogenesis'. *Cell* 126 (6), 1037-1048

Steinberg, S. F. (2008) 'Structural Basis of Protein Kinase C Isoform Function'. *Physiological Reviews* 88 (4), 1341-1378

Steinberg, S. F. (2004) 'Distinctive Activation Mechanisms and Functions for Protein Kinase Cdelta'. *The Biochemical Journal* 384 (Pt 3), 449-459

Stewart, B. and Wild, C. P. (2017) 'World Cancer Report 2014'. *Health*

Stratton, M. R., Campbell, P. J., and Futreal, P. A. (2009) 'The Cancer Genome'. *Nature* 458 (7239), 719-724

Strevel, E. L., Ing, D. J., and Siu, L. L. (2007) 'Molecularly Targeted Oncology Therapeutics and Prolongation of the QT Interval'. *Jco* 25 (22), 3362-3371

Su, J., Xu, J., and Zhang, S. (2015) 'RACK1, Scaffolding a Heterotrimeric G Protein and a MAPK Cascade'. *Trends in Plant Science* 20 (7), 405-407

Sucharov, C., Bristow, M. R., and Port, J. D. (2008) 'miRNA Expression in the Failing Human Heart: Functional Correlates'. *Journal of Molecular and Cellular Cardiology* 45 (2), 185-192

Sundarrajan, M., Boyle, D. L., Chabaud-Riou, M., Hammaker, D., and Firestein, G. S. (2003) 'Expression of the MAPK Kinases MKK-4 and MKK-7 in Rheumatoid Arthritis and their Role as Key Regulators of JNK'. *Arthritis & Rheumatism* 48 (9), 2450-2460

Svilaas, T., Lefrandt, J. D., Gietema, J. A., and Kamphuisen, P. W. (2016) 'Long-Term Arterial Complications of Chemotherapy in Patients with Cancer'. *Thrombosis Research* 140, Supplement 1, S109-S118

Tachibana, H., Perrino, C., Takaoka, H., Davis, R. J., Prasad, S. V. N., and Rockman, H. A. (2006) 'JNK1 is Required to Preserve Cardiac Function in the Early Response to Pressure Overload'. *Biochemical and Biophysical Research Communications* 343 (4), 1060-1066

Taimor, G., Schluter, K. D., Best, P., Helmig, S., and Piper, H. M. (2004) 'Transcription Activator Protein 1 Mediates Alpha- but Not Beta-Adrenergic Hypertrophic Growth Responses in Adult Cardiomyocytes'. *American Journal of Physiology.Heart and Circulatory Physiology* 286 (6), H2369-75

Takano, H., Bolli, R., Black, R. G.,Jr, Kodani, E., Tang, X. L., Yang, Z., Bhattacharya, S., and Auchampach, J. A. (2001) 'A(1) Or A(3) Adenosine Receptors Induce Late Preconditioning Against Infarction in Conscious Rabbits by Different Mechanisms'. *Circulation Research* 88 (5), 520-528

Takekawa, M., Tatebayashi, K., and Saito, H. (2005) 'Conserved Docking Site is Essential for Activation of Mammalian MAP Kinase Kinases by Specific MAP Kinase Kinase Kinases'. *Molecular Cell* 18 (3), 295-306

Tam, W., Hughes, S. H., Hayward, W. S., and Besmer, P. (2002) 'Avian Bic, a Gene Isolated from a Common Retroviral Site in Avian Leukosis Virus-Induced Lymphomas that Encodes a Noncoding RNA, Cooperates with C-Myc in Lymphomagenesis and Erythroleukemogenesis'. *Journal of Virology* 76 (9), 4275-4286

Tam, W., Ben-Yehuda, D., and Hayward, W. S. (1997) 'Bic, a Novel Gene Activated by Provital Insertions in Avian Leukosis Virus-Induced Lymphomas, is Likely to Function through its Noncoding RNA'. *Molecular and Cellular Biology* 17 (3), 1490-1502

Tang, B., Du, J., Wang, J., Tan, G., Gao, Z., Wang, Z., and Wang, L. (2012) 'Alpinetin Suppresses Proliferation of Human Hepatoma Cells by the Activation of MKK7 and Elevates Sensitization to Cis-Diammined Dichloridoplatium'. *Oncology Reports* 27 (4), 1090-1096

Taniike, M., Yamaguchi, O., Tsujimoto, I., Hikoso, S., Takeda, T., Nakai, A., Omiya, S., Mizote, I., Nakano, Y., Higuchi, Y., Matsumura, Y., Nishida, K., Ichijo, H., Hori, M., and Otsu, K. (2008) 'Apoptosis Signal-Regulating Kinase 1/p38 Signaling Pathway Negatively Regulates Physiological Hypertrophy'. *Circulation* 117 (4), 545-552

Telli, M. L., Witteles, R. M., Fisher, G. A., and Srinivas, S. (2008) 'Cardiotoxicity Associated with the Cancer Therapeutic Agent Sunitinib Malate'. *Annals of Oncology* 19 (9), 1613-1618

Teng, C. J., Yu, C. R., Hwang, W., Tsai, J., Liu, H., Hwang, G., and Hsu, S. (2013) 'Effector Mechanisms of Sunitinib-Induced G1 Cell Cycle Arrest, Differentiation, and Apoptosis in

Human Acute Myeloid Leukaemia HL60 and KG-1 Cells'. *Annals of Hematology* 92 (3), 301-313

Thornton, B. and Basu, C. (2011) 'Real-Time PCR (qPCR) Primer Design using Free Online Software'. *Biochemistry and Molecular Biology Education* 39 (2), 145-154

Thuc, L. C., Teshima, Y., Takahashi, N., Nishio, S., Fukui, A., Kume, O., Saito, S., Nakagawa, M., and Saikawa, T. (2012) 'Inhibition of Na -H Exchange as a Mechanism of Rapid Cardioprotection by Resveratrol'. *British Journal of Pharmacology* 166 (6), 1745-1755

Thum, T., Galuppo, P., Wolf, C., Fiedler, J., Kneitz, S., van Laake, L. W., Doevendans, P. A., Mummery, C. L., Borlak, J., Haverich, A., Gross, C., Engelhardt, S., Ertl, G., and Bauersachs, J. (2007) 'MicroRNAs in the Human Heart: A Clue to Fetal Gene Reprogramming in Heart Failure'. *Circulation* 116 (3), 258-267

Tijsen, A. J., Pinto, Y. M., and Creemers, E. E. (2012) 'Non-Cardiomyocyte microRNAs in Heart Failure'. *Cardiovascular Research* 93 (4), 573-582

Tobiume, K., Saitoh, M., and Ichijo, H. (2002) 'Activation of Apoptosis Signal-regulating Kinase 1 by the Stress-induced Activating Phosphorylation of Pre-formed Oligomer'. *Journal of Cellular Physiology* 191 (1), 95-104

Tobiume, K., Matsuzawa, A., Takahashi, T., Nishitoh, H., Morita, K., Takeda, K., Minowa, O., Miyazono, K., Noda, T., and Ichijo, H. (2001) 'ASK1 is Required for Sustained Activations of JNK/p38 MAP Kinases and Apoptosis'. *EMBO Reports* 2 (3), 222-228

Toldo, S., Breckenridge, D., Mezzaroma, E., Van Tassell, B., Kannan, H. R., Shryock, J., Voelkel, N. F., and Abbate, A. (2012) 'Inhibition of Apoptosis Signal-Regulating Kinase 1 (ASK1) Reduces Myocardial Ischemia-Reperfusion Injury in the Mouse'. *Journal of the American College of Cardiology* 59 (13s1), E548-E548

Tooze, S. A. and Yoshimori, T. (2010) 'The Origin of the Autophagosomal Membrane'. *Nature Cell Biology* 12 (9), 831-835

Torre, L. A., Bray, F., Siegel, R. L., Ferlay, J., Lortet-Tieulent, J., and Jemal, A. (2015) 'Global Cancer Statistics, 2012'. *CA: A Cancer Journal for Clinicians* 65 (2), 87-108

Tournier, C., Whitmarsh, A. J., Cavanagh, J., Barrett, T., and Davis, R. J. (1999) 'The MKK7 Gene Encodes a Group of C-Jun NH2-Terminal Kinase Kinases'. *Molecular and Cellular Biology* 19 (2), 1569-1581

Toutain, P.L., Ferran, A. and Bousquet-Mélou, A., (2010) 'Species differences in pharmacokinetics and pharmacodynamics'. In *Comparative and veterinary pharmacology*. Ed by Cunningham, F., Elliott, J., Lees, P. Berlin Heidelberg: Springer, 19-48

Tracey, W. R., Magee, W., Masamune, H., Oleynek, J. J., and Hill, R. J. (1998) 'Selective Activation of Adenosine A3 Receptors with N6-(3-Chlorobenzyl)-5'-N-

Methylcarboxamidoadenosine (CB-MECA) Provides Cardioprotection Via KATP Channel Activation'. *Cardiovascular Research* 40 (1), 138-145

Tracey, W. R., Magee, W., Masamune, H., Kennedy, S. P., Knight, D. R., Buchholz, R. A., and Hill, R. J. (1997) 'Selective Adenosine A3 Receptor Stimulation Reduces Ischemic Myocardial Injury in the Rabbit Heart'. *Cardiovascular Research* 33 (2), 410-415

Tsuchiya, A. and Nishizaki, T. (2015) 'Anticancer Effect of Adenosine on Gastric Cancer Via Diverse Signaling Pathways'. *World Journal of Gastroenterology: WJG* 21 (39), 10931

Tsujimoto, Y. and Shimizu, S. (2005) 'Another Way to Die: Autophagic Programmed Cell Death'. *Cell Death & Differentiation* 12, 1528-1534

Uchida, C., Gee, E., Ispanovic, E., and Haas, T. L. (2008) 'JNK as a Positive Regulator of Angiogenic Potential in Endothelial Cells'. *Cell Biology International* 32 (7), 769-776

Uraizee, I., Cheng, S., and Moslehi, J. (2011) 'Reversible Cardiomyopathy Associated with Sunitinib and Sorafenib'. *New England Journal of Medicine* 365 (17), 1649-1650

van Rooij, E., Marshall, W. S., and Olson, E. N. (2008) 'Toward microRNA-Based Therapeutics for Heart Disease: The Sense in Antisense'. *Circulation Research* 103 (9), 919-928

van Rooij, E. and Olson, E. N. (2007) 'MicroRNAs: Powerful New Regulators of Heart Disease and Provocative Therapeutic Targets'. *The Journal of Clinical Investigation* 117 (9), 2369-2376

van Rooij, E., Sutherland, L. B., Liu, N., Williams, A. H., McAnally, J., Gerard, R. D., Richardson, J. A., and Olson, E. N. (2006) 'A Signature Pattern of Stress-Responsive microRNAs that can Evoke Cardiac Hypertrophy and Heart Failure'. *Proceedings of the National Academy of Sciences of the United States of America* 103 (48), 18255-18260

Vandamme, T. F. (2014) 'Use of Rodents as Models of Human Diseases'. *Journal of Pharmacy & Bioallied Sciences* 6 (1), 2-9

Vanlangenakker, N., Berghe, T. V., and Vandenabeele, P. (2012) 'Many Stimuli Pull the Necrotic Trigger, an Overview'. *Cell Death & Differentiation* 19 (1), 75-86

Varfolomeev, E. E., Schuchmann, M., Luria, V., Chiannilkulchai, N., Beckmann, J. S., Mett, I. L., Rebrikov, D., Brodianski, V. M., Kemper, O. C., and Kollet, O. (1998) 'Targeted Disruption of the Mouse Caspase 8 Gene Ablates Cell Death Induction by the TNF Receptors, Fas/Apo1, and DR3 and is Lethal Prenatally'. *Immunity* 9 (2), 267-276

Vegter, E. L., van der Meer, P., de Windt, L. J., Pinto, Y. M., and Voors, A. A. (2016) 'MicroRNAs in Heart Failure: From Biomarker to Target for Therapy'. *European Journal of Heart Failure 18*(5), 457-468

Vogelstein, B., Papadopoulos, N., Velculescu, V. E., Zhou, S., Diaz, L. A.,Jr, and Kinzler, K. W. (2013) 'Cancer Genome Landscapes'. *Science (New York, N.Y.)* 339 (6127), 1546-1558

Volynets, G. P., Chekanov, M. O., Synyugin, A. R., Golub, A. G., Kukharenko, O. P., Bdzhola, V. G., and and Yarmoluk, S. M. (2011) 'Identification of 3H-Naphtho[1,2,3-De]Quinoline-2,7-Diones as Inhibitors of Apoptosis Signal-Regulating Kinase 1 (ASK1)'. *Journal of Medicinal Chemistry* 54 (8), 2680-2686

von Brandenstein, M., Pandarakalam, J. J., Kroon, L., Loeser, H., Herden, J., Braun, G., Wendland, K., Dienes, H. P., Engelmann, U., and Fries, J. W. U. (2012) 'MicroRNA 15a, Inversely Correlated to PKCα, is a Potential Marker to Differentiate between Benign and Malignant Renal Tumors in Biopsy and Urine Samples'. *The American Journal of Pathology* 180 (5), 1787-1797

Wada, T., Joza, N., Hai-ying, M. C., Sasaki, T., Kozieradzki, I., Bachmaier, K., Katada, T., Schreiber, M., Wagner, E. F., and Nishina, H. (2004) 'MKK7 Couples Stress Signalling to G2/M Cell-Cycle Progression and Cellular Senescence'. *Nature Cell Biology* 6 (3), 215-226

Wagner, E. F. and Nebreda, Á R. (2009) 'Signal Integration by JNK and p38 MAPK Pathways in Cancer Development'. *Nature Reviews Cancer* 9 (8), 537-549

Walsh, D., Donnelly, S., and Rybicki, L. (2000) 'The Symptoms of Advanced Cancer: Relationship to Age, Gender, and Performance Status in 1,000 Patients'. *Supportive Care in Cancer* 8 (3), 175-179

Wang, E., Nie, Y., Zhao, Q., Wang, W., Huang, J., Liao, Z., Zhang, H., Hu, S., and Zheng, Z. (2013) 'Circulating miRNAs Reflect Early Myocardial Injury and Recovery After Heart Transplantation'. *Journal of Cardiothoracic Surgery* 8 (1), 1

Wang, Y., Su, B., Sah, V. P., Brown, J. H., Han, J., and Chien, K. R. (1998) 'Cardiac Hypertrophy Induced by Mitogen-Activated Protein Kinase Kinase 7, a Specific Activator for C-Jun NH2-Terminal Kinase in Ventricular Muscle Cells'. *Journal of Biological Chemistry* 273 (10), 5423-5426

Wang, G. K., Zhu, J. Q., Zhang, J. T., Li, Q., Li, Y., He, J., Qin, Y. W., and Jing, Q. (2010) 'Circulating microRNA: A Novel Potential Biomarker for Early Diagnosis of Acute Myocardial Infarction in Humans'. *European Heart Journal* 31 (6), 659-666

Wang, J., Liu, X., Sentex, E., Takeda, N., and Dhalla, N. S. (2003) 'Increased Expression of Protein Kinase C Isoforms in Heart Failure due to Myocardial Infarction'. *American Journal of Physiology.Heart and Circulatory Physiology* 284 (6), H2277-87

Wang, J., Wang, H., Chen, J., Wang, X., Sun, K., Wang, Y., Wang, J., Yang, X., Song, X., Xin, Y., Liu, Z., and Hui, R. (2008) 'GADD45B Inhibits MKK7-Induced Cardiac Hypertrophy and the Polymorphisms of GADD45B is Associated with Inter-Ventricular Septum Hypertrophy'. *Biochemical and Biophysical Research Communications* 372 (4), 623-628

Wang, X., Destrument, A., and Tournier, C. (2007) 'Physiological Roles of MKK4 and MKK7: Insights from Animal Models'. *Biochimica Et Biophysica Acta (BBA) - Molecular Cell Research* 1773 (8), 1349-1357

Watanabe, T., Otsu, K., Takeda, T., Yamaguchi, O., Hikoso, S., Kashiwase, K., Higuchi, Y., Taniike, M., Nakai, A., Matsumura, Y., Nishida, K., Ichijo, H., and Hori, M. (2005) 'Apoptosis Signal-Regulating Kinase 1 is Involved Not Only in Apoptosis but also in Non-Apoptotic Cardiomyocyte Death'. *Biochemical and Biophysical Research Communications* 333 (2), 562-567

Wei, M. C., Lindsten, T., Mootha, V. K., Weiler, S., Gross, A., Ashiya, M., Thompson, C. B., and Korsmeyer, S. J. (2000) 'tBID, a Membrane-Targeted Death Ligand, Oligomerizes BAK to Release Cytochrome C'. *Genes & Development* 14 (16), 2060-2071

Westfall, M. V. and Metzger, J. M. (2004) 'Gene Transfer of Troponin I Isoforms, Mutants, and Chimeras'. *Molecular and Cellular Aspects of Muscle Contraction*, 169-174

Whitmarsh, A. J. (2006) 'The JIP Family of MAPK Scaffold Proteins'. *Biochemical Society Transactions* 34 (Pt 5), 828-832

Whitmarsh, A. J., Kuan, C., Kennedy, N. J., Kelkar, N., Haydar, T. F., Mordes, J. P., Appel, M., Rossini, A. A., Jones, S. N., Flavell, R. A., Rakic, P., and Davis, R. J. (2001) 'Requirement of the JIP1 Scaffold Protein for Stress-Induced JNK Activation'. *Genes & Development* 15 (18), 2421-2432

Widera, C., Gupta, S. K., Lorenzen, J. M., Bang, C., Bauersachs, J., Bethmann, K., Kempf, T., Wollert, K. C., and Thum, T. (2011) 'Diagnostic and Prognostic Impact of Six Circulating microRNAs in Acute Coronary Syndrome'. *Journal of Molecular and Cellular Cardiology* 51 (5), 872-875

Will, Y., Dykens, J. A., Nadanaciva, S., Hirakawa, B., Jamieson, J., Marroquin, L. D., Hynes, J., Patyna, S., and Jessen, B. A. (2008) 'Effect of the Multitargeted Tyrosine Kinase Inhibitors Imatinib, Dasatinib, Sunitinib, and Sorafenib on Mitochondrial Function in Isolated Rat Heart Mitochondria and H9c2 Cells'. *Toxicological Sciences : An Official Journal of the Society of Toxicology* 106 (1), 153-161

Windak, R., Müller, J., Felley, A., Akhmedov, A., Wagner, E. F., Pedrazzini, T., Sumara, G., and Ricci, R. (2013) 'The AP-1 Transcription Factor C-Jun Prevents Stress-Imposed Maladaptive Remodeling of the Heart'. *PloS One* 8 (9), e73294

Winter, J., Jung, S., Keller, S., Gregory, R. I., and Diederichs, S. (2009) 'Many Roads to Maturity: microRNA Biogenesis Pathways and their Regulation'. *Nature Cell Biology* 11 (3), 228-234

Xiao, G., Tang, H., Wei, W., Li, J., Ji, L., and Ge, J. (2014) 'Aberrant Expression of MicroRNA-15a and MicroRNA-16 Synergistically Associates with Tumor Progression and Prognosis in Patients with Colorectal Cancer'. *Gastroenterology Research and Practice* 2014, 364549

Xiao, J., Luo, X., Lin, H., Zhang, Y., Lu, Y., Wang, N., Zhang, Y., Yang, B., and Wang, Z. (2007) 'MicroRNA miR-133 Represses HERG K+ Channel Expression Contributing to QT

Prolongation in Diabetic Hearts'. *The Journal of Biological Chemistry* 282 (17), 12363-12367

Xin, M., Olson, E. N., and Bassel-Duby, R. (2013) 'Mending Broken Hearts: Cardiac Development as a Basis for Adult Heart Regeneration and Repair'. *Nature Reviews Molecular Cell Biology* 14 (8), 529-541

Xu, Z., Jang, Y., Mueller, R. A., and Norfleet, E. A. (2006) 'IB-MECA and Cardioprotection'. *Cardiovascular Drug Reviews* 24 (3-4), 227-238

Xu, C., Lu, Y., Pan, Z., Chu, W., Luo, X., Lin, H., Xiao, J., Shan, H., Wang, Z., and Yang, B. (2007) 'The Muscle-Specific microRNAs miR-1 and miR-133 Produce Opposing Effects on Apoptosis by Targeting HSP60, HSP70 and Caspase-9 in Cardiomyocytes'. *Journal of Cell Science* 120 (Pt 17), 3045-3052

Yamaguchi, O., Higuchi, Y., Hirotani, S., Kashiwase, K., Nakayama, H., Hikoso, S., Takeda, T., Watanabe, T., Asahi, M., Taniike, M., Matsumura, Y., Tsujimoto, I., Hongo, K., Kusakari, Y., Kurihara, S., Nishida, K., Ichijo, H., Hori, M., and Otsu, K. (2003) 'Targeted Deletion of Apoptosis Signal-Regulating Kinase 1 Attenuates Left Ventricular Remodeling'. *Proceedings of the National Academy of Sciences of the United States of America* 100 (26), 15883-15888

Yanaihara, N., Caplen, N., Bowman, E., Seike, M., Kumamoto, K., Yi, M., Stephens, R. M., Okamoto, A., Yokota, J., Tanaka, T., Calin, G. A., Liu, C., Croce, C. M., and Harris, C. C. (2006) 'Unique microRNA Molecular Profiles in Lung Cancer Diagnosis and Prognosis'. *Cancer Cell* 9 (3), 189-198

Yang, B., Lin, H., Xiao, J., Lu, Y., Luo, X., Li, B., Zhang, Y., Xu, C., Bai, Y., and Wang, H. (2007) 'The Muscle-Specific microRNA miR-1 Regulates Cardiac Arrhythmogenic Potential by Targeting GJA1 and KCNJ2'. *Nature Medicine* 13 (4), 486-491

Yao, X., Ping, Y., Liu, Y., Chen, K., Yoshimura, T., Liu, M., Gong, W., Chen, C., Niu, Q., and Guo, D. (2013) 'Vascular Endothelial Growth Factor Receptor 2 (VEGFR-2) Plays a Key Role in Vasculogenic Mimicry Formation, Neovascularization and Tumor Initiation by Glioma Stem-Like Cells'. *PLoS One* 8 (3), e57188

Yeap, X.Y., Dehn, S., Adelman, J., Lipsitz, J., and Thorp, E.B. (2013) 'Quantitation of acute necrosis after experimental myocardial infarction'. *Necrosis: Methods and Protocols* 115-133.

Yujiri, T., Sather, S., Fanger, G. R., and Johnson, G. L. (1998) 'Role of MEKK1 in Cell Survival and Activation of JNK and ERK Pathways Defined by Targeted Gene Disruption'. *Science* 282 (5395), 1911-1914

Zhang, H., Li, M., Han, Y., Hong, L., Gong, T., Sun, L., and Zheng, X. (2010) 'Down-Regulation of miR-27a might Reverse Multidrug Resistance of Esophageal Squamous Cell Carcinoma'. *Digestive Diseases and Sciences* 55 (9), 2545-2551

Zhang, J., Yang, P. L., and Gray, N. S. (2009) 'Targeting Cancer with Small Molecule Kinase Inhibitors'. *Nature Reviews Cancer* 9 (1), 28-39

Zhang, N., Liu, L., Dou, Y., Song, D., and Deng, H. (2016) 'Glycogen Synthase Kinase-3β Antagonizes ROS-Induced Hepatocellular Carcinoma Cell Death through Suppression of the Apoptosis Signal-Regulating Kinase 1'. *Medical Oncology* 33 (7), 60

Zhang, X., Azhar, G., and Wei, J. Y. (2012) 'The Expression of microRNA and microRNA Clusters in the Ageing Heart'. *PloS One* 7 (4), e34688

Zhang, H., Tao, L., Jiao, X., Gao, E., Lopez, B. L., Christopher, T. A., Koch, W., and Ma, X. L. (2007) 'Nitrative Thioredoxin Inactivation as a Cause of Enhanced Myocardial Ischemia/Reperfusion Injury in the Ageing Heart'. *Free Radical Biology and Medicine* 43 (1), 39-47

Zhang, L., Chen, J., and Fu, H. (1999) 'Suppression of Apoptosis Signal-Regulating Kinase 1-Induced Cell Death by 14-3-3 Proteins'. *Proceedings of the National Academy of Sciences* 96 (15), 8511-8515

Zhao, T. C. and Kukreja, R. C. (2002) 'Late Preconditioning Elicited by Activation of Adenosine A 3 Receptor in Heart: Role of NF-K B, iNOS and Mitochondrial K ATP Channel'. *Journal of Molecular and Cellular Cardiology* 34 (3), 263-277

Zhao, Y. and Srivastava, D. (2007) 'A Developmental View of microRNA Function'. *Trends in Biochemical Sciences* 32 (4), 189-197

Zhao, Y., Ransom, J. F., Li, A., Vedantham, V., von Drehle, M., Muth, A. N., Tsuchihashi, T., McManus, M. T., Schwartz, R. J., and Srivastava, D. (2007) 'Dysregulation of Cardiogenesis, Cardiac Conduction, and Cell Cycle in Mice Lacking miRNA-1-2'. *Cell* 129 (2), 303-317

Zhao, Y., Xue, T., Yang, X., Zhu, H., Ding, X., Lou, L., Lu, W., Yang, B., and He, Q. (2010) 'Autophagy Plays an Important Role in Sunitinib-Mediated Cell Death in H9c2 Cardiac Muscle Cells'. *Toxicology and Applied Pharmacology* 248 (1), 20-27

Zhou, G., Myers, R., Li, Y., Chen, Y., Shen, X., Fenyk-Melody, J., Wu, M., Ventre, J., Doebber, T., Fujii, N., Musi, N., Hirshman, M. F., Goodyear, L. J., and Moller, D. E. (2001) 'Role of AMP-Activated Protein Kinase in Mechanism of Metformin Action'. *The Journal of Clinical Investigation* 108 (8), 1167-1174

Zhou, Q. Y., Li, C., Olah, M. E., Johnson, R. A., Stiles, G. L., and Civelli, O. (1992) 'Molecular Cloning and Characterization of an Adenosine Receptor: The A3 Adenosine Receptor'. *Proceedings of the National Academy of Sciences of the United States of America* 89 (16), 7432-7436

Zhuang, G., Shu-yan, H., Chen, Y., Jun, G., and Li, P. (2011) 'Mitochondrial Reactive Oxygen Species in Sunitinib Induced Cardiomyocytes Apoptosis'. *Chin J Pharmacol Toxicol* 25, 188-192

Zimmer, H. G. (1998) 'The Isolated Perfused Heart and its Pioneers'. *News in Physiological Sciences : An International Journal of Physiology Produced Jointly by the International Union of Physiological Sciences and the American Physiological Society* 13, 203-210

Appendices

Normalised haemodynamic data in tables

Haemodynamic data from chapter 3

Table 0.1: Time points at which Sunitinib (1 µM) significantly alters LVDP compared to control in (3 month, 12 month and 24 month aged rat hearts.

*Stats: students t-test between Control vs Sunitinib * = p < 0.05, **= p < 0.01, *** = p <0.01.*

Time point		3 month	12 month	24 month
15	Control	106. 62 ± 4.23	107.04 ± 4.42	104.07 ± 1.20
	Sunitinib	107.38 ± 6.13	100.40 ± 5.17	76.28 ± 6.72 **
30	Control	106.46 ± 4.47	97.23 ± 5.35	97.42 ± 3.14
	Sunitinib	93.04 ± 3.39 *	96.50 ± 2.90	73.49 ± 5.54 **
35	Control	104.61 ± 4.63	100.60 ± 4.27	94.45 ± 3.42
	Sunitinib	93.90 ± 3.39	97.38 ± 4.67	71.81 ± 4.28 *
50	Control	101.65 ± 7.23	98.98 ± 4.34	86.21 ± 5.17
	Sunitinib	85.04 ± 4.69**	91.18 ± 5.39	69.39 ± 3.01
65	Control	98.50 ± 5.94	90.04 ± 3.43	77.78 ± 3.09
	Sunitinib	81.67 ± 4.79**	89.64 ± 5.68	60.36 ± 3.18
80	Control	92.62 ± 4.41	90.85 ± 4.93	76.14 ± 1.84
	Sunitinib	80.50 ± 4.56	83.86 ± 4.58	57.28 ± 3.21
95	Control	90.46 ± 4.13	87.68 ± 2.60	76.70 ± 0.71
	Sunitinib	81.95 ± 5.61	81.43 ± 5.16	56.08 ± 2.17 *
110	Control	85.27 ± 3.51	84.84 ± 2.11	75. 68 ± 0.58
	Sunitinib	70.39 ± 3.38	75.32 ± 3.75	57.35 ± 3.21
125	Control	85.27 ± 3.51	80.32 ± 1.57	73.50 ± 1.21
	Sunitinib	70.39 ± 3.38 ***	69.47 ± 1.29	55.14 ± 2.70

Table 0.2: Time points at which Sunitinib (1 µM) significantly alters HR compared to control in (3 month, 12 month and 24 month aged rat hearts.

Stats: students t-test between Control vs Sunitinib * = $p < 0.05$, **= $p < 0.001$.

Time point		3 month	12 month	24 month
80	Control	96.77 ± 2.99	98.29 ± 4.16	91.72 ± 3.01
	Sunitinib	86.51 ± 4.38	81.60 ± 2.09 **	88.41 ± 6.20
95	Control	98.81 ± 1.74	97.44 ± 4.47	93.39 ± 4.16
	Sunitinib	84.87 ± 4.86	84.34 ± 2.85	89.19 ± 7.19
110	Control	99.63 ± 2.50	97.68 ± 2.68	95.24 ± 4.76
	Sunitinib	82.37 ± 5.28 **	81.21 ± 3.96 **	89.67 ± 7.18
125	Control	100.48 ± 2.22	98.00 ± 2.76	92.06 ± 7.94
	Sunitinib	79.78 ± 4.99 ***	79.73 ± 2.88 **	89.93 ± 7.05

Haemodynamic data from chapter 4

Table 0.3*: Time points which produced significant changes (p<0.05) in LVDP.*

Stats: one way ANOVA Comparing: Control versus Sunitinib (A), Control versus Sunitinib + NQDI-1 (B), Control versus NQDI-1 (C). Sunitinib versus Sunitinib + NQDI-1 (D).

Time/min	Control	Sunitinib	Suntinib+NQDI-1	NQDI-1
50	101.65 ± 7.23	83.84 ± 5.04 ^{A}	85.04 ± 4.70	85.71 ± 5.51
65	98.50 ± 5.94	81.37 ± 3.73	81.67 ± 4.79	80.42 ± 5.43 ^{C}
80	92.62 ± 4.41	77.86 ± 2.86	80.50 ± 4.56	73.57 ± 5.51^{C}
95	90.46 ± 4.13	76.23 ± 3.43	81.95 ± 5.61	69.33 ± 4.13 ^{C}
110	85.57 ± 3.28	70.72 ± 3.72	74.29 ± 3.62	69.31 ± 4.53 ^{C}
125	85.27 ± 3.50	68.53 ± 4.05	70.39 ± 3.38	67.57 ± 5.54 ^{C}

Table 0.4*: Time points which produced significant changes (p<0.05) in HR*

Stats: One way ANOVA Comparing: *Control versus Sunitinib (A), Control versus Sunitinib + NQDI-1 (B), Control versus NQDI-1 (C). Sunitinib versus Sunitinib + NQDI-1 (D).*

Time/min	Control	Sunitinib	Suntinib+NQDI-1	NQDI-1
95	98.81 ± 1.74	84.87 ± 4.86 ^{A}	87.78 ± 4.52	90.83 ± 3.78
110	99.63 ± 2.50	82.37 ± 5.28 ^{AA}	84.84 ± 4.15 ^{B}	90.06 ± 3.65
125	100.48 ± 2.22	79.78 ± 4.99 ^{AAA}	83.42 ± 4.39 ^{BB}	89.35 ±4.45

Table 0.5: *Time points which produced significant changes (p<0.05) in CF.*

Stats: One way ANOVA comparing: Control versus Sunitinib (A), Control versus Sunitinib + NQDI-1 (B), Control versus NQDI-1 (C). Sunitinib versus Sunitinib + NQDI-1 (D

Time/min	Control	Sunitinib	Suntinib+NQDI-1	NQDI-1
5	92.69 ± 2.76	103.98 ± 1.96 [A]	100.87 ± 1.71	94.32 ± 3.92
10	89.46 ± 2.81	106.54 ± 3.48 [A]	95.50 ± 4.13 [D]	96.24 ± 3.39
15	87.03 ± 2.31	102.91 ± 4.51 [A]	94.65 ± 3.48	95.03 ± 4.47

Haemodynamic data from chapter 5

Table 0.6: *Time points which produced significant changes (p<0.05) in LVDP.*

Stats: One way ANOVA comparing: *Control versus Sunitinib (A), Control versus Sunitinib + IB-MECA (B), Control versus IB-MECA (C). Sunitinib versus Sunitinib + IB-MECA (D).*

Time/ min	Control	Sunitinib	Sunitinib + IB-MECA	IB-MECA
30	106.29 ± 5.53	88.01 ± 3.49 [A]	98.96 ± 5.13	94.50 ± 4.38
35	101.69 ± 5.36	90.44 ± 3.03	96.76 ± 6.07	97.01 ± 3.47
50	99.40 ± 7.77	78.25 ± 4.27 [AA]	92.43 ± 6.52	87.31 ± 3.39
65	92.04 ± 6.37	76.32 ± 3.35	87.35 ± 5.98	85.00 ± 4.13
80	88.70 ± 3.40	76.26 ± 3.51	82.23 ± 3.84	82.45 ± 3.71
95	90.98 ± 4.13	76.68 ± 4.61	82.38 ± 4.75	82.97 ± 6.75
110	84.26 ± 3.62	69.61 ± 2.23	80.30 ± 3.33	79.83 ± 7.11
125	86.08 ± 2.37	65.63 ± 2.23 [A]	78.36 ± 4.56	76.16 ± 7.92

Table 0.7: Time points which produced significant changes in HR.

Stats: One way ANOVA comparing: Control versus Sunitinib (A), Control versus Sunitinib + IB-MECA (B), Control versus IB-MECA (C) and Sunitinib versus Sunitinib + IB-MECA (D) ($p<0.05$).

Time/min	Control	Sunitinib	Sunitinib + IB-MECA	IB-MECA
30	99.44 ± 2.93	85.52 ± 3.23 [A]	89.07 ± 1.97	99.01 ± 5.20
35	102.72 ± 2.45	88.83 ± 3.75 [A]	88.72 ± 1.97	101.01 ± 4.78
50	97.20 ± 2.20	84.82 ± 3.82	89.39 ± 3.01	104.13 ± 4.11
65	97.50 ± 1.80	85.58 ± 4.02	88.09 ±3.23	105.96 ± 4.00
80	96.77 ± 2.99	85.33 ± 3.84	86.13 ± 2.88	102.80 ± 4.50
95	98.81 ± 1.74	86.34 ± 3.42 [A]	87.19 ± 3.91	97.90 ± 6.53
125	95.97 ± 5.15	82.53 ± 4.82 [AA]	86.37 ± 5.23[B]	96.97 ± 8.11

Representative Western blots

Western Blots from chapter 3

MKK7 western blot

Age (months)	3	3	12	12	24	24	3	12	24
Sunitinib	-	+	-	+	-	+	+	+	+

p-MKK7 48 kDa →

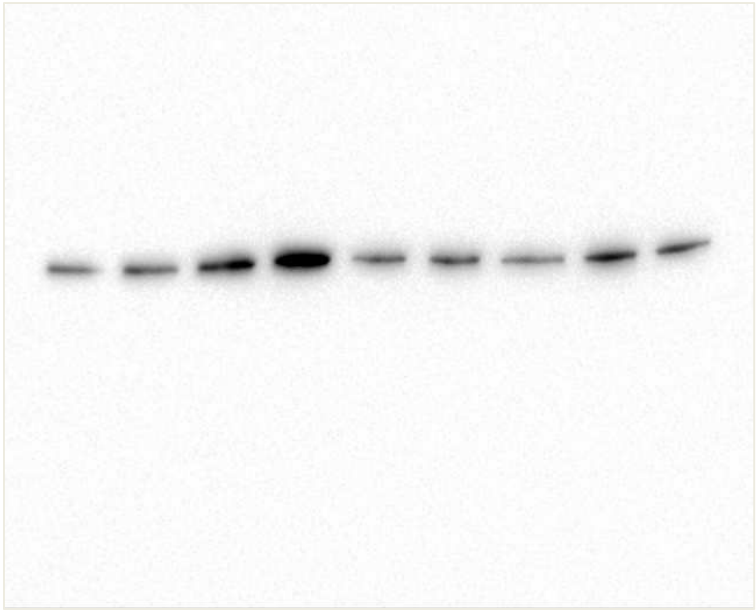

Total MKK7 48 kDa →

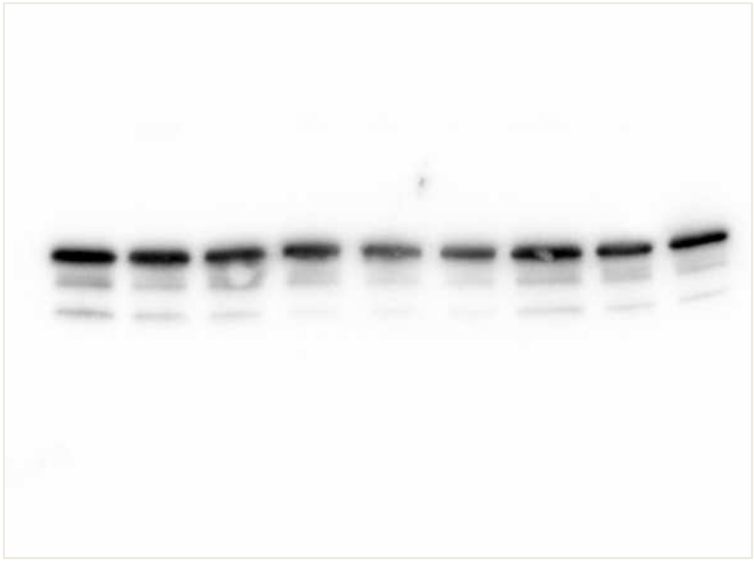

Western blots from chapter 4

ASK1 western blot

Sunitinib	-	+	+	-
NQDI-1	-	-	+	+

p-ASK1 155 kDa →

Total ASK1 155 kDa →

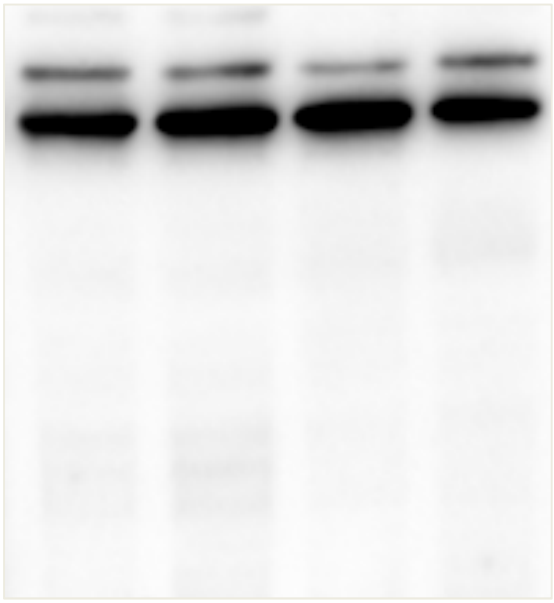

MKK7 western blots

Sunitinib	-	+	-	+
NQDI-1	-	-	+	+

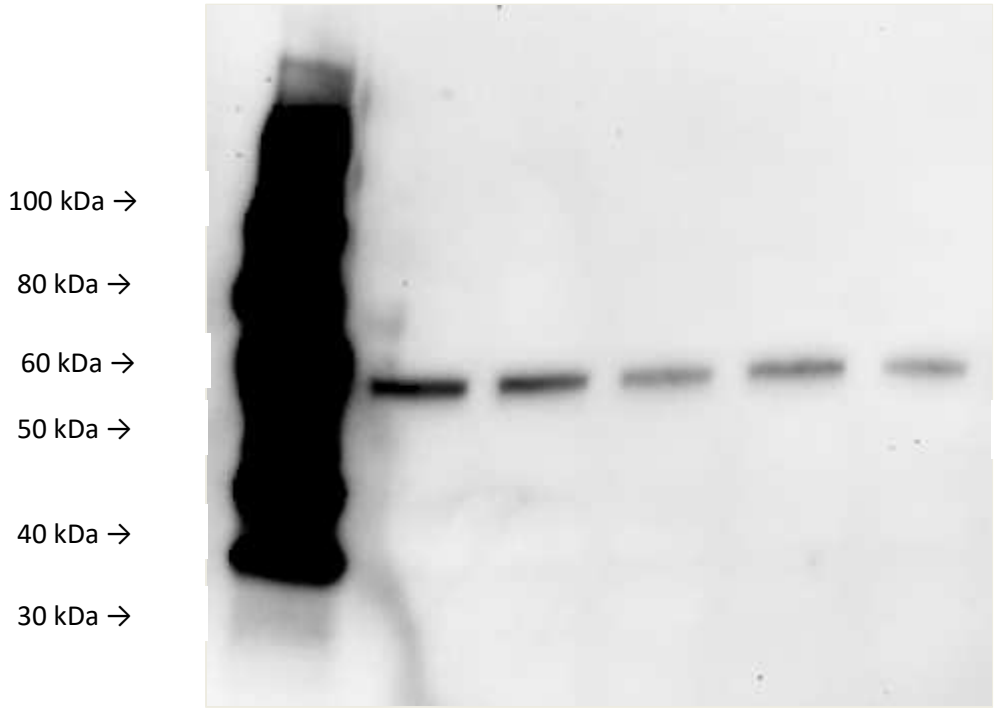

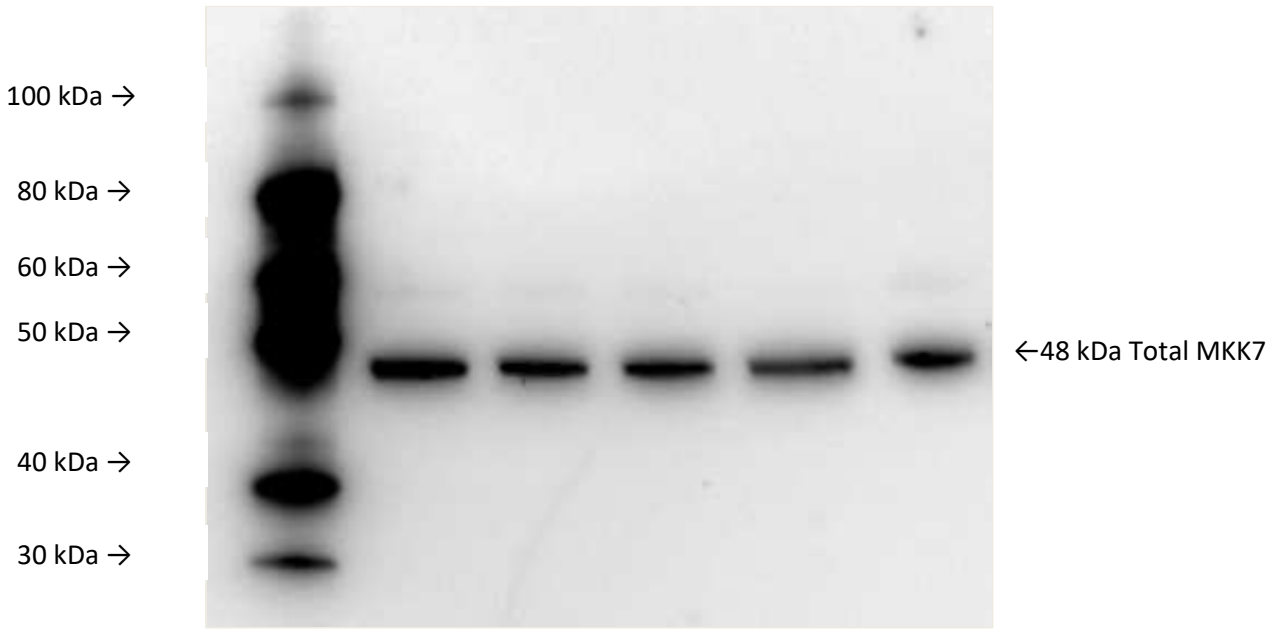

JNK western blots

Sunitinib	-	+	+	-
NQDI-1	-	-	+	+

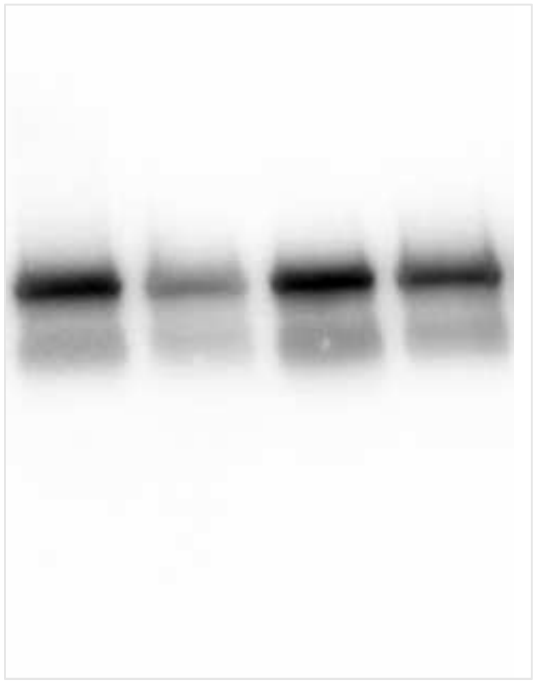

← 54 kDa p-JNK

← 46 kDa p-JNK

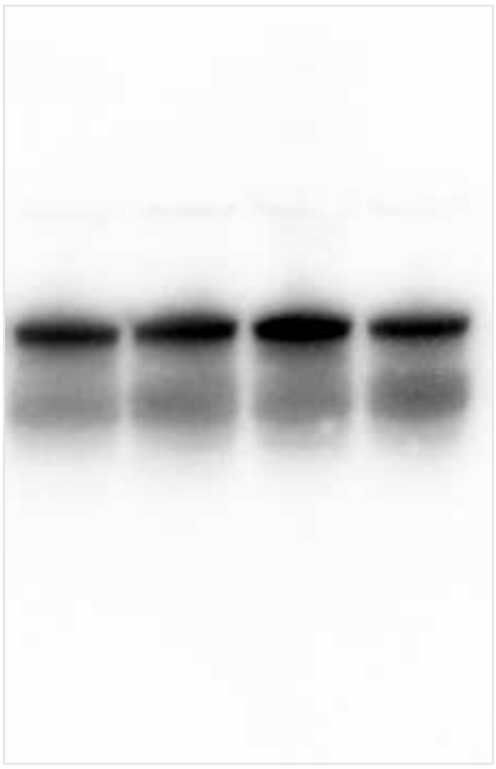

← 54 kDa Total MKK7

← 46 kDa Total JNK

Western blots from chapter 5

MKK7 Western Blot

Sunitinib	-	+	+	-
IB-MECA	-	-	+	+

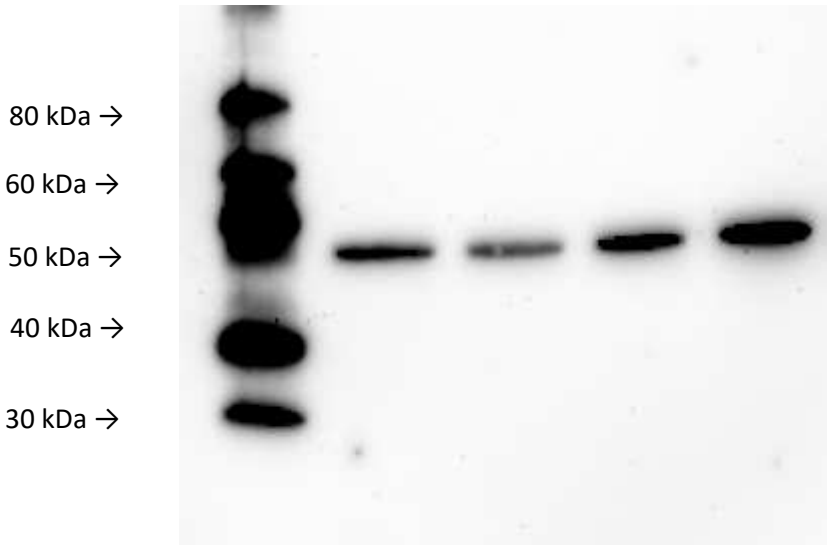

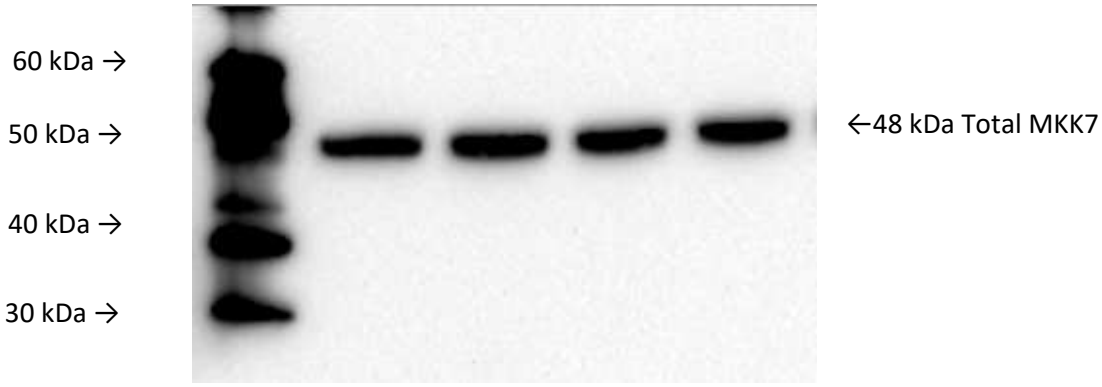

JNK Western blot

Sunitinib	-	+	+	-
IB-MECA	-	-	+	+

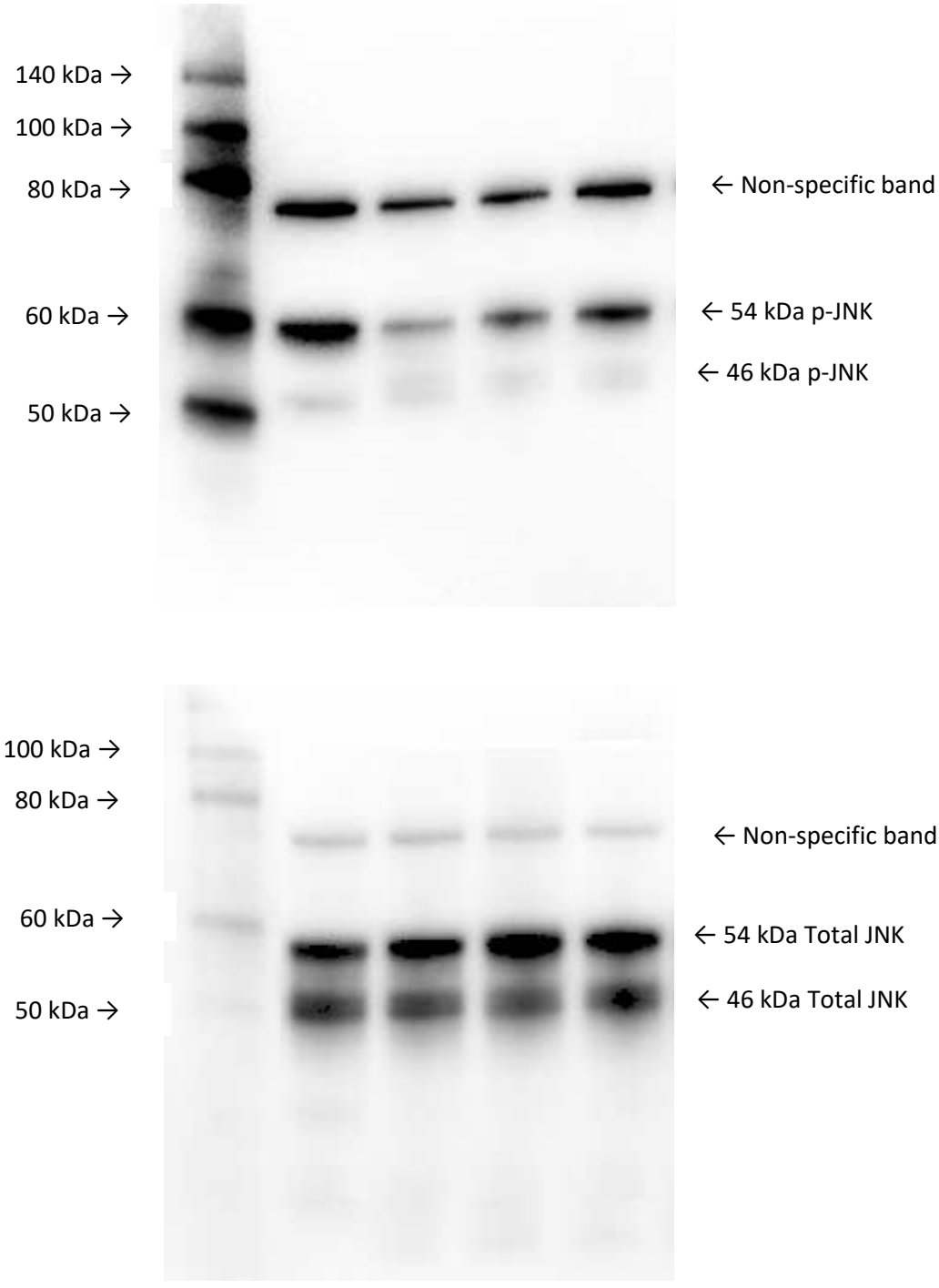

PKC western blots

Left ventricular tissue

Sunitinib	-	+	+	-
IB-MECA	-	-	+	+

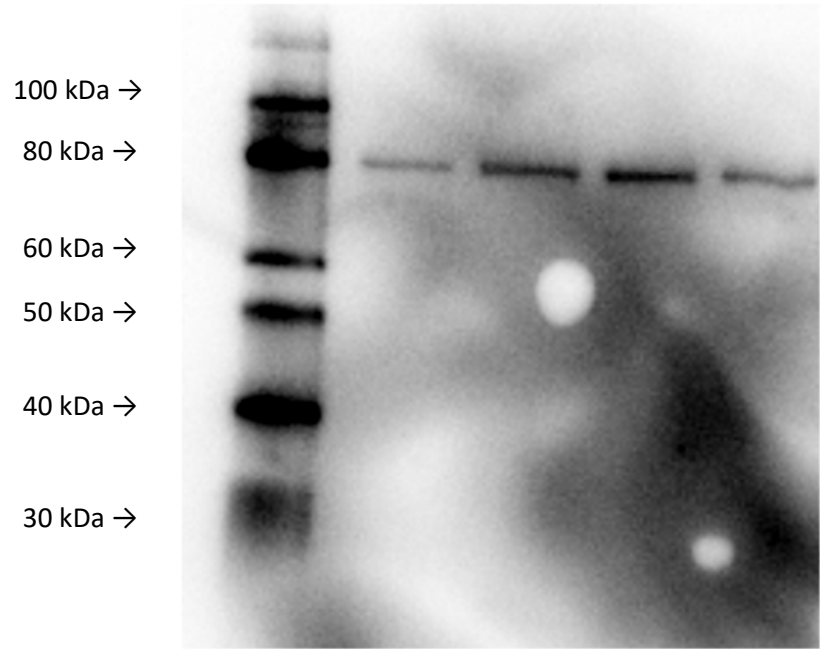

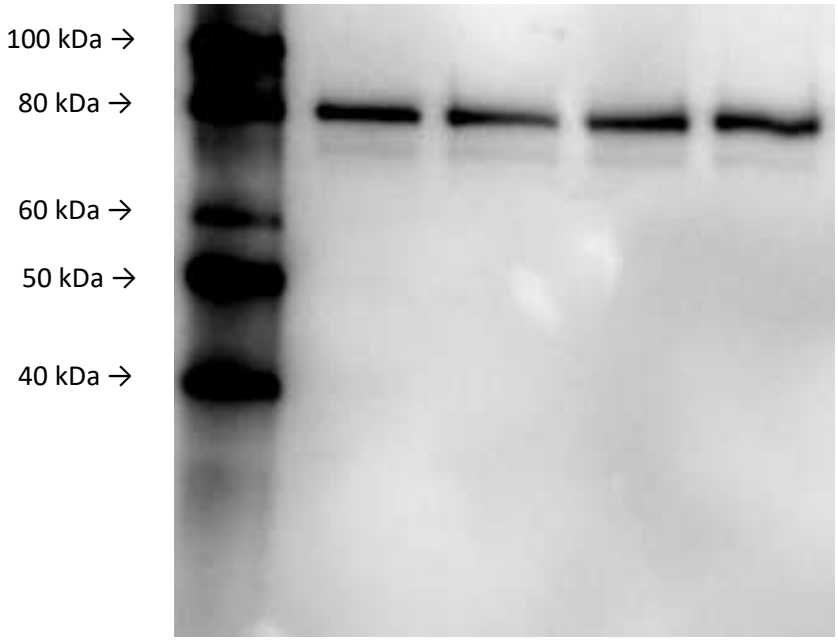

HL60 cell PKCα Western Blot

Sunitinib	-	+	+	-
IB-MECA	-	-	+	+